AN INVESTIGATION INTO THE EFFECT OF SALT (SODIUM CHLORIDE) ON IMMUNITY IN PATIENTS WITH KIDNEY DISEASE

RHYS D R EVANS

UCL

THESIS SUBMITTED FOR THE DEGREE OF DOCTOR OF PHILOSOPHY

Declaration of originality

I, Rhys D R Evans, confirm that the work presented in this thesis is my own. Where information has been derived from other sources, I confirm that this has been indicated in the thesis.

Abstract

The salt (sodium chloride; NaCl) content of a western diet far exceeds the amount that we consumed through most of our evolutionary history. It is accepted that excess sodium intake causes hypertension and cardiovascular disease, but it has been recently shown that sodium also affects immunity, and high salt diets worsen animal models of autoimmune disease. Sodium has been shown to activate multiple immune cells, including Th17 cells, which provide protection from bacterial and fungal infection but which are also implicated in autoimmune disease. The mechanism by which sodium polarises Th17 cells, whether salt depletion has clinical consequences, and if altering sodium balance affects the development of inflammatory kidney diseases are unknown. In this project, I investigate the effect of salt on IL-17 responses and how this is relevant in patients with kidney disease.

I demonstrate that NaCl promotes IL-17 responses in both CD4+ (Th17) and CD8+ (Tc17) cells. This effect is mediated by sodium altering calcium flux during T cell activation and may be abrogated by inhibition of the sodium-potassium-chloride (NKCC) transporter and the epithelial sodium channel (ENaC) on immune cells. Patients with inherited salt losing tubulopathies (SLTs) have clinical features of immunodeficiency with increased infections and allergic disease. This is associated with a reduced ratio of circulating Th17:Th2 cells, and Th17 polarisation in SLT patients is impaired compared with controls. I show that SLT patients have reduced sodium stores and that the typical extracellular ionic environment in SLT is inhibitory to Th17 polarisation. Salt supplementation *in vitro* rescues IL-17 responses in SLT patients. Lastly, I demonstrate that Th17 cells are salt responsive in patients with inflammatory kidney disease despite *in vivo* immunosuppression. A high salt diet did not alter the development of an animal model of glomerulonephritis, but a low salt diet was a feasible therapeutic intervention in kidney transplant recipients.

Impact Statement

The findings in this research project impact scientists, clinicians, patients, and society. From a scientific perspective, I provide data that expands our understanding of the effect of sodium on IL-17 responses and the basic mechanisms that underlie this effect. In demonstrating the role of multiple ions promoting Th17 polarisation and the involvement of specific ion channels and transporters involved in this process, I highlight the possibility of using commonly used sodium channel and transporter inhibitors as adjunctive immunosuppressive drugs. This is relevant in a variety of clinical disciplines (e.g. immunology, nephrology, rheumatology, dermatology, and transplantation) where abrogation of harmful IL-17 responses is therapeutically desirable.

Through investigating immunity in patients with inherited SLT, I provide the first description of human immunodeficiency mediated by changes in the extracellular ionic environment, and describe a novel cause for impaired IL-17 immunity. This is of relevance to clinicians who manage SLT patients and to researchers who investigate immunodeficiency, but above all to SLT patients themselves. The recognition of immunological features as part of what is considered a physiological disease and the provision of reasons for previously unexplained clinical features in this condition may bring great comfort to this patient cohort. Moreover, it provides the basis for studies in to treatments that may improve morbidity in SLT, such as better correction of electrolyte imbalance and prophylactic antimicrobials in those with severe or recurrent infectious disease. No evidence-based treatments improving symptoms or outcomes in SLT patients currently exist.

The possibility of using changes in dietary salt intake to impact immunity is relevant not only to patients with allo- and autoimmune kidney disease, but also to patients with extra-renal inflammatory disease and clinicians who manage these conditions. By demonstrating current immunosuppressive regimens do not impact IL-17 salt responsiveness and by showing low dietary salt interventions are feasible, I provide the basis for larger studies

investigating whether reduced sodium balance may improve outcomes in immune mediated diseases. Data from this research highlights that patients are more supportive of investigating such lifestyle interventions as opposed to using more medications in efforts to improve clinical outcomes in immune mediated diseases.

Finally, this research has a societal impact. Our data highlights that both too little and too much salt have immunological consequences. It remains unclear what the optimal set point for sodium balance should be for society, whether this is different for individuals in different parts of the world, and how the immunological and physiological consequences of altered sodium balance interact. These should be addressed in public health approaches targeting salt intake at a population level.

Acknowledgements

I would firstly like to thank my supervisors, Alan and Ben. Your continuous support, guidance, and enthusiasm at every step had made this research not only possible but also one of the best experiences of my professional life. You are tremendous role models and mentors and I hope we can continue this research collaboration in our future careers.

A huge thanks to everyone at UCL who has helped me along the way. Special thanks to those in the Department of Renal Medicine, particularly Marilina, not only for your help with my experiments but also for making it such fun to come in to the lab every day. I will miss the hot cross buns, mince pies, cakes, and coffee every day!

Thanks also to Janani and others in the immunology department for your patience and advice with the FACS. Thanks to Marilena for your help and persistence in setting up the Na-MRI. Thanks to Winnie and Kate for all you do behind the scenes. And lastly thanks to Magdi (QMUL), Kamal (HCA), Felix, and Christoph (Erlangen) who helped me get the research up and running at the start.

Thanks to KRUK for believing in the project and me, and for all you do for kidney research in the UK.

This would not have been possible without all the patients who so kindly participated in the research. I will always be grateful for everything you have done to support the work and I hope my findings will one day lead to improvements in your care.

Lastly, I would like to thank my family. Mum, Dad, and Cez, thank you for your help and support over many years. And Pandora, Giselle, and Maria Clara: I could not have done this without your endless love, kindness, support and guidance, and I dedicate this work to you all.

List of publications

Publications directly related to research within this thesis

Evans RDR, et al. Inherited Salt Losing Tubulopathies are associated with immunodeficiency due to impaired IL-17 responses. *Nature Communications*. 2020. Under review

Evans RDR, Antonelou M, Henderson S, Walsh SB, Salama AD. Emerging evidence of an effect of salt on innate and adaptive immunity. *Nephrol Dial Transplant Off Publ Eur Dial Transpl Assoc - Eur Ren Assoc.* 2019 Dec 1;34(12):2007–14

Publications related to relevant clinical studies undertaken during this research period

Evans, R. et al. Clinical Manifestations and Long-term Outcomes of IgG4-Related Kidney and Retroperitoneal Involvement in a United Kingdom IgG4-Related Disease Cohort. *Kidney Int. Rep*. 0, (2018).

Evans, R. D. R. *et al.* Assessment of a Dedicated Transplant Low Clearance Clinic and Patient Outcomes on Dialysis After Renal Allograft Loss at 2 UK Transplant Centers. *Transplant. Direct* **4,** e352 (2018)

Evans RDR, Laing CM, Ciurtin C, Walsh SB. Tubulointerstitial nephritis in primary Sjögren syndrome: clinical manifestations and response to treatment. *BMC Musculoskelet Disord*. 2016;17(1):2

Evans R, Zdebik A, Ciurtin C, Walsh SB. Renal involvement in primary Sjögren's syndrome. *Rheumatol Oxf Engl*. 2015 Sep;54(9):1541–8.

Publications related to other collaborative laboratory work undertaken during this research period

Antonelou M, **Evans RDR**, Henderson SR, Salama A. Neutrophils are key mediators in crescentic glomerulonephritis and targets for new therapeutic approaches. NDT 2020. *In Press*.

Antonelou M, Michaëlsson E, **Evans RDR**, Wang CJ, Henderson SR, Walker LSK, et al. Therapeutic Myeloperoxidase Inhibition Attenuates Neutrophil Activation, ANCA-Mediated Endothelial Damage, and Crescentic GN. J Am Soc Nephrol JASN. 2020 Feb;31(2):350–64

Table of Contents

1 CHAPTER 1: INTRODUCTION 26

1.1 Dietary salt intake and clinical consequences 26

1.1.1 Historical aspects of salt intake 26

1.1.2 Known and emerging adverse effects of excess salt 28

1.2 Novel concepts of sodium balance 31

1.2.1 Sodium and water balance are coupled in traditional theories of sodium balance 31

1.2.2 Novel theories suggest sodium and water balance become uncoupled during chronic sodium loading 32

1.2.3 Non-osmotic sodium storage 32

1.2.4 The use of sodium MRI to visualise sodium storage 33

1.2.5 Natural rhythms of sodium excretion and total body sodium balance unrelated to sodium intake 35

1.3 The effect of salt on innate and adaptive immunity 37

1.3.1 SALT AND INNATE IMMUNITY 39

1.3.2 SALT AND ADAPTIVE IMMUNITY 43

1.3.3 Human studies of dietary salt modification and its effect on immunity 60

1.4 Renal sodium handling and salt losing tubulopathy 63

1.4.1 Proximal tubule sodium transport and renal Fanconi syndromes 64

1.4.2 Thick ascending limb sodium transport and Bartter Syndrome 66

1.4.3 Distal convoluted tubule sodium transport and Gitelman syndrome 70

1.4.4 Further clinical considerations in Bartter and Gitelman syndromes 73

1.4.5 Cortical collecting duct sodium reabsorption and pseudohypoaldosteronism type 1 75

1.5 Summary 77

1.6 Aims and hypotheses 78

2 CHAPTER 2: MATERIALS AND METHODS 79

2.1 Methods for techniques used throughout the project 79

2.1.1 Peripheral blood mononuclear cell (PBMC) isolation 79

2.1.2 PBMC freezing and defrosting 79

2.1.3 Cell culture 80

2.1.4 FACS staining 80

2.2 Methods pertaining specifically to investigations reported in Chapter 3 80
2.2.1 Th17 polarisation assay 80
2.2.2 Naïve and memory T cell isolation 82
2.2.3 Analysis of the relationship between osmolality and IL-17 responses 83
2.2.4 Epithelial sodium channel (ENaC) and sodium chloride cotransporter (NCC) expression on lymphocytes 83
2.2.5 Sodium transport inhibition experiments 85
2.2.6 Calcium flux experiments 85
2.2.7 Autosomal recessive Pseudohypoaldosteronism type 1 (AR PHA1) patients 86
2.3 Methods pertaining specifically to investigations reported in Chapter 4 87
2.3.1 Salt losing tubulopathy (SLT) and control cohorts 87
2.3.2 ^{23}Na-MRI Imaging 88
2.3.3 Urine Culture experiments 91
2.3.4 Initial immunological analysis 92
2.3.5 T cell subset analysis 93
2.3.6 Th17 and Tc17 polarisation analysis 96
2.3.7 STAT1 and STAT3 phosphorylation assays 97
2.3.8 NCC expression and calcium flux experiments 98
2.3.9 IL-23 Receptor expression 99
2.3.10 SGK1 expression 99
2.3.11 NFAT5 expression 99
2.3.12 Innate cytokine stimulation assays 100
2.3.13 Monocyte analysis 101
2.3.14 NK cell analysis 103
2.3.15 Statistics 105
2.3.16 Study Approval 106
2.4 Methods pertaining to investigations reported in Chapter 5 106
2.4.1 Patient recruitment for *in vitro* assessment of IL-17 responses 106
2.4.2 T follicular helper (TfH) cell polarisation assay 107
2.4.3 Nephrotoxic nephritis animal model of glomerulonephritis 109
2.4.4 Investigating the feasibility of dietary salt restriction in healthy controls and its impact on IL-17 responses 112
2.4.5 Prospective cohort study of immune responses to sodium minimisation through dietary salt restriction in kidney transplant recipients (KTRs) 115

2.5 Buffers and solutions 120
2.5.1 FACS 120
2.5.2 ELISA 120
3 CHAPTER 3: THE EFFECT AND MECHANISM OF SODIUM CHLORIDE ON *IN VITRO* IL-17 RESPONSES 122
3.1 Introduction 122
3.2 Aims 123
3.3 Brief Methods 124
3.4 Results 125
3.4.1 Th17 polarisation assay 125
3.4.2 Sodium chloride increases IL-17 expression by both CD4+ (Th17) and CD8+ (Tc17) cells 129
3.4.3 The polarising effect of NaCl on Th17 and Tc17 cells is consistent across healthy controls 136
3.4.4 NaCl effects both naïve and memory T cell populations 139
3.4.5 Sodium predominantly mediates the polarising effect of sodium chloride on IL-17 responses 142
3.4.6 Sodium channels and transporters are expressed on diverse immune cells 149
3.4.7 Sodium transport inhibition abrogates sodium chloride driven IL-17 responses 152
3.4.8 T cell activation in the presence of sodium is associated with an alteration in calcium flux 163
3.4.9 Extrapolating *in vitro* findings to patients with Pseudohypoaldosteronism type 1 (PHA1) 169
3.5 Discussion 184
4 CHAPTER 4: INVESTIGATING IMMUNITY IN PATIENTS WITH INHERITED SALT LOSING TUBULOPATHY 188
4.1 Introduction 188
4.2 Aims 189
4.3 Brief Methods 190
4.4 Results 193
4.4.1 SLT and control cohorts 193
4.4.2 SLT patients have reduced sodium stores 198
4.4.3 SLT patients have clinical features of immunodeficiency 200

4.4.4 SLT patients have an altered urinary microbial community 204
4.4.5 Initial immunological analysis of SLT patients suggests a quantitative defect in NK cells 207
4.4.6 Circulating Th17 cells are reduced in SLT patients 212
4.4.7 Th17 and Tc17 polarisation are reduced in SLT patients 215
4.4.8 The clinical phenotype in SLT patients is consistent with an IL-17 defect, but STAT1 and STAT3 phosphorylation are normal 217
4.4.9 Reduced IL-17 responses in SLT patients are not due to altered ion channel or transporter activity on immune cells 224
4.4.10 Multiple ions influence IL-17 responses and alterations in the *in vivo* extracellular ionic environment may explain altered immunity in SLT 226
4.4.11 The intracellular pathway which mediates salt-driven IL-17 inflammation is intact in SLT patients 236
4.4.12 Th17 polarisation defects can be rescued by the addition of salt to culture conditions 239
4.4.13 SLT patients do not have defective innate immune responses 241
4.4.14 Monocyte analysis in SLT patients 246
4.4.15 Further analysis of NK cells in SLT patients 248
4.5 Discussion 252

5 CHAPTER 5: INVESTIGATION AND TARGETING OF SODIUM BALANCE IN INFLAMMATORY KIDNEY DISEASES 257

5.1 Introduction 257
5.2 Aims 258
5.3 Brief Methods 258
5.4 Results 260
5.4.1 Sodium chloride increases *in vitro* IL-17 responses in patients with native autoimmune kidney disease and kidney transplant recipients on *in vivo* immunosuppression 260
5.4.2 Salt responsiveness of IL-17 responses is not different in AIKD patients and kidney transplant recipients on immunosuppression compared to healthy controls 268
5.4.3 T follicular helper (TfH) cell responses were not affected by NaCl 271
5.4.4 Altering dietary salt intake did not affect the development of an animal model of glomerulonephritis 275

5.4.5 Dietary salt restriction is feasible in healthy controls but does not alter Th17 and Treg cells 291
5.4.6 Prospective cohort study of immune responses to sodium minimisation through dietary salt restriction in kidney transplant recipients (KTRs) 296
5.5 Discussion 309

6 CHAPTER 6: DISCUSSION 313
6.1 Summary of results and interpretation 313
6.2 Limitations and future work 315
6.3 Summary of planned and potential future work 318
6.4 Concluding remarks 319

7 REFERENCES 321

8 Appendix 341
8.1 Structured clinical history proforma used for assessment of clinical features of altered immunity 341
8.2 Questionnaire used in pilot studies for assessment of dietary salt intake 343
8.3 Questionnaire used to assess tolerability of low salt intervention 348
8.4 List of organisms isolated from urine sediment cultures in Salt Losing Tubulopathy patients and healthy controls 349

List of Figures

FIGURE 1.1: HISTORICAL PERSPECTIVE OF SALT DISCOVERY AND INTAKE. 27
FIGURE 1.2: SOURCES OF SALT INTAKE IN A WESTERN DIET. DATA FROM[5]. 28
FIGURE 1.3: KNOWN AND EMERGING ADVERSE EFFECTS OF EXCESS SALT INTAKE 31
FIGURE 1.4: ^{23}NA-MRI IMAGE OF THE LOWER LIMB OF A PATIENT WITH PRIMARY ALDOSTERONISM PRE- AND POST-SURGICAL REMOVAL OF AN ALDOSTERONE SECRETING TUMOUR. 35
FIGURE 1.5: MECHANISM OF SODIUM STORAGE AT INTERSTITIAL SITES IN THE MUSCLE AND SKIN, AND PATHWAYS INVOLVED IN INNATE CELL SODIUM CLEARANCE. DATA FROM[35]. 40
FIGURE 1.6: SALT EFFECTS ON M1 AND M2 MACROPHAGES AND PATHWAYS INVOLVED. DATA FROM[45,46]. 41
FIGURE 1.7: SUMMARY OF PATHWAYS INVOLVED IN CD4+ T CELL POLARISATION. 44
FIGURE 1.8: REGULATION OF TH17-TREG BALANCE THROUGH SGK1 ACTIVITY UNDER ISOTONIC CONDITIONS. DATA FROM[53,79]. 46
FIGURE 1.9: INBORN ERRORS OF IL-17 IMMUNITY. FIGURE FROM[82]. 48
FIGURE 1.10: SUMMARY OF INFLAMMATORY KIDNEY DISEASES ASSOCIATED WITH IMBALANCE IN TH17 AND TREG CELLS 52
FIGURE 1.11: INTRACELLULAR PATHWAYS INVOLVED IN SALT INDUCED TH17 POLARISATION. DATA FROM[52,53]. 56
FIGURE 1.12: SODIUM TRANSPORT IN NEPHRON SEGMENTS AND ASSOCIATED SALT LOSING TUBULOPATHY SYNDROMES. FIGURE FROM[118] 64
FIGURE 1.13: SODIUM TRANSPORT MECHANISMS IN THE PROXIMAL CONVOLUTED TUBULE. FIGURE FROM[118]. 65
FIGURE 1.14: SODIUM TRANSPORT MECHANISMS IN THE THICK ASCENDING LIMB OF THE LOOP OF HENLE. FIGURE FROM[118] 68
FIGURE 1.15: SODIUM TRANSPORT MECHANISMS IN THE DISTAL CONVOLUTED TUBULE. FIGURE FROM[118]. 72
FIGURE 1.16: SODIUM TRANSPORT MECHANISMS IN THE COLLECTING DUCT. FIGURE FROM[118]. 76
FIGURE 2.1: GATING USED DURING FACS ANALYSIS OF TH17 AND TC17 POLARISATION 81
FIGURE 2.2: GATING USED DURING FACS ANALYSIS OF ENAC AND NCC EXPRESSION 84
FIGURE 2.3: VARIABLES DETERMINED FROM THE CALCIUM FLUX CURVES 86
FIGURE 2.4: CONVENTIONAL (HYDROGEN) AND ^{23}NA-MRI IMAGES OF THE LOWER LIMB IN A HEALTHY CONTROL 90
FIGURE 2.5: DEMONSTRATION OF REGIONS OF INTEREST IN WHICH SODIUM WAS QUANTITATED IN LOWER LIMB ^{23}NA-MRI SCANS. 90
FIGURE 2.6: GATING USED DURING ANALYSIS OF CD4 SUBSETS 94
FIGURE 2.7: GATING USED DURING ANALYSIS OF THE EFFECT OF IONS ON CD4 SUBSET BALANCE 95
FIGURE 2.8: GATING USED IN STAT1 AND STAT3 PHOSPHORYLATION ASSAYS 98
FIGURE 2.9: GATING USED FOR ANALYSIS OF MONOCYTE SUBSETS 102
FIGURE 2.10: GATING USED FOR ANALYSIS OF MONOCYTE EXPRESSION OF TNFA 103

FIGURE 2.11: GATING USED FOR ANALYSIS OF NK CELL SUBSETS 104
FIGURE 2.12: GATING USED FOR ANALYSIS OF NK CELL EXPRESSION OF IFNΓ 105
FIGURE 2.13: GATING USED DURING ANALYSIS OF TFH CELLS 108
FIGURE 2.14: GATING USED DURING ANALYSIS OF KIDNEY TH17 CELLS 112
FIGURE 2.15: GATING USED DURING ANALYSIS OF TH17 AND TREG CELLS IN HEALTHY CONTROLS UNDERGOING DIETARY SALT RESTRICTION 113
FIGURE 2.16: PILOT STUDY FLOWCHART (SALT RESTRICTION IN HEALTHY VOLUNTEERS) 115
FIGURE 2.17: STUDY PROTOCOL FLOWCHART (SALT RESTRICTION IN KTRS) 119
FIGURE 3.1: CONFIRMATION OF THE EFFECT OF POLARISING CYTOKINES ON IL-17 RESPONSES ... 126
FIGURE 3.2: THE EFFECT OF NACL ON TH17 AND TC17 POLARISATION IN CYTOKINE STIMULATED CELLS 130
FIGURE 3.3: THE EFFECT OF NACL ON TH17 AND TC17 POLARISATION IN ANTI-CD3/28 STIMULATED CELLS 134
FIGURE 3.4: THE EFFECT OF NACL ON IL-17 RESPONSES IN HEALTHY CONTROLS (N=26) 136
FIGURE 3.5: SALT RESPONSIVENESS OF TH17 AND TC17 CELLS 138
FIGURE 3.6: EFFECT OF NACL ON SUPERNATANT IFNΓ CONCENTRATION (N=9) 139
FIGURE 3.7: PURITY OF NAÏVE AND MEMORY T CELL ISOLATION 140
FIGURE 3.8: EFFECT OF NACL ON IL-17 RESPONSES IN NAÏVE AND MEMORY T CELLS 140
FIGURE 3.9: IL-17 RESPONSES ACCORDING TO HYPEROSMOLAR CONDITIONS CREATED BY NACL, MANNITOL AND UREA 143
FIGURE 3.10: IL-17 RESPONSES ACCORDING TO HYPEROSMOLAR CONDITIONS CREATED BY NACL, NA GLUCONATE, AND MANNITOL 146
FIGURE 3.11: AENAC AND NCC EXPRESSION ON LYMPHOCYTE SUBTYPES 150
FIGURE 3.12: REPRESENTATIVE FACS PLOTS OF HIGH AND LOW LEVEL ENAC EXPRESSION 150
FIGURE 3.13: EXPRESSION LEVELS OF ENAC AND NCC ON LYMPHOCYTE SUBTYPES 151
FIGURE 3.14: EFFECT OF AMILORIDE ON CELL VIABILITY, TH17 AND TC17 POLARISATION, AND SUPERNATANT IL-17 CONCENTRATION 152
FIGURE 3.15: EFFECT OF FUROSEMIDE ON CELL VIABILITY, TH17 AND TC17 POLARISATION, AND SUPERNATANT IL-17 CONCENTRATION 154
FIGURE 3.16: EFFECT OF HYDROCHLOROTHIAZIDE ON CELL VIABILITY, TH17 AND TC17 POLARISATION, AND SUPERNATANT IL-17 CONCENTRATION 156
FIGURE 3.17: EFFECT OF KB-R7943 ON CELL VIABILITY, TH17 AND TC17 POLARISATION, AND SUPERNATANT IL-17 CONCENTRATION 158
FIGURE 3.18: SUMMARY OF THE EFFECT OF AMILORIDE 20UM, FUROSEMIDE 10-20UM, HYDROCHLOROTHIAZIDE 20UM, AND KB-R7943 200NM ON IL-17 RESPONSES 159
FIGURE 3.19: EFFECT OF AMILORIDE ON SUPERNATANT IFNΓ CONCENTRATION 161
FIGURE 3.20: EFFECT OF AMILORIDE ON IL-17 EXPRESSION IN ISOLATED NAÏVE CD4+ AND CD8+ CELLS 162
FIGURE 3.21: CALCIUM FLUX IN CD4+ CELLS AFTER T CELL ACTIVATION IN THE PRESENCE OF NACL. 163

FIGURE 3.22: CALCIUM FLUX IN CD4+ CELLS AFTER T CELL ACTIVATION IN THE PRESENCE OF NA GLUCONATE AND MANNITOL 166
FIGURE 3.23: AMILORIDE, FUROSEMIDE, AND HCT EFFECT ON CALCIUM FLUX IN CD4+ CELLS AFTER T CELL ACTIVATION 167
FIGURE 3.24: EFFECT OF AMILORIDE ON CALCIUM FLUX IN CD4+ CELLS AFTER T CELL ACTIVATION IN HIGH SALT CONDITIONS 168
FIGURE 3.25: FAMILY TREE OF PATIENTS WITH PSEUDOHYPOLADOSTERONISM TYPE 1 169
FIGURE 3.26: LYMPHOCYTE CALCIUM FLUX IN PATIENTS WITH PHA1 173
FIGURE 3.27: T CELL PROLIFERATION AND ACTIVATION IN PATIENTS WITH PHA1 175
FIGURE 3.28: IL-17 RESPONSES IN PHA1 PATIENTS AND HEALTHY CONTROLS 177
FIGURE 3.29: SUPERNATANT IL-17 AND IFNΓ CONCENTRATIONS IN PHA1 PATIENT 1 AND HEALTHY CONTROLS 178
FIGURE 3.30: SALT RESPONSIVENESS OF IL-17 RESPONSES IN PHA1 PATIENTS AND CONTROLS, AND THE EFFECT OF AMILORIDE ON IL-17 RESPONSES IN PHA1 PATIENT 1 178
FIGURE 3.31: IFNΓ, IL-17, AND TNFA CONCENTRATIONS IN PHA1 PATIENT 1 FROM WHOLE BLOOD CYTOKINE STIMULATION ASSAYS PLOTTED AGAINST CONCENTRATIONS IN 42 HEALTHY CONTROLS 182
FIGURE 4.1: ^{23}NA-MRI IMAGES DEMONSTRATING INCREASED SKIN AND MUSCLE SODIUM STORAGE IN A DIALYSIS PATIENT COMPARED TO AN AGE MATCHED HEALTHY CONTROL (HC) 198
FIGURE 4.2: ^{23}NA-MRI IMAGES DEMONSTRATING REDUCED SKIN SODIUM STORES IN SALT LOSING TUBULOPATHY (SLT) PATIENTS COMPARED TO AGE MATCHED HEALTHY CONTROLS (HC).... 199
FIGURE 4.3: RECURRENT FUNGAL TOENAIL AFFECTING ALL TOES IN A PATIENT WITH BARTTER SYNDROME TYPE 3 204
FIGURE 4.4: MICROBIAL CULTURE (SERIAL DILUTIONS NEAT, 10^{-1}, 10^{-2}, 10^{-3}) IN TRYPTONE SOYA AGAR MEDIA, WITH AND WITHOUT ADDITIONAL NACL (+0-160MM) 206
FIGURE 4.5: ABNORMALITIES ON INITIAL IMMUNOLOGICAL WORK-UP OF SLT PATIENTS 209
FIGURE 4.6: T CELL PROLIFERATION ASSESSMENT IN SLT PATIENTS AND CONTROLS 209
FIGURE 4.7: T CELL ACTIVATION ASSESSMENT IN SLT PATIENTS AND CONTROLS 210
FIGURE 4.8: ANTIGEN SPECIFIC IMMUNOGLOBULIN RESPONSES IN SLT PATIENTS 211
FIGURE 4.9: CD4 SUBSET ANALYSIS IN SALT LOSING TUBULOPATHY (SLT) PATIENTS AND CONTROLS. 213
FIGURE 4.10: BALANCE OF TH1, TH2 AND TH17 CELLS IN SLT PATIENTS AND CONTROLS 214
FIGURE 4.11: TH17 AND TC17 POLARISATION IN SALT LOSING TUBULOPATHY (SLT) PATIENTS, HEALTHY CONTROLS (HC) AND DISEASE CONTROLS (DC). 216
FIGURE 4.12: SUPERNATANT IL-17 CONCENTRATIONS IN SLT PATIENTS AND CONTROLS 217
FIGURE 4.13: IL-17 RELATED INFECTION SCORE IN SLT PATIENTS AND CONTROLS 218
FIGURE 4.14: PHOSPHORYLATION OF STAT1 AND STAT3 IN SALT LOSING TUBULOPATHY (SLT) PATIENTS 221
FIGURE 4.15: NCC EXPRESSION ON LYMPHOCYTES IN GITELMAN SYNDROME PATIENTS 225
FIGURE 4.16: CALCIUM FLUX AFTER T CELL ACTIVATION IN GITELMAN SYNDROME 225

FIGURE 4.17: EFFECT OF ALTERING EXTRACELLULAR IONS DURING T CELL ACTIVATION ON CD4 SUBSET BALANCE 227
FIGURE 4.18: CALCIUM FLUX AFTER T CELL ACTIVATION IN THE PRESENCE OF $MgCl_2$ AND KCL ... 231
FIGURE 4.19: EFFECT OF ALTERING EXTRACELLULAR ION CONCENTRATION ON TH17 AND TC17 POLARISATION 232
FIGURE 4.20: EFFECT OF ANGIOTENSIN II ON IL-17 RESPONSES 233
FIGURE 4.21: IL-17 RELATED INFECTION SCORE ACCORDING TO SERUM BIOCHEMICAL PARAMETERS AND DISEASE SUBTYPES IN SALT LOSING TUBULOPATHY (SLT) PATIENTS 235
FIGURE 4.22: SGK1 EXPRESSION IN SLT PATIENTS AND CONTROLS 236
FIGURE 4.23: NFAT5 EXPRESSION IN SLT PATIENTS AND CONTROLS 237
FIGURE 4.24: IL23-R EXPRESSION IN SLT PATIENTS AND CONTROLS 238
FIGURE 4.25: SALT RESCUE OF *IN VITRO* IL-17 RESPONSES IN SALT LOSING TUBULOPATHY (SLT) PATIENTS 239
FIGURE 4.26: SALT RESPONSIVENESS OF IL-17 RESPONSES IN SLT PATIENTS AND CONTROLS 240
FIGURE 4.27: MONOCYTE ANALYSIS IN SALT LOSING TUBULOPATHY (SLT) PATIENTS 246
FIGURE 4.28: EFFECT OF ALTERING EXTRACELLULAR IONS ON MONOCYTE FUNCTION 248
FIGURE 4.29: ANALYSIS OF NATURAL KILLER (NK) CELLS IN SALT LOSING TUBULOPATHY (SLT) PATIENTS. 249
FIGURE 4.30: THE EFFECT OF NACL ON NK RESPONSES 250
FIGURE 5.1: THE EFFECT OF NACL ON IL-17 RESPONSES IN PATIENTS WITH AIKD (N=9) ON MAINTENANCE IMMUNOSUPPRESSION 261
FIGURE 5.2: THE EFFECT OF NACL ON IL-17 RESPONSES IN KIDNEY TRANSPLANT RECIPIENTS (N=14) ON MAINTENANCE IMMUNOSUPPRESSION 266
FIGURE 5.3: SALT RESPONSIVENESS OF IL-17 RESPONSES IN HEALTHY CONTROLS, PATIENTS WITH AIKD, AND KTRS. 269
FIGURE 5.4: THE EFFECT OF NACL ON TFH RESPONSES IN HEALTHY CONTROLS (N=7) 271
FIGURE 5.5: URINE VOLUME (24 HOUR) AND PROTEINURIA IN NTN MICE ON A STANDARD AND HIGH SALT DIET (ANIMAL EXPERIMENT 1) 276
FIGURE 5.6: SERUM SODIUM AND CREATININE IN NTN MICE ON A STANDARD AND HIGH SALT DIET (ANIMAL EXPERIMENT 1) 278
FIGURE 5.7: KIDNEY HISTOLOGY SCORES IN NTN MICE ON A STANDARD AND HIGH SALT DIET (ANIMAL EXPERIMENT 1) 280
FIGURE 5.8: MOUSE WEIGHTS IN ANIMAL EXPERIMENT 2 283
FIGURE 5.9: URINE VOLUME (24 HOUR) AND PROTEINURIA IN NTN MICE ON A STANDARD AND HIGH SALT DIET (ANIMAL EXPERIMENT 2) 284
FIGURE 5.10: SERUM CREATININE IN NTN MICE ON A STANDARD AND HIGH SALT DIET (ANIMAL EXPERIMENT 2) 286
FIGURE 5.11: KIDNEY HISTOLOGY SCORES IN NTN MICE ON A STANDARD AND HIGH SALT DIET (ANIMAL EXPERIMENT 2) 287

Figure 5.12: Infiltrating IL-17 expressing cells in the kidneys of NTN mice on a standard and high salt diet (animal experiment 2) 289
Figure 5.13: Analysis of T cell subsets in healthy controls undergoing dietary salt restriction..... 293
Figure 5.14: Changes in salt intake and physiological parameters with low salt diet intervention..... 301
Figure 5.15: Muscle and skin sodium stores quantified by 23Na-MRI pre and post low salt diet in KTRs (n=5) 303
Figure 5.16: Th1, Th2, and Th17 cells pre low salt (T1), post low salt (T2), and at 2-4 weeks back on standard diet (T3) in KTRs (n=4) 306
Figure 5.17: Tc1, Tc2, and Tc17 cells pre low salt (T1), post low salt (T2), and at 2-4 weeks back on standard diet (T3) in KTRs (n=4) 306
Figure 5.18: Th1, Th2, and Th17 cells (expressed as a ratio to each other) pre low salt (T1), post low salt (T2), and at 2-4 weeks back on standard diet (T3) in KTRs (n=4) 307
Figure 5.19: Tc1, Tc2, and Tc17 cells (expressed as a ratio to each other) pre low salt (T1), post low salt (T2), and at 2-4 weeks back on standard diet (T3) in KTRs (n=4) 307
Figure 5.20: TfH polarisation and IL-21 expression by TfH cells pre low salt (T1), post low salt (T2), and at 2-4 weeks back on standard diet (T3) in KTRs (n=3)..... 308

List of Tables

TABLE 1.1: SUMMARY OF THE KNOWN EFFECTS OF SALT ON IMMUNE CELL FUNCTION, THE INTRACELLULAR PATHWAYS INVOLVED, AND THE *IN VIVO* CLINICAL CONSEQUENCES OF THE HIGH SALT EFFECT 37

TABLE 1.2: CLINICAL FEATURES IN COHORTS OF PATIENTS WITH STAT3 AND STAT1 MUTATION[86,87,90] 50

TABLE 1.3: SUMMARY OF STUDIES INVESTIGATING THE IMMUNOLOGICAL EFFECTS OF DIETARY SALT MODIFICATION IN HEALTHY HUMAN VOLUNTEERS AND IN PATIENTS WITH AUTOIMMUNE DISEASE. 62

TABLE 1.4: INHERITED SALT LOSING TUBULOPATHIES CAUSING DEFECTIVE SODIUM REABSORPTION IN THE LOOP OF HENLE AND DISTAL CONVOLUTED TUBULE 70

TABLE 1.5: CLINICAL MANIFESTATIONS OF GITELMAN SYNDROME. TABLE ADAPTED FROM[126] 74

TABLE 2.1: SCORING SYSTEM USED TO ASSESS INFECTION RELATED TO IL-17 DEFECTS 88

TABLE 3.1: MEASURED IONIC CONCENTRATIONS OF UNADJUSTED XVIVO15 MEDIA 130

TABLE 3.2: TREATMENT AND SERUM BIOCHEMISTRY AT TIME OF RECRUITMENT IN PHA1 PATIENTS 170

TABLE 3.3: CLINICAL FEATURES OF ALTERED IMMUNITY IN PATIENTS WITH PHA1 171

TABLE 3.4: INITIAL IMMUNOLOGICAL INVESTIGATION IN PATIENTS WITH PHA1 172

TABLE 3.5: WHOLE BLOOD CYTOKINE STIMULATION ASSAY RESULTS IN PATIENT 1 181

TABLE 4.1: DEMOGRAPHIC DATA AND GENOTYPE OF SALT LOSING TUBULOPATHY PATIENTS 194

TABLE 4.2: SERUM BIOCHEMISTRY IN SALT LOSING TUBULOPATHY (SLT) COHORT. 197

TABLE 4.3: SERUM BIOCHEMISTRY IN SALT LOSING TUBULOPATHY PATIENTS AND DISEASE CONTROLS. 197

TABLE 4.4: CLINICAL FEATURES OF DYSREGULATED IMMUNITY IN PATIENTS WITH SALT LOSING TUBULOPATHY (SLT) COMPARED TO HEALTHY AND DISEASE CONTROLS. 201

TABLE 4.5: URINARY MICROBIAL COMMUNITY IN SALT LOSING TUBULOPATHY (SLT) PATIENTS AND HEALTHY CONTROLS (HC). 205

TABLE 4.6: INITIAL IMMUNOLOGICAL ANALYSIS OF PATIENTS WITH SALT LOSING TUBULOPATHY (SLT). 208

TABLE 4.7: CLINICAL FEATURES IN THE SALT LOSING TUBULOPATHY COHORT IN THIS STUDY AND IN COHORTS OF PATIENTS WITH INHERITED DEFECTS IN IL-17 MEDIATED IMMUNITY DUE TO MUTATIONS IN STAT1 AND STAT3. 219

TABLE 4.8: WHOLE BLOOD CYTOKINE STIMULATION ASSAYS TO ASSESS INNATE CYTOKINE RESPONSES IN SALT LOSING TUBULOPATHY PATIENTS. 243

TABLE 5.1: DEMOGRAPHIC AND CLINICAL DATA OF PATIENTS WITH NATIVE AIKD IN WHOM IL-17 RESPONSES WERE ASSESSED 260

TABLE 5.2: DEMOGRAPHIC AND CLINICAL DATA OF KIDNEY TRANSPLANT RECIPIENTS IN WHOM IL-17 RESPONSES WERE ASSESSED 264

TABLE 5.3: DIPSTICK PROTEINURIA (ANIMAL EXPERIMENT 1) 275

TABLE 5.4: DIPSTICK PROTEINURIA (ANIMAL EXPERIMENT 2)..... 284
TABLE 5.5: PHYSIOLOGICAL PARAMETERS IN HEALTHY CONTROLS (N=9) UNDERGOING LOW SALT DIETARY INTERVENTION FOR 1 WEEK 293
TABLE 5.6: KTR COHORT ENROLLED IN PILOT STUDY 297
TABLE 5.7: POST INTERVENTION QUESTIONNAIRE DESIGNED TO ASSESS TOLERABILITY OF THE LOW SALT DIET INTERVENTION 299
TABLE 5.8: RENAL FUNCTION AND SERUM BIOCHEMICAL PARAMETERS AT PRE AND POST INTERVENTION..... 300
TABLE 5.9: LEUCOCYTE COUNT AND DIFFERENTIAL, C-REACTIVE PROTEIN, AND TOTAL IMMUNOGLOBULINS PRE AND POST LOW SALT DIET IN KTRS (N=7) 305

Abbreviations

AAV	ANCA associated vasculitis
AD HIES	autosomal dominant hyperIgE syndrome
ADH	anti diuretic hormone
AIKD	autoimmune kidney disease
AKI	acute kidney injury
Akt/PKB	protein kinase B
ANCA	anti neutrophil cytoplasmic antibody
APC	antigen presenting cell
AR PHA1	autosomal recessive pseudohypoaldosteronism type 1
AU	arbitrary units
B-GLUC	beta-glucan
BCC	basal cell carcinoma
BS	Bartter syndrome
BSA	bovine serum albumin
CaSR	calcium sensing receptor
CD	cluster of differentiation
CD	collecting duct
CFA	complete Freud's adjuvant
CFU	colony forming units
CKD	Chronic Kidney Disease
CLC	chloride channel
CMC	chronic mucocutaneous candidiasis
CNS	central nervous system
COX	cyclooxygenase
CRP	c-reactive protein
CSF2/GM-CSF	granulocyte-macrophage colony stimulating factor
CVA	cerebrovascular accident
DASH	Dietary approaches to stop hypertension
DC	disease control
DCT	distal convoluted tubule
DM	diabetes mellitus
DMSO	dimethyl sulfoxide
DNA	deoxyribonucleic acid

DVT	deep vein thrombosis
EAE	experimental autoimmune encephalomyelitis
EAST	epilepsy ataxia sensorineural deafness and tubulopathy
EBV	Epstein Barr virus
ECW	extracellular water
EDTA	Ethylenediaminetetraacetic acid
ELISA	enzyme linked immunosorbent assay
ENaC	epithelial sodium channel
ESKD	end stage kidney disease
ESR	erythrocyte sedimentation rate
FACS	fluorescence activated cell sorting
FBS	fetal bovine serum
FMO	fluorescence minus one
FOX	Forkhead Box
FSC	forward scatter
FSC-A	forward scatter area
FSC-H	forward scatter height
GAPDH	Glyceraldehyde 3-phosphate dehydrogenase
GATA3	GATA binding protein 3
GFR	glomerular filtration rate
GS	Gitelman syndrome
GVHD	graft versus host disease
HC	healthy control
HCT	hydrochlorothiazide
HIV	human immunodeficiency virus
HNF4a	hepatocyte nuclear factor 4 alpha
HPV	human papilloma virus
HRA	health research authority
HRP	horseradish peroxidase
HSV	herpes simplex virus
HTN	hypertension
IFN-γ	interferon gamma
Ig	immunoglobulin
IL	interleukin
IL-23R	Interleukin-23 receptor
ILC	innate lymphoid cell

IONO	ionomycin
IQR	interquartile range
KDIGO	Kidney Disease Improving Global Outcomes
KRUK	Kidney Research UK
KTR	kidney transplant recipient
LN	lupus nephritis
LPS	lipopolysaccharide
LRTI	lower respiratory tract infection
MAGED2	melanoma associated antigen D2
MAGT1	magnesium transporter 1
MALDI-TOF	matrix-assisted laser desorption ionisation time-of-flight mass
MS	spectrometry
MAPK	mitogen-activated protein kinase
MD	macula densa
MDP	muramyldipeptide
MDRD	modification of diet in renal disease
MFI	median fluorescence intensity
MHC	major histocompatibility complex
MMF	mycophenolate mofetil
MNP	mononuclear phagocyte
MRC	medical research council
MRI	magnetic resonance imaging
mTOR	mammalian target of rapamycin
NADPH	Nicotinamide adenine dinucleotide phosphate
NCC	sodium-chloride cotransporter
NCX	sodium calcium exchanger
NDI	nephrogenic diabetes insipidus
NFAT5	nuclear factor of activated T cells 5
NHE	sodium hydrogen exchanger
NHS	National Health Service
NK	natural killer
NKCC	sodium-potassium-chloride cotransporter
NR	not recorded
NSAID	Non-steroidal anti-inflammatory drug
NTN	nephrotoxic nephritis
NTS	nephrotoxic serum

ORAI1	calcium release-activated calcium channel protein 1
PBMC	peripheral blood mononuclear cells
PBS	phosphate buffered saline
PCP	pneumococcus
PCR	polymerase chain reaction
PGE	prostaglandin E
PHA	phytohaemagglutinin
PKD	polycystic kidney disease
PMA	phorbol myristate acetate
pSS TIN	Primary Sjögren's Syndrome associated tubulointerstitial nephritis
PT	proximal tubule
QMUL	Queen Mary University London
RA	rheumatoid arthritis
RAAS	renin-angiotensin-aldosterone-system
RAG	recombination activating genes
RNA	ribonucleic acid
ROMK	renal outer medulla potassium channel
RORγT	retinoic acid-related orphan receptor gamma t
RPM	revolutions per minute
SGK1	serum and glucocorticoid regulated kinase 1
SLE	systemic lupus erythematosus
SLT	salt losing tubulopathy
SOCE	store operated calcium entry
SPAK	SPS1 related proline alanine rich kinase
SSC	side scatter
STAT	signal transducer and activator of transcription
STIM1	stromal interaction molecule 1
TAL	thick ascending limb
TBW	total body water
Tc	T cytotoxic cell
Teff	Effector T cell
TET2	Ten-eleven translocation-2
TfH	T follicular helper cell
TGF-β	transforming growth factor beta
Th	T helper cell
TNF-α	tumour necrosis factor alpha

Treg	Regulatory T cell
UCL	University College London
UCLH	University College London Hospital
UK	United Kingdom
URTI	upper respiratory tract infection
US	United States
UTI	urinary tract infection
VEGF-C	vascular endothelial growth factor C
VZV	varicella zoster virus
WHO	World Health Organisation
WNK	with no lysine K
XMEN	X-linked immunodeficiency with magnesium defect, EBV viraemia, and neoplasia
ZYM	zymosan

1 CHAPTER 1: INTRODUCTION

1.1 Dietary salt intake and clinical consequences

1.1.1 Historical aspects of salt intake

Salt (sodium chloride; NaCl) has been a prominent feature of the human diet for a relatively short time, at least in evolutionary terms. Our ancestors survived for millions of years on a diet that contained less than 1g salt per day[1,2]. Sodium is the principal extracellular ion, and through its osmotic effect is required for the maintenance of extracellular (including plasma) volume, as well as playing an integral part in acid-base balance, the transmission of nerve impulses, muscle contraction, and normal cell function. Given the limited salt composition of our natural diet, humans evolved under an intense evolutionary pressure for the selection of salt-conserving genes[3]. This enables us to maintain plasma volume even when salt intake is minimal, and to recreate to some extent the extracellular saline environment of the sea from where we originally evolved.

Salt was discovered as a way of preserving food around 5000 years ago, and since then salt intake has increased rapidly (

Figure 1.1).

Figure 1.1: Historical perspective of salt discovery and intake.

BP - before present

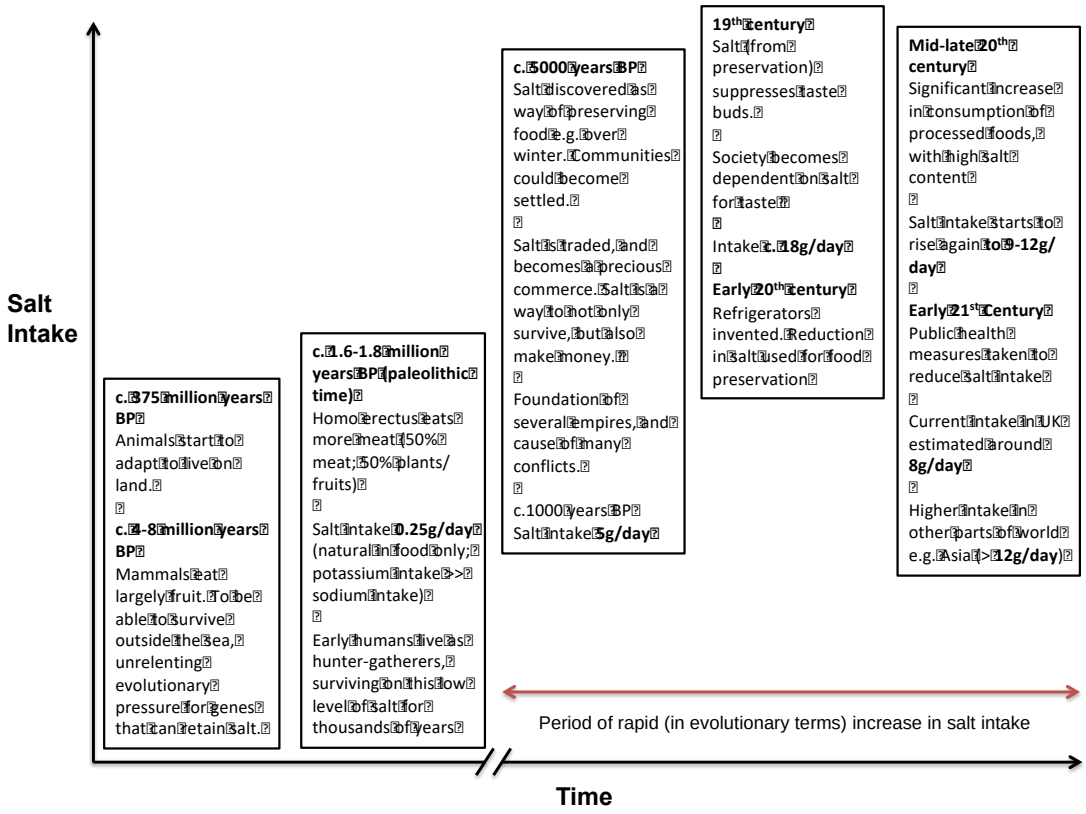

Current estimated salt intake is 8g per day in the United Kingdom, with even greater intake in other parts of the world, in particular in central and eastern Asia[4]. Salt is found in small amounts in natural animal products (e.g. milk, meat and fish), but is much more abundant in processed and packaged foods, such as crackers, breads, processed meats, cheese, sauces, and ready-meals. In high-income settings most dietary salt is consumed from processed foods and restaurant meals, whilst adding salt during cooking and eating contributes to a greater degree in lower income countries worldwide (

Figure 1.2). Across almost all diets globally, though, current salt intake is far in excess of the amount with which we are physiologically programmed to handle[4].

Figure 1.2: Sources of salt intake in a western diet. Data from[5].

1.1.2 Known and emerging adverse effects of excess salt

Given our ability to retain salt, in steady state the minimum amount required to replace losses is less than 0.5g per day. Adverse effects of excess salt are largely considered to be mediated by sodium, although there is some evidence that chloride may play an independent role[6]. In reality, as the majority (approximately 85-90% in a European diet) of our sodium intake is in the form of sodium chloride, the relevance of the contribution of each of the individual ions in terms of interventions to improve patients outcomes is largely academic.

The most robust evidence of an adverse effect of salt is in hypertension. There is good evidence from both observational (e.g. INTERSALT) and interventional (e.g. DASH-Sodium) studies that excess sodium intake increases blood pressure and results in the development of hypertension[7,8]. In INTERSALT, blood pressure and sodium intake were recorded in over 10,000 adults in 52 different communities worldwide[7]. Across all communities, sodium intake positively correlated with blood pressure, blood pressure increased with age in most communities, and the rate of increase in blood pressure was related to sodium intake. Notable in INTERSALT was the observation that 4 remote communities (e.g. Yanomami Indians in the Amazon, Brazil) who exist away from the influence of a 'western diet', had minimal sodium excretion (<200mg/24 hours) and in these communities there was no evidence of hypertension, nor an increase in blood pressure with age[9]. These data support the concept that our dietary salt requirements are minimal, and also highlights that hypertension, a condition that is estimated to affect over 1 billion people worldwide, is predominantly driven by lifestyle, and therefore should be preventable by changes in lifestyle alone, if instituted at a young enough age.

The Dietary Approaches to Stop Hypertension (DASH) trial subsequently investigated the effect of a 30-day diet composed of three different levels of sodium (3.45g, 2.3g, and 1.15g/day) on the blood pressure of adults in the United States (US)[8]. Lowering sodium intake across these ranges resulted in

a step-wise reduction in systolic blood pressure in both normo- and hypertensive patients. There have been numerous further studies supporting the role of sodium in the development of hypertension[10,11], there is also strong evidence that sodium intake is linked to the development of cardiovascular disease[12,13], and there is some evidence for a role in the progression of kidney disease[14]. Based on this, the World Health Organization (WHO) recommends limiting salt intake to <5g/day, which it estimates could prevent 2.5 million deaths globally each year[15]. The Kidney Disease Improving Global Outcomes (KDIGO) group makes a similar recommendation in patients with chronic kidney disease (CKD)[16].

It should be noted however, that not all studies have supported a direct relationship between sodium intake and cardiovascular disease, with some proposing a J shaped or even an inverse relationship[17,18]. Moreover there is inconclusive evidence linking increasing sodium intake to mortality[19]. Adverse effects of sodium restriction proposed include reduction in effective circulating volume with activation of the renin-angiotensin-aldosterone-system (RAAS), concentration of lipids within plasma, and worsening renal function. A systematic review however conducted by the WHO concluded there was no evidence to support these proposals[19]. More likely explanations for these conflicting data are methodological issues, particularly in observational studies where patients with cardiovascular disease are more likely to sodium restrict (i.e. reverse causation), and most importantly significant challenges in determining sodium intake over the long term. Alongside the use of food diaries, sodium intake has traditionally been determined by measurement of urinary sodium excretion, this being done either with a spot urine sodium concentration (with formulae used to determine 24 hour excretion[20]) or with a single 24-hour urine collection. These methods are inaccurate on the whole. Sodium intake varies greatly on a day-day basis and 24-hour collections are often incomplete. Moreover, as outlined below, recent evidence on sodium balance shows that sodium excretion over a single 24-hour period varies independently of sodium intake, and hence all salt studies to date must be interpreted with this caveat in mind.

Beyond hypertension and cardiovascular disease, there are other, perhaps less well appreciated adverse effects of high salt intake which are becoming apparent (Figure 1.3). These include the development of malignancy, in particular gastric cancer[21], obesity, and the metabolic syndrome[22]. Excess salt is also implicated in autoimmune and inflammatory disease. In addition to the laboratory and animal data outlined in the subsequent sections on how salt impacts immunity, observational human studies have suggested that increased salt intake is associated with the development of rheumatoid arthritis[23], and correlates with disease severity in multiple sclerosis[24]. Furthermore, in renal transplantation, peri-operative salt loading worsens short-term outcomes[25], and adherence to a low salt diet improves renal outcomes and survival in the longer term[26]. The consequences of changes in salt intake may therefore extend beyond the widely accepted consequences on hypertension and cardiovascular disease.

Figure 1.3: Known and emerging adverse effects of excess salt intake

Known and emerging adverse effects of excess salt intake
Hypertension[10,11]
Cardiovascular disease (including coronary artery disease and cerebrovascular disease) [12,13]
Progression of chronic kidney disease[14]
Left ventricular hypertrophy[27]
Renal stone disease and osteoporosis (increased Na excretion is associated with hypercalciuria)[28]
Malignancy, in particular gastric cancer[21]
Obesity and metabolic syndrome (may be direct salt effect as well as through association with increased sugar intake)[22]
Autoimmune and inflammatory disease (below)

1.2 Novel concepts of sodium balance

1.2.1 Sodium and water balance are coupled in traditional theories of sodium balance

The classical theory of sodium balance states that if you go from low to high sodium intake, you can excrete about half of this increased load within 24 hours, but the rest is retained and this retained sodium is coupled to an increase in body water[29]. Sodium absorption increases serum osmolality, which will stimulate a thirst and antidiuretic hormone (ADH) response, to increase total body water with a resultant return of serum osmolality back down to normal levels thereby preventing any changes in cell volume. This increase in water is associated with an increase in body weight, plasma volume and blood pressure, which will lead to increased sodium excretion by the kidney through the process of pressure natiuresis. The kidney therefore increases sodium excretion to match increased intake and a new steady state is reached whereby excretion is the same as intake maintaining neutral overall sodium balance and preventing any changes in interstitial sodium concentrations. In this model, sodium accumulation is associated with water retention and increases in body weight, which resolve only when sodium intake is reduced back down again.

1.2.2 Novel theories suggest sodium and water balance become uncoupled during chronic sodium loading

This classical view, based on relatively short term balance studies conducted in the 20th century[30,31], in which it is proposed sodium and water are always coupled, has been challenged by a new body of research which has emerged over the last decade, conducted largely by Titze and colleagues. A key component of this work has been the undertaking of longer-term sodium balance studies during experiments that simulated space flights to Mars[32,33].

In these studies healthy male volunteers (astronauts) were isolated in highly controlled conditions, sodium intake was known and sodium excretion in urine carefully recorded over a period of up to 6 months.

In the initial work, the subjects had free access to food and water, but the researchers knew exactly how much sodium was going in and out[32]. In the short term, sodium accumulation occurred in all subjects with increased sodium intake, and this correlated with an increase in body weight in accordance with traditional theories as above. However, towards the end of this initial experiment (total duration 135 days), sodium accumulated without an increase in body weight suggesting that sodium accumulation was occurring in an osmotically inactive form.

1.2.3 Non-osmotic sodium storage

It has subsequently been shown where this sodium is stored and how this non-osmotic storage occurs, through experiments firstly in animals where sodium concentrations in individual compartments of the body are measured by atomic absorption spectrometry after dry ashing of tissues (the same technique used by the food industry to determine the sodium content of foods), and subsequently in experiments in humans by visualising sodium through the development and use of Sodium Magnetic Resonance Imaging (^{23}Na-MRI). Through the use of both of these techniques sodium has been shown to be stored at interstitial sites in muscle and skin bound to negatively charged glycosaminoglycans[34–37]. As sodium intake increases, it is proposed that glycosaminoglycan polymerization and sulfation increases, binding and storing sodium within the skin, resulting in sodium concentrations at these sites of up to 250mM, levels well above the concentration within the serum where sodium concentrations are tightly regulated due to their influence on osmolality[34,38].

1.2.4 The use of sodium MRI to visualise sodium storage

The use of ^{23}Na-MRI has revolutionised our understanding of sodium storage in humans. MRI relies upon the ability of atomic nuclei to absorb and emit radio frequency energy when placed within a magnetic field, which is measured by a receiving coil. Conventional MRI uses hydrogen atoms as a source of this energy, and anatomical structures are deciphered based on their varying hydrogen content. ^{23}Na-MRI uses the same approach using specially adapted emission/receiver coils that can detect energy created by sodium nuclei. The initial use of this technique measured sodium in skin and muscle just below the knee. These images were calibrated by imaging patients prior to scheduled amputation and directly measuring leg sodium using atomic absorption spectrometry in the same manner to measurement of compartmental sodium employed in the mouse experiments above[36]. Phantoms of known sodium concentration are imaged alongside the leg and used to create a standard curve from which tissue sodium concentrations can be determined (**Figure 1.4**). Importantly, ^{23}Na-MRI measures total sodium within each compartment and therefore the readout reflects sodium concentrations across both intra- and extracellular sites, albeit efforts are ongoing to create methods to specifically measure sodium within the extracellular space.

The use of ^{23}Na-MRI has confirmed sodium storage within the skin of healthy individuals and demonstrated sodium accumulates at these sites with age[36,37]. Furthermore, increased sodium storage has been demonstrated in a number of disease states including hypertension[37], primary hyperaldosteronism[36], congestive cardiac failure[39], and end stage kidney disease (ESKD)[40,41]. Moreover, it has been shown that skin and muscle sodium is rapidly exchangeable. This has included the demonstration of a reduction in sodium stores after medical and surgical treatment of primary hyperaldosteronism (**Figure 1.4**), after sodium removal by haemodialysis in patients with ESRD, and after diuretic management of decompensated congestive cardiac failure[36,39,41].

Figure 1.4: ^{23}Na-MRI image of the lower limb of a patient with primary aldosteronism pre- and post-surgical removal of an aldosterone secreting tumour. Data from[36,42].

Phantoms of known sodium concentrations (10, 20, 30, and 40mM; red arrows) are imaged alongside the leg to create a standard curve. Removal of the aldosterone secreting tumour results in a reduction in tissue sodium storage. This was not associated with a change in weight, supporting evidence for an uncoupling of sodium and water balance.

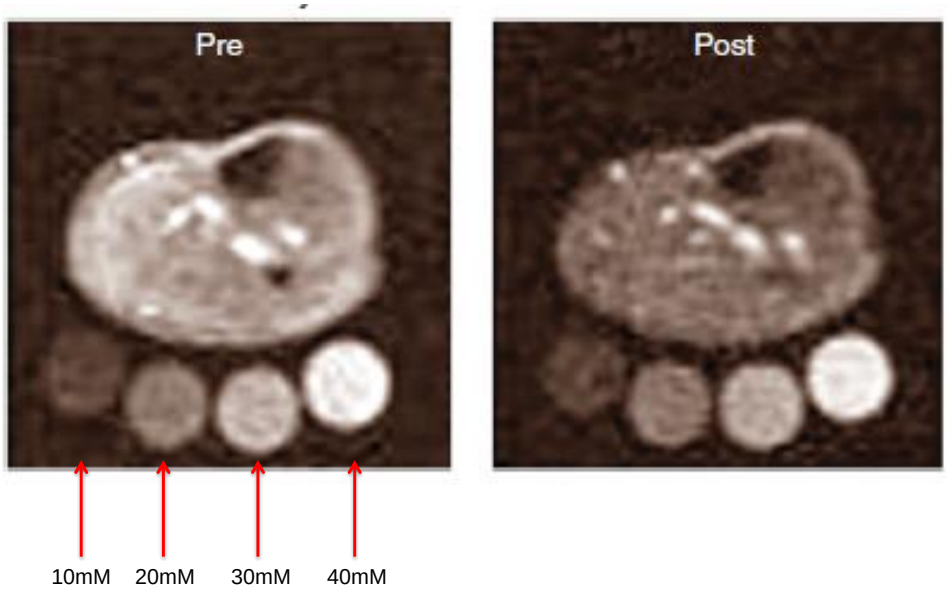

1.2.5 Natural rhythms of sodium excretion and total body sodium balance unrelated to sodium intake

Further Mars space flight simulation experiments were subsequently undertaken in attempts to add to our contemporary understanding of sodium balance[33]. In these experiments (Mars105 and Mars520) sodium intake was fixed and altered over time, with subjects undergoing a diet containing 12g, 9g, and 6g salt simultaneously for approximately 35 days each, with salt intake increasing again to 12g in one of the experiments[33]. Importantly, other dietary components including other electrolytes were consistent across changes in salt, and in addition to blood pressure, body weight and urinary sodium excretion, urinary levels of aldosterone and cortisol were also recorded.

These studies confirmed that lowering sodium reduces blood pressure in healthy individuals, and also that sodium and water balance become uncoupled during prolonged sodium loading, confirming the concept of non-osmotic sodium storage described above. Of further interest was the finding of

marked variability in urinary sodium excretion on a day-day basis within the fixed sodium intake periods, i.e. sodium excretion was independent of intake. In addition to this day-day variation, sodium excretion was also shown to fluctuate rhythmically on a weekly basis (circaseptan rhythm) related to changes in urinary aldosterone, which was inversely related to sodium excretion irrespective of sodium intake at this time. Moreover total body sodium naturally fluctuated on a roughly monthly basis, linked to rhythms of urinary cortisol despite fixed sodium intake during this period. These data provide the novel concept that urinary sodium excretion and balance vary over weekly and monthly periods respectively, and are determined primarily by natural cycles of hormone release, unrelated to sodium intake. This variation in sodium excretion independently of intake has clinical and research implications in the use of a 24-hour urine collection to estimate sodium intake. Based on the findings of this study, a 1-day urine collection is only 50% accurate at determining sodium intake, a 3-day urine collection is better but still only 75% accurate, and a 7-day collection is required to increase accuracy to 92%[43]. This supports older studies that highlight urine collections over a prolonged period are required to accurately estimate sodium intake[44].

Titze and colleague's experiments have thus challenged our traditional view that sodium and water balance are coupled, and moreover that sodium concentrations are the same across the extracellular space. They have demonstrated a third compartment of sodium, stored extracellularly in a non-osmotic manner at interstitial sites in the muscle and skin, with sodium concentrations exceeding those in plasma. Negatively charged glycosaminoglycans at these sites act like a reservoir for sodium, which can be mobilised through a mechanism subsequently shown to involve the innate immune system, described in more details in the sections that follow.

1.3 The effect of salt on innate and adaptive immunity

There have been significant advances over the last 10 years in our appreciation and understanding of the direct effects on salt on the immune

system. *In vitro* studies have focused on changing extracellular sodium concentrations and measuring effects on specific cell populations and the mechanisms involved, whilst animal models have been used to determine the effect of altering dietary salt intake on the development of inflammatory disease. Initial work described the inflammatory effect of salt on macrophages and Th17 cells, but since then salt has been shown to affect most components of innate and adaptive immunity, summarised in **Table 1.1**.

Table 1.1: Summary of the known effects of salt on immune cell function, the intracellular pathways involved, and the *in vivo* clinical consequences of the high salt effect

Cell type	Salt Effect	Intracellular signalling molecules and pathways mediating salt effect	Clinical consequences of high salt effect *in vivo*
INNATE IMMUNE SYSTEM			
M1 Macrophage[45]	Activation	p38-MAPK, NFAT5	Enhanced clearance of cutaneous infection
M2 Macrophage[46]	Inhibition	Akt, mTOR	Reduced wound healing
Monocytes[47]	Expansion of CD14++CD16+ (intermediate) monocytes	Formation of reactive oxygen species	Renal hypoxia and inflammation
Tissue resident mononuclear phagocytes (MNPs)[48]	Increased phagocytic activity of CD14+ MNPs	NFAT5	Protection against pyelonephritis
Dendritic Cell[49,50]	Activation	NADPH Oxidase (reactive oxygen species formation), formation of isolevuglandin protein adducts	Gut inflammation, Hypertension

Neutrophils[51]	Activation as a consequence of increased IL-23 production (direct effect unknown)	Unknown	Exacerbated gut inflammation
Innate lymphoid cells (ILC)[51]	Activation of ILC3	Unknown	Exacerbated gut inflammation
ADAPTIVE IMMUNE SYSTEM			
Th17[51–56]	Activation	p38-MAPK, NFAT5, SGK1, FOXO1	Exacerbated EAE, colitis, and lupus nephritis. Increased progression AKI to CKD.
Treg[57,58]	Inhibition	SGK1, FOXO1/3	Exacerbated transplant rejection, EAE.
Th1[54]	Increased activity *in vivo*, possibly conversion from Th17 or Treg (no direct effect *in vitro*)	N/A	Exacerbated lupus nephritis
Th2[52,59]	Activation (although conflicting data)	NFAT5, SGK1	Exacerbated allergic disease
TfH[60]	Activation	TET2	Exacerbated SLE
CD8+ T cell[49]	Increased IFN-γ and IL-17 from CD8+ cells from salt sensitive mice when cultured with salt primed dendritic cells	Unknown	Unknown
B cells[61]	Biphasic response: initial activation, followed by impaired plasmablast differentiation	p38-MAPK (*downregulation*), NFAT5	Unknown

1.3.1 SALT AND INNATE IMMUNITY

1.3.1.1 Initial evidence of an effect of salt on macrophages

The mechanism by which excess salt causes hypertension is unclear, and given the findings above cannot be explained by an effect on extracellular volume[62]. Over the last decade, in addition to the discovery of these novel findings with regards to sodium storage has been the increasing awareness of a role for immunity in the development of hypertension. A link between both these concepts was demonstrated in a seminal paper in 2009 which demonstrated a high salt diet in rats results in elevated skin sodium concentrations, which in turn activate resident macrophages, which through production of vascular endothelial growth factor C (VEGF-C) clear this stored sodium through the lymphatic system (

Figure 1.5)[35]. Macrophage depletion promoted skin sodium storage and the development of hypertension. Hence, salt loading leads to sodium storage at interstitial sites, resulting in immune cell activation and sodium clearance via the lymphatic system. Either excess salt intake, or impaired immune-mediated sodium clearance, can lead to hypertension. Whether clearance of elevated tissue sodium leads to elevated sodium concentrations in the draining lymph node or in the lymphatic system more generally is unclear[63,64].

Figure 1.5: Mechanism of sodium storage at interstitial sites in the muscle and skin, and pathways involved in innate cell sodium clearance. Data from[35].

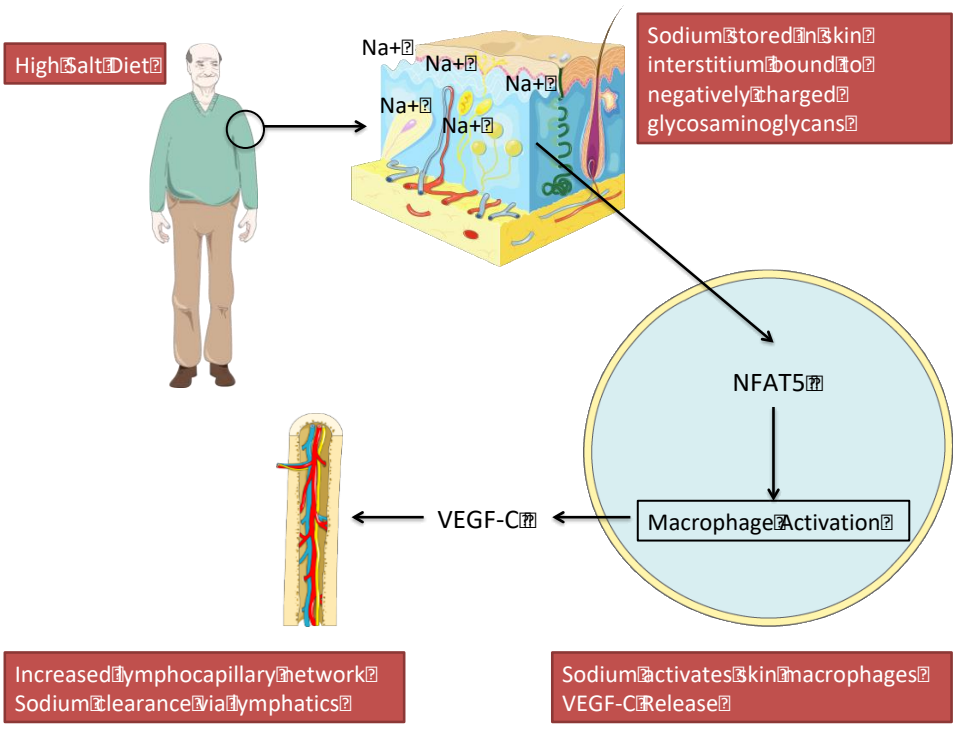

1.3.1.2 Further studies on the effect of salt on macrophage activation

Following this initial work, there have been several other studies investigating how salt affects macrophage activation. Like other cells of the immune system, macrophages display a spectrum of activation states with plasticity along this spectrum. At one end, are pro-inflammatory M1 macrophages, which secrete inflammatory cytokines IL-1, IL-6, IL-12, and TNF-α and activate effector T cells (Teff), and at the other end are reparative M2 macrophages which secrete anti-inflammatory cytokines IL10 and TGF-β, with reduction in Teff and increase in regulatory T cell (Treg) activity[65]. M2 macrophage activity is important in wound healing, and experimentally, they have been shown to reduce the development of autoimmune disease[66,67].

Salt has been shown to have a pro-inflammatory effect on macrophages, increasing M1 activation and reducing M2 activation (

Figure 1.6)[45,46]. In cell culture, the addition of 40mM NaCl increases M1 macrophage activation and this is dependent on a signalling pathway

involving p38-mitogen activated protein kinase (p38-MAPK) and the transcription factor nuclear factor of activated T-cells 5 (NFAT5; also known as tonicity-responsive enhancer binding protein, TonEBP)[45]. Sodium accumulates at sites of skin infection in mice and in humans, adding NaCl to cell cultures *in vitro* led to increased M1 clearance of infection, and a high salt diet in animals resulted in enhanced clearance of cutaneous leishmaniasis. By contrast, M2 activation is blunted *in vitro* in high salt culture conditions, and a high salt diet is associated with reduced wound healing and reduced M2 activity in a mouse model of peritonitis[46]. Unlike the salt effect on M1 macrophages, and indeed that on Th17 cells, which is dependent on NFAT5, the inhibitory salt effect on M2 macrophages is dependent on reduction in signalling through a pathway involving protein kinase B (PKB, also known as Akt) and the mammalian target of rapamycin (mTOR).

Figure 1.6: Salt effects on M1 and M2 macrophages and pathways involved. Data from[45,46].

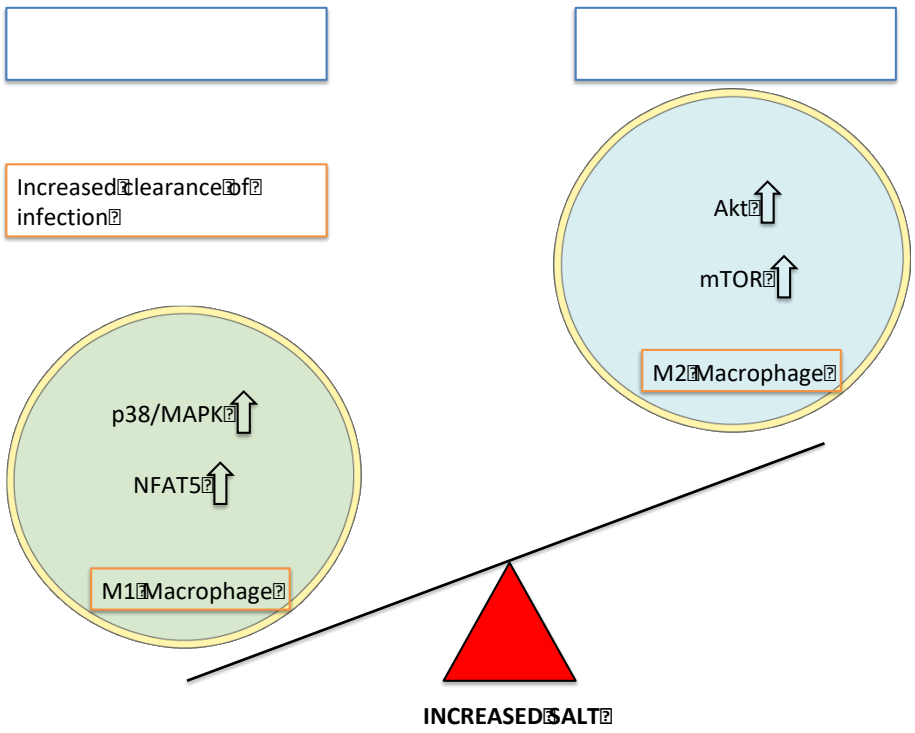

Taken together, these data on macrophage activation states and high interstitial sodium concentrations provide an insight in to the potential evolutionary reasons for why the immune system responds to salt. Infection is associated with the creation of localised hypersalinity[45], which may allow for local activation of pro-inflammatory cells whilst limiting such activation in the body more generally. A similar high sodium environment is created at sites of body-environmental interface (e.g. skin, kidney/genitourinary tract) providing protection from pathogens at these locations.

1.3.1.3 The effect of the sodium gradient on tissue resident mononuclear phagocytes in the kidney

Tissue resident leucocytes stably occupy tissue and do not traffic through blood or lymphoid organs[68]. As such they cannot be sampled in peripheral venous blood and have therefore remained relatively hidden from detailed analysis. More recently, there has been increased focus on this important part of the innate and adaptive immune sensing network, and their ability to detect local changes in homeostasis, participate in protection from infection, and likely contribute to the development of autoimmune disease.

Further evidence for a role of hypersalinity in providing protection from infection was provided in a recent study, which assessed the role of interstitial sodium concentrations on tissue resident mononuclear phagocytes (MNPs) in the kidney[48]. Tissue MNPs include distinct subsets of macrophages and dendritic cells. *Berry et al* demonstrated that CD14+ MNPs, a subset of MNPs with enhanced phagocytic capability, were enriched in the medulla compared to the cortex of human kidneys; this positioning was dependent on NFAT5 mediated production of the chemokines CCL2 and CX3CL1 by renal tubular epithelial cells in response to hypersalinity. Medullary CD14+ MNPs demonstrated increased phagocytosis of uropathogenic E.Coli, and phagocytic activity increased with increasing extracellular sodium concentrations in an NFAT5 dependent manner. The induction of nephrogenic diabetes insipidus (NDI) resulted in increased bacteraemia and death

following intravesical uropathogenic E.Coli challenge in mice; this was interpreted as being due to disruption of the medullary renal sodium gradient. Moreover, NDI in patients, either in the setting of tolvaptan use, or as a result of sickle cell disease, is associated with increased urinary tract infection risk[48].

Taken together, these data demonstrate that high interstitial salt concentrations in the kidney, primarily required for water reabsorption and the maintenance of extracellular volume, also promote medullary localisation of specific subsets of MNPs, which in turn provide protection from infection. It is tempting to speculate that autoimmune kidney disease might in part arise due to the hypertonic environment found in the kidneys, created through evolution for these volume and infectious purposes.

1.3.2 SALT AND ADAPTIVE IMMUNITY

1.3.2.1 CD4+ T cell polarisation

Antigen is presented to naïve CD4+ T cells on MHC class II (MHC-II). This is done by a select group of antigen presenting cells, including dendritic cells, macrophages, and B cells. After antigen presentation, naïve CD4+ T cells become activated and polarise towards one of a number of CD4+ T cell subsets, including Th1, Th2, Th17, and Treg cells, each of which has different effects on the immune response, in part through the cell-specific cytokines produced (

Figure 1.7).

Figure 1.7: **Summary of pathways involved in CD4+ T cell polarisation.** APC – antigen presenting cell; GATA-3 – GATA binding protein 3; RORγT – retinoic acid-related orphan receptor gamma t; FOXP3 – forkhead box P3.

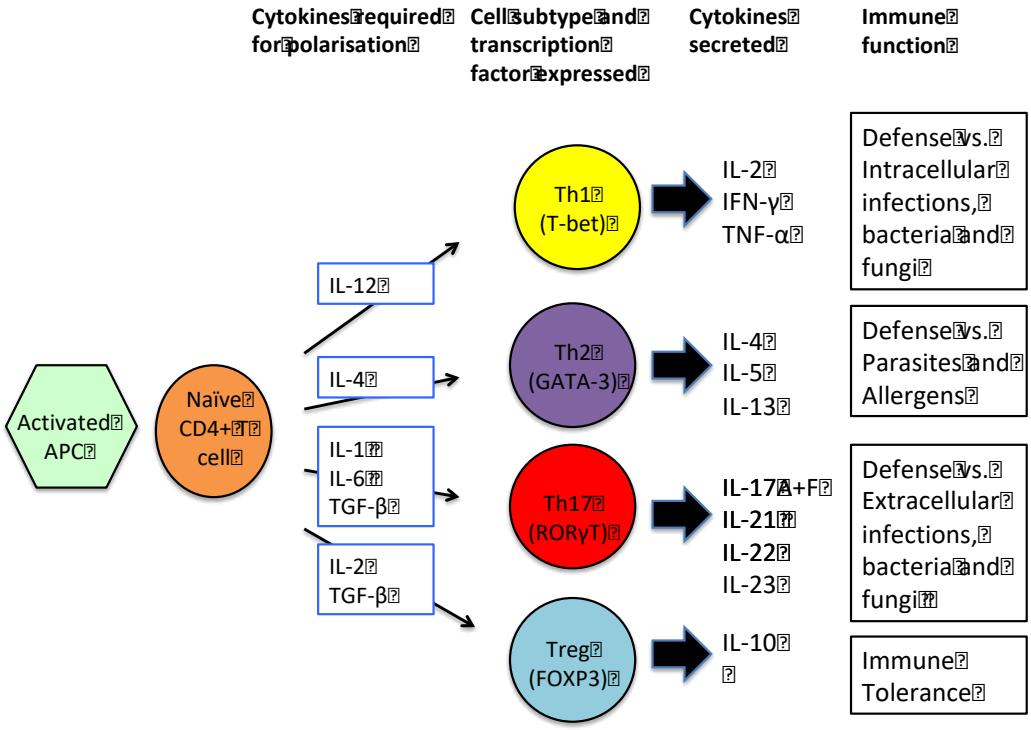

1.3.2.2 Th17 function and plasticity

Th17 cells are pro-inflammatory, and provide protection against extracellular bacterial and fungal infections, particularly at epithelial cell surfaces[69]. Polarisation requires stimulation by IL-1β, IL-6, TGF-β, while full maturation requires IL-21 and IL-23. Th17 cells secrete various cytokines including IL-17,

which acts on stromal cells and is important for neutrophil recruitment, and others such as IL-26 and IL-22, which act on non-immune cells, enhancing inflammation or serving to attenuate damage, depending on the tissue and environment. IL-17 is also produced by other immune cells, specifically CD8+ (Tc17) cells and various innate cells including γδT cells, natural killer T (NKT) cells, and group 3 innate lymphoid cells (ILCs)[70]. The IL-17 family of cytokines consists of a number of homologs (IL-17A-F), with IL17-A being the most abundant and well-studied in human health and disease.

Tregs have opposing effects to Th17 cells. Naturally occurring and peripherally induced Tregs are characterised by expression of the transcription factor Forkhead Box P3 (FOXP3), and provide peripheral tolerance through inhibiting the function of effector CD4+ and CD8+ T cells, B cells, and cells of the innate immune system, through cell-cell contact mechanisms and release of suppressive cytokines (e.g. TGF- β, IL-10)[71]. Lack of Treg function (e.g. through mutation in FOXP3) results in a severe and rapidly fatal autoimmune disease[72].

It was originally thought that CD4+ T cells could only become polarised to one particular subtype during their lifespan, but it is becoming increasingly apparent that this is not the case, especially in the case of Tregs and Th17 cells[71]. We now know that CD4+ T cells demonstrate significant plasticity, and commitment to a particular subtype does not necessarily represent terminal differentiation. Studies, often using fate reporter mice, have shown that during inflammation, Th17 cells can either develop a Th1 signature and secrete IFN-γ[73], or develop a regulatory phenotype[74]. Similarly, Tregs are plastic and can become inflammatory, up-regulating IL-17 and IFN-γ[75,76]. The potential to harness the plasticity of Th17 and Tregs therapeutically has been demonstrated in animal models of autoimmune kidney disease; for example, in a mouse model of crescentic glomerulonephritis it has been shown that Th17 can up-regulate IL-10 and promote tolerance in response to anti-CD3 treatment[77].

Whilst a full understanding of the mechanisms which govern the balance between Th17 and Tregs remains elusive, intracellular pathways are beginning to emerge. The serine-threonine kinase serum and glucocorticoid regulated kinase 1 (SGK1) plays a pivotal role[53,78]. SGK1 is a widely expressed intracellular kinase, which acts as an important mediator of renal sodium reabsorption, for example through regulation of the epithelial sodium channel (ENaC)[79,80]. More recently, it has been shown to be expressed in CD4+ T cells, in particular Th17 and Tregs, and this kinase provides a crucial link between sodium homeostasis and immunity.

SGK1 acts to direct the immune response towards a pro-inflammatory Th17 phenotype, whilst inhibiting the activation of Tregs. It does this under both standard conditions, and as outlined further below, in response to salt. Isotonic up-regulation of SGK1 occurs in response to IL23-receptor (IL23-R) signalling resulting in phosphorylation of the transcription factor forkhead box protein O1 (FOXO1). FOXO1 is prevented from entering the nucleus, and as FOXO1 normally down-regulates FOXP3 (expressed by Tregs) and up-regulates RORγT (expressed by Th17), increased SGK1 activity results in Th17 activation and secretion of IL-17 and IL-23 (

Figure 1.8). A positive feedback loop is established with further IL23-R signalling, further SGK1 activity and enhanced Th17 mediated inflammation. *In vivo*, SGK1 knock out mice demonstrate attenuated Th17 cell responses, increased regulatory T cell activity, and less severe autoimmune disease[78].

Figure 1.8: Regulation of Th17-Treg balance through SGK1 activity under isotonic conditions. Data from[53,78].

SGK1 activation leads to increased Th17 (RORγT) and reduction in Treg (FOXP3).

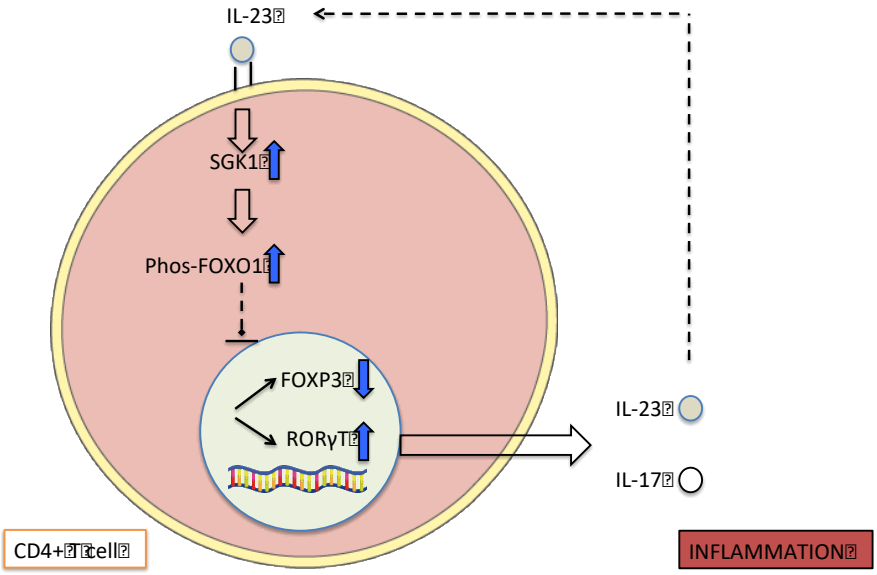

1.3.2.3 Alterations in IL-17 responses and clinical consequences

- *Defects in IL-17 immunity*

Defects in IL-17 immunity result in the clinical syndrome of chronic mucocutaneous candidiasis (CMC), characterised by recurrent or persistent infections affecting the nails, skin and oral or genital mucosae caused by *Candida sp*., often *Candida albicans*[81]. The mucosal nature of fungal infection highlights the importance of IL-17 immunity at epithelial/mucosal surfaces, whereas primary quantitative or qualitative defects in neutrophil function more commonly result in invasive fungal disease. CMC may occur without other clinical features (termed CMC disease), but is more commonly associated with other microbial, in particular with bacterial, infections.

CMC is caused by inherited mutations in components of the pathway of IL-17 production and its subsequent action on target cells. Defects may occur at any point in this pathway (**Figure 1.9**). Specific defects of IL-17 immunity may also be acquired, for example in patients with thymoma (production of neutralizing antibodies to IL-17)[82], and in patients taking anti-IL-17

monoclonal antibodies for the treatment of inflammatory disease (e.g. psoriasis)[83].

Figure 1.9: **Inborn errors of IL-17 immunity.** Figure from[81].

Inherited defects in IL-17 immunity may occur at multiple points along the pathway of IL-17 production and its action on target cells. These include:

- Antigen recognition and presentation by antigen presenting cells (APCs) (CARD9 *deficiency*)
- Secretion of pro-inflammatory cytokines (e.g. IL-6, IL-12, and IL-23) by APCs (*IL-12p40 deficiency*)
- Binding of these polarising cytokines to cytokine receptors on T cells (*IL-12RB1 deficiency*)
- Signalling downstream of cytokine receptors in T cells through a pathway involving STAT1 (*STAT1 gain of function mutation*) and STAT3 (*STAT3 loss of function mutation*)
- Upregulation of the key Th17 transcription factor RORγT (*RORγT deficiency*)
- Production of IL-17A and IL-17F (*IL-17A and F deficiency; neutralizing antibodies to IL-17*)
- IL-17 binding to the IL-17 receptor on target cells (*IL-17RC and IL-17RA deficiency*)
- Signalling downstream of the IL-17 receptor (*ACT1 deficiency*).

Molecular defects leading to CMC syndrome (i.e. additional clinical features) in blue; molecular defects leading to CMC disease (i.e. no additional clinical features) in pink.

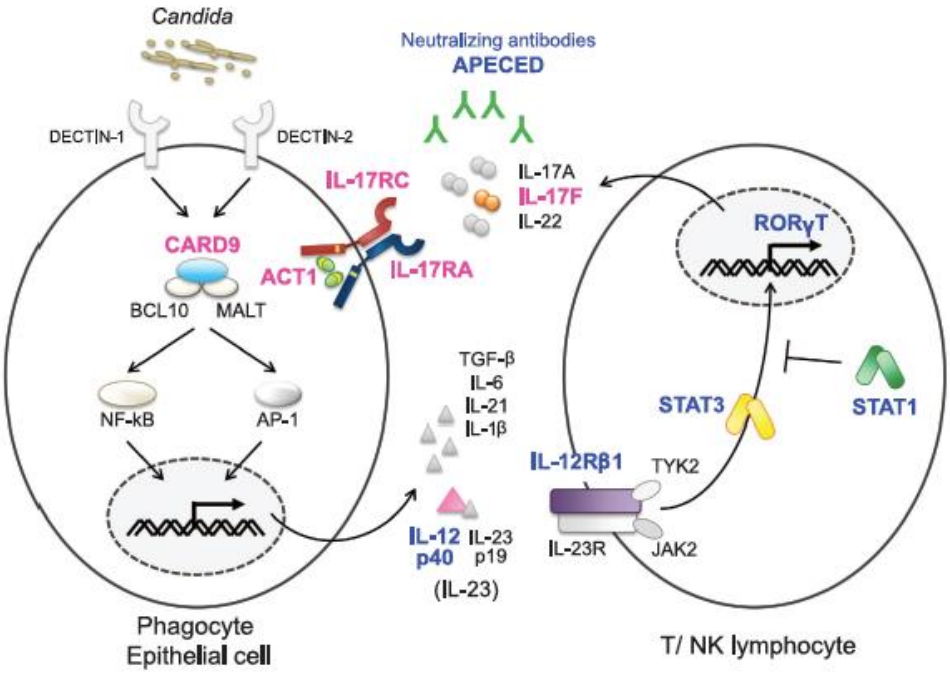

Two important causes of Th17 dysfunction result from loss of function mutations in STAT3, manifesting as Autosomal Dominant HyperIgE syndrome (AD HIES), and gain of function mutations in STAT1. The clinical (immunological) features of cohorts with each of these mutations are summarised in Table 1.2.

AD HIES, originally called Job's syndrome, was first described in the 1960s[84]. It is a primary immunodeficiency characterised by recurrent staphylococcal skin abscesses, pulmonary infections, eczema, mucocutaneous candidiasis, and elevated serum levels of IgE, in addition to a number of musculoskeletal anomalies[85,86]. The molecular cause in most cases is loss of function mutation of STAT3, which is involved in the signalling pathways of a number of cytokines important in the IL-17 response (e.g. IL-6, IL-21, and IL-23). This results in reduced Th17 polarisation, with the resultant increased risk of bacterial and fungal infections described.

STAT1 gain of function mutations have been more recently described as a predominant causes of CMC[87,88]. Mutation results in hyperphosphorylation of STAT1 in response to IFNγ, IFNα, and IL-27 stimulation. These STAT1

transduced cytokines inhibit IL-17 responses *in vivo*, and whilst the precise mechanism how STAT1 hyperphosphorylation leads to impaired Th17 responses remains unclear, it is suggested to be via an increase in this negative feedback loop. In addition to reduced Th17 responses, some patients also have defects in B cells[81]. The clinical phenotype includes increased bacterial and mucocutaneous fungal infections, in addition to autoimmune manifestations in over a third of patients[89]. The presence of autoimmune phenomena and allergic disease in STAT1 and STAT3 mutations suggest a more global dysregulation of the immune system, but the exact mechanisms by which this occurs are unclear.

Table 1.2: Clinical features in cohorts of patients with STAT3 and STAT1 mutation[85,86,89].

Study Reference	**Autosomal Dominant Hyper-IgE Syndrome in the USIDNET Registry.** Gernez et al. J Allergy Clin Immunol Pract 2018.	**Autosomal dominant STAT3 deficiency and hyper-IgE syndrome: molecular, cellular, and clinical features from a French national survey.** Chandesris et al. Medicine (Baltimore) 2012.	**Heterozygous STAT1 gain-of-function mutations underlie an unexpectedly broad clinical phenotype.** Toubiana J et al. Blood 2016.
Location	North America	France	International (62% European)
Genetic cause of chronic mucocutaneous candiasis	STAT3 deficiency (Autosomal Dominant Hyper-IgE Syndrome)	STAT3 deficiency (Autosomal Dominant Hyper-IgE Syndrome)	STAT1 gain-or-function

Number of patients in cohort	85	60	274
Demographics	59% male; 62.4% Caucasian	Mean age 21 (time of study)	M:F ratio 1.03; median age 22 (time of study)
Bacterial Infections			
Any bacterial infection			74%
Abscess	74%	73%	28% (recurrent skin infections including cellulitis, abscess, and paronychia)
Lower Respiratory Tract Infection	72%	90%	47%
Upper respiratory tract infection	48.8% sinusitis; 42.7% otitis; 11.7% tonsillectomy	90%	44%
Urinary Tract Infection	2.4% pyelonephritis		2.9% recurrent pyelonephritis
Other severe bacterial infection	18.2% cellulitis, 7.3% sepsis, 6.1% meningitis, 5.8% lymphadenitis	45% impetigo, pustulosis, and pyodermatitis; 13% sepsis	2.9% severe gastroenteritis, 2.6% sepsis, 6% mycobacterial diseases.
Fungal Infections			
Recurrent oral/vaginal candidiasis	21%	85%	98% chronic mucocutaneous candidiasis (93% oral thrush, glossitis, and/or chelitis; 56% oesophageal/genital)
Fingernail fungal infection	28%		56%
Other fungal infection			10% invasive fungal infections.
Viral Infections			
Any recurrent or severe viral infection	7.4% herpes.		38% at least 1 systemic or atypical viral infection, or recurrent mucocutaneous viral infection
Recurrent VZV			12% shingles and 7% severe chicken-pox
Recurrent HPV			12% moluscum contagiosum or warts
Recurrent HSV		13% HSV	32% recurrent mucocutaneous viral infection HSV or VZV)
Other viral infection			8% severe systemic viral infection
Atopic disease			

Asthma	39%		
Eczema	57%	93%	
Allergic disease			
Any allergic disease	65%		
Contact and environmental allergy (inc wasp stings, dust, dander pollens)	18%		
Food allergy	37%		
Drug allergy	43%		
Angioedema/hives unexplained	8.5% anaphylaxis, 15.9% urticaria		
Other features			
Malignancy	7% malignancy (lymphoma 3, thyroid 1, brain 1, squamous cell carcinoma 1)		
Autoimmune			37% autoimmune manifestation (largely thyroid disease, 22%)

- *Th17 cells in Autoimmune Kidney Disease (AKID)*

Whilst a reduction in Th17 cell activity leads to immunodeficiency, increased Th17 function leads to inflammation, and Th17 cells along with Tregs play a major role in AIKD and kidney transplant rejection. Th17 cells are implicated in the development of both glomerular and tubulointerstitial disease in patients and animal models including ANCA-associated glomerulonephritis (AAV)[90,91], Lupus Nephritis (LN)[92], IgA Nephropathy[93], and Primary Sjögren's Syndrome associated tubulointerstitial nephritis (pSS TIN)[94,95]. Conversely, Treg activity limits inflammatory glomerular disease and autoimmune disease relapses, both clinically and in experimental models[96]. Furthermore, it is becoming increasingly clear that excessive Th17 and reduced Treg activity are important components in the development of acute and chronic allograft rejection[97]. Hence, excess Th17 activation and reduced Treg activity underlie a number of inflammatory kidney diseases in both the native and transplant setting. This augmented-Th17 and attenuated-Treg phenomenon is the same effect that salt has on these CD4+ T cell subtypes, as described below.

Figure 1.10: **Summary of inflammatory kidney diseases associated with imbalance in Th17 and Treg cells**

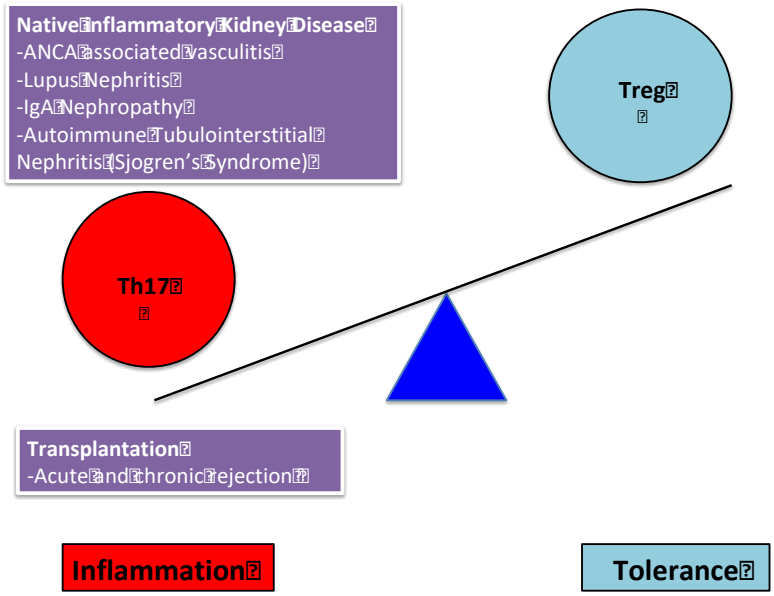

To mediate organ specific autoimmune disease, such as that affecting the kidney, Th17 cells must migrate to sites of inflammation. This process is controlled by chemokines and their receptors, in the case of Th17 through CCR6 expression on Th17 interacting with CCL20, up-regulated by mesangial cells and tubular epithelial cells in response to IL17 signalling[98]. Renal injury mediated by Th17 cells is dependent on CCR6 in animal models of immune-mediated glomerulonephritis[99]. IL-17 also promotes glomerular cells to express CXCL5, which further recruits Th17 cells and neutrophils to the kidney via interaction with CCR6 and CXCR2 respectively[98].

Th17 cells are found most abundantly in the gut under physiological conditions. A recent study demonstrated that in experimental crescentic glomerulonephritis, gut-derived Th17 cells traffic to the kidney to mediate injury[100]. Migration of Th17 cells from the gut was dependent on sphingolipid sphingosine-1-phosphate (S1P), and subsequent infiltration into the kidney was dependent, as above, on the chemokine CCL20. Furthermore, it was shown that gut bacteria could influence this process. Germ-free mice or

treatment with oral antibiotics ameliorated renal inflammation, whereas expansion of gut Th17 cells occurred in response to citrobacter infection, and renal pathology was exacerbated. Hence, gut-derived Th17 cells may mediate inflammatory kidney disease, and intestinal constituents such as the gut microbiome may influence Th17 behaviour. Using dietary modification (e.g. salt) to modulate intestinal Th17 cells may therefore offer a potentially novel adjunctive therapeutic strategy in inflammatory kidney disease.

- *Unmet clinical need in inflammatory kidney disease*

Together autoimmune kidney diseases are an important cause of CKD, particularly in young patients, and a proportion of these patients will progress to ESKD. Inflammatory glomerular disease, for example, is the cause of 14% of ESKD across all age groups in the UK, whereas it is the cause of 30% of cases in patients aged 18-35 years[101]. ESKD brings with it significant morbidity and mortality but much of this can be mitigated with renal transplantation, which offers the best outcomes.

Short-term outcomes in AIKD and renal transplantation have improved significantly over the last decade; however, longer-term outcomes have not improved to the same extent[102,103]. Relapse of lupus nephritis occurs in up to 66% of cases[104], 14% of patients with ANCA vasculitis still reach ESKD within 7 years[105], and immune mediated mechanisms remain the commonest cause of cause of renal allograft loss[106]. Moreover, much of the morbidity and mortality in AIKD and ESKD treated with transplantation are the result of adverse effects and consequences of immunosuppressive therapy, as opposed to the diseases themselves. Infection and malignancy caused 24% and 22% of deaths respectively, in patients with renal transplants in the UK in 2015[107]. There is therefore an urgent need to develop new management strategies in auto- and allo-immune settings, that maintain disease remission, but that are associated with fewer long-term side effects associated with immunosuppressive drugs.

1.3.2.4 Initial evidence of an effect of salt on Th17 cells

Two studies published in Nature in 2013 provided the initial evidence of an effect of salt on Th17 polarisation[52,53]. Kleinewietfeld et al isolated naïve CD4+ T cells from healthy volunteers, and cultured these for 7 days in optimal Th17 polarising conditions in standard media and in media supplemented with varying concentrations of NaCl (0-80mM). There was a dose dependent increase in Th17 polarisation with salt up to 40mM NaCl, which provided optimal polarisation and cell survival. The authors concluded on the basis of control experiments in which media was supplemented with sodium gluconate, magnesium chloride, or mannitol, that sodium, as opposed to chloride or tonicity, was mediating this pro-inflammatory effect. Further *in vitro* work showed that salt stimulation affected naïve, rather than memory CD4+ T cells, and did not influence Th1 and Th2 polarisation. A more recent study has contradicted these data, demonstrating salt affects both naïve and memory T cell populations, and may promote Th2 responses leading to exacerbated allergic disease[59]. The addition of NaCl in the original Th17 work not only polarised Th17 cells but also promoted a pathogenic Th17 phenotype with increased expression of IL-2, TNF-α, IL-9, and CSF2/GM-CSF. It was subsequently shown that the intracellular pathway mediating this response to hypersalinity involved up-regulation of phosphorylated p38-MAPK, NFAT5, and serum- and glucocorticoid-inducible kinase 1 (SGK1) (

Figure 1.11). Knocking down any of these molecules resulted in a sharp reduction in salt mediated Th17 polarisation. The authors then investigated the salt effect on Th17 cells *in vivo*, in an animal model of multiple sclerosis (experimental autoimmune encephalitis; EAE), a Th17-mediated disease. A high salt diet exacerbated disease severity, and this was associated with

increased Th17 cells in the central nervous system (CNS). The use of a p38-MAPK inhibitor abrogated both salt-induced Th17 CNS infiltration, and clinical markers of disease severity.

Wu et al focused further on the role of SGK1 in salt mediated Th17 polarisation. They described the pathway downstream of SGK1, which involves phosphorylation of FOXO1 and upregulation of the main Th17 transcription factor, RAR-related orphan receptor gamma T (RORγT; Figure 1.11). They also confirmed the polarising effect of salt on Th17 cells *in vitro*, and demonstrated this Th17 polarisation was prevented in SGK1-deficient cells. They showed that a high salt diet in mice is associated with increased gut Th17 cell frequency, confirmed that a high salt diet exacerbates EAE, and showed that this was prevented in SGK1 knock out mice. Since this initial work, the same group has demonstrated a pivotal role of SGK1 in mediating the balance between Th17 and Treg in isotonic conditions, as described[78]. Taken together, these initial studies demonstrate that Th17 cell polarisation is enhanced by high salt conditions both *in vitro* and *in vivo*, that this is dependent on signalling through p38-MAPK, NFAT5 and SGK1, and that salt mediated Th17 polarisation exacerbates animal models of extra-renal autoimmune disease.

Figure 1.11: Intracellular pathways involved in salt induced Th17 polarisation. Data from[52,53].

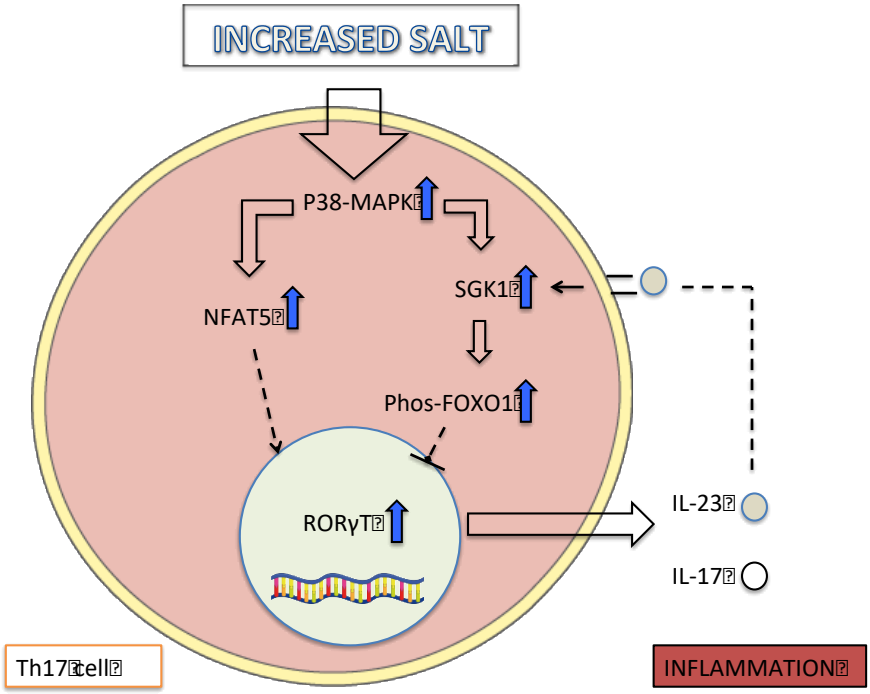

1.3.2.5 The effect of salt on suppressor Treg function and transplant rejection

Given the interrelationship between Th17 cells and Tregs, and the effect of salt on Th17 polarisation, subsequent work investigated whether there was an effect of salt on Treg function, firstly *in vitro*, and then in mouse models of graft versus host disease (GVHD), colitis, and mismatched cardiac transplantation[57,58]. Hernandez et al demonstrated that addition of salt to co-culture of Tregs with effector T cells inhibited regulatory cell function in a dose dependent manner over the range 10-40mM NaCl[57]. Further analysis of purified Tregs cultured under high salt conditions demonstrated that the mechanism of this loss of suppressor function was Treg shift to a Th1 phenotype with up-regulation of pro-inflammatory molecules such as IFN-γ; knock-down of IFN-γ resulted in maintenance of suppressor function. The

authors demonstrated that the same pathway, increased SGK1 activity and phosphorylation of FOXO1 and FOXO3, that is involved in Th17-Treg balance in isotonic conditions, and in the polarisation of Th17 in hypertonic conditions, also mediates the salt effect on Tregs. Inhibition or knock down of SGK1 resulted in recovery of suppressor function; high salt conditions increased phosphorylation of FOXO1 and FOXO3, which resulted in impaired stabilization of the FOXP3 locus. This inhibitory effect of salt on Tregs was then confirmed *in vivo*. A high salt diet was associated with increased IFN-γ secreting Tregs in the spleen and mesenteric lymph nodes, and this was associated with increased SGK1 expression. Moreover, a high salt diet increased IFN-γ secreting Tregs and worsened disease in a mouse model of GVHD, while transfer of Tregs cultured under high salt, as opposed to standard conditions, led to exacerbation of disease in an animal model of colitis[57].

Safa et al investigated the effect of high salt on the allo-immune response, using a mouse model of MHC-II mismatched cardiac transplantation, which is dependent on Treg suppressor function for graft survival[58]. Despite having no effect on blood pressure, a high salt diet reduced allograft survival, and this was associated with a reduction in Tregs within the transplant and the spleen. This high salt effect on rejection was abolished in SGK1 knock out mice. Together, these initial studies demonstrate an inhibitory effect of salt on Treg suppressor function, which is mediated through an SGK1-FOXO1/3 pathway. High salt exacerbates animal models of autoimmune disease and worsens murine transplant rejection.

1.3.2.6 The effect of salt on the development of autoimmune diseases

Subsequent studies have investigated further aspects of the effect of salt on immunity in models of multiple sclerosis (EAE), colitis, lupus nephritis, and also in the setting of the progression of acute kidney injury (AKI) to chronic

kidney disease (CKD). The results of this work, and the effects of salt on the immune cells involved, are summarised below.

- *Animal models of multiple sclerosis*

Wilck et al proposed an alternative indirect *in vivo* mechanism by which a high salt affects Th17 cells and the development of EAE[108]. This was through alteration in the gut microbiome, and provides a link to studies which demonstrate gut derived Th17 cells traffic to, and mediate the development of extra-intestinal disease, including inflammatory kidney disease[100]. Salt loading inhibited the growth of lactobacillus sp. *in vitro*, in mice and in healthy human volunteers. In an EAE model, lactobacillus administration ameliorated Th17 CNS infiltration and the development of disease. The mechanism of the effect on Th17 polarisation was proposed to be due to reduced bacterial production of indole derivatives, which have previously been shown to associate with improvement in EAE. Hence, multiple extracellular cues may affect Th17 polarisation, and several pathways may mediate the pro-inflammatory salt effect *in vivo*.

Jorg et al investigated whether alteration of dendritic cell function occurred in response to salt and mediated the *in vitro* effects of salt on Th17 and the development of EAE[109]. They found no effect on dendritic cell function, suggesting the salt effect on Th17 is a direct effect on Th17 cells themselves. By contrast, Barbaro et al demonstrated that high salt conditions increased both macrophage and dendritic cell activation directly, and that co-culture of salt activated dendritic cells with T cells from salt sensitive mice led to increased pro-inflammatory cytokine production (IL-17 and IFN-γ) from CD4+ and CD8+ cells[49]. The intracellular pathway mediating this effect involved sodium entry in to dendritic cells through amiloride sensitive sodium channels, formation of reactive oxygen species, and the production of isolevuglandin protein adducts, with ultimately enhanced antigen presentation to T cells. A subsequent study demonstrated that this increase in dendritic cell isolevuglandins may also be mediated by a high-salt driven alteration in the

gut microbiome, resulting in not only gut inflammation, but also the development of hypertension[50].

- *Animal models of inflammatory bowel disease*

Several studies have investigated the role of salt on intestinal immunity and the development of colitis, perhaps unsurprising given the abundance of Th17 cells within the gut[51,56,57]. In these studies, salt loading of mice without disease results in increased gut Th17 cells and reduced Treg suppressor function. This is associated with increased SGK1 expression, increased gut permeability and histological features of inflammation. High salt has also been shown to worsen mouse models of inflammatory bowel disease, associated with increased gut IL-17. One study investigated the source of this IL-17 and demonstrated that salt not only affects CD4+ T cells, but also innate lymphoid cells (ILCs), in particular ILC3, the innate lymphoid equivalent of Th17 cells[51]. Indeed, RAG knock out (i.e. lymphocyte deplete) mice still get IL-17 mediated gut inflammation in response to a high salt diet, highlighting that salt promotes IL-17 production from multiple immune cells.

- *Animal models of Systemic Lupus Erythematosus (SLE)*

Elevated salt concentrations *in vitro* have been shown to increase follicular helper T cell (TfH) polarisation, and a high salt diet worsens lupus features in an animal model[60]. A further study demonstrated that a high salt diet leads to exacerbated experimental lupus nephritis, with more significant disease on histology, increased proteinuria and worse survival[54]. This was associated with increased Th17 and Th1 cells in the spleen, and reduced splenic Tregs. The salt response of isolated CD4+ T cells from patients with SLE was then analysed; Th17 cell polarisation increased with anti-CD3 and anti-CD28 stimulation in the presence of NaCl. This, as in healthy volunteers, was abrogated by the addition of an SGK1 inhibitor. Of note, high salt conditions do not promote increased polarisation of naïve T cells to Th1 cells *in vitro*, under Th1 polarising conditions[110], but this and other studies have shown a

high salt diet does promote a Th1 phenotype *in vivo*[54,110]. This may reflect CD4+ T cell plasticity, with Th17 cells or Tregs developing a pro-inflammatory Th1 phenotype with expression of IFN-γ in response to high salt conditions.

TfH cells are integral to the generation of antibody responses in B cells, but whether salt affects antibody production indirectly through this mechanism has not been studied. A direct effect of salt, however, on B cells *in vitro* was recently demonstrated[61]. Salt produced a biphasic response in B cells with an early enhancement of differentiation into antibody secreting plasma cells, which was followed by an increase in cell death and impaired plasmablast differentiation. Whilst NFAT5 was upregulated, in contrast to the effects on other cell types, increased NaCl reduced signalling via p38-MAPK, demonstrating the context and cell specific dependency of salt and its signalling pathways within the immune system.

- *Animal models of acute kidney injury*

Acute Kidney Injury (AKI), particularly if recurrent, can lead to CKD, and high salt has been shown to increase the progression of AKI to CKD in animal models[111]. The mechanism behind this phenomenon is unclear, but has been proposed to be immune mediated as immunosuppression with mycophenolate mofetil abrogates the salt effect. More recent work has demonstrated that Th17 cells mediate interstitial inflammation in AKI; salt loading worsened Th17 mediated inflammation and this resulted in more significant CKD[55]. This was prevented by angiotensin receptor blockade, which was shown *in vitro* to directly affect Th17 cells. Receptors for multiple components of the RAAS system are expressed on immune cells, and alterations in RAAS components may themselves directly lead to altered immunity, independently of any effect on sodium balance[112].

1.3.3 Human studies of dietary salt modification and its effect on immunity

Given the growing body of laboratory and animal work that have demonstrated a polarising effect of salt on diverse immune cells (**Table 1.1**), using dietary modifications to limit salt intake in the management of patients with autoimmune disease provides an intriguing and potentially beneficial, low-cost, therapeutic avenue. Initial interventional studies have investigated the effect of changing salt intake on the immune response, in healthy volunteers and in patients with autoimmune disease. The results of these studies are outlined in
Table 1.3. Together, these demonstrate dietary salt modification may be used to modulate the immune response to varying degrees, but whether this translates to changes in clinical outcomes, is yet to be determined. Moreover, all studies to date have assessed the effect of changing salt intake within a range above the WHO recommended 5g/day, and the effect of reducing salt to below this level in terms of its effect on immunity or the development of inflammatory disease is unknown.

Table 1.3: **Summary of studies investigating the immunological effects of dietary salt modification in healthy human volunteers and in patients with autoimmune disease.**

Study Reference	Subjects included	Dietary Modification	Main results
Zhou et al, 2013[47]	Healthy volunteers (n=20)	3-day run in on normal diet, then fixed daily salt intake of 15g (high salt) for 7 days, then 5g (low salt) for 7 days. Food provided to subjects.	Increase in CD14++CD16+ (intermediate) monocytes; decrease in CD14++CD16- (classical) and CD14+CD16++ (non-classical) monocytes with high salt intake.
Yi et al, 2015[113] *(part of Mars flight simulation study)*	Healthy volunteers (n=6)	Fixed daily salt intake of 12g, 9g, then 6g for 1-2 months, then reverted back to 12g for 1 month. Food provided to subjects.	Serum cytokines analyzed after each intervention period: increased pro-inflammatory cytokines (IL-6 and IL-23) and reduced anti-inflammatory cytokines (IL-10) with high salt intake
Luo et al, 2016[114]	Healthy volunteers (n=15)	3-day run in on normal diet, then fixed daily salt intake of 15g (high salt) for 7 days, then 5g (low salt) for 7 days. Food provided to subjects.	T cell subset analysis: increased Th17 and reduced Treg populations with high salt intake. Associated with increased expression of NFAT5 and SGK1.
Wen et al, 2016[115]	Healthy volunteers (n=49)	Fixed daily salt intake of 3g (low salt) for 7 days, then 7 days high salt (18g), then 7 days high salt (18g) plus potassium supplementation (4.5g KCl; 60mmol K)	Serum IL17 and PBMC IL17 mRNA increased with high salt. Associated with increased SGK1. High salt effect abolished with potassium supplementation of diet.
Scrivo et al, 2017[116]	Patients with	Dietary counseling used to limit daily salt intake to 5g for	RA patients: no effect in Th17 or Treg subsets. SLE

	rheumatoid arthritis (RA; n=15) and SLE (n=15)	3 weeks. Then reverted back to standard diet for 2 weeks. 24-hour urine Na measurement used to assess adherence to diet.	patients: increase in Treg after salt restriction; no effect on Th17 cells

1.4 Renal sodium handling and salt losing tubulopathy

When animals evolved to live on land as opposed to in the sea, a system had to be developed to recreate the extracellular saline environment that our cells had become accustomed to. Moreover, mammals subsequently needed a method to maintain plasma volume even when salt and water intake were limited. Hence, one of the most crucial homeostatic functions of the kidney is maintenance of salt and water balance. 'Intelligent design' may have not created the system by which the kidney handles salt and water[117]. Glomerular filtration of greater than 120mls/minute, which allows excretion of toxins in tiny concentrations in the extracellular space, means 150L of water and greater than half a kilogram of sodium are filtered from the plasma each day. The kidney must then reabsorb this salt and water, with fine adjustments made according to needs.

Sodium reabsorption occurs in almost all segments of the nephron, and is dependent on the energy dependent active transport of sodium via the sodium-potassium ATPase in the basolateral membrane of renal epithelial cells which creates the electrochemical gradient for sodium reabsorption and the passive reabsorption of water[118]. The energy requirements for this process and the lack of tubular anaerobic capacity make the proximal tubule highly susceptible to ischemic injury. The majority of sodium is reabsorbed proximally, with fine-tuning occurring in more distal segments. Because most tubular cells are involved in sodium reabsorption and because sodium transport is often linked directly or indirectly to the transport of other solutes, defects in sodium reabsorption lead to major alterations in other homeostatic functions of the kidney, such as other electrolyte and acid-base balance, and control of total body water. Inherited defects in sodium transport are mostly

due to mutations of channels and transporters involved in sodium reabsorption, termed *salt losing tubulopathies (SLTs)*. The clinical phenotype of these patients is dependent on the specific segment of the nephron affected. SLT syndromes collectively describe a number of different mutations that lead to defective transport in a specific segment (**Figure 1.12**). In the following sections, sodium transport mechanisms and inherited defects of these processes in different segments of the nephron are described, with a particular focus on Bartter and Gitelman Syndromes.

Figure 1.12: **Sodium transport in nephron segments and associated salt losing tubulopathy syndromes.** Figure from[117]

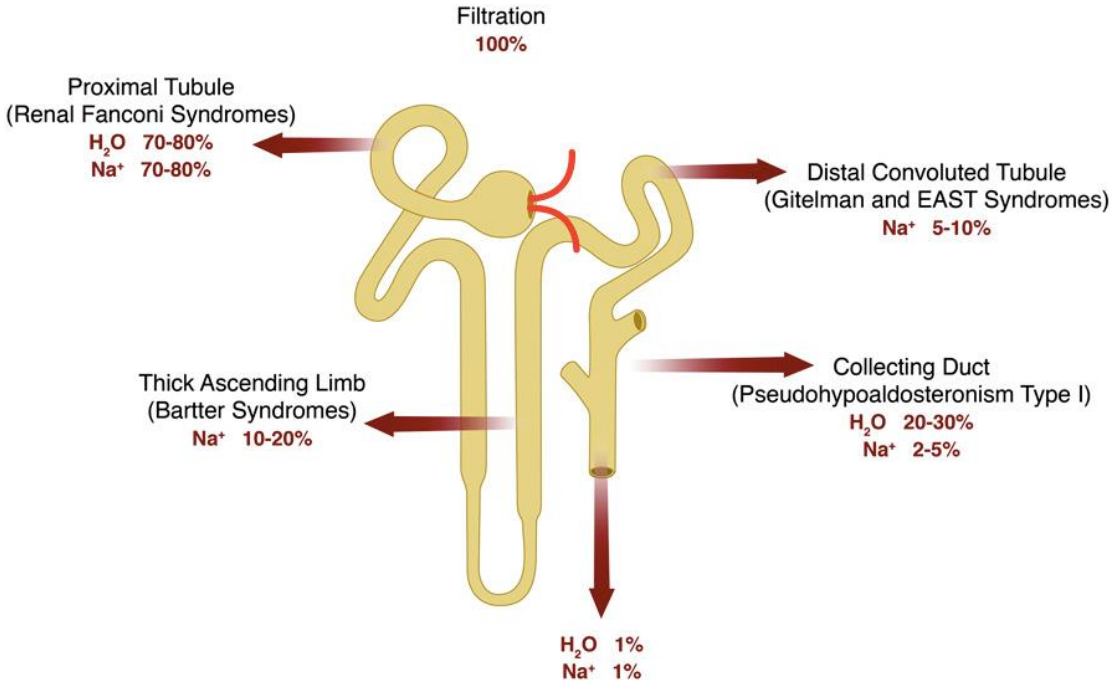

1.4.1 Proximal tubule sodium transport and renal Fanconi syndromes

The proximal tubule (PT) acts as the workhorse of the nephron with approximately 70% of filtered sodium being reabsorbed here. Reabsorption is isotonic (i.e. occurring at the same rate as water) and the filtrate sodium concentration remains constant along the length of this segment. Sodium reabsorption is directly related to the rate of filtration (glomerulotubular

balance) such that sodium and water losses are prevented with increased filtration rates[118].

The Na-K ATPase creates an electrochemical gradient for the luminal transport of sodium by a variety of transcellular and paracellular mechanisms (

Figure 1.13). The predominant mechanism is via sodium-hydrogen exchange (NHE3), which links sodium reabsorption to acid-base balance. In addition, sodium may be transported linked to a number of other solutes (Na-X) such as glucose, phosphate, amino acids, and lactate, and wasting of these solutes alongside sodium characterise the renal Fanconi syndrome. Sodium reabsorption also occurs paracellularly through claudins in the PT[117].

Figure 1.13: Sodium transport mechanisms in the proximal convoluted tubule. Figure from[117].

Na-K ATPase generates the electrochemical gradient for transcellular sodium reabsorption via NHE3 and Na-X cotransporters (X = other solutes such as phosphate, amino acids, glucose). Paracellular reabsorption through claudin channels (e.g. Claudin 2) also occurs.

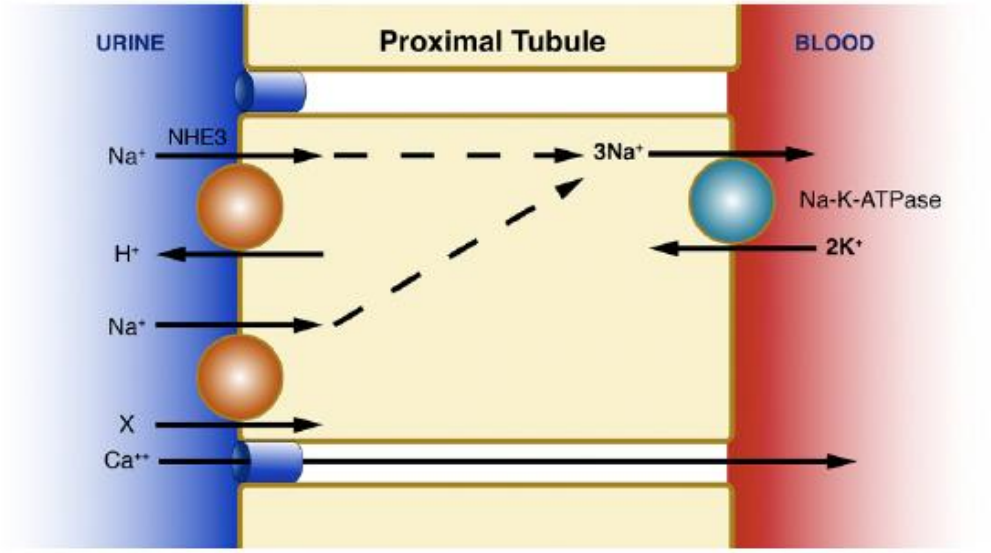

Reabsorption in PT is particularly energy intensive making it especially susceptible to defects that result in impaired energy supply. Most commonly

this is acquired due to drugs or heavy metals affecting mitochondrial function (e.g. tenofovir for HIV; fumarate esters for psoriasis; lead exposure) but may also be inherited due to genes involved in mitochondrial fatty acid oxidation (e.g. EHHADH, renal Fanconi syndrome type 3)[119], or through a specific mutation in the transcription factor HNF4a (renal Fanconi syndrome type 4, associated with maturity onset diabetes type 1[120,121]). The phenotype of diffuse proximal tubule dysfunction, described originally by Guido Fanconi, includes renal salt wasting and the consequences of defective solute transport linked to sodium reabsorption in this segment, i.e. proximal tubular acidosis, phosphaturia with or without hypophosphataemia and osteomalacia, aminoaciduria, uricosuria, and glycosuria.

1.4.2 Thick ascending limb sodium transport and Bartter Syndrome

The thick ascending limb (TAL) of the loop of Henle accounts for around 20% of total sodium reabsorption. Sodium uptake in the TAL is predominantly through the furosemide sensitive sodium-potassium-chloride (NKCC2) transporter; NHE3 also contributes (

Figure 1.14). Defects in sodium transport within this segment of the nephron, which can be due to mutations in a number of genes, leads to Bartter syndrome (BS) (Table 1.4). As in other tubular cells, the Na-K ATPase provides the electrochemical gradient for sodium uptake. Transport of sodium in the TAL through NKCC2 is electroneutral, with one sodium being accompanied by one potassium and two chloride ions. All four ions must be bound to the luminal surface of NKCC2 for sodium uptake and given its lower luminal concentration potassium binding becomes the rate-limiting step. To ensure sufficient luminal potassium for sodium reabsorption, it is recycled back from inside the cell to the tubular lumen through the potassium channel ROMK. Mutations in SLC12A1 encoding NKCC2, and KCNJ1 encoding ROMK, leads to BS types 1 and 2 respectively. The recycling of potassium creates a positive luminal charge, which drives the paracellular uptake of calcium and magnesium (and sodium) through claudins 16 and 19. A reduction in this process is the cause of calcium and magnesium wasting in BS and the subsequent development of nephrocalcinosis, which may contribute to the development of renal failure in some BS patients.

Basolateral chloride exit is mediated by chloride channels, CLC-Kb and CLC-Ka. CLCNKB mutations, which encode CLC-Kb, cause BS type 3. CLC-Kb is also expressed in the distal convoluted tubule (DCT) and hence the clinical phenotype of BS type 3 is heterogenous with overlapping clinical features (mixed loop and DCT phenotype) with patients with Gitelman syndrome (GS)[122]. There is likely some redundancy to chloride exit by each of these channels, as the severity of the disease is often reduced compared to patients with other forms of BS. Inactivation of both CLC-Ka and CLC-Kb chloride channels cause BS type 4. This can occur either through defects in Barttin, encoded by BSND (BS type 4a), which is an essential subunit of both channels, or through other mutations in all 4 alleles of both of the channels (BS type 4b). These chloride channels are also expressed in the middle ear and loss of both of their function leads to the sensorineural hearing loss associated with BS type 4.

Figure 1.14: Sodium transport mechanisms in the thick ascending limb of the loop of Henle. Figure from[117].

Na-K ATPase creates the electrochemical gradient for sodium uptake along with potassium and chloride via NKCC2. Potassium is recycled via ROMK to ensure persistent potassium supply for NKCC2. Potassium recycling creates a luminal positive charge favouring paracellular magnesium and calcium reabsorption. Basolateral chloride exit is via CLC-Kb and CLC-Ka.

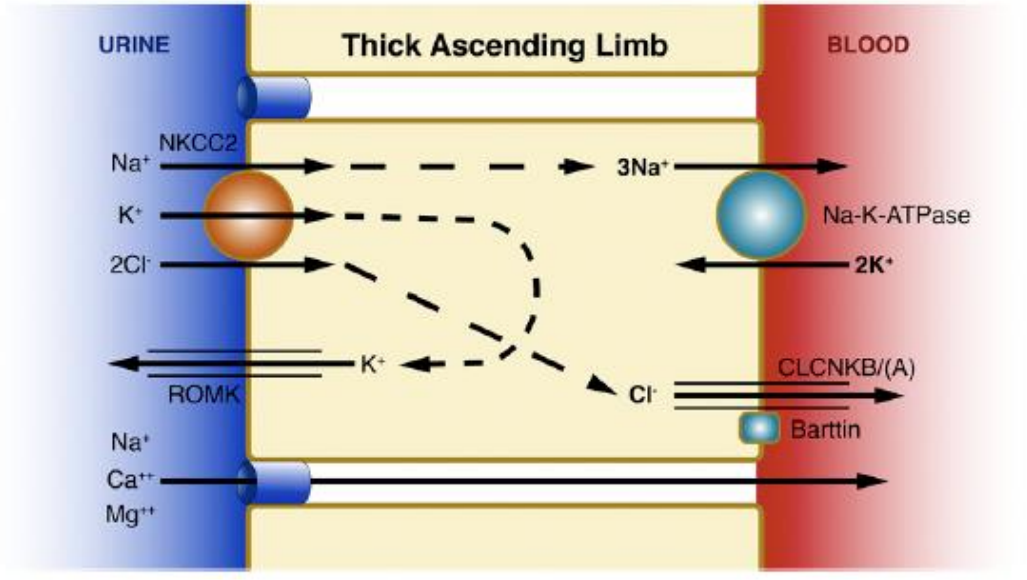

Rare other causes of BS include activating mutations of the calcium sensing receptor (CaSR; leading to autosomal dominant hypocalcaemia), which as well as being expressed in the parathyroid gland is also expressed on the basolateral surface of the TAL tubular cell (hypercalcaemia reduces TAL solute transport leading to increased urinary calcium excretion). Persistent activation leads to marked hypocalcaemia, largely due to its parathyroid effects, but also to salt wasting in the TAL. X-linked mutations in MAGED2 lead to a transient BS in the perinatal period due to defects in a protein important in the regulation of TAL reabsorption at this stage, but not later in life. Both CaSR and MAGED2 mutations have been referred to as BS type 5 so to avoid confusion the term BS type 5 is best avoided. Similarly, due to their earlier onset, BS types 1,2 and 4 were previously referred to as 'antenatal BS' with BS type 3 termed 'classical BS'. Due to the phenotypic overlap across BS and SLT more generally, again theses terms are best avoided[123].

A clinical feature unique to BS in some patients is the loss of tubuloglomerular feedback. The macula densa (MD) consists of 15-20 renal tubular cells at the end of TAL which act as a sodium, and hence, plasma volume, sensors within the kidney. These cells are anatomically adjacent to the feeding glomerulus forming a region called the juxtaglomerular apparatus. MD cells communicate to the glomerulus to alter glomerular filtration, dependent on sodium reaching this segment. Reduced sodium delivery results in increased renin production and afferent arteriole vasodilation, which maintains filtration rate. This autoregulatory process thereby maintains GFR even when systemic blood pressure is reduced. The cellular processes involved include NaCl uptake in to the MD cells in the same way as elsewhere in the TAL, through a process involving NKCC2. Reduced NaCl uptake increases COX2 activity, which subsequently increases PGE2, in turn leading to increased renin production by juxtaglomerular cells and activation of the RAAS to maintain filtration rate[124]. In BS, especially BS type 1 and 2, this regulatory process linking sodium delivery and glomerular filtration becomes uncoupled; the same thing happens with furosemide use. Due to impaired NaCl uptake through NKCC2, MD cells are 'tricked' in to thinking sodium delivery is low, resulting in

persistent PGE2 and renin release. This compounds the activation of the RAAS seen as a result of relative hypovolaemia in SLT more generally. Therapeutically, COX2 inhibition (e.g. with NSAID, or COX-2 inhibitor) may be used to prevent this process with the aim of reducing PGE2 levels. Whilst this should theoretically only benefit patients with BS, some effect in GS may also be seen, although is not recommended[125]. Of note, PGE2 itself has been shown to affect a wide range of immune cells, but whether this is relevant in patients with BS is unknown[126].

BS patients also often have a defect in urinary concentrating capability. The primary role of the loop of Henle is the development of a hypertonic interstitium, which allows subsequent reabsorption of water driven by anti-diuretic hormone (ADH) acting on aquaporin channels in the collecting duct dependent on requirement. Hypertonicity may also impact on resident immune cells and protect from infection, as described above. Defects in sodium reabsorption in the loop therefore mean that despite maximal ADH production, urinary concentration is suboptimal, resulting in a form of secondary nephrogenic diabetes insipidus. This can lead to high normal serum sodium levels, a concept that seems somewhat paradoxical without an understanding of this physiology in 'salt losing' tubulopathy.

Table 1.4: Inherited salt losing tubulopathies causing defective sodium reabsorption in the loop of Henle and distal convoluted tubule

AR – autosomal recessive; EAST – epilepsy, ataxia, sensorineural deafness, tubulopathy

Disorder	Gene	Inheritance	Gene product	Extra renal features
Defective thick ascending limb sodium reabsorption				
Bartter Syndrome Type 1	SLC12A1	AR	NKCC2	
Bartter Syndrome Type 2	KCNJ1	AR	ROMK	
Bartter Syndrome	CLCKNB	AR	CLC-Kb	

Type 3				
Bartter Syndrome Type 4a	BSND	AR	Barttin	Sensorineural deafness
Bartter Syndrome Type 4b	CLCKNA and CLCKNB	AR	CLC-Ka and CLC-Kb	Sensorineural deafness
Defective distal convoluted tubule sodium reabsorption				
Gitelman Syndrome	SLC12A3	AR	NCC	
EAST Syndrome	KCNJ10	AR	Kir4.1	Epilepsy, ataxia, sensorineural deafness

1.4.3 Distal convoluted tubule sodium transport and Gitelman syndrome

Only around 5-10% of sodium is reabsorbed in the DCT, but given the large amount of filtered sodium, defects in reabsorption here still lead to significant salt wasting. Reabsorption, driven by the Na-K ATPase, is via the electroneutral sodium chloride cotransporter (NCC) encoded by SLC12A3 (

Figure 1.15). Inactivating mutations in NCC cause GS. As in the TAL, chloride exit is via the chloride channel CLC-Kb, explaining the overlapping phenotype of BS type 3 as described above. Like BS, GS is associated with magnesium wasting but in GS this is due to downregulation of the magnesium channel TRPM6 in the DCT. In contrast to BS, GS patients have *hypo*calciuria, thought to be due to an increase in calcium reabsorption proximally, itself a consequence of an adaptive process to increase sodium reabsorption in this part of the tubule[127]. Chronic hypomagnesaemia can lead to condrocalcinosis and arthritis, due to reduced solubility of calcium pyrophosphate in the bones and joints. Renal impairment is less frequently seen in GS than BS, but can occur[128].

Figure 1.15: Sodium transport mechanisms in the distal convoluted tubule. Figure from[117].

Sodium is transported via NCC along a sodium gradient created by the Na-K ATPase. Chloride exit is via CLC-Kb, akin to the TAL. Potassium is recycled on the basolateral membrane by Kir4.1 (encoded by KCNJ10), which acts as a potassium sensor in the part of the nephron. Mutations in NCC cause Gitelman syndrome; mutations in KCNJ10 cause EAST syndrome.

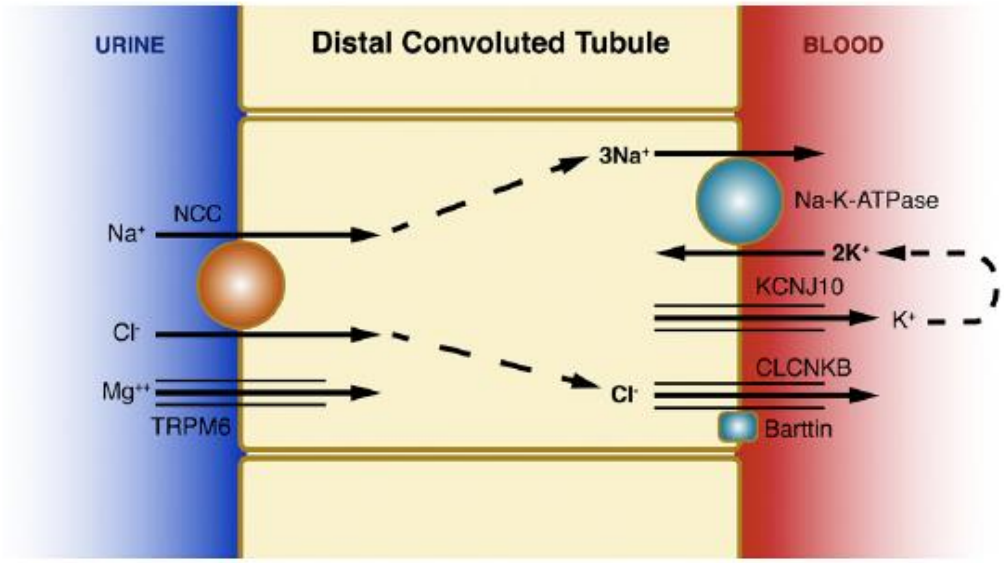

Interest has more recently also focused on the basolateral potassium channel Kir4.1, encoded by KCNJ10. This channel recycles potassium to permit persistent activity of the Na-K ATPase. Mutations in KCNJ10 lead to EAST syndrome (Epilepsy, Ataxia, Sensorineural deafness, and tubulopathy)[129]. The salt wasting phenotype in this condition is identical to GS; expression of this channel in the brain, ear, and eye explain its extra renal features. This channel has also, though, been shown to be an important potassium sensor in the kidney, and links potassium intake to sodium balance[130,131]. Hypokalaemia hyperpolarises the basolateral membrane in the DCT, which favours chloride exit via CLC-Kb. Reduced intracellular chloride activates WNK-SPAK signalling to increase phosphorylation and therefore activity of NCC (mutations resulting in constitutively active WNK signalling cause Gordon's syndrome). The reverse happens in hyperkalaemia, with reduced activity of NCC, and in doing so the kidney shifts sodium reabsorption more distally to the cortical collecting duct, where sodium is exchanged for potassium, through the mechanisms described below. Hence, hypokalaemia is associated with sodium reabsorption in the DCT whilst increased blood

potassium levels favour natiuresis. Increased potassium intake has been shown to be beneficial and the WHO recommends not only restricting sodium intake, but also that potassium and sodium intake should be at least in the ratio of 1:1. A recent community based study in which potassium chloride was substituted for sodium chloride demonstrated a beneficial blood pressure effect[132].

This highlights the potential complexities of dietary intervention studies in clinical practice. Unlike the space flight experiments conducted to determine sodium balance, where all electrolytes aside from sodium were precisely controlled, in 'real-life' dietary interventions such control is not possible and increases and decreases aimed at a particular solute may in turn impact alternative dietary components, making cause and effect difficult to determine.

1.4.4 Further clinical considerations in Bartter and Gitelman syndromes

Bartter and Gitelman syndromes, both originally described in the 1960s[133,134], are the commonest salt losing tubulopathies. As outlined above, they are due to autosomal recessive defects in sodium reabsorption in the loop, and distal convoluted tubule respectively; they are akin to being on a loop and a thiazide diuretic. They share many of the same characteristic biochemical abnormalities including renal salt wasting (elevated fractional excretion of chloride), activation of RAAS leading to a hypokalaemic metabolic alkalosis with evidence of renal potassium wasting (increased fractional excretion of potassium), in addition to low or normal blood pressure in the majority, but not all, patients[128]. In both syndromes, patients may be hypomagnesaemic (with evidence of renal magnesium wasting), whilst hypercalciuria (with or without nephrocalcinosis) is a feature of loop dysfunction. Renal failure is more common in BS, but does occur in GS for unknown reasons[128].

Clinical presentation is *in utero*, perinatally, or during infancy for severe forms of BS. BS type 3 and GS may present later in life. As mentioned, there is significant phenotypic overlap. Patients may be asymptomatic, and be

diagnosed after workup of the discovery of biochemical abnormalities on bloods undertaken for other reasons; otherwise they may present with one of a number of relatively non-specific symptoms, which may be disabling (Table 1.5). The mechanisms by which these symptoms develop are somewhat unexplained. Whilst often attributed directly to electrolyte imbalance, there is no correlation observed between symptoms and electrolyte abnormalities, and symptoms may persist even when electrolytes have been normalised[117]. More recently, novel manifestations of GS have been described such as an increased susceptibility to diabetes[135]. Of note febrile episodes during childhood and a link to autoimmunity in GS have been suggested, but are as yet unexplained[125,136]. A direct impact on the immune system has not been described in either syndrome.

Table 1.5: Clinical manifestations of Gitelman Syndrome. Table adapted from[125].

Most common (>50% patients)	Prominent (20-50% patients)	Occasional (<20%)	Rare
Salt craving	Fainting	Failure to thrive	Seizure
Cramps, muscle weakness	Polyuria	Growth retardation	Ventricular tachycardia
Fatigue	Arthralgia	Pubertal delay	Rhabdomyolysis
Dizziness	Chondrocalcinosis	Vertigo	Blurred vision
Nocturia	Prolonged QT interval	Carpopedal spasm, tetany	Pseudotumor cerebri
Thirst, polyuria	Febrile episodes	Vomiting	Sclerochoroidal calcifications
Numbness, paraesthesia		Constipation	
Palpitations		Enuresis	
Low blood pressure		Paralysis	

Diagnosis is dependent on genetic testing demonstrating biallelic mutations in one of the genes known to result in BS and GS, as above. Heterozygous mutations in these genes are thought to occur in around 1% of the general population; people with these may have a mild phenotype but their long term outcomes are unexplored[135]. Management of BS and GS targets correction of electrolyte abnormalities with oral supplementation of sodium, potassium, and

magnesium salts. However, supplementation of salt and correction of other electrolytes results in increased glomerular filtration, which in turn increases renal losses therefore complete normalisation of electrolyte abnormalities are almost impossible to achieve. Supplements are combined with avoidance of dehydration. COX-2 inhibitors and inhibition of sodium-potassium exchange in the cortical collecting duct (e.g. aldosterone receptor or ENaC antagonists) are used in BS, but may be complicated by adverse effects, and the latter may exacerbate salt wasting due to its effect on compensatory mechanisms to maintain sodium balance.

Whilst patients with BS and GS waste significant amounts of sodium, how this impacts total body sodium is unexplored. Long-term sodium balance studies in patients with GS and BS have not been performed. Compensatory mechanisms, such as increased sodium reabsorption in the PT or in cortical collecting duct due to an activated RAAS are proposed to maintain at least neutral total body sodium balance in the longer term. Persistent total body sodium depletion would seem inherently incompatible with life. How renal salt wasting impacts on salt stores though, especially in the light of our new understanding of a third compartment of non-osmotic sodium storage, and if any alteration may impact immunity, is unknown.

1.4.5 Cortical collecting duct sodium reabsorption and pseudohypoaldosteronism type 1

The abundance of NCC reduces along the length of the DCT, and is replaced by ENaC, which is the sodium channel responsible for sodium reabsorption in the late distal tubule and within the cortical collecting duct (CD). This process is highly regulated according to needs, largely through the action of aldosterone. As exemplified by remote indigenous populations, urinary sodium excretion can be as little as <1mmol/day when intake is minimal[137].

As throughout the nephron, the Na-K ATPase creates the electrochemical gradient for sodium reabsorption, through ENaC in the principal cells of the

collecting duct. Sodium reabsorption in the CD is coupled to potassium and proton excretion through ROMK and the vH+ ATPase respectively. This process is mediated by aldosterone, which through intracellular binding of the mineralocorticoid receptor increases the expression of ENaC and the activity of the Na-K ATPase. As in patients with BS and GS, hyperaldosteronism thereby results in a hypokalaemic metabolic alkalosis.

Figure 1.16: Sodium transport mechanisms in the collecting duct. Figure from[117].

The Na-K ATPase generates the electrochemical gradient for sodium reabsorption through ENaC. Sodium reabsorption is coupled to potassium excretion through ROMK, and proton excretion through the vH+ ATPase.

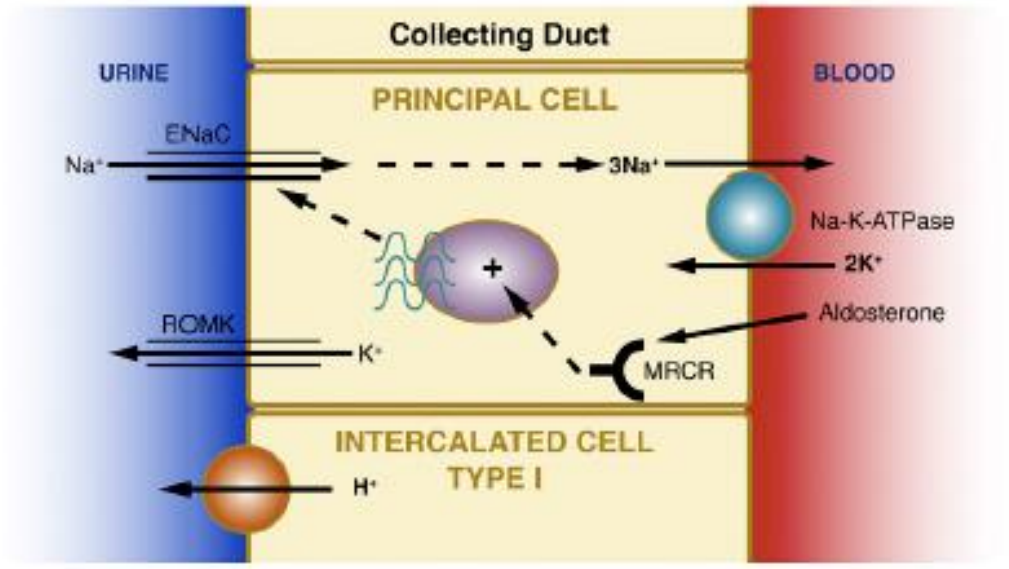

Defects in sodium reabsorption in this segment of the nephron may be due to mutations in genes encoding one of the subunits of ENaC (SCNN1A – alpha subunit; SCNN1B – beta subunit; or SCNN1G – gamma subunit) or due to mutations in NR3C2, which encodes the mineralocorticoid receptor. These defects result in Autosomal Recessive and Autosomal Dominant Pseudohypoaldosteronism Type 1 (PHA1) respectively. This is akin to being on a potassium sparing diuretic (e.g. amiloride which inhibits ENaC) or an aldosterone receptor antagonist (e.g. spironolactone). PHA1 tends to present in infancy with weight loss, hypovolaemia, and failure to thrive. In contrast to

BS and GS, patients with PHA1 are hyperkalaemic and acidotic. Interestingly, AR PHA1 patients have an increased risk of respiratory infections, attributed to extra-renal defective sodium transport and a cystic fibrosis like phenotype in the lungs[138]. Both the mineralocorticoid receptor and ENaC are expressed in immune cells[49,139], and whether there is a direct effect on immunity in PHA1 is unknown.

1.5 Summary

Salt intake as part of current diets globally is in excess of the amount with which we evolved. Excess salt intake is associated with hypertension and cardiovascular disease, but more recently salt has been linked to autoimmunity and the development of inflammatory disease. Novel concepts of sodium balance highlight that sodium loading is associated with non-osmotic sodium storage, with the development of interstitial sodium concentrations higher than those of plasma. High interstitial sodium concentrations activate tissue resident macrophages, which clear sodium through the lymphatics. *In vitro* and animal studies have demonstrated salt effects multiple components of immunity. Initial evidence demonstrated a salt effect on macrophage and Th17 cell polarisation, but many cells within both the innate and adaptive immune systems have now been shown to be affected. Whilst some of the intracellular mechanisms that mediate this effect have been described, the precise mechanism by which cells ‘sense’ changes in extracellular sodium is unknown. The *in vivo* consequences of salt loading are improved clearance of infection and the development of inflammatory disease. Short-term salt loading in humans has been shown to augment IL-17 immunity, but whether salt minimisation has a counter effect in diminishing immunity is unexplored. Patients with inherited salt losing tubulopathy have defects in sodium reabsorption in the kidney and chronically salt waste. An effect on immunity in these patients has not been described.

1.6 Aims and hypotheses

This project aims to investigate the effect of salt on immunity and its relevance in patients with kidney disease, with a particular focus on IL-17 responses. Specifically I aim to:

- Confirm previous evidence of a polarising effect of salt on *in vitro* IL-17 responses
- Determine the mechanism by which salt exerts its polarising effect, with a particular focus on sodium transport and associated signalling mechanisms
- Understand the consequences of chronic salt depletion on the immune system by studying immunity in patients with inherited salt losing tubulopathy
- Investigate whether altering salt intake may be used to affect severity of kidney injury in animal models of glomerular disease and immunity in human kidney transplant recipients

My hypotheses are:

1. Salt promotes IL-17 production by CD4+ and non CD4+ cells
2. This salt effect is mediated by sodium, which is transported in to cells through specific sodium transport mechanisms and this may be inhibited to abrogate its inflammatory effect
3. Salt losing tubulopathy is associated with dampened IL-17 responses and associated clinical features of immunodeficiency
4. Increasing salt intake worsens mouse models of inflammatory kidney disease
5. Dietary salt restriction is feasible in kidney transplant recipients and leads to a reduction in circulating Th17 cells

2 CHAPTER 2: MATERIALS AND METHODS

2.1 Methods for techniques used throughout the project

2.1.1 Peripheral blood mononuclear cell (PBMC) isolation

PBMCs were isolated via density centrifugation. 20ml blood was collected via peripheral venipuncture in Ethylenediaminetetraacetic acid (EDTA) coated tubes. Blood was diluted 1:1 with sterile phosphate buffered saline (PBS; Gibco, cat#14190250), layered on top of 15ml Lymphoprep (Stemcell, cat#07861) in a 50ml falcon tube, and centrifuged for 30 minutes at 1750 revolutions per minute (RPM) with the break off. The PBMC layer was aspirated, resuspended in PBS (total volume 50ml), and centrifuged for 10 minutes at 1350 RPM (break on). Cells were washed once with PBS and then pelleted cells were resuspended in 10ml PBS for counting. 50ul of suspended cells were diluted 1:1 with trypan blue (0.4%; Sigma Aldrich, cat#93595) and the number of cells counted with a haemocytometer. Cells were pelleted by centrifugation and either resuspended in the appropriate media for culture or frozen as below for future analysis.

2.1.2 PBMC freezing and defrosting

20-40 million cells were resuspended in 1ml 10% dimethyl sulfoxide (DMSO)/90% fetal bovine serum (FBS) and transferred to cryovial tubes on ice. Cells were then placed in a freezing container (Mr Frosty; ThermoFisher, cat#5100-001) at -80^{o}C to achieve a rate of cooling of -1^{o}C per minute. Cells were stored at -80^{o}C until subsequent analysis.

To defrost cells, cryovials were submerged in a 37^{o}C water bath for 1-2 minutes. Cell suspensions were diluted immediately in 50ml PBS, washed twice, and then PBMCs were counted and resuspended as above for subsequent use and analysis.

2.1.3 Cell culture

Unless otherwise specified, cell culture experiments were undertaken in round bottom 96-well culture plates with PBMCs at a starting concentration of 5 million cells/ml in 200ul total volume of XVIVO15 media (Lonza, cat# BE02-060F). Each culture condition was performed at a minimum of 2 replicates in each experiment.

2.1.4 FACS staining

FACS staining was undertaken on ice in the dark within round bottom 96 well culture plates unless otherwise specified. Viability staining was undertaken in PBS and cell surface staining in FACS wash (0.1% NaN_3, 0.5% bovine serum albumin in PBS). In experiments that required intracellular staining, cells were fixed and permeabilised for 30 minutes on ice with 200ul of fix/perm solution (Invitrogen, Cat# 00-5523-00), and intracellular stains were undertaken in perm buffer (ThermoFisher, cat#00-8333-56). In experiments where no intracellular staining was undertaken, cells were fixed with 4% paraformaldehyde (150ul for 10 minutes at room temperature). Cells were washed at least once between staining steps. Compensation was performed using compensation beads (Ultra Comp eBeads, ThermoFisher, cat#01-2222-41). FACS was undertaken either on a LSRII or LSR Fortessa flow cytometer (BD Biosciences). Analysis was undertaken using FlowJo v10 software (https://www.flowjo.com). Gates were determined using a fluorescence minus one (FMO) strategy unless otherwise specified.

2.2 Methods pertaining specifically to investigations reported in Chapter 3

2.2.1 Th17 polarisation assay

PBMCs were isolated from healthy controls and fresh cells were stimulated for 7 days with anti-human CD3 (10ug/ml plate bound) and anti-human CD28

(1ug/ml), with and without cytokines required for Th17 polarisation: IL-1β (12.5ng/ml; Peprotech, cat#200-01B), IL-6 (25ng/ml; Peprotech, cat#200-06), IL-21 (25ng/ml; Peprotech, cat#200-21), IL-23 (25ng/ml; Peprotech, cat#200-23), and TGFβ (5ng/ml; Peprotech, cat#100-36E). This was performed in XVIVO15 media with media supplemented on day 4. On day 7, cells were restimulated for 4 hours with PMA (50ng/ml) and ionomycin (1ug/ml; Sigma, cat#I9657) in the presence of brefeldin A (5ug/ml). Cells were then stained for viability (eFluor450, Invitrogen, cat# 65-0863-14), CD4 (CD4-FITC, BioLegend, cat# 300538), CD8 (CD8-PE/Cy7, BioLegend, cat#300914), and IL-17 (IL-17-PE, BioLegend, cat#512306), and analysed by FACS. Gates for cytokine expression were determined by fluorescence minus one (FMO) (**Figure 2.1**). The proportion of viable CD4+ and CD8+ cells expressing IL-17, representing Th17 and Tc17 cells respectively, in addition to the median fluorescence intensity (MFI) of IL-17 staining in CD4+ and CD8+ cells, were determined. Supernatant IL-17 and IFNγ concentrations were measured by enzyme linked immunosorbant assay (ELISA) (R&D systems, cat#DY317 and cat#DY285).

Experiments were subsequently undertaken in media supplemented with NaCl (ranging from 0-80mM), and IL-17 responses were compared between conditions. Electrolyte concentrations in unsupplemented XVIVO15 media were measured by automated analyser (Cobas 8000 modular analyser series, Roche) to determine baseline conditions.

Figure 2.1: Gating used during FACS analysis of Th17 and Tc17 polarisation

Gates for IL-17 were determined by fluorescence minus one (FMO)
Top panel: Lymphocytes were gated on a FSC-SSC plot; live cells were gated on a FSC-Viability dye plot.
Middle Panel: IL-17 expression was determined by CD4-IL-17 gating; left panel demonstrates FMO.
Bottom panel: IL-17 expression was determined by CD8-IL-17 gating; left panel demonstrates FMO.

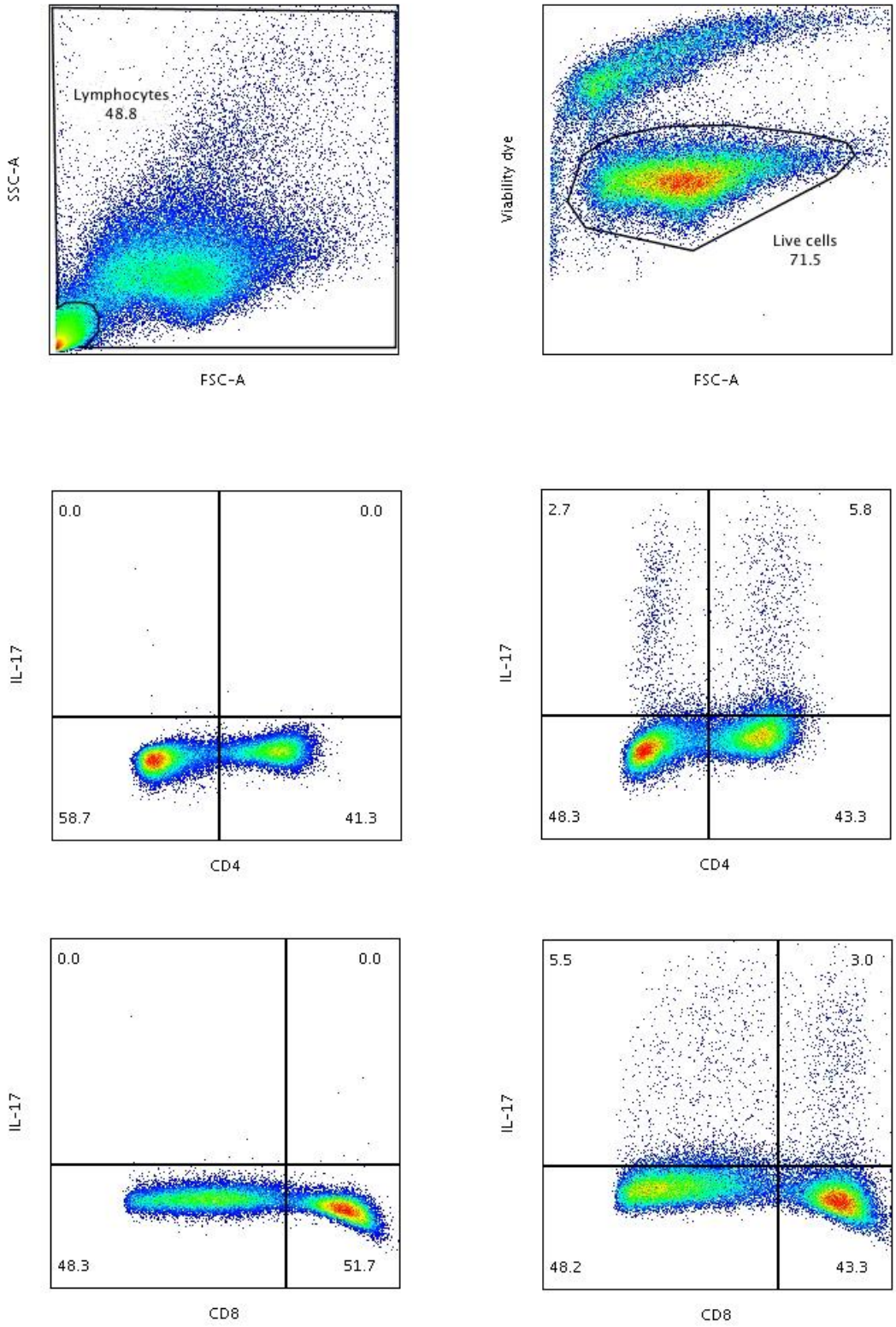

2.2.2 Naïve and memory T cell isolation

Naïve CD4+CD45RA+ and memory CD4+CD45RO+ cells were isolated from PBMCs using isolation kits (EasySep Human Naïve CD4+ T cell Isolation Kit; Stemcell, cat#17515; EasySep Human Memory CD4+ T cell Isolation Kit; Stemcell, cat#19117). Cell purity was confirmed by staining for CD4 (CD4-FITC) and CD45RO (CD45RO-PE; BioLegend, cat#304206) and analysed with FACS. Isolated cells, as well as whole PBMCs were then stimulated with anti-CD3/28 and Th17 polarising cytokines in XVIVO15 media as above. This was done in standard conditions and in media supplemented with 40mM NaCl. The effect of NaCl on IL-17 responses in whole PBMCs and in isolated naïve and memory cells was determined.

2.2.3 Analysis of the relationship between osmolality and IL-17 responses

Th17 polarisation experiments were undertaken as described above in the presence of NaCl 0-80mM, mannitol 0-160mM, urea 0-80mM and sodium gluconate 0-80mM. In addition to assessing Th17 and Tc17 polarisation, final supernatant osmolality was also measured (Osmomat 030, Gonotec, Berlin). Final supernatant osmolality was then correlated with IL-17 responses (Th17 and Tc17 polarisation, and supernatant IL-17 concentration) for each osmole creating the hyperosmolar conditions. The nature of the relationship was assessed using a linear regression analysis.

2.2.4 Epithelial sodium channel (ENaC) and sodium chloride cotransporter (NCC) expression on lymphocytes

Healthy control PBMCs were isolated and stained for NCC (rabbit anti-SLC12A3 polyclonal primary antibody; Life technologies, cat# PA5-80004; goat anti-rabbit APC conjugated secondary antibody; Invitrogen, cat#A-10931) or ENaC (rabbit anti-alpha ENaC polyclonal primary antibody Invitrogen, cat#PA5-35364; goat anti-rabbit APC conjugated secondary antibody). Cells were then stained for CD4 (CD4-FITC), CD8 (PE-Cy7), and

CD45RA (CD45RA-AF700; BioLegend, cat#304120), and analysed by FACS (**Figure 2.2**). Separate staining was performed for NCC and ENaC (APC), alongside CD45 (CD45-FITC), CD3 (CD3-BV711), and CD56 (CD56-BV510), in addition to NCC and ENaC (APC) with CD19 (CD19-PE/Cy7; Invitrogen, cat#25-0199042). The percentage of each cell type expressing NCC was determined.

Figure 2.2: Gating used during FACS analysis of ENaC and NCC expression

Gates for ENaC/NCC were determined by fluorescence minus one (FMO) – an example of ENaC gating is shown

Top panel: Lymphocytes were gated on a FSC-SSC plot; single cells were gated on a FCS-A-FSC-H plot.

Middle Panel: ENaC expression was determined by CD4-ENaC gating; left panel demonstrates FMO.

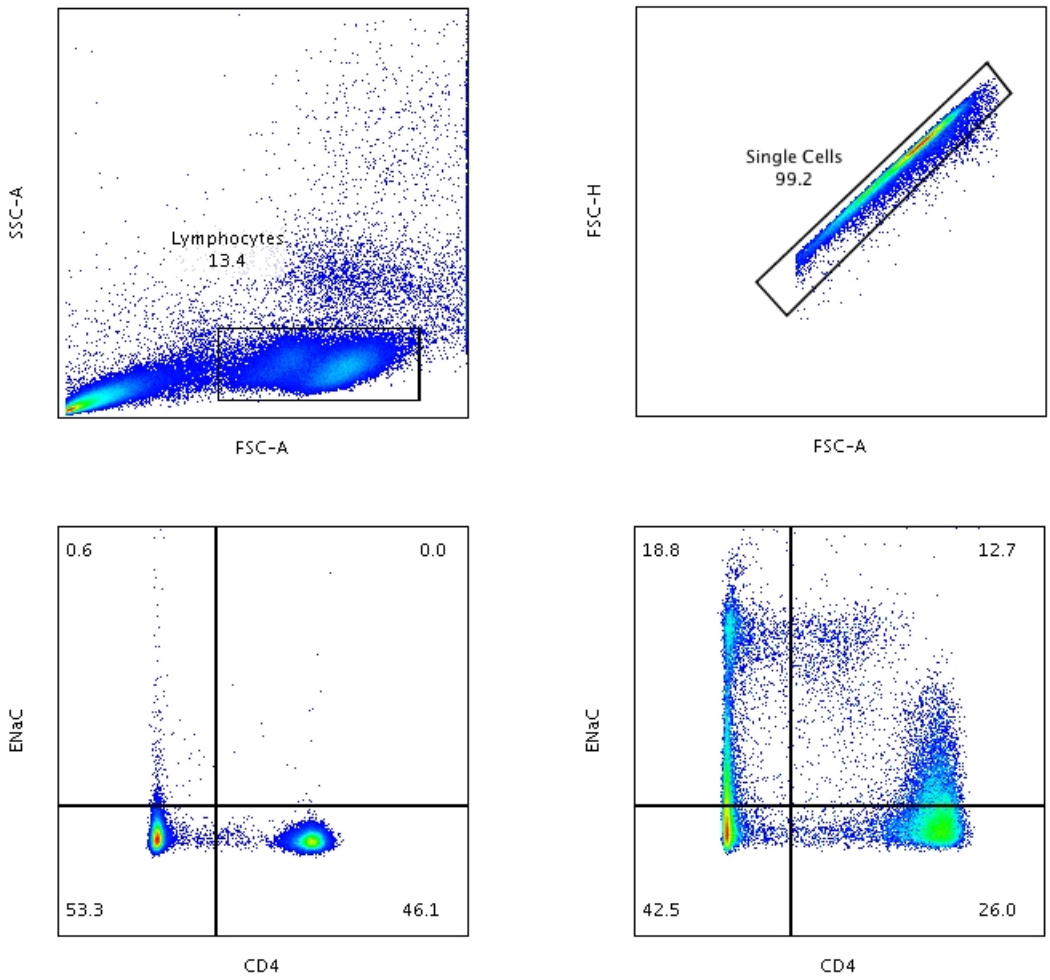

2.2.5 Sodium transport inhibition experiments

7 day Th17 polarisation experiments were performed as above in media supplemented with 40mM NaCl with and without sodium channel and transporter inhibitors: amiloride 20uM (Sigma Aldrich cat#A7410), furosemide 10-20uM (Sigma Aldrich cat#F4381), hydrochlorothiazide (HCT) 20uM (Sigma Aldrich cat#H4759), and the sodium-calcium exchanger (NCX) inhibitor KB-R7943 200nM (Tocris Bioscience, cat#K4144). Concentrations were chosen on the basis of the known minimum inhibitory concentration of the molecules. IL-17 responses (Th17 and Tc17 polarisation, and supernatant IL-17 concentration) were compared between high salt conditions with inhibitor present to high salt conditions alone.

2.2.6 Calcium flux experiments

PBMCs were isolated from healthy controls, and fresh cells loaded with the ratiometric calcium indicator Indo-1 (4uM; Indo-1 AM cell permeant; Thermo Fisher cat#I1223) for 45 minutes in XVIVO15 (calcium containing) media. Cells were washed and stained for CD4 (CD4-PerCP/Cy5.5; BioLegend, cat#300530) at room temperature and then incubated with biotinylated anti-CD3 (BioLegend; cat#317320) in XVIVO15 media for 15-30 minutes at 37^{o}C in an incubator. The ratio of Indo-1 fluorescence in CD4+ cells at 400nM compared to 475nm (representing free intracellular calcium) was then analysed in real time by FACS. FACS tubes were placed within a polystyrene coat throughout the FACS analysis to maintain cells as warm as possible. Fluorescence data were collected for 1 minute to determine baseline calcium concentrations, prior to T cell activation with the addition of streptavidin (40ug/ml; Avivasysbio, cat#OPPA01200), and fluorescence recorded for a further 5 minutes. A calcium flux curve was created and the peak x, peak y, and area under this curve determined (**Figure 2.3**). Experiments were performed in standard conditions and in media supplemented with NaCl 0-80mM, Na gluconate 0-80mM, mannitol 0-160mM, $MgCl_2$ 0-1mM, KCl 0-1mM,

amiloride 20-100uM, furosemide 20-100uM, and HCT 20-100uM. These were added at the time of incubation with anti-CD3. The characteristics of the calcium flux curves were compared to standard conditions.

Figure 2.3: Variables determined from the calcium flux curves

Area under the curve, peak X (time in seconds for curve peak) and peak Y (maximum indo-1 ratio representative of maximum free intracellular calcium) were determined.

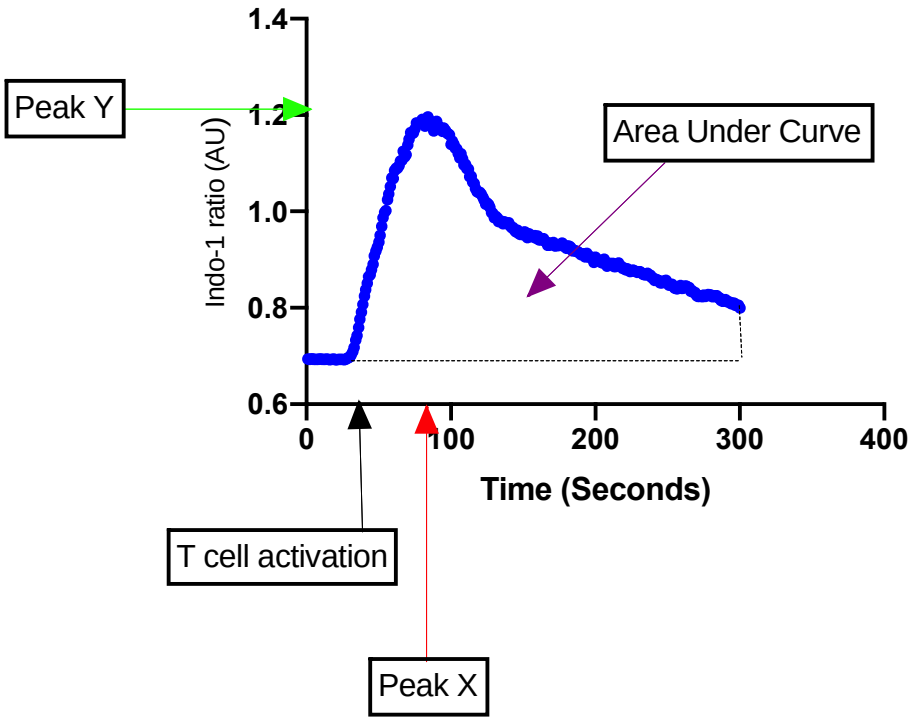

2.2.7 Autosomal recessive Pseudohypoaldosteronism type 1 (AR PHA1) patients

AR PHA1 patients were recruited from the Tubular Disorders Clinics at the Royal Free Hospital and Great Ormond Street Hospital, London, UK. Demographic and clinical data were collected. This included serum biochemistry and treatment on the day of recruitment, as well as clinical features of dysregulated immunity. Patients underwent initial immunological analysis in the NHS laboratories (full blood count, immunoglobulins, lymphocyte subsets). Further immunological analysis was undertaken in the

research laboratory. T cell proliferation and activation were assessed (2.3.4), as were 7-day IL-17 responses as described above (2.2.1). One patient underwent whole blood cytokine stimulation assay analysis (2.3.12). Variables were compared between PHA1 patients and controls. All patients provided written informed consent prior to participation in the study (Royal Free Hospital Research and Development committee study identification number 7727).

2.3 Methods pertaining specifically to investigations reported in Chapter 4

2.3.1 Salt losing tubulopathy (SLT) and control cohorts

Patients with genotyped BS, GS, or EAST syndrome were recruited from the Royal Free Hospital and Great Ormond Street Hospital Tubular Disorders Clinics, London, UK[140]. Demographic, genetic, biochemical, and clinical data on the day of recruitment were recorded. Biochemical parameters were compared between SLT patients with loop dysfunction (BS types 1, 2, and 4), distal tubule dysfunction (GS and EAST syndrome), and a mixed phenotype (BS type 3).

SLT patients underwent a structured clinical history focused on clinical features of dysregulated immunity (Appendix 8.1). This was also undertaken in age and sex matched healthy and disease control cohorts. Disease controls included patients attending the Tubular Disorders Clinics, but who had no evidence of a significant salt wasting phenotype (conditions included are outlined within the results, 4.4.1). The prevalence of each clinical variable was compared between SLT and controls. Biochemical parameters were also compared between SLT patients and disease controls.

An infection score was subsequently determined for each subject related to infections known to arise from defects in IL-17 mediated immunity. To do this,

the infection related scoring system employed in the diagnostic criteria of Hyper-IgE syndrome[141], which results from inherited defects in IL-17 immunity, was used (Table 2.1). IL-17 related infection scores were compared between SLT and controls. Infection scores were also compared between SLT subtypes and were correlated to serum biochemical parameters and blood pressure in SLT patients.

Table 2.1: Scoring system used to assess infection related to IL-17 defects

Points attributed to each answer in red parentheses; scoring system is based on the infection related criteria and scores used in the Hyper-IgE syndrome diagnostic criteria; maximum score is 26 points.

Total number of skin abscesses in lifetime	None (0)	1-2 (2)	3-4 (4)	>4 (8)
Total number x-ray proven pneumonias in lifetime	None (0)	1 (2)	2 (4)	3 (6)
Other serious infections (requiring hospital admission or intravenous antibiotics)	None (0)	Severe (4)		
Number of upper respiratory tract infections (tonsillitis, sinusitis and otitis) in worst year	0-2 (0)	3 (1)	4-6 (2)	>6 (or tonsillectomy) (4)
Fungal infection?	None (0)	Oral, vaginal (candida) (1)	Fingernail (2)	Systemic (4)

2.3.2 ^{23}Na-MRI Imaging

To investigate interstitial sodium storage, ^{23}Na-MRI capability was established at University College London Hospital (UCLH) in collaboration with the UCL department of Imaging and the UCL-UCLH Biomedical Research Centre. Dr.

Marilena Rega (Physicist, UCLH) performed the ^{23}Na-MRI and produced quantified ^{23}Na maps. To determine skin and muscle sodium stores, subjects underwent ^{23}Na-MRI imaging of the right lower limb. Tubes ('phantoms') of known ^{23}Na concentration (0, 20, 40, 60, and 80mM respectively) were placed on the participants' limb within the field of view and were used for quantification (

Figure 2.4). All participants were scanned on a 3T mMR Biograph with a transmit/receive birdcage ^{23}Na coil (Stark Contrast MRI Coils Research). Three ^{23}Na weighted MR images were acquired with a balance steady state free precision (BSSFP) sequence (Bandwidth = 289Hz/pixel, Echo Time = 3.33ms, Repetition Time = 21ms, Signal Averages = 100, resolution = 3.1x3.1x20mm^3, acquisition time = 2:17). Quantified ^{23}Na maps were calculated with an in-house script (Matlab). Regions of interests were drawn per acquisition per participant on each sodium phantom and the averaged signal per phantom was used to calculate a calibration curve as: [Known ^{23}Na Concentration] = p1*[Averaged signal]+p2, where p1 and p2 are the slope and intercept respectively. The values of p1 and p2 were then used to calculate the ^{23}Na concentration per pixel using: [^{23}Na Concentration in mM] = ([Signal] – p2)/p1. Mean sodium concentrations in the skin, bone, and in 4 muscle groups were determined for each patient (Figure 2.5). Image analysis was performed using ITK-Snap v3.0 software (http://www.itksnap.org/). Mean sodium concentrations in the skin and muscles were compared between SLT patients (n=4) and controls (n=4). Peritoneal dialysis patients (n=3) were imaged for optimisation purposes and to act as salt loaded positive controls.

Figure 2.4: Conventional (hydrogen) and ^{23}Na-MRI Images of the lower limb in a healthy control

Arrows highlight phantoms of known NaCl concentrations (in solution; 0-80mM), which were used to quantitate the sodium images acquired; other phantoms are known concentrations of NaCl in agar, which were used for a separate research project attempting to distinguish intra and extracellular sodium

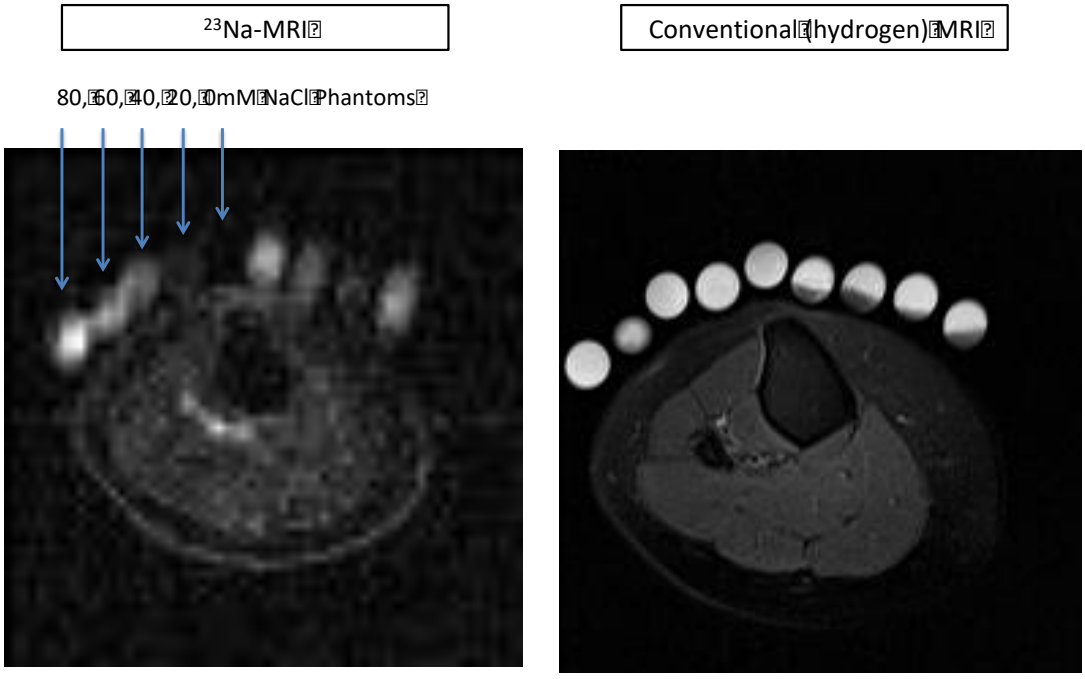

Figure 2.5: Demonstration of regions of interest in which sodium was quantitated in lower limb ^{23}Na-MRI scans.

Regions of interest analysed were: 1. Muscles x4 (peroneus - pink, medial gastrocnemius - grey, lateral gastrocnemius - orange, soleus - purple); 2. Bone (tibia - green); and 3. Skin (red). Panels below represent three ^{23}Na images and one hydrogen image (bottom right). Regions of interest are drawn on to the hydrogen image and automatically mapped to the identical area on the ^{23}Na scan. The mean sodium concentration within the region of interest across scans performed in triplicate was reported.

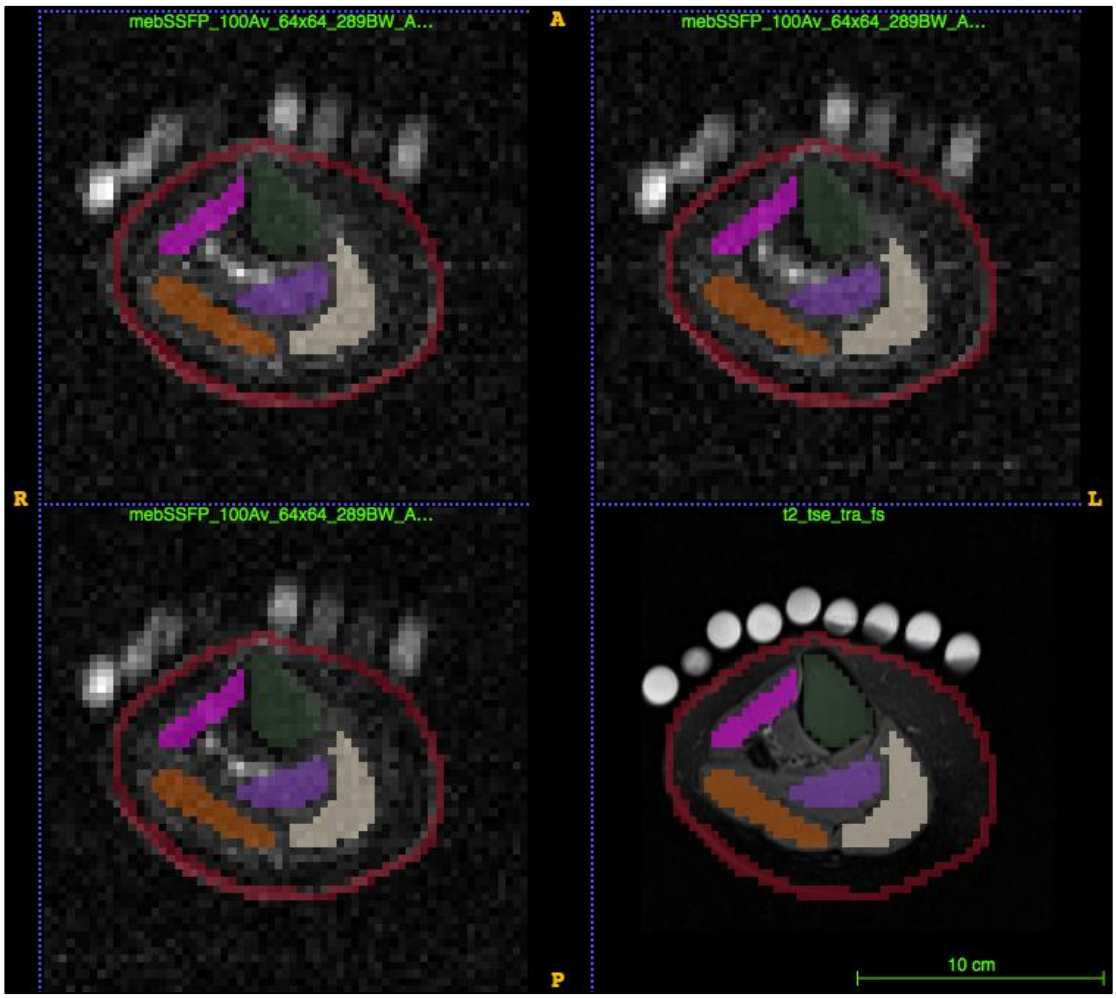

2.3.3 Urine Culture experiments

To characterise the urinary microbial community, urine specimens were collected from SLT patients (n=14) and healthy controls (n=12) and sediment cultures undertaken. This was done in collaboration with the chronic urinary tract infection group within the UCL department of renal medicine. A 20ml

volume of each urine specimen was centrifuged at 1400 x *g* for 10 minutes. The supernatant was removed and the resulting cell pellet was resuspended in 400µl of phosphate buffered saline (PBS) (Life Technologies, UK). Ten-fold serial dilutions were performed in PBS to facilitate the quantification of microbial colonies. Cultures were kept in an ordinary incubator at 37°C for 18-24 hours. Following incubation, the resulting microbial growth was quantified in colony forming units per millilitre (cfu/ml).

Cultured organisms were grown separately on Columbia blood agar (Oxoid, UK) for species-level identification using matrix-assisted laser desorption ionisation time-of-flight mass spectrometry (MALDI-TOF MS). This analysis was undertaken by Dr. Sanchutha Sathiananthamoorthy (post-doctoral fellow, chronic urinary tract infection group, UCL). The direct colony protocol was adopted on the MicroFlex LT mass spectrometer (Bruker Daltonics, USA). Briefly, each cultured isolate was spotted on a 96-well target plate and overlayed with matrix solution consisting of alpha-cyano-4-hydroxycinnamic acid dissolved in 50% acetonitrile and 2.5% trifluoroacetic acid. Once air-dried for 5 minutes, the target plate was loaded and analysed using the MALDI Biotyper 3.0 software programme containing the Bruker Taxonomy 16S reference library. The number of different isolates identified, the microbial burden of each isolate, and the microbial identity of the isolates were recorded for each patient, and summarised and compared between SLT patients and controls.

To determine if increasing extracellular sodium directly affected microbial growth, strains of *Escherichia coli*, *Staphylococcus aureus*, *Candida albicans* and *Corynebacterium amycolatum* were grown on chromogenic agar (Biomerieux, France) in an ordinary incubator at 37°C. A bacterial suspension in sterile distilled water with turbidity equivalent to a 0.5 McFarland standard was made for each strain. Seven ten-fold serial dilutions were made for each strain and 25µl of each dilution, along with the undiluted bacterial suspension, were plated onto one quadrant of four tryptone soya agar plates, which had been prepared with and without additional NaCl (unadjusted plate, +40mM,

+80mM, +160mM). Plates were incubated at 37°C and microbial growth was examined by visual inspection after 24 hours.

2.3.4 Initial immunological analysis

Initial immunological analysis of SLT patients was undertaken in the National Health Service clinical laboratories of the Royal Free Hospital, London. This included full blood count, erythrocyte sedimentation rate (ESR), C-reactive protein (CRP), total immunoglobulin A, G, M, and E concentrations, complement protein C3 and C4 concentrations, and lymphocyte counts/subsets (CD3+, CD4+, CD8+, CD19+, CD16/56+).

To assess T cell proliferation and activation, peripheral blood mononuclear cells (PBMCs) were isolated from SLT (n=6) and healthy controls (n=7) by density centrifugation (Lymphoprep; Stemcell, cat#07861), and fresh cells were stimulated for 72 hours with anti-human CD3 (10ug/ml plate bound; BD Pharmigen, cat# 555336) and anti-human CD28 (1ug/ml; Invitrogen, cat# 16-0289-85) in XVIVO15 media (Lonza, cat# BE02-060F). Cells were stained for viability (Fixable viability dye – efluor450), CD4 (CD4-FITC), and CD25 (CD25-PE/Cy7; BioLegend, cat# 302612), prior to fixation and permeabilisation (Invitrogen, Cat# 00-5523-00) and intracellular staining for Ki67 (Ki67-APC; BioLegend, cat#350514). The proportion of viable CD4+ cells expressing Ki67 and CD25, analysed by fluorescent activated cell sorting (FACS), are reported.

To assess antigen specific immunoglobulin responses to vaccines/prior infection, varicella zoster and pneumococcal specific immunoglobulin G levels in SLT (n=12) serum were measured via enzyme linked immunosorbent assay (ELISA) (VaccZyme VZV and PCP kits; Binding site, Cat#MK012 and MK092). Antibody levels were compared to the levels recorded in the healthy adult population as specified by the assay data information sheet.

2.3.5 T cell subset analysis

PBMCs were isolated from SLT patients (n=20), healthy controls (n=19), and disease controls (n=18) and fresh cells were stimulated for 4 hours with phorbol myristate acetate (PMA, 50ng/ml; Sigma, cat#P8139) and ionomycin (1ug/ml; Sigma, cat#I9657) in the presence of brefeldin A (5ug/ml). This was performed in XVIVO15 media in round bottom 96-well plates. Cells were subsequently stained for CD4 (CD4-FITC), IL-17 (IL-17-PE), IFNγ (IFNγ-APC) and IL-4 (IL-4-PE/Cy7; BioLegend; cat#500824), and analysed by FACS. Gates for cytokine expression were determined by fluorescence minus one (FMO) (Figure 2.6). The proportion of CD4+ cells expressing each of these cytokines was determined and compared between groups.

Figure 2.6: Gating used during analysis of CD4 subsets

Cytokine (IFNγ, IL-4, and IL-17) gates in CD4+ cells were determined by FMO
Top panel: Lymphocytes were gated on a FSC-SSC plot; live cells were gated on a FSC-Viability dye plot
Middle Panel: Cytokine expression was determined by CD4-cytokine gating; middle panel demonstrates FMO for each cytokine.
Bottom panel: Representative staining of IFNγ, IL-4, and IL-17 against CD4 in a healthy control

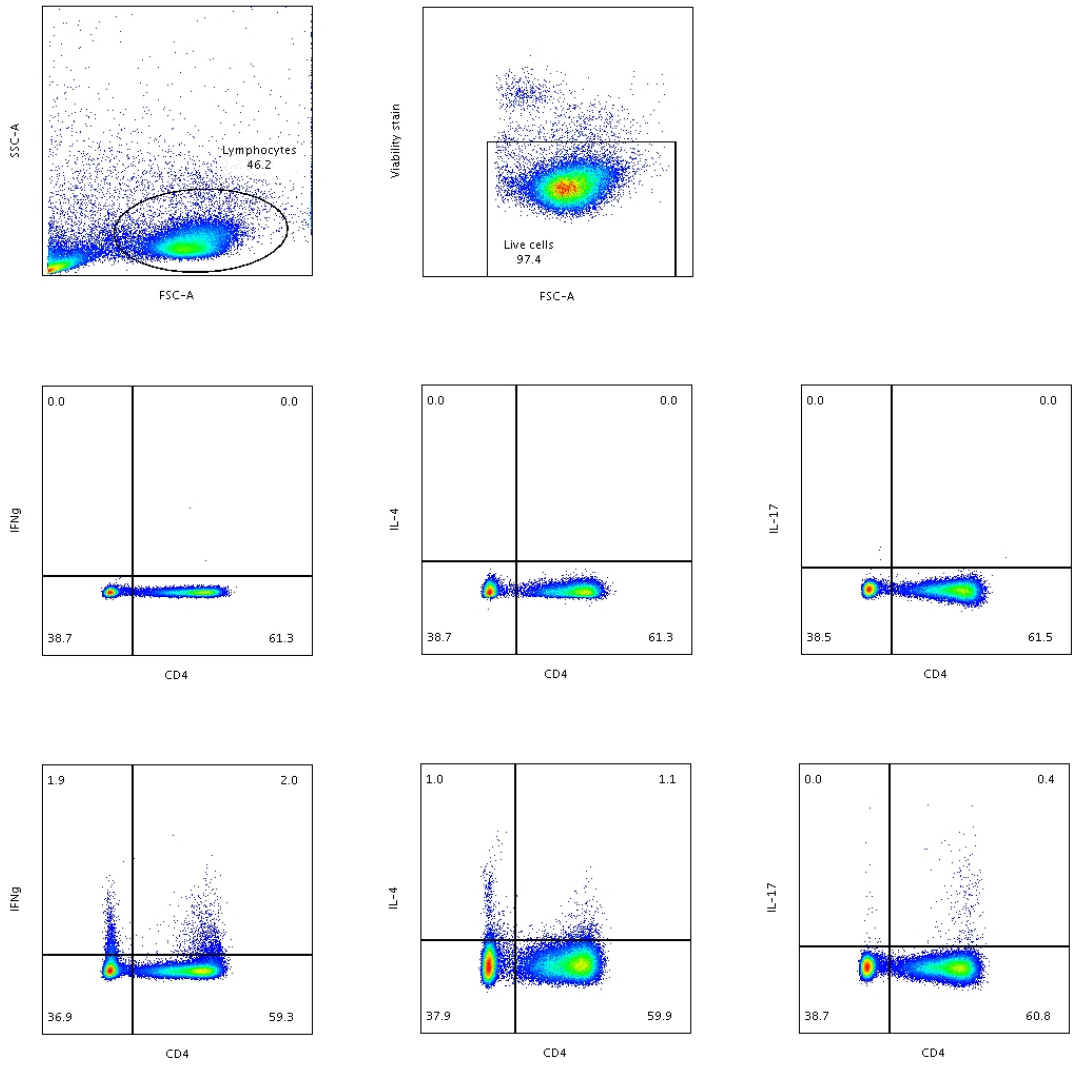

To investigate the effect of extracellular ions on CD4+ subset balance, healthy control PBMCs were isolated and stimulated for 72 hours with anti-human CD3 (10ug/ml plate bound) and anti-human CD28 (1ug/ml) in XVIVO15 media with additional 0-40mM NaCl, 0-2mM KCl, and 0-1mM $MgCl_2$. On day 3, cells were restimulated for 4 hours with PMA (50ng/ml) and ionomycin (1ug/ml; Sigma, cat#I9657) in the presence of brefeldin A (5ug/ml). Cells were then stained for viability (eFluor450), CD4 (CD4-FITC), IFNγ (IFNγ-APC), IL-4 (IL-4-PE/Cy7) and IL-17 (IL-17-PE), and analysed by FACS. Gates for cytokine expression were determined by fluorescence minus one (FMO) (Figure 2.7). The ratio of cytokine expression in viable CD4+ cells was determined, and compared between conditions.

Figure 2.7: Gating used during analysis of the effect of ions on CD4 subset balance

Cytokine (IFNγ, IL-4, and IL-17) gates in CD4+ cells were determined by FMO
Top panel: Lymphocytes were gated on a FSC-SSC plot; Single cells were gated on a FCS-A-FSC-H plot; live cells were gated on a FSC-Viability dye plot
Middle Panel: Cytokine expression was determined by CD4-cytokine gating; middle panel demonstrates FMO for each cytokine.
Bottom panel: Representative staining of IFNγ, IL-4, and IL-17 against CD4 in a healthy control

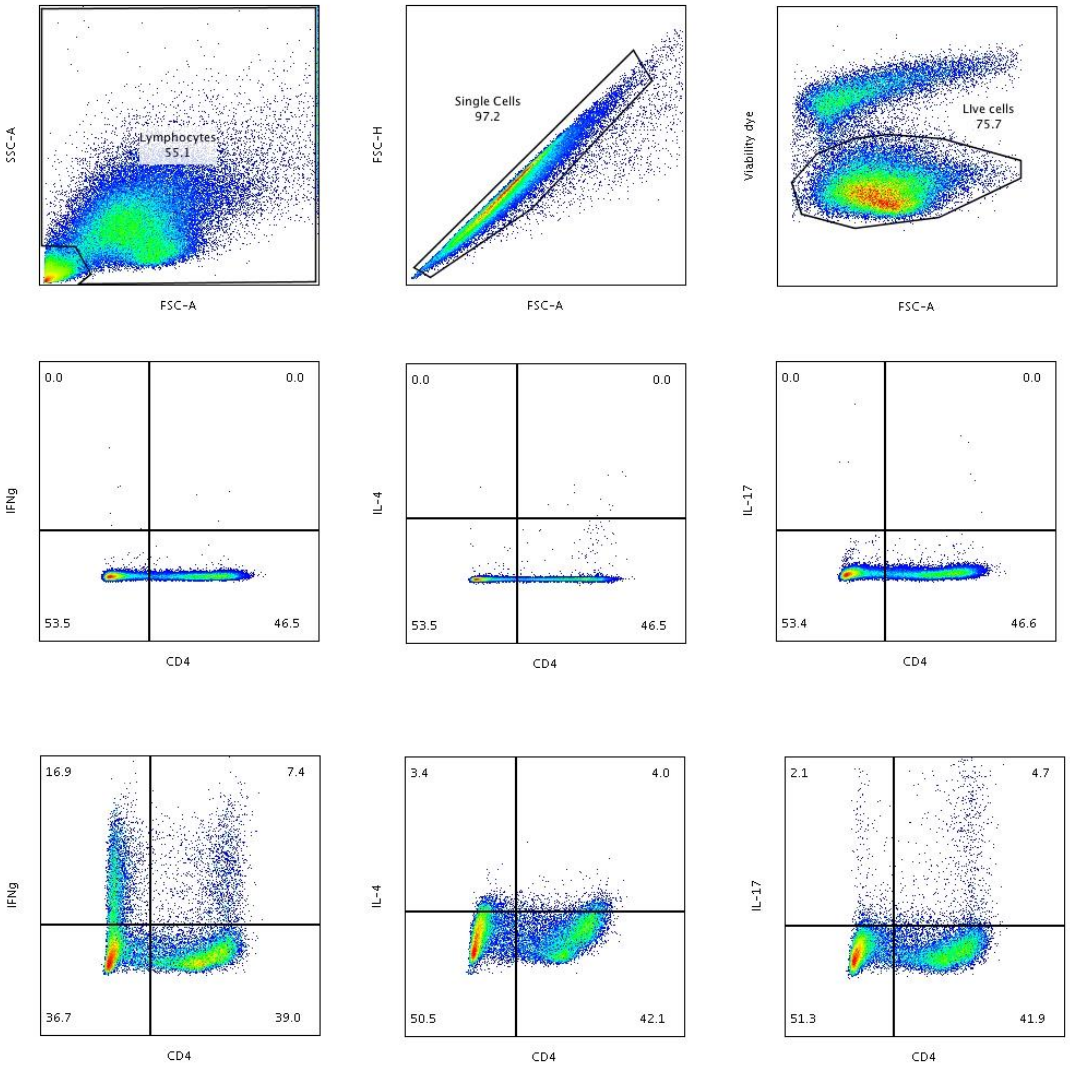

2.3.6 Th17 and Tc17 polarisation analysis

PBMCs were isolated from SLT patients (n=27), healthy controls (n=21) and disease controls (n=19) and fresh cells stimulated with anti-human CD3 (10ug/ml plate bound), anti-human CD28 (1ug/ml), IL-1β (12.5ng/ml; Peprotech, cat#200-01B), IL-6 (25ng/ml; Peprotech, cat#200-06), IL-21 (25ng/ml; Peprotech, cat#200-21), IL-23 (25ng/ml; Peprotech, cat#200-23), and TGFβ (5ng/ml; Peprotech, cat#100-36E) in XVIVO15 media for 7 days. On day 7, cells were restimulated for 4 hours with PMA (50ng/ml) and ionomycin (1ug/ml; Sigma, cat#I9657) in the presence of brefeldin A (5ug/ml). Cells were then stained for viability (eFluor450), CD4 (CD4-FITC), CD8 (CD8-PE/Cy7, BioLegend, cat#300914), and IL-17 (IL-17-PE), and analysed by FACS. Gates for cytokine expression were determined by fluorescence minus one (FMO) (**Figure 2.1**). The proportion of viable CD4+ and CD8+ cells expressing IL-17, representing Th17 and Tc17 cells respectively, were determined and compared between groups. Supernatant IL-17 concentrations were measured by ELISA (R&D systems, cat#DY317) and compared between groups.

In all subjects, experiments were undertaken in standard media and in media supplemented with 40mM NaCl. In a subset of healthy controls, experiments were also undertaken with the addition of other cations to culture conditions (KCl 0-2mM and $MgCl_2$ 0-1mM) in addition to experiments with aldosterone (100nM; Cambridge biosciences, cat#B2153), and angiotensin II (0.1-1uM; Sigma, cat#A9525). IL-17 responses in supplemented media were compared to standard culture conditions.

2.3.7 STAT1 and STAT3 phosphorylation assays

To investigate for phosphorylation defects in STAT1 and STAT3, PBMCs from SLT patients (n=13) were isolated and fresh cells were stimulated for 15 minutes with IL-6 (100ng/ml), IL-21 (100ng/ml), and IFNα (11500U/ml; R&D Systems, cat#11101-1). Cells were fixed immediately (Cytofix Fixation Buffer; BD Biosciences, cat#554655), permeabilised (Phosflow Perm Buffer III; BD Biosciences, cat#558050), and stained for CD4 (CD4-FITC), pSTAT1 (STAT1

pY701 – Alexa647; BD Biosciences, cat#612597) and pSTAT3 (STAT3 pY705 – PE; BD Biosciences, cat#612569). The expression of pSTAT1 and pSTAT3 was determined by the median fluorescence intensity of staining within CD4+ cells (

Figure 2.8). Phosphorylation of STAT1 was assessed in response to IFNα, and phosphorylation of STAT3 assessed in response to IL-6 and IL-21. For each subject, the increase in phosphorylation of STAT1 and STAT3 in stimulated compared to unstimulated CD4+ cells was determined; in SLT patients this increase was expressed as a ratio with the increase seen in a healthy control subject in each experiment.

Figure 2.8: Gating used in STAT1 and STAT3 phosphorylation assays

Top panel: Lymphocytes were gated on a FSC-SSC plot; single cells were gated on a FSC-A-FSC-H plot; CD4 cells were then gated on a FSC-CD4 plot.
Median fluorescence staining intensity (MFI) of pSTAT1 and pSTAT3 were determined in the CD4+ population.
Bottom panel: Histograms represent pSTAT1 staining in unstimulated and stimulated cells.
Increase in MFI was determined for each subject

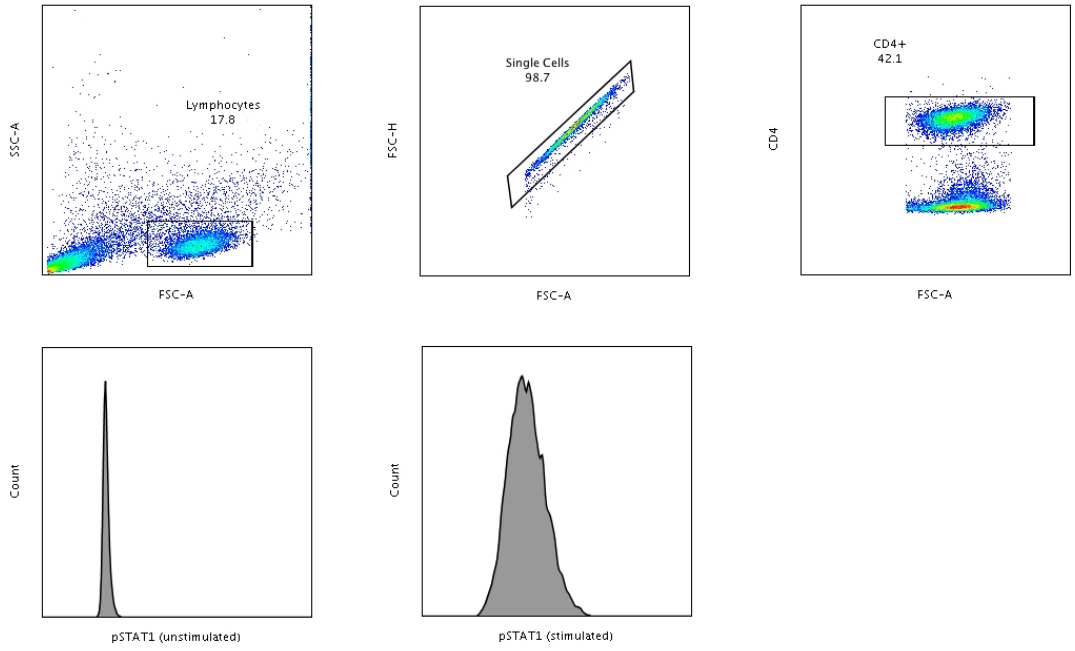

2.3.8 NCC expression and calcium flux experiments

Lymphocyte NCC expression was determined in 2 GS patients using the methods outlined in Chapter 3 (2.2.4). Similarly, calcium flux after T cell activation was assessed using the previously described technique (2.2.6). This was done in SLT patients (n=5) and compared to calcium flux in healthy controls (n=13).

2.3.9 IL-23 Receptor expression

PBMCs were isolated from healthy controls (n=8) and SLT patients (n=7) and stored at -80^{o}C in 10% DMSO/90% FCS until analysis. Cells were defrosted, washed, and then stained for CD4 (CD4-FITC) and the IL-23 receptor (IL23R-PE; R&D Systems, cat#FAB14001P) and analysed with FACS. Gates for IL23-R expression were determined by fluorescence minus one (FMO). The percentage of CD4+ and CD4- cells expressing the IL23-R were determined and compared between groups.

2.3.10 SGK1 expression

PBMCs were isolated from healthy controls (n=7) and SLT patients (n=13) and protein lysates prepared by digestion in RIPA buffer (Sigma, cat#R0278) containing protease inhibitors (Halt protease inhibitor cocktail; Thermo Scientific, cat#1862209). Protein was quantified (Pierce BCA assay; Thermo Scientific, cat#23227) and 35ug samples loaded onto a 10% SDS-PAGE electrophoresis gel run at 120V for 60-90 minutes (BioRad PowerPac Basic). The gel was transferred (70V for 90 minutes) to a nitrocellulose membrane (GE Healthcare, cat#106000006) and blocked for 1 hour at room temperature in 5% milk. The membrane was incubated with primary antibody at 4^{o}C overnight and secondary antibody for 1 hour at room temperature. Rabbit anti-SGK1 primary antibody (Abcam, cat#ab43606) was used at 1:900 dilution and

mouse anti-GAPDH primary antibody (Abcam, cat#ab8245) at 1:10000 dilution. Anti-rabbit HRP (Abcam, cat#ab205718) and anti-mouse HRP (Abcam, cat#ab205719) secondary antibodies were used at 1:3000 and 1:5000 dilutions respectively. Blots were developed with the BioSpectrum 810 Imaging System (UVP) and images quantified using ImageJ software (https://imagej.net). The expression of SGK1 relative to that of GAPDH was determined and compared between SLT patients and HCs.

2.3.11 NFAT5 expression

PBMCs were isolated from healthy controls (n= 13) and SLT patients (n=12) and RNA extracted using an RNA purification kit (Direct-zol RNA MicroPrep; Zymo Research, cat#R2061). Yields were analysed using nanodrop spectrophotometry and complementary DNA synthesis undertaken using a high capacity cDNA reverse transcription kit (Applied biosystems, cat#4374966) using a G-Storm GS1 thermal cycler. Reverse Transcriptase Polymerase Chain Reaction (RT-PCR) was then performed using Taqman reagents (Taqman Fast Advanced Master mix; Applied biosystems, cat#4444556) in the LightCycler96 (Roche) thermal cycler. Primers were used to detect NFAT5 (Taqman gene expression assay ID Hs00232437_m1; Applied biosystems, cat#4331182) and 18S (Taqman gene expression assay ID Hs99999901_s1; Applied biosystems, cat#4331182). PCR conditions used were: 1. Hold 50^{o}C for 2 minutes; 2. Hold 95^{o}C for 10 minutes; 3. 40 cycles of 95^{o}C 15 seconds / 60^{o}C 1 minute. The expression of NFAT5 relative to 18S in each subject was determined using $2^{-\Delta CT}$ and then compared to one healthy control subject using $2^{-\Delta\Delta CT}$. Relative expression was compared between SLT patients and HCs.

2.3.12 Innate cytokine stimulation assays

Innate cytokine assays were undertaken by Dr. Rainer Doffinger (Immunology department, University of Cambridge). Whole blood of SLT patients (n=13) and healthy controls (n=42) was diluted 1:5 in RPMI and activated in 96-well

plates with the following stimuli used alone or in combination: IFNγ ($2x10^4$IU/ml, Immuno Tools); IL-12 (5ug/ml; Immuno Tools); Lipopolysaccharide (LPS, 1ug/ml; List Biochemicals); IL-18 (5ug/ml; R&D Systems); Zymosan (ZYM, 10mg/ml; InvivoGen); Beta-glucan (B-GLUC, 5mg/ml, InvivoGen); IL-15 (5ug/ml; Immuno Tools); Pam2 (1mg/ml; EMC Microcollections); Muramyldipeptide (MDP, 4mg/ml; InvivoGen).

Cells were incubated for 24 hours and supernatant cytokines then measured by multiplex bead array (TNFα, IL-1β, IL-6, IL-10, IL-12, and IFN-γ; R+D Systems Fluorokinemap) on a Luminex analyzer (Bio-Plex, Bio-Rad, UK). Cytokine concentrations were compared for each stimulating condition between SLT patients and healthy controls.

2.3.13 Monocyte analysis

PBMCs were isolated from SLT patients (n= 14) and healthy controls (n=12) and stained for CD14 (CD14-APC/Cy7; BioLegend, cat#325619) and CD16 (CD16-FITC; BioLegend, cat#302006) and analysed with FACS. Classical (CD14+CD16-), intermediate (CD14+CD16+) and non-classical (CD14-CD16+) monocyte populations were determined and compared between groups (

Figure 2.9). Cells were also stimulated for 4 hours with LPS (100ng/ml; LPS from E.Coli Serotype R515; Hycult Biotech, cat#HC4048) in the presence of Brefeldin A (5ug/ml). Cells were stained for viability (alexafluor450) and CD14 (APC/Cy7), prior to being fixed and permeabilised, stained for TNFα (TNFα-Alexafluor488; BD Biosciences, cat#557722) and analysed with FACS. Gates for TNFα expression were determined by fluorescence minus one (FMO) (**Figure 2.10**). This was done in standard media and, in healthy controls, in media supplemented with 40mM NaCl, 2mM KCl, 1mM $MgCl_2$, and aldosterone (10-100nM). The proportion of viable CD14+ cells expressing TNFα was compared between SLT and controls, and between supplemented media and standard conditions.

Figure 2.9: Gating used for analysis of monocyte subsets

Top Panel: Monocytes were gated on a FSC-SSC plot, and single cells on a FSC-A-FSC-H plot
Bottom Panel: Live cells were gated on a FSC-viability dye plot; CD14-CD16 gates then determined classical (CD14+CD16-), intermediate (CD14+CD16+) and non-classical (CD14-CD16+) monocyte populations.

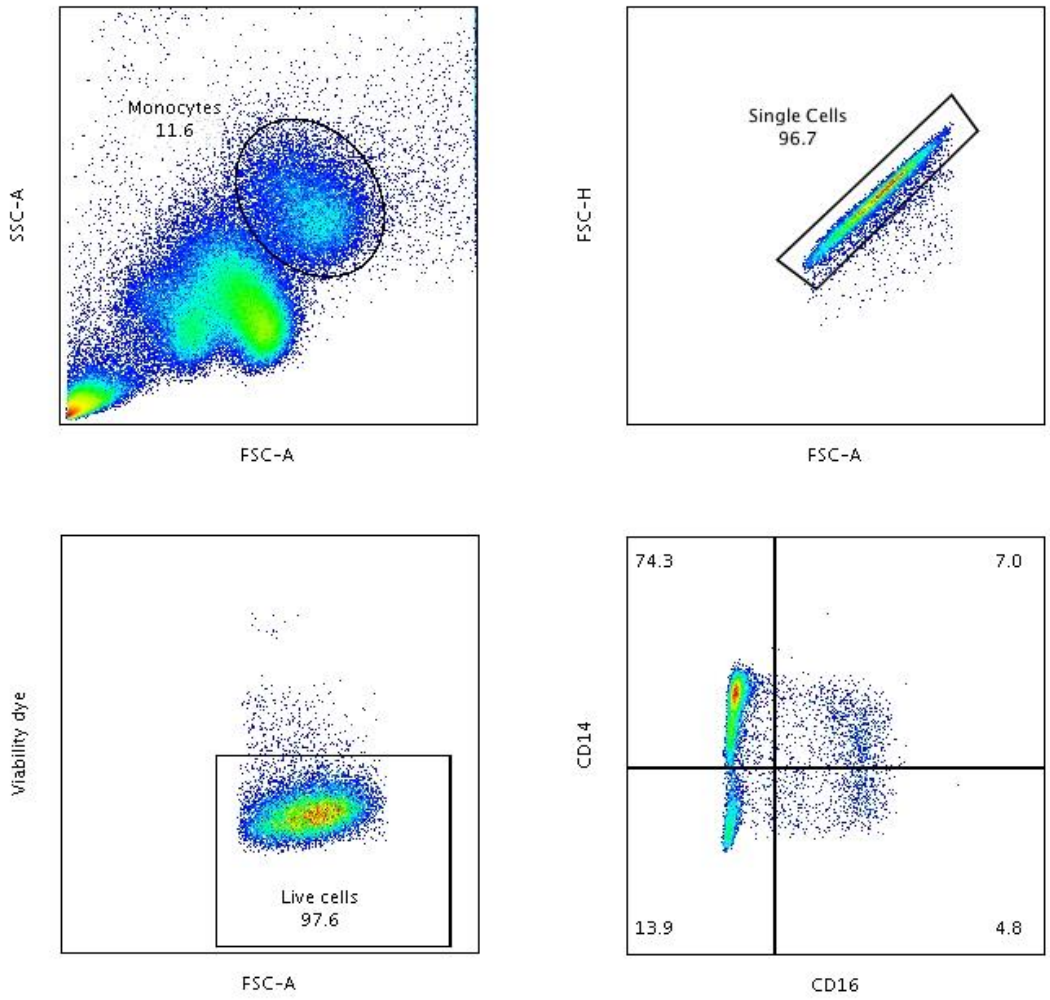

Figure 2.10: Gating used for analysis of monocyte expression of TNFα

Top panel: Stimulated monocytes were gated on a FSC-SSC plot; single cells were gated on a FSC-A-FSC-H plot; live cells were gated on a FSC-Viability dye plot. Bottom Panel: TNFα expression was determined by CD14-TNFα gating; bottom left panel demonstrates FMO for TNFα and bottom right panel demonstrates TNFα staining in a HC.

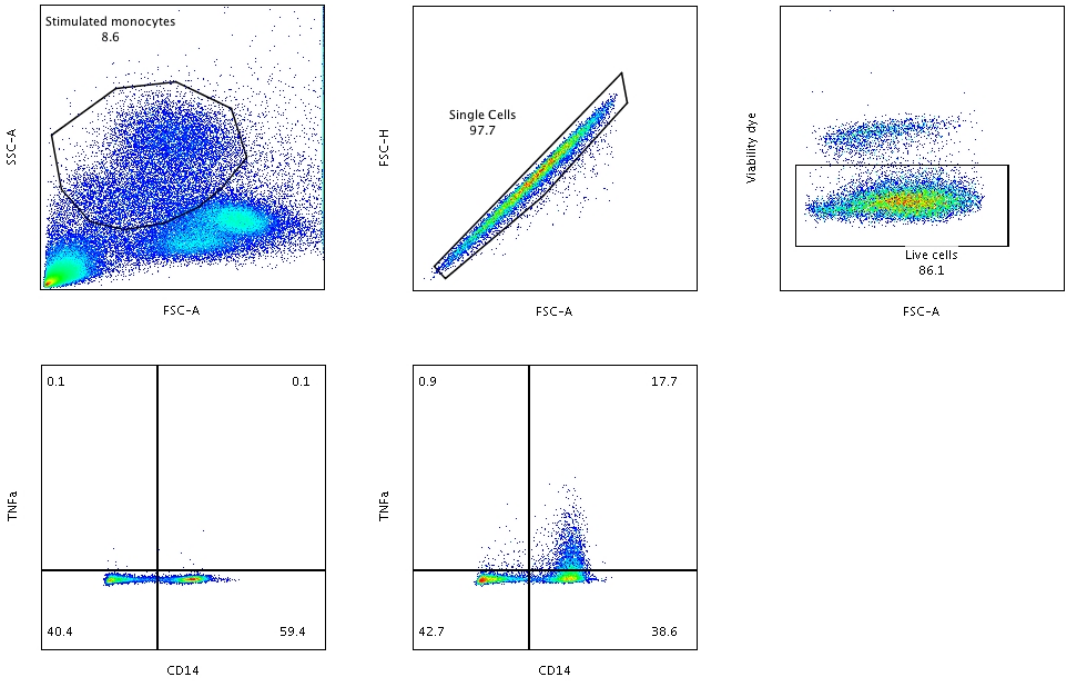

2.3.14 NK cell analysis

PBMCs were isolated from SLT patients (n=16) and healthy controls (n=17), and cells were stained for CD45 (CD45-FITC; BioLegend, cat#304006), CD3 (CD3-BV711; BioLegend, cat#317328), CD56 (CD56 – BV510; BioLegend, cat#318340), and CD16 (CD16-PE/Cy7; BioLegend, cat#302016), and analysed via FACS (**Figure 2.11**). CD45+CD3-CD56+CD16+ (NK) cells as a proportion of CD45+ cells were calculated, as were the ratio of CD56+CD16+ to CD56+CD16- cells. PBMCs were also stimulated with IL-12 (50ng/ml; Peprotech, cat#200-12) and IL-18 (50ng/ml; Cambridge bioscience, cat#230-00229-10) in the presence of brefeldin A (5ug/ml; Sigma, cat#B7651) for 4 hours and stained for viability, CD45, CD3, CD56, and IFNγ (IFNγ-APC; BioLegend, cat#502512). The proportion of viable CD45+CD3-CD56+ cells expressing IFNγ was determined. Gates for IFNγ expression were determined by fluorescence minus one (FMO) (**Figure 2.12**). Stimulation was also performed in healthy controls (n=8) in media supplemented with 40mM NaCl. The proportion of NK cells (CD45+CD3-CD56+) was determined as was

expression of IFNγ by CD56+ cells, and compared between standard and high salt conditions.

Figure 2.11: Gating used for analysis of NK cell subsets

Top Panel: Lymphocytes were gated on an FCS-SSC plot; single cells were gated on a FSC-A-FSC-H plot; CD45+ cells were gated on a FSC-CD45 plot.
Bottom Panel: CD3-CD56+ cells were gated on a CD3-CD56 plot (bottom left panel, top left quadrant); CD56 bright versus dim was then gated against CD16 to determine $CD56^{bright}CD16^{neg}$, $CD56^{bright}CD16^{pos}$, and $CD56^{dim}CD16^{pos}$ cells.

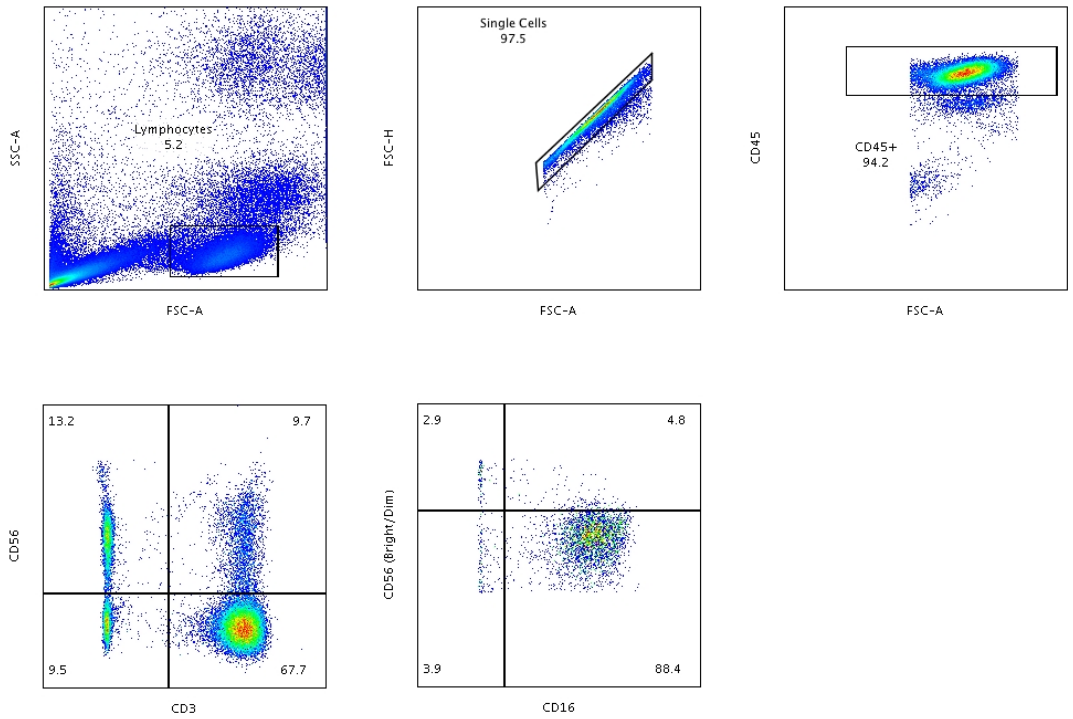

Figure 2.12: Gating used for analysis of NK cell expression of IFNγ

Top panel: Lymphocytes were gated on a FSC-SSC plot; single cells were gated on a FSC-A-FSC-H plot; live cells were gated on a FSC-Viability dye plot.
Middle panel: CD45+ cells were gated on a FSC-CD45 plot; CD3- cells were gated on a FSC-CD3 plot

Bottom Panel: IFN*γ* expression was determined by CD56-IFNγ gating; bottom left panel demonstrates FMO for IFN*γ* and bottom right panel demonstrates IFN*γ* staining in a HC.

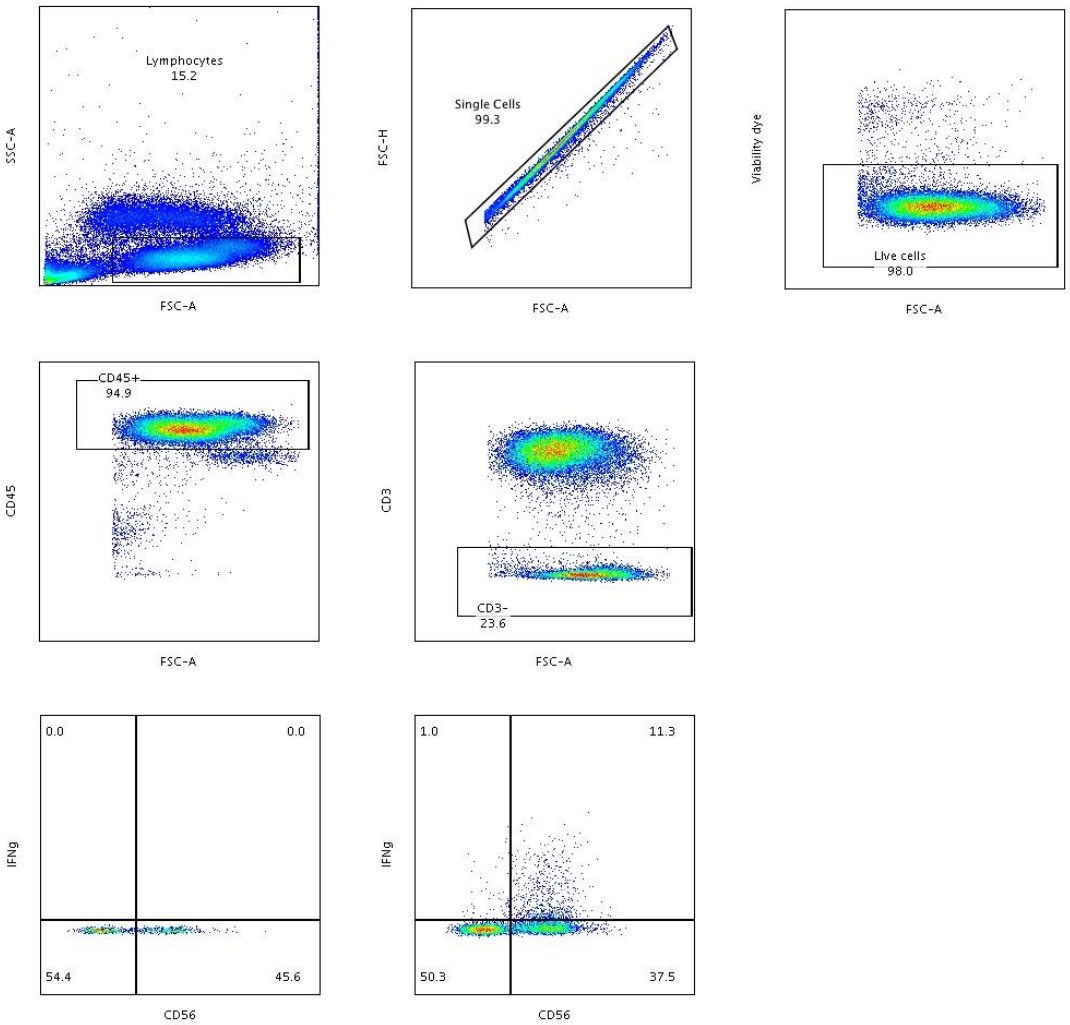

2.3.15 Statistics

Data are presented as number and percentages for categorical variables, and mean and standard deviation or median and interquartile range for numerical variables depending on distribution. Categorical variables were compared using the Fisher's exact or Chi-squared test. Non-parametrically distributed numerical variables were compared between two groups using the Mann-Whitney test and the Wilcoxon test for unpaired and paired data respectively.

Parametrically distributed numerical variables were compared with an unpaired or paired T test. Variables are compared across greater than two groups with a one-way analysis of variance with multiple comparison testing; specifically, for non-parametric data we used the Kruskall-Wallis test with Dunn's test for multiple comparisons. Numerical variables were correlated with a Pearson and Spearman correlation for parametric and nonparametric data respectively.

Analysis was performed using Graphpad Prism version 7 (www.graphpad.com). A p-value of ≤0.05 was considered statistically significant.

2.3.16 Study Approval

The Royal Free Hospital Research and Development committee approved the study (identification number 7727) and all subjects provided written informed consent prior to enrollment.

2.4 Methods pertaining to investigations reported in Chapter 5

2.4.1 Patient recruitment for *in vitro* assessment of IL-17 responses

Adult (>18 years of age) patients with native AIKD (AAV, pSS TIN, or LN) and KTRs (>3 months post transplant) were recruited from the Nephrology Outpatient Department of the Royal Free Hospital, London. All patients were on maintenance immunosuppression at the time of recruitment. Demographic and clinical data were recorded. PBMCs were isolated and IL-17 responses were determined in standard media and in media supplemented with 40mM NaCl using the assay outlined in 2.2.1. Th17 and Tc17 cell polarisation, and supernatant IL-17 concentrations, were compared between standard and high salt conditions. In addition, salt responsiveness of each of these readouts was determined for each subject. Salt responsiveness was defined by the readout

(Th17 and Tc17 cell frequency, IL-17 concentration) in high salt conditions expressed as a ratio to the readout in standard conditions (i.e. salt responsiveness of 1 = no difference between normal and high salt; salt responsiveness of 2 = result in high salt double that in normal media). Salt responsiveness was then compared between healthy controls, patients with AIKD, and KTRs.

All patients provided written informed consent prior to participation in the study (Royal Free Hospital Research and Development committee study identification number 7727).

2.4.2 T follicular helper (TfH) cell polarisation assay

To investigate the effect of NaCl on TfH responses, healthy control PBMCs were isolated and stored at -80^{o}C in 10% DMSO/90% fetal bovine serum until analysis. Cells were defrosted, washed, and stimulated for 72 hours with anti-human CD3 (10ug/ml plate bound) and anti-human CD28 (1ug/ml) in XVIVO15 media with and without additional 40mM NaCl. On day 3, cells were restimulated for 4 hours with PMA (50ng/ml) and ionomycin (1ug/ml; Sigma, cat#I9657) in the presence of brefeldin A (5ug/ml). Cells were then stained for viability (eFluor450), CD4 (CD4-FITC), CXCR5 (anti-human CD185 (CXCR5) – APC; BioLegend, Cat# 356908), and IL-21 (anti-human IL21 – PE; BioLegend, cat# 516704), and analysed by FACS. Gates for cytokine expression were determined by fluorescence minus one (FMO) (**Figure 2.13**). The proportion of CD4+ cells expressing CXCR5 (TfH cells) and IL-21 were determined, as was the proportion of TfH cells (CD4+CXCR5+) expressing IL-21. These were then compared between standard stimulating conditions and stimulation in the presence of +40mM NaCl.

Figure 2.13: Gating used during analysis of TfH Cells

CXCR5 and IL-21 gates in CD4+ cells were determined by FMO
Top panel: Lymphocytes were gated on a FSC-SSC plot; single cells on a FCS-A-FCS-H plot; and live cells were gated on a FSC-Viability dye plot

Second Panel: CXCR5 expression in CD4+ cells was determined by CD4-CXCR5 gating; left panel demonstrates FMO.
Third panel: IL-21 expression in CD4+ cells was determined by CD4-IL-21 gating; left panel demonstrates FMO.
Bottom panel: IL-21 expression by TfH cells was determined by gating single live lymphocytes on an FCS-CD4 plot (not shown), followed by CXCR5-IL21 gating; left panel demonstrates FMO.

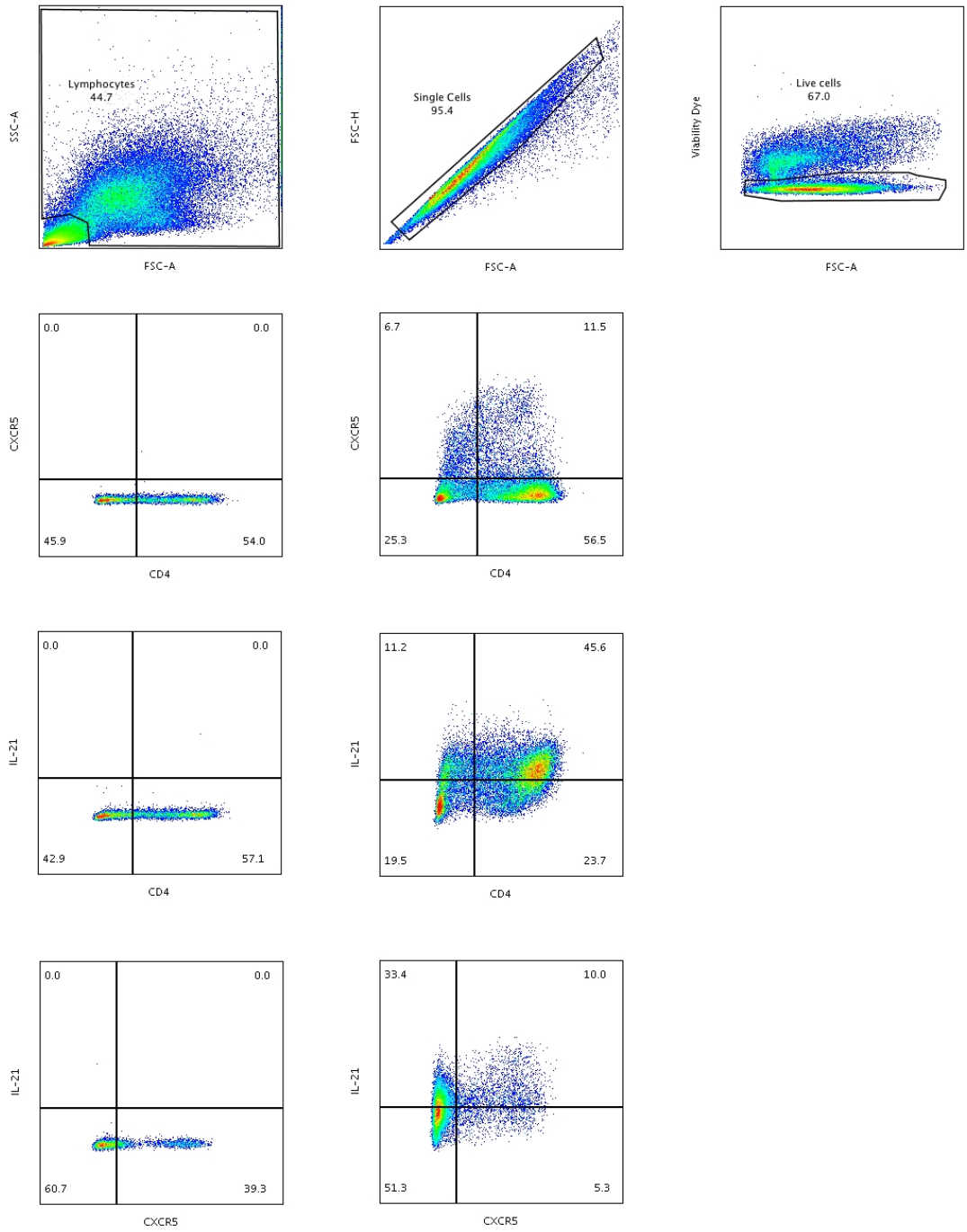

2.4.3 Nephrotoxic nephritis animal model of glomerulonephritis

The nephrotoxic nephritis (NTN) model was used to investigate the effect of high dietary salt on the development of glomerulonephritis. This model is mediated by the injection of nephrotoxic serum (NTS), which contains sheep

immunoglobulin targeted against mouse glomerular antigens. 2 experiments were undertaken.

Experiment 1

C57Bl/6 8-12 week male mice were pre-immunised by subcutaneous injection of sheep immunoglobulin (200ug per mouse; Sigma-Aldrich, cat# I5131) in Complete Freud's Adjuvant (CFA) (100ul per mouse; Sigma-Aldrich, Cat# F5881). 5 days later, NTS (100ul per mouse) and lipopolysaccharide (LPS) (0.5ug per mouse) were injected via the tail vein to induce disease. On day 6 after disease induction, mice were transferred to metabolic cages, and sacrificed 24 hours later. 8 mice were fed standard chow and tap water ('normal salt' diet), and 8 mice were fed chow supplemented with 4% NaCl and 1% NaCl drinking water from the time of pre-immunisation until time of sacrifice ('high salt' diet).

Experiment 2

A subsequent experiment was undertaken with a period of salt loading prior to the induction of milder disease. In this experiment C57Bl/6 8-12 week male mice had disease induced via tail vein injection of NTS (100ul per mouse) and LPS (0.75ug per mouse) without preimmunisation. On day 12 and 13 (half the mice in each group on each day for logistic reasons), mice were transferred to metabolic cages, and sacrificed 24 hours later. 7 mice were fed standard chow and tap water ('normal salt' diet), and 7 mice were fed chow supplemented with 4% NaCl and 1% NaCl drinking water from 2 weeks prior to induction of disease until time of sacrifice ('high salt' diet).

In both experiments, all urine was collected during the 24-hour period mice were in metabolic cages, blood was collected via cardiac puncture at the time of sacrifice, and kidneys were retrieved after sacrifice. One kidney was preserved in formalin for histological analysis and in experiment 2 the other in phosphate buffered saline (PBS) for FACS analysis of Th17 cells infiltrating the kidney, as below. 24-hour urine volume was recorded, urine dipstick

undertaken, and urine protein (sulphasalicylic acid test) and creatinine were quantified (Jaffe method; R and D Systems). Serum creatinine and sodium were measured by an automated analyser (The MRC Harwell Institute). Kidneys were stained with haematoxylin and eosin, and periodic acid-schiff stains. Each histological section was scored in a blinded manner according to the following criteria:

1. Glomerular crescents: not present =0; present = 1. A total of 25 glomeruli were scored and the mean score reported.
2. Glomerular thrombosis: not present = 0, present affecting ¼ of the glomerulus = 1, present affecting ½ of the glomerulus = 2, present affecting ¾ of the glomerulus = 3, present affecting all of the glomerulus = 4. A total of 25 glomeruli were scored and the mean score reported
3. Tubular Dilatation (area of biopsy affected at x10 magnification): 0-5% = 0; 6-10% = 1; 11-25% = 2; 26-45% = 3; 46-75% = 4; 76-100% = 5.
4. Tubular Casts (area of biopsy affected at x10 magnification): 0-10% = 0; 11-30% = 1; 31-50% = 2; 51-75% = 3; >75% = 4.

A combined histological score was defined by the sum of these individual component scores. All variables were compared between normal salt and high salt fed animals.

FACS analysis of lymphocytes infiltrating the kidney was undertaken in experiment 2. For this, kidneys were cut into small pieces, washed in PBS, and then digested through a 70uM filter. Further digestion was undertaken by incubation in 1ml of digestion solution (RPMI with 1% penicillin/streptomycin, 0.4mg/ml collagenase D, 0.01mg/ml DNAase, 10% fetal bovine serum, 1% 1M HEPES) for 40 minutes at 37^{o}C. Kidneys were then digested through a 40uM filter, followed by incubation in red blood cell lysis buffer for 2 minutes in the dark. Cells were washed, counted, and transferred to a 96 well round bottom plate at 0.5million cells/well. Cells were then stimulated for 4 hours with PMA (50ng/ml) and ionomycin (1ug/ml) in the presence of brefeldin A (5ug/ml). Cells were subsequently stained for viability (eFluor450), blocked for

15 minutes with Fc block (purified anti-mouse CD16/32; BioLegend, cat#101302), then stained for CD4 (anti-mouse CD4-AF647; BioLegend, cat#100424), fixed/permeabilised (FOXP3/Transcription Factor staining set; eBioscience, cat#00-5523-00) and stained for IL-17 (anti-mouse IL-17A-PE; BioLegend, cat#506904), and analysed with FACS. The proportion of viable CD4+ and CD4- cells expressing IL-17 was determined; FMO was used to determine IL-17 gates (**Figure 2.14**).

Figure 2.14: Gating used during analysis of kidney Th17 Cells

IL-17 gating was determined by FMO

Top panel: Lymphocytes were gated on a FSC-SSC plot; single cells on a FCS-A-FCS-H plot; and live cells were gated on a FSC-Viability dye plot

Bottom Panel: IL-17 expression in CD4+ and CD4- cells was determined by CD4-IL-17 gating; left panel demonstrates FMO and right panel IL-17 stained sample.

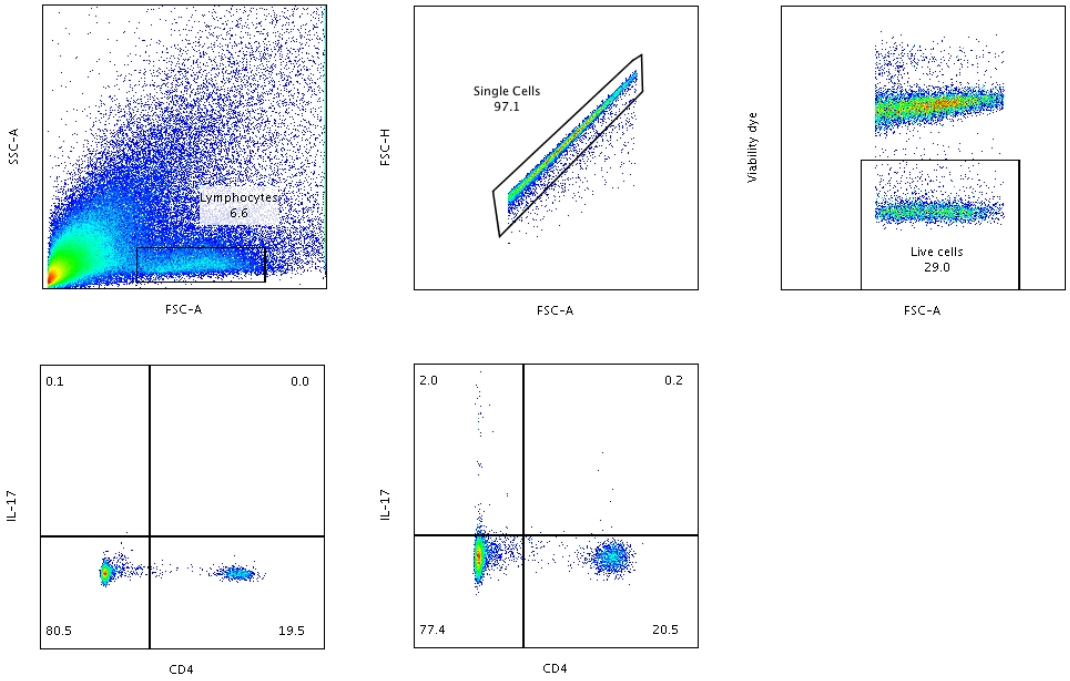

2.4.4 Investigating the feasibility of dietary salt restriction in healthy controls and its impact on IL-17 responses

A pilot study was undertaken to assess the feasibility of a 1-week low salt diet, and to determine its effect on T cell subtypes. Healthy volunteers were

recruited and baseline demographic data collected. The following were measured:

a. **Physiological parameters**: weight, systolic blood pressure, diastolic blood pressure, pulse rate. Blood pressure and pulse were measured by automated machine; the mean of 3 measurements was recorded.
b. **Body composition** as determined by bioelectrical impedance analysis (InBody Technology). Total body water (TBW), and extracellular water/total body water (ECW/TBW) are reported.
c. An assessment of **salt intake:** through use of a validated questionnaire (Appendix 8.2)**.** A score of >65 on this questionnaire represents high salt intake.
d. An assessment of **T cell subsets** (Th17 and Treg), as below.

For T cell subset analysis, PBMCs were isolated and fresh cells were stimulated for 4 hours with PMA (50ng/ml) and ionomycin (1ug/ml) in the presence of brefeldin A (5ug/ml). Cells were stained for viability (eFluor450), CD4 (CD4-FITC), fixed/permeabilised (Foxp3 / Transcription Factor Staining Buffer Set), and then stained for FOXP3 (anti-human FOXP3 – Alexa fluor 647; BioLegend, cat#320114) and IL-17 (IL-17–PE), and analysed by FACS. The proportion of CD4+ and CD4- cells expressing IL-17, and the proportion of CD4+ cells expressing FOXP3, were determined (**Figure 2.15**).

Figure 2.15: Gating used during analysis of Th17 and Treg cells in healthy controls undergoing dietary salt restriction

FOXP3 and IL-17 gating were determined by FMO
Top panel: Lymphocytes were gated on a FSC-SSC plot; and live cells were gated on a FSC-Viability dye plot
Middle Panel: FOXP3 expression in CD4+ cells was determined by CD4-FOXP3 gating; left panel demonstrates FMO and right panel FOXP3 stained sample.
Bottom Panel: IL-17 expression in CD4+ and CD4- cells was determined by CD4-IL-17 gating; left panel demonstrates FMO and right panel IL-17 stained sample.

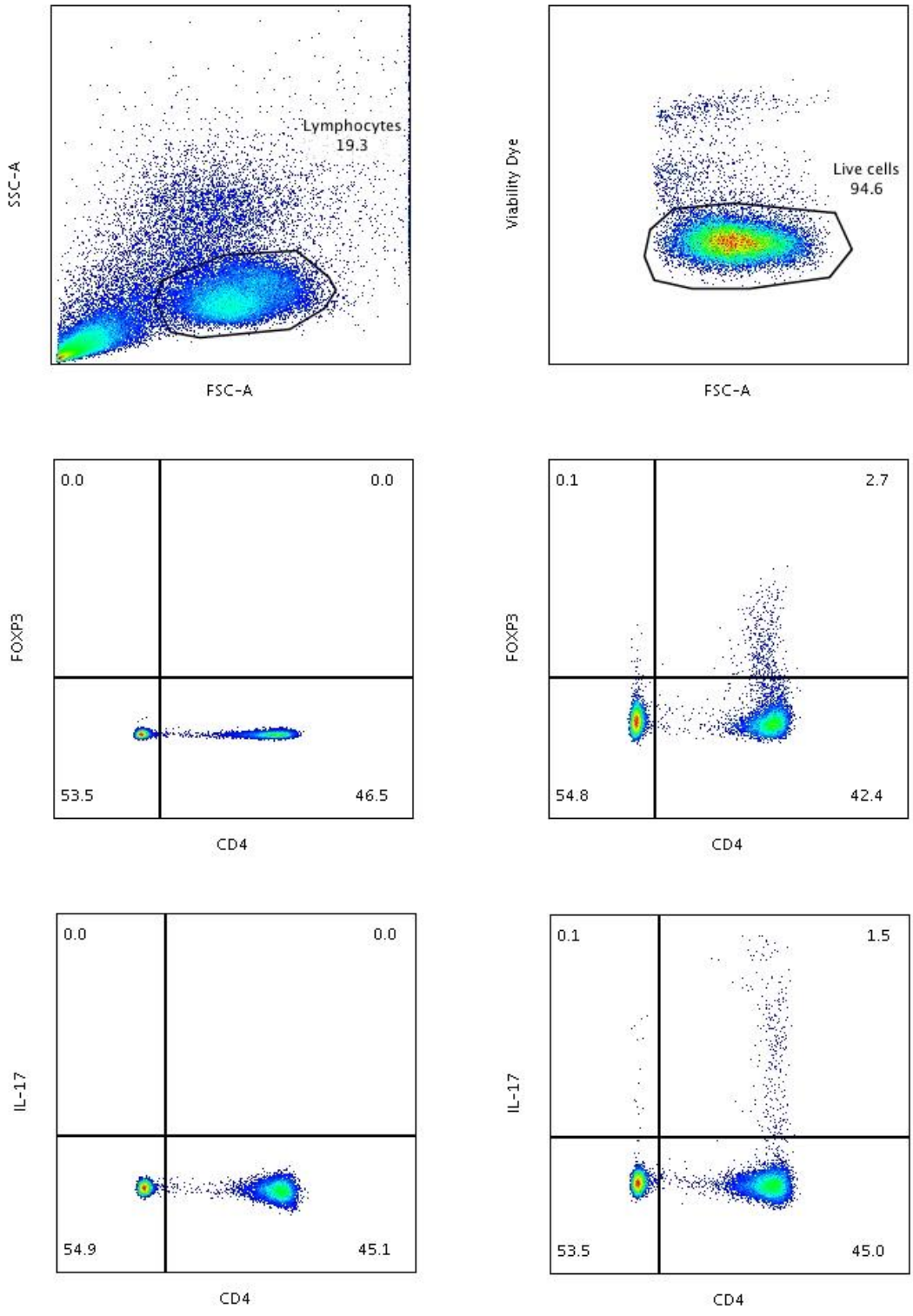

After baseline analysis ('pre-low salt'), subjects were counseled on the salt content of common foodstuffs and requested to eat a diet containing a

maximum of 2.5g salt (1g sodium) per day for 7 days. At the end of intervention, all analyses undertaken at baseline were repeated ('post-low salt'). These analyses were repeated a third time 10-14 days after return to standard diet ('2 weeks back on normal diet') (**Figure 2.16**). Results were compared between the 3 time-points using a non-parametric analysis of variance (Friedman), with multiple comparison testing (Dunn's).

Figure 2.16: Pilot study flowchart (salt restriction in healthy volunteers)

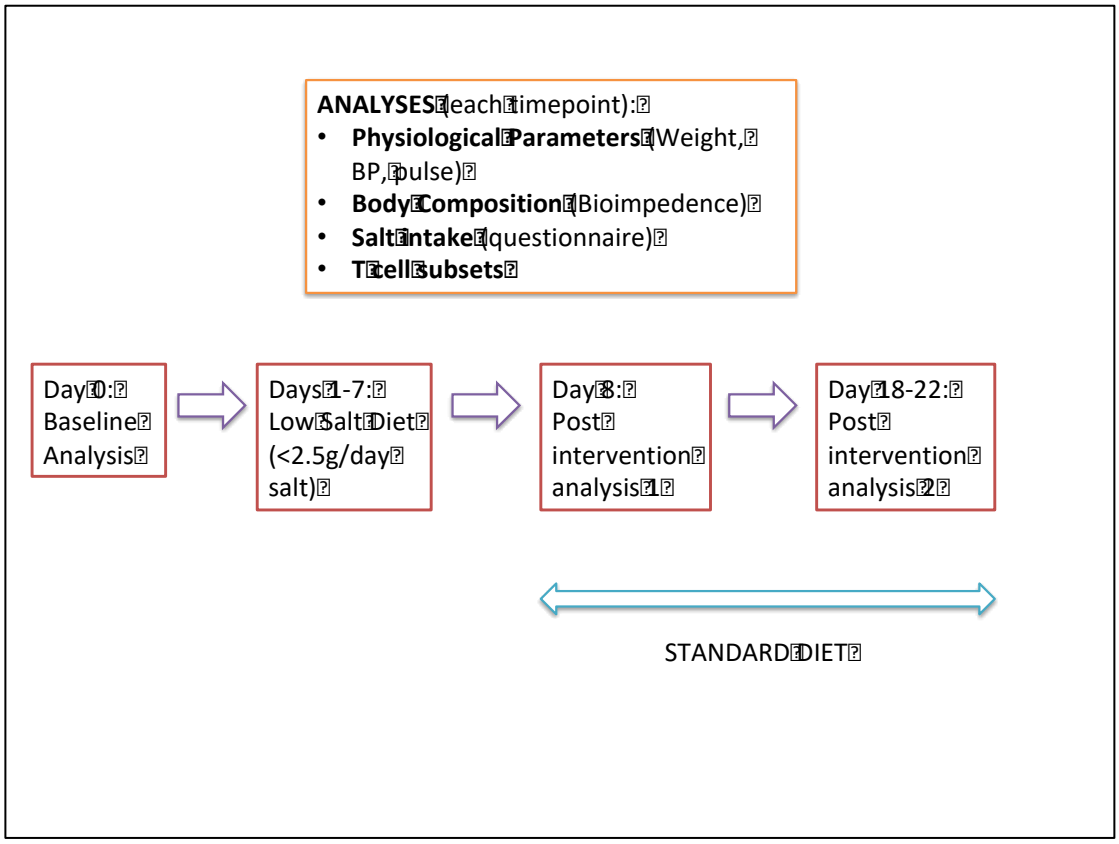

2.4.5 Prospective cohort study of immune responses to sodium minimisation through dietary salt restriction in kidney transplant recipients (KTRs)

A prospective cohort study was designed to investigate the safety and feasibility of short-term sodium restriction in KTRs and determine its effect on sodium storage and IL-17 immune responsiveness. The full study protocol

that received Health Research Authority (HRA) approval has been provided alongside this thesis. A summary of the methods is outlined below.

2.4.5.1 Objectives

Primary

To determine if short-term dietary salt restriction to < 2.5g/day over 1 week is safe and feasible in KTRs.

Secondary

To determine if short term dietary salt restriction to < 2.5g/day over 1 week affects:

- Skin and muscle sodium stores, as assessed by ^{23}Na-MRI
- Circulating CD4+ T cell subsets (Th1, Th2, and Th17)
- TfH responses, as assessed in 3 day culture experiments

2.4.5.2 Inclusion and exclusion criteria

Inclusion criteria

- Renal allograft recipients (cadaveric or live donor): age >18, male or female, >1 year post transplant, eGFR >30ml/min (estimated using modification of diet in renal disease [MDRD] equation).

All patients were required to be taking minimal immunosuppression, defined as: ≤10mg/day prednisolone, ≤150mg/kg azathioprine, ≤1g/day MMF, no depleting or non-depleting antibody treatment (including antithymocyte globulin, alemtuzumab, and rituximab) within the last 6 months.

Exclusion criteria

- Patients <18 years old, and patients unable to provide written informed consent.

- Patients with hypotension (symptomatic or systolic blood pressure <90mmHg) at baseline, and those already taking a diuretic (any).

Other medications that may interfere with sodium transport (e.g. Angiotensin converting enzyme inhibitors, angiotensin receptor blockers, aldosterone receptor antagonists) were permitted as long as there is no dose alteration during intervention.

- Patients with electrolytes (serum sodium and potassium) outside the normal range at baseline.

- Pregnant and breastfeeding women.

2.4.5.3 Trial design and methods

Patients meeting inclusion criteria were recruited from transplant clinics at the Royal Free Hospital, London, UK.

Baseline assessment

The following were recorded:

1. *Demographic and clinical data*

Including details of underlying kidney disease, details of transplantation, and current medications. Baseline haematology (full blood count) and biochemistry (serum urea, creatinine, electrolytes, C-reactive protein, and immunoglobulins) analyses were performed by automated analyser in NHS clinical laboratories.

2. *Sodium intake assessment*

Via a validated questionnaire (Appendix 8.2). A total score of >65 points signifies increased salt intake.

3. *Sodium Store assessment*

Via lower limb 23Na-MRI, using the method outlined in 2.3.2.

4. *Blood pressure and weight*

Blood pressure was measured via automated machine after the patient was seated for 5 minutes. 3 blood pressures were undertaken, and a mean of the second and third recordings taken. Weight was recorded with shoes removed.

5. *Immune responses*

20ml blood was collected in EDTA tubes and PBMCs isolated and frozen as per the procedure outlined in 2.1. Once samples from each of the assessment time points had been collected, these were then defrosted together and analysed at the same time. The following analyses were undertaken:

i. **CD4+ subsets**. Circulating Th1, Th2, and Th17 subsets were determined as per the method outlined in 2.3.5.
ii. **TfH responses**. TfH cell polarisation was assessed in the method outlined in 2.4.2.

<u>Treatment procedures</u>

Patients underwent sodium minimisation through dietary salt restriction to <2.5g/day over 1 week. This was achieved through counselling on the salt content of foods, and advice on how to minimise salt intake. This was individually tailored to responses in the baseline sodium intake questionnaire.

<u>Subsequent assessments</u>

At the end of intervention, all assessments undertaken at baseline were repeated. A questionnaire on the tolerability of the intervention was also undertaken (Appendix 8.3). A further clinical assessment and an assessment

of immune responses were repeated again at 2-4 weeks after completion of intervention (**Figure 2.17**).

Any adverse events were recorded throughout the intervention period.

Figure 2.17: Study Protocol Flowchart (salt restriction in KTRs)

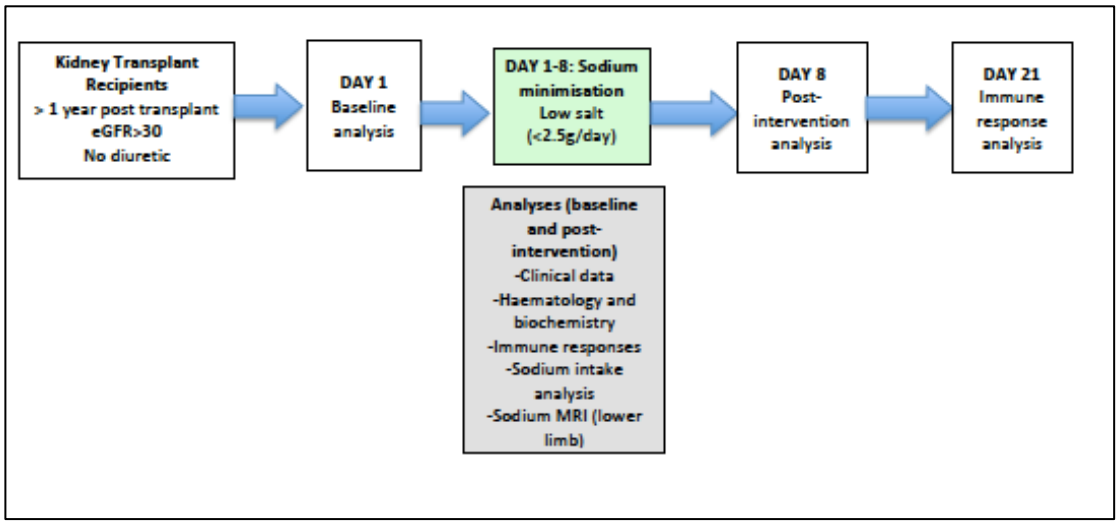

2.4.5.4 Sample size and recruitment

A sample size of 10 patients was estimated to be sufficient to detect a difference of at least 1% in the th17 population using a paired-sample t-test, assuming a standard deviation of 0.5% for the Th17 population within a patient with a power of 90% and a significance level of 5%. This sample size calculation has accounted for the possibility of patient dropout, with an anticipated rate of 10% and was adjusted to account for the possibility of non-normal/skewed outcome data.

The aim was to recruit one patient per month, allowing the target of 10 patients to be recruited, and the subsequent analyses undertaken, within a 1-year period.

2.4.5.5 Statistical methodology and analysis

For variables that were recorded at all 3 assessment time points, differences were assessed with a one-way analysis of variance (non-parametric given small number of subjects) with multiple comparison testing. For variables collected only before and after intervention, differences were assessed with a Wilcoxon test. Variables compared included clinical data (haematology/biochemistry), sodium intake and stores, physiological parameters such as blood pressure and weight, and immune responses (CD4 subsets, and TfH polarisation).

2.4.5.6 Ethical and regulatory approvals

Approval for the study was provided by the Health Research Authority (London – Fulham Research Ethics Committee reference 18/LO/0214; protocol number 17/0620; IRAS project ID 223362). All patients were provided with a written information sheet and provided written informed consent prior to enrollment.

2.5 Buffers and solutions

2.5.1 FACS

FACS Wash

0.5% BSA, 0.1% NaN_3 diluted in PBS

Fixation solutions

Non-permeabilised cells: 4% paraformaldehyde

Permeabilised cells: Fix/perm solution (Invitrogen, Cat# 00-5523-00)

2.5.2 ELISA

Wash buffer

0.05% Tween 20 in PBS (pH 7.5)

Blocking buffer

3% BSA in PBS (pH 7.5)

Reagent diluent

1% BSA in PBS (pH 7.5)

Substrate solution

1:1 mixture of colour Reagent A (H_2O_2) and colour Reagent B (Tetramethylbenzine) (R&D Systems)

Stop Solution

1M H2SO4 diluted in dH2O

3 CHAPTER 3: THE EFFECT AND MECHANISM OF SODIUM CHLORIDE ON *IN VITRO* IL-17 RESPONSES

3.1 Introduction

Initial research on the effect of salt on adaptive immunity focused on its polarising effect on IL-17 expressing CD4+ cells (Th17 cells)[52,53]. *In vitro* experiments demonstrated that adding NaCl (40mM) to isolated naïve CD4+ cells cultured in optimal IL-17 conditions increased Th17 polarisation. The *in vivo* consequence of salt driven Th17 activation demonstrated in these studies was an exacerbated animal model of multiple sclerosis in mice fed a high salt diet. Since this initial work, further *in vivo* studies have shown that high salt diets exacerbate animal models of other autoimmune diseases including inflammatory bowel disease and lupus nephritis, and the polarising effect of NaCl on CD4+ T cells has been confirmed[51,54,56]. The effect, however, of NaCl on IL-17 expression by CD4-negative cells (e.g. IL-17 expressing CD8+ cells; Tc17 cells) is undetermined; moreover, there is debate over the respective effects of NaCl on naïve and memory cell populations[59].

The intracellular pathway that mediates the NaCl effect on Th17 cells has been shown to include up-regulation of p38-MAPK, SGK1, and NFAT5[52,53]. However, how increased extracellular sodium signals to intracellular pathways in human T cells is unknown. In mice, sodium has been shown to enter dendritic cells through amiloride sensitive channels including the alpha and gamma subunits of the epithelial sodium channel (ENaC) and the sodium hydrogen exchanger 1 (NHE1); sodium is then exchanged for calcium via reverse mode action of the sodium-calcium exchanger (NCX) leading to an increase in intracellular calcium that subsequently mediates inflammation[49]. In murine T cells, sodium entry and up-regulation of SGK1 is dependent on the furosemide sensitive sodium potassium chloride transporter NKCC1[142].

Multiple sodium channels and transporters have therefore been shown to be involved in the inflammatory effect of sodium on leucocytes in animals, but which sodium transport mechanisms are relevant in human IL-17 expressing T cells is unknown. Moreover, how sodium flux alters the intracellular concentrations of other cations, in particular calcium, and whether this is relevant in sodium T cell signalling is undetermined.

Autosomal recessive Pseudohypoaldosteronism Type 1 (AR PHA1) results from inherited inactivating mutations in one of the SCNN1 subunit genes which encode the subunits of the epithelial sodium channel (ENaC)[117]. Impaired ENaC function results in defective sodium reabsorption in the distal nephron and a biochemical phenotype that mimics aldosterone deficiency: salt wasting and relative hypotension associated with hyperkalaemic metabolic acidosis. Recurrent lower respiratory tract infections are reported in AR PHA1 patients and this has been attributed to defective respiratory salt transport and a clinical phenotype mimicking cystic fibrosis[138]. ENaC, as above, has been shown to be expressed on innate immune cells and be involved in sodium-mediated inflammation. Whether ENaC is involved in sodium signalling in adaptive immune cells and whether patients with AR PHA1 (defective ENaC) have altered immunity has not been previously investigated.

3.2 Aims

i. to investigate the effect of NaCl on *in vitro* IL-17 responses in CD4+ and CD4- cells
ii. to determine the mechanism of NaCl induced inflammation focusing on sodium transport mechanisms in human T cells, and the effect of sodium on calcium flux during T cell activation
iii. to investigate immunity in patients with AR PHA1

3.3 Brief Methods

Initial experiments were undertaken to optimise the 7-day Th17 polarisation assay, subsequently used in multiple parts of the project. Healthy control PBMCs were stimulated with anti-CD3/28 with and without Th17 polarising cytokines for 7 days. Supernatant IL-17 concentrations were measured by ELISA and Th17 polarisation was measured with FACS. Once consistent, 7-day culture experiments were undertaken in the presence of NaCl (0-80mM) and the effect on Th17 and Tc17 polarisation recorded. The effect of NaCl on isolated naïve and memory cells was also determined.

To investigate the mechanism of sodium mediated IL-17 inflammation experiments were repeated in the presence of alternative osmoles (Na gluconate, mannitol, and urea). Final supernatant osmolality was measured and correlated with Th17 and Tc17 polarisation. ENaC and NCC expression on immune cells were determined by immunostaining and flow cytometry. Sodium channel and transporter inhibitors (amiloride, furosemide, hydrochlorothiazide and the NCX inhibitor KB-R7943) were added to culture conditions and their effect on IL-17 responses assessed. Next the effect of sodium and alternative osmoles on calcium flux during T cell activation was investigated. This was done using a ratiometric calcium dye (Indo-1) with real time analysis using FACS. The effect of sodium transport inhibitors on calcium flux was also assessed.

Lastly, immunity was investigated in patients with AR PHA1. Patients were recruited from tertiary tubular disorder clinics. Clinical features of altered immunity were recorded. Patients subsequently underwent analysis of lymphocyte subsets, T cell activation and proliferation, calcium flux during T cell activation, and IL-17 responses in the presence and absence of salt. One patient underwent a comprehensive assessment of cytokine production using whole blood assays.

3.4 Results

3.4.1 Th17 polarisation assay

14 experiments using cells from 8 healthy controls were undertaken to confirm the effect of polarising cytokines on IL-17 responses. Upregulation of IL-17 expression in the presence of polarising cytokines (IL-1, IL-6, IL-21, IL-23, TGFβ), as determined by both FACS and ELISA, was consistently demonstrated (Figure 3.1). Th17 polarisation in optimal conditions was assessed in the same subject at 5 different time points. The coefficients of variation in Th17 polarisation as determined by FACS (% CD4+ cells expressing IL-17) and ELISA (supernatant IL-17 concentration) were 56.5% and 75.4% respectively. A consistent effect of using polarising cytokines to promote IL-17 responses was therefore confirmed, albeit with data to suggest reasonable variation across time points within individuals, which may reflect true biological variation or variability within the assay.

Figure 3.1: Confirmation of the effect of polarising cytokines on IL-17 responses

ns – not significant (p>0.05), *p≤0.05, **p≤0.01, ***p≤0.001, ****p≤0.0001

A. Th17 polarisation, expressed as the percentage of CD4 cells expressing IL-17 determined by FACS. Anti-CD3/28 stimulated 2.5% (1.6-5.6); anti-CD3/28 + cytokines 5.3% (2.6-9.1); p=0.0012. Compared with Wilcoxon test.

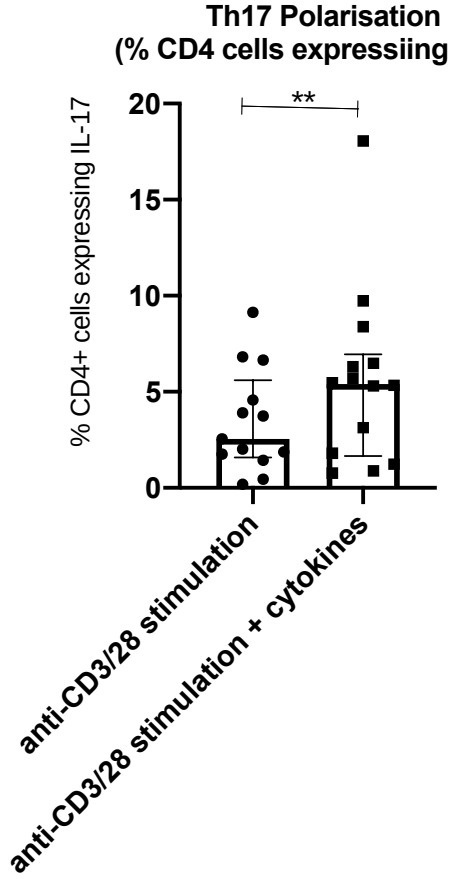

B. Th17 polarisation, expressed as median fluorescence intensity (MFI) of IL-17 staining in CD4+ cells as determined by FACS. Anti-CD3/28 stimulated 273AU (234-358); anti-CD3/28 + cytokines 327AU (286-419); p=0.0002. Compared with Wilcoxon test.

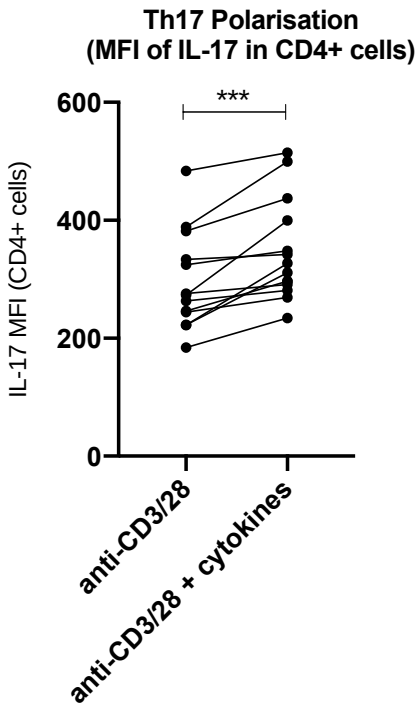

C. Supernatant IL-17 concentration, as determined by ELISA. Anti-CD3/28 stimulated 5215 pg/ml (2494-19403); anti-CD3/28 + cytokines 10766 pg/ml (6312-87509); p=0.002. Compared with Wilcoxon test.

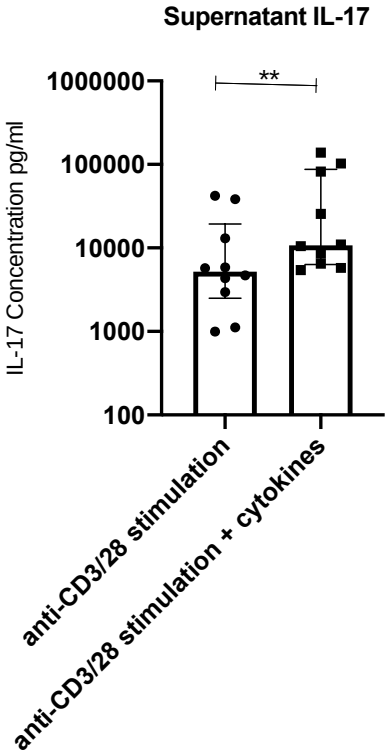

D. Th17 polarisation and supernatant IL-17 concentration (expressed as a ratio of polarisation in culture conditions containing cytokines compared to polarisation with anti-CD3/28 stimulation only; red line drawn at ratio of 1 representing no difference between conditions)

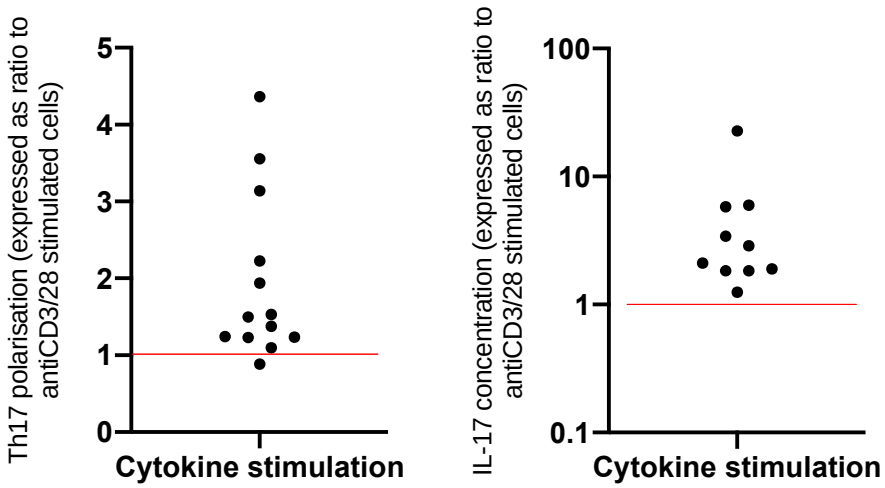

E. Representative FACS plots of IL-17 expression in CD4+ and CD8+ cells after stimulation with anti-CD3 and anti-CD28 with and without Th17 polarising cytokines (IL-1, IL-6, IL-21, IL-23, TGFβ)

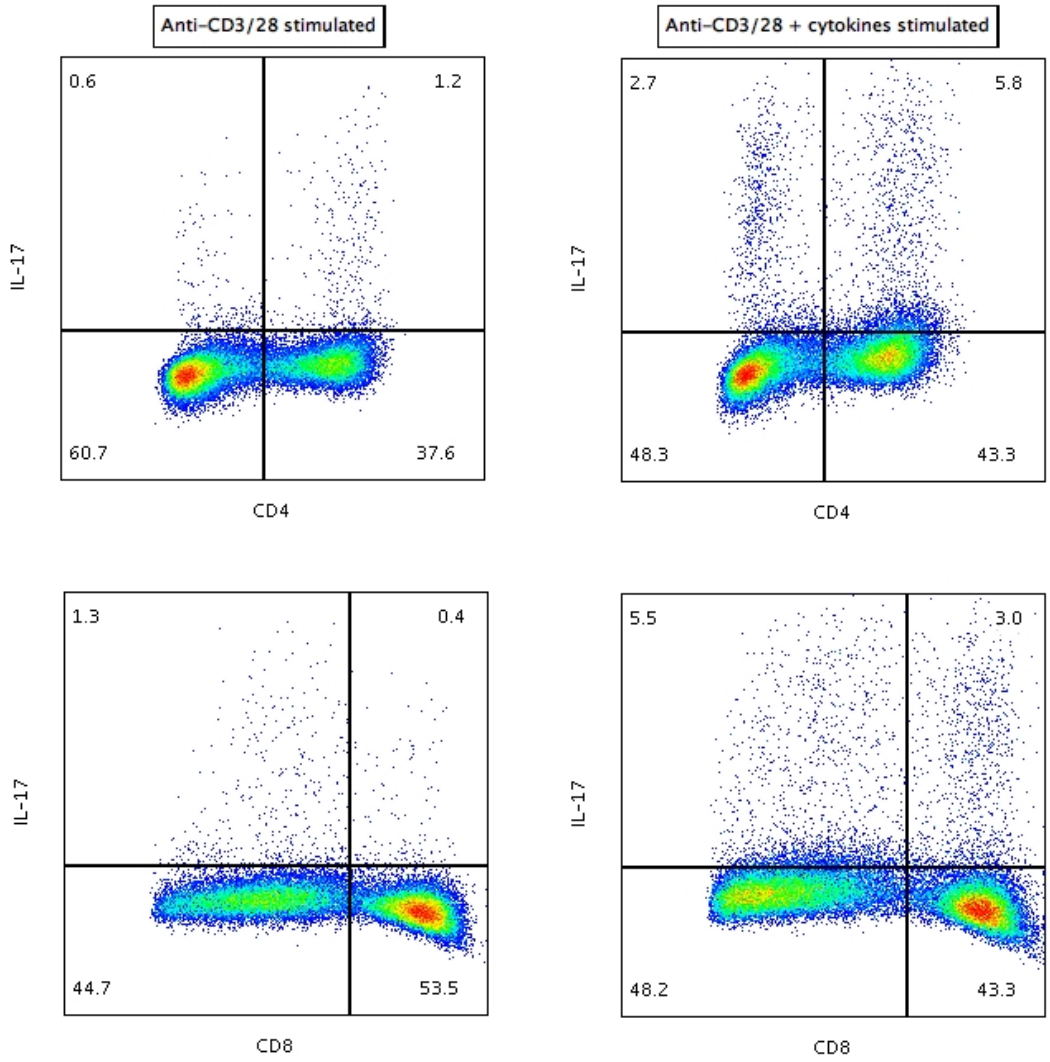

3.4.2 Sodium chloride increases IL-17 expression by both CD4+ (Th17) and CD8+ (Tc17) cells

The electrolyte concentrations of XVIVO15 media were measured to determine baseline extracellular ionic conditions (Table 3.1). NaCl +0-80mM (final Na concentration of 131-211mM) was then added to culture conditions (7 day culture in the presence of Th17 polarising cytokines) to assess its effect on IL-17 responses. NaCl promoted a dose dependent increase in IL17 expression in CD4+ (Th17) and CD8+ (Tc17) cells (Figure 3.2). Cell viability was unaffected in the +0-40mM range; there was an increase in cell death however when +80mM NaCl was added (Figure 3.2). Hence, +40mM NaCl

was used in subsequent experiments as the optimal high salt conditions for promotion of IL-17 responses.

Table 3.1: Measured ionic concentrations of unadjusted XVIVO15 media

Electrolyte	Concentration in XVIVO15 (measured; mmol/l)
Sodium	131
Chloride	98
Potassium	4.4
Magnesium	0.75
Calcium	1.29
Phosphate	0.92

Figure 3.2: The effect of NaCl on Th17 and Tc17 polarisation in cytokine stimulated cells

A. The effect of +0-80mM NaCl added to 7-day culture conditions on Th17 polarisation, shown as the percentage of CD4+ cells expressing IL-17 measured by FACS. Conditions compared with Kruskall-Wallis test. P=0.048.

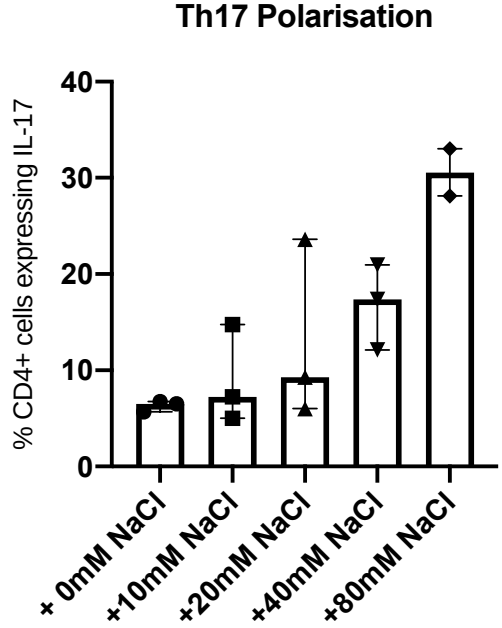

B. The effect of +0-80mM NaCl added to 7-day culture conditions on Th17 polarisation, shown as the MFI of IL-17 staining in CD4+ cells as measured by FACS. Conditions compared with Kruskall-Wallis test. P=0.02.

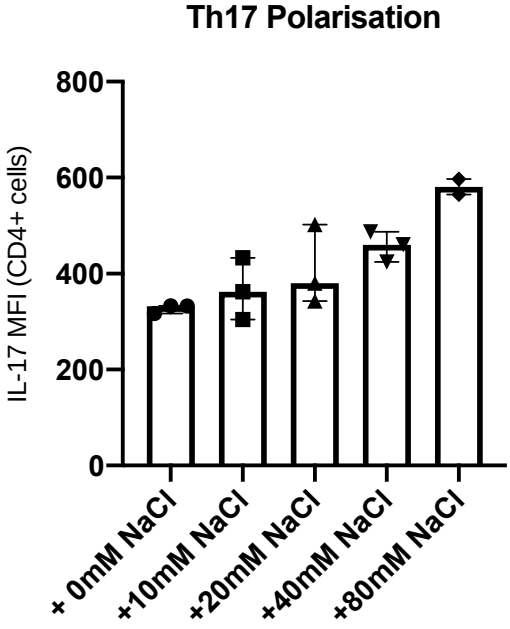

C. The effect of +0-80mM NaCl added to 7-day culture conditions on Tc17 polarisation, shown as the percentage of CD8+ cells expressing IL-17 measured by FACS. Conditions compared with Kruskall-Wallis test. P=0.037.

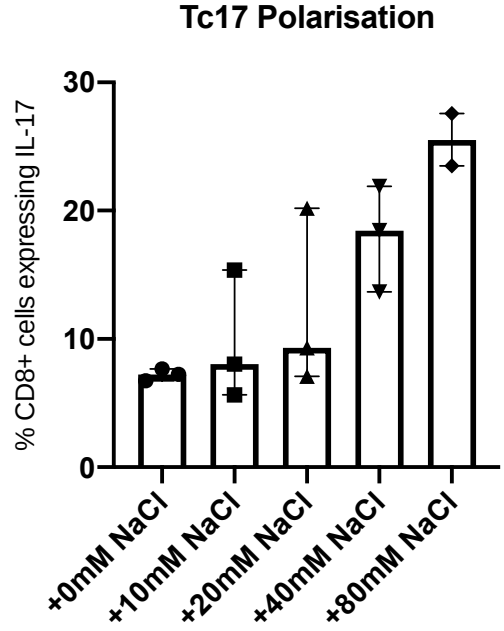

D. The effect of +0-80mM NaCl added to 7-day culture conditions on Tc17 polarisation, shown as the MFI of IL-17 staining in CD8+ cells as measured by FACS. Conditions compared with Kruskall-Wallis test. P=0.017.

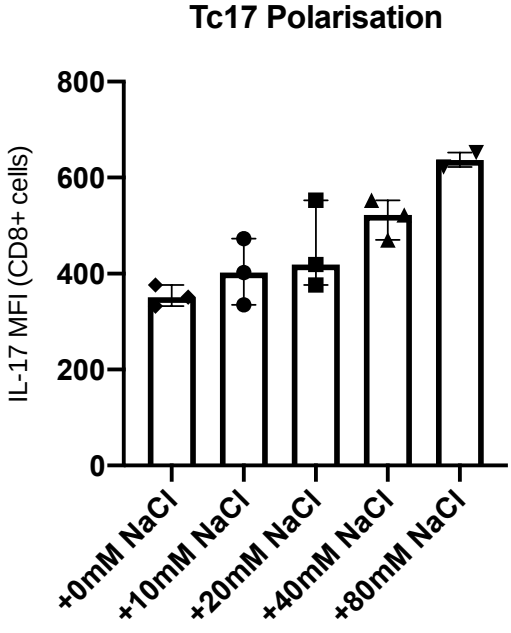

E. Representative FACS Plots of IL-17 expression in CD4 (top panel) and CD8 (bottom panel) cells with 0-80mM (left to right panels) NaCl added to culture conditions.

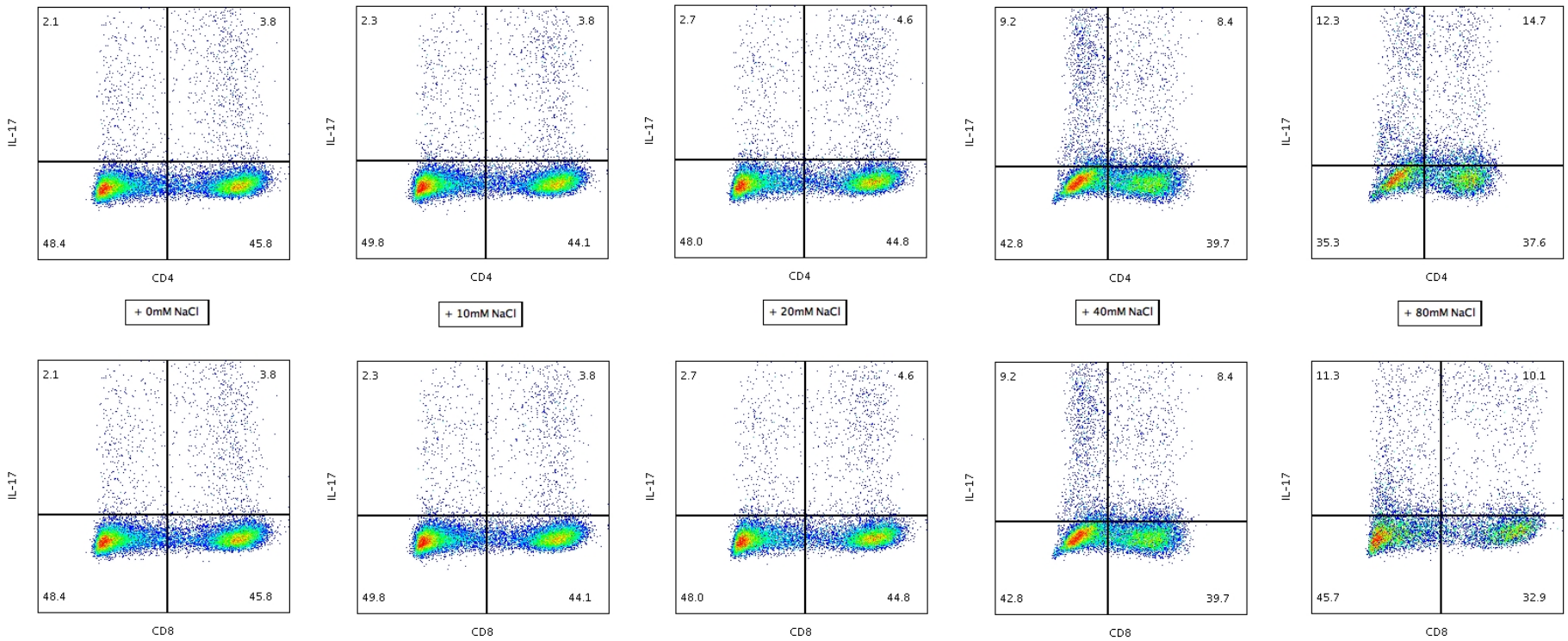

F. The effect of +0-80mM NaCl added to 7-day culture conditions on Lymphocyte viability

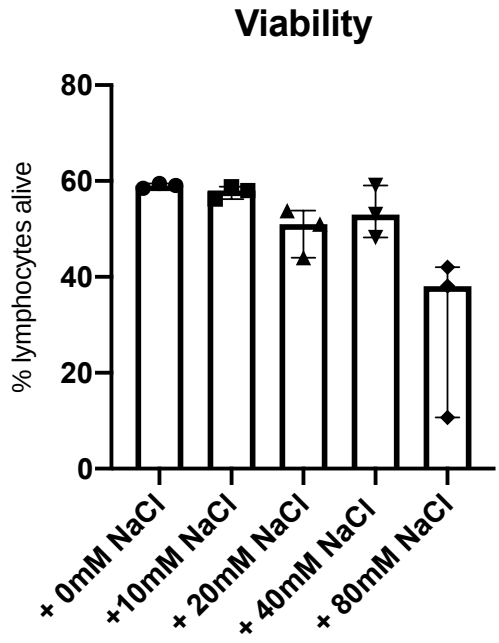

In addition to assessing the effect of NaCl on cells stimulated in the presence of Th17 polarising cytokines, the effect of NaCl was also assessed on anti-CD3 and anti-CD28 stimulated cells. NaCl promoted IL-17 expression in CD4+ and CD8+ cells stimulated with anti-CD3/28. Th17 and Tc17 polarisation in cells stimulated with anti-CD3/28 in the presence of +80mM NaCl was equivalent to cells stimulated with polarising cytokines in standard NaCl conditions (Figure 3.3). These initial experiments confirm the polarising effect of NaCl on Th17 cells, demonstrate that NaCl also promotes IL-17 expression in other T cell subtypes (Tc17 cells), and demonstrate that NaCl promotes IL-17 expression with non-specific T cell stimulation even in the absence of polarising cytokines.

Figure 3.3: The effect of NaCl on Th17 and Tc17 polarisation in anti-CD3/28 stimulated cells

A. Th17 polarisation in anti-CD3/28 stimulated cells and anti-CD3/28 + cytokine stimulated cells in different NaCl concentrations.

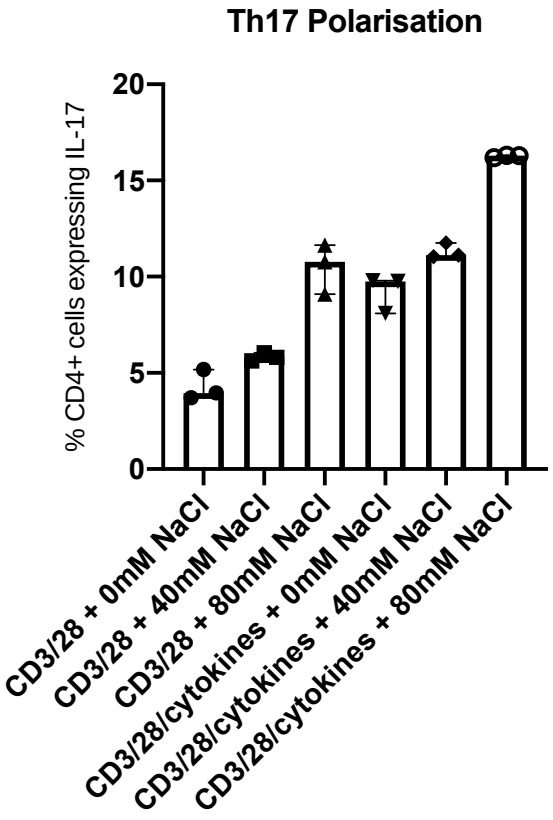

B. Tc17 polarisation in anti-CD3/28 stimulated cells and anti-CD3/28 + cytokine stimulated cells in different NaCl concentrations.

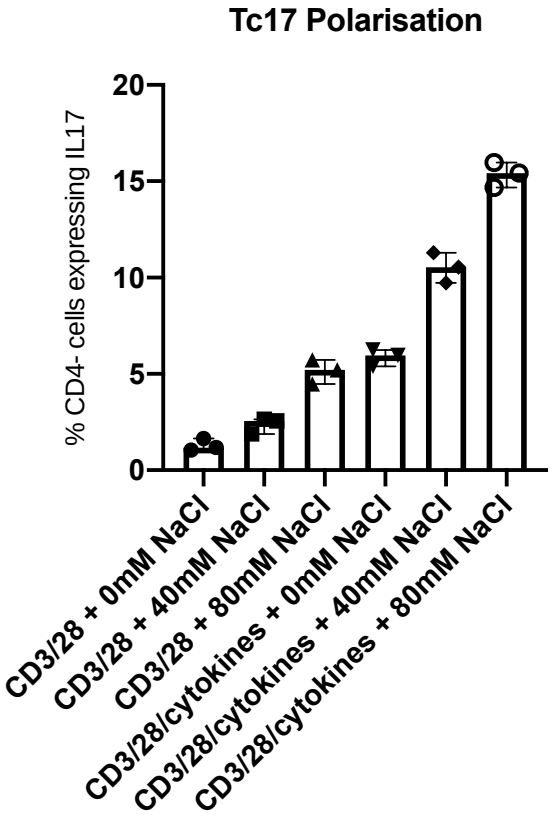

C. Supernatant IL-17 concentration in anti-CD3/28 stimulated cells and anti-CD3/28 + cytokine stimulated cells in different NaCl concentrations.

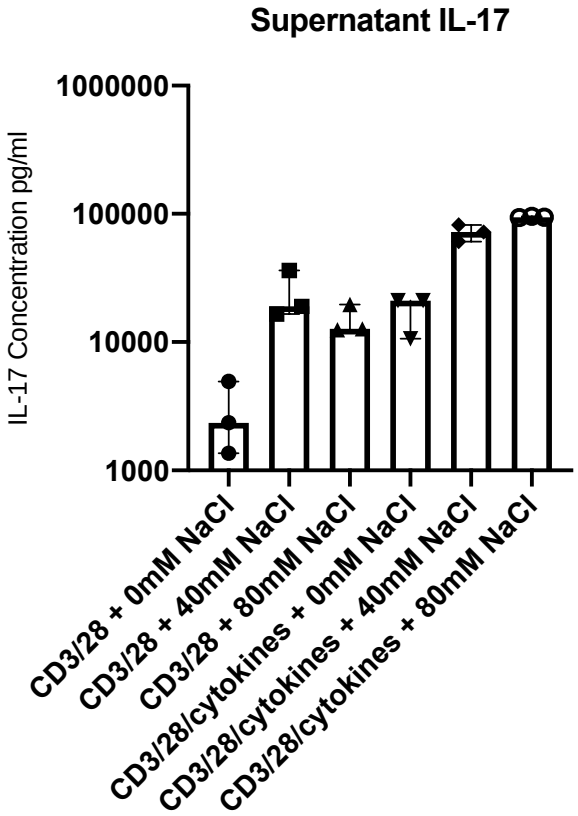

3.4.3 The polarising effect of NaCl on Th17 and Tc17 cells is consistent across healthy controls

The effect of NaCl on IL-17 responses was assessed in 26 healthy controls (aged 32 (28-42) years, 15 (58%) female). PBMCs were cultured in standard media and in media supplemented with 40mM NaCl. Th17 and Tc17 polarisation, and supernatant IL-17 concentrations increased in high salt conditions (Figure 3.4).

Figure 3.4: The effect of NaCl on IL-17 responses in healthy controls (n=26)

ns – not significant (p>0.05), *p≤0.05, **p≤0.01, ***p≤0.001, ****p≤0.0001
A. Th17 polarisation in unsupplemented media and in media supplemented with 40mM NaCl. Th17 cells as a percentage of CD4+ cells: +0mM NaCl 3.2% (2.5-6.3); +40mM NaCl 7.6% (4.6-12.4), median difference 2.9% (1.8-5.3), p<0.0001. Compared with Wilcoxon test.

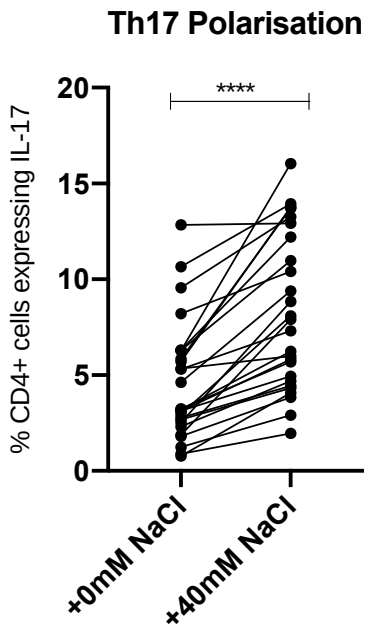

B. Tc17 polarisation in unsupplemented media and in media supplemented with 40mM NaCl. Tc17 cells as a percentage of CD4- cells: +0mM NaCl 1.5% (0.6-2.9); +40mM NaCl 3.2% (1.5-5.7), median difference 1.7% (0.7-3.3), p<0.0001. Compared with Wilcoxon test.

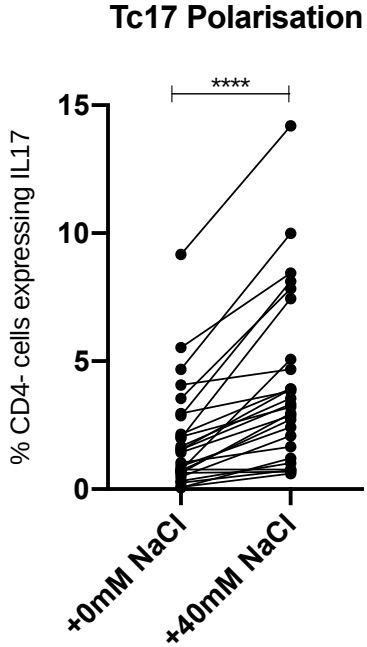

C. Supernatant IL-17 in cells stimulated in unsupplemented media and in media supplemented with 40mM NaCl. IL-17 concentration: +0mM NaCl 4287pg/ml (1681-11045); +40mM NaCl 9264pg/ml (4507-17565), median difference 3212pg/ml (1327-7078), p<0.0001. Compared with Wilcoxon test.

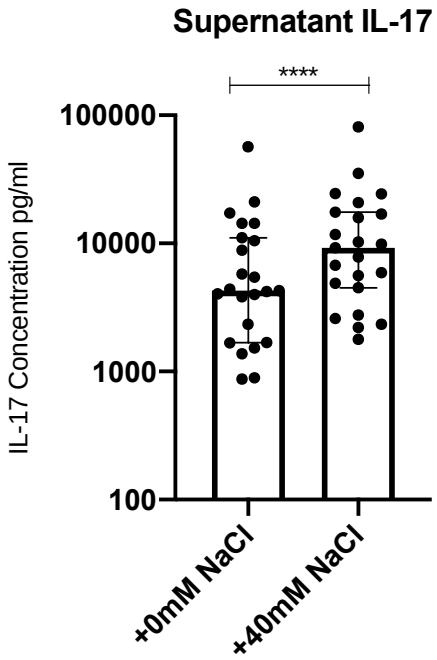

Median salt responsiveness (ratio of variable in high salt conditions: standard conditions) of Th17 and Tc17 cells across healthy controls were 1.9 (1.5-2.4) and 2.1 (1.6-3.4) respectively (Figure 3.5). Salt had no effect on supernatant IFNγ concentration (Figure 3.6). These experiments demonstrate a consistent polarising effect of NaCl on IL-17 responses across healthy individuals.

Figure 3.5: Salt responsiveness of Th17 and Tc17 cells

Salt responsiveness represents polarisation in high salt media (+40mM NaCl) as a ratio with polarisation in media with no NaCl supplementation; red line drawn at ratio = 1 represents no difference between conditions.

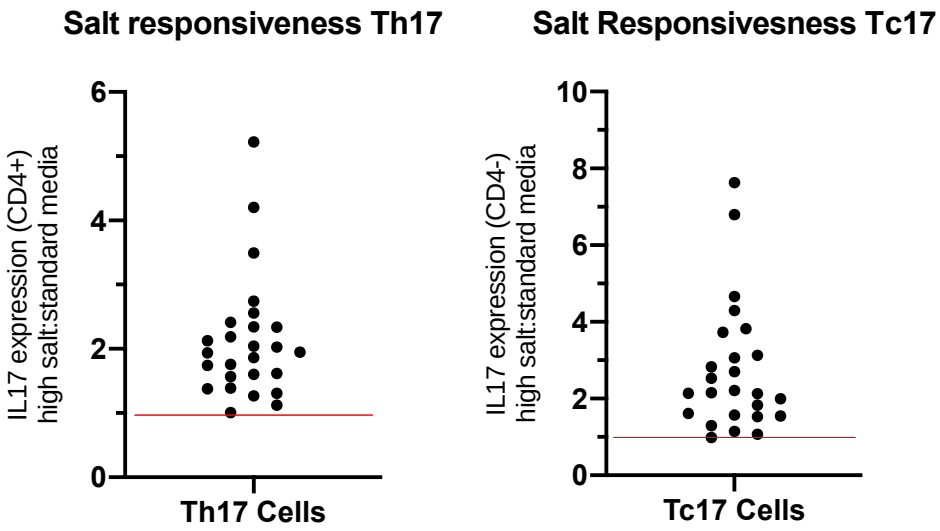

Figure 3.6: Effect of NaCl on supernatant IFNγ concentration (n=9)

IFNγ concentration: +0mM NaCl 27330pg/ml (18991-57668); +40mM NaCl 35309pg/ml (23647-49623); median difference -1922pg/ml (-11598-13306); p=0.82.

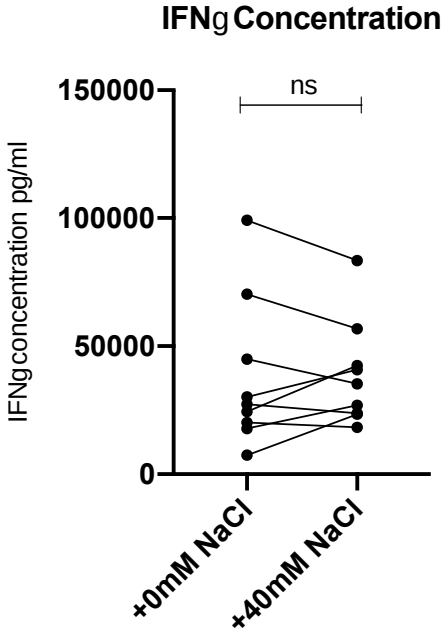

3.4.4 NaCl effects both naïve and memory T cell populations

Naïve (CD4+CD45RA+) and memory (CD4+CD45RO+) T cells were isolated from PBMCs and polarised to a Th17 phenotype in the presence and absence of salt (+40mM NaCl). Purity of cells isolated was confirmed (Figure 3.7).

NaCl increased Th17 polarisation in both isolated naïve and memory cell populations; naïve cells were more salt responsive than memory cells (Figure 3.8).

Figure 3.7: Purity of naïve and memory T cell isolation

Representative FACS plots and summary data of CD4 and CD45RO staining in whole PBMCs (left panel), isolated naïve (CD4+CD45RA+) and isolated memory (CD4+CD45RO+) cells

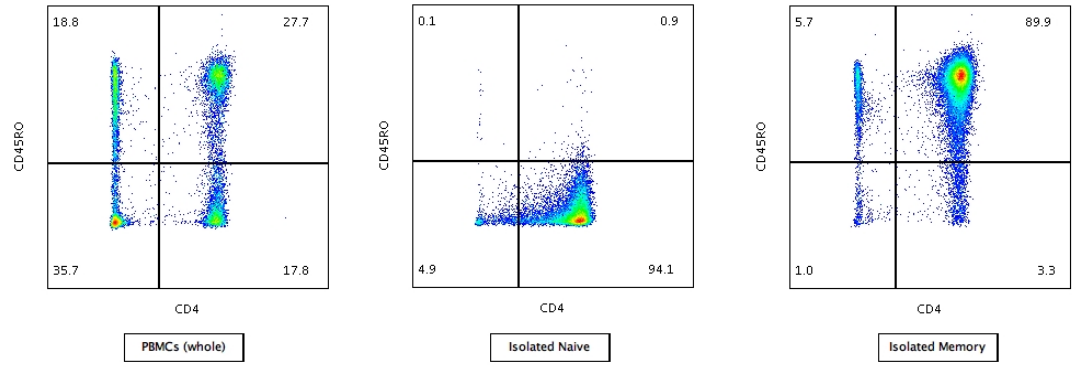

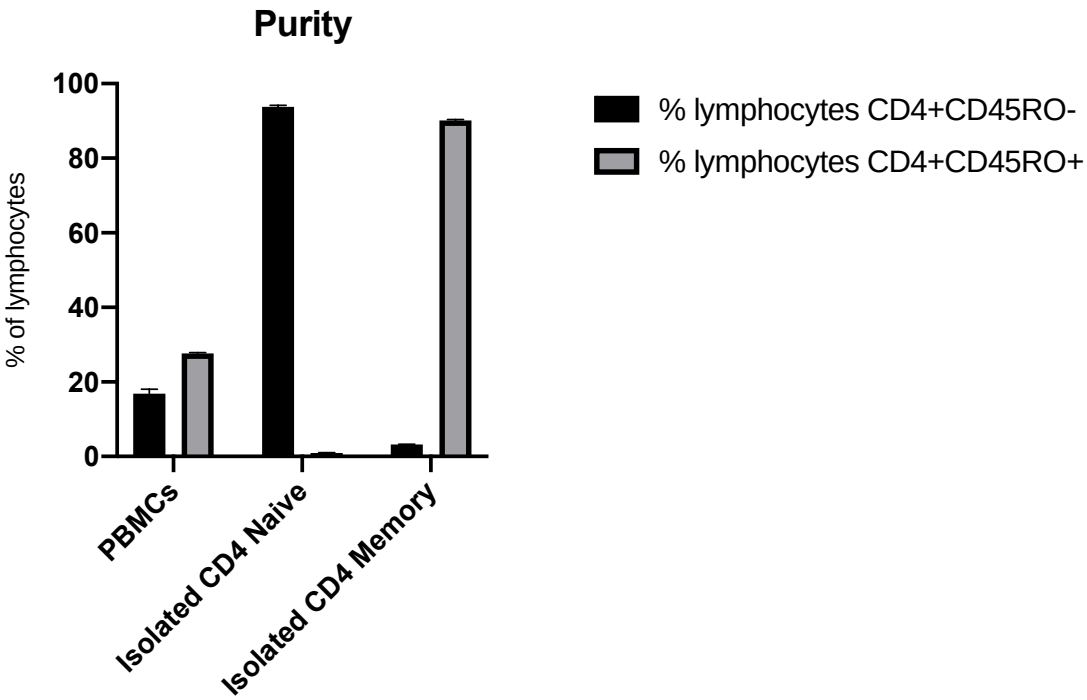

Figure 3.8: Effect of NaCl on IL-17 responses in naïve and memory T cells

Data represent one subject with analyses in triplicate.

A. Th17 polarisation in normal media and in media supplemented with 40mM NaCl in whole PBMCs and in isolated naïve and memory CD4+ cells.

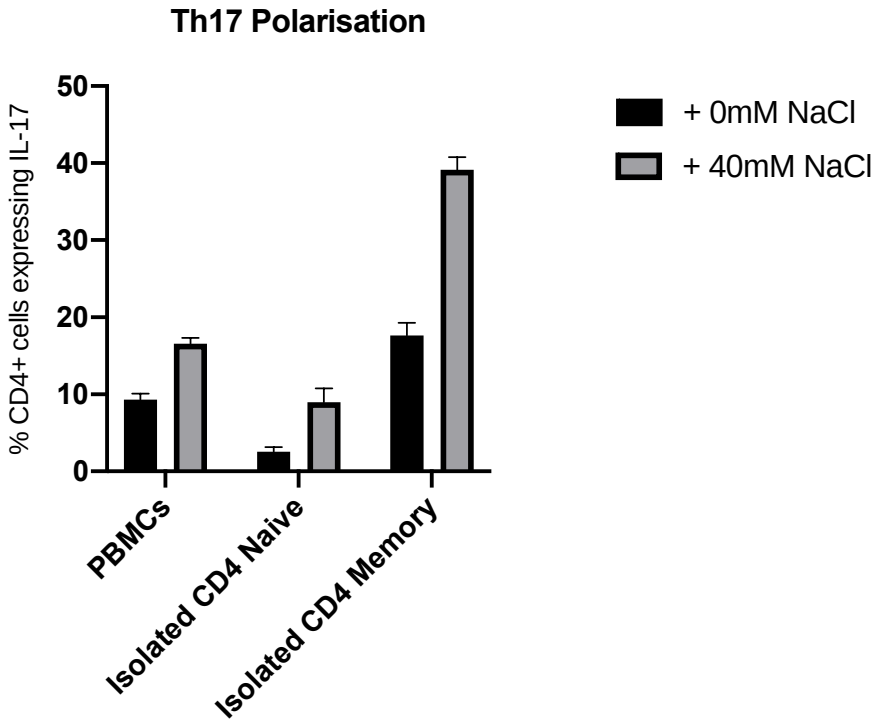

B. Salt responsiveness (Th17 polarisation in high salt media as a ratio to normal media) of whole PBMCs, isolated naïve and isolated memory CD4+ cells; red line drawn at ratio = 1 represents no difference between conditions.

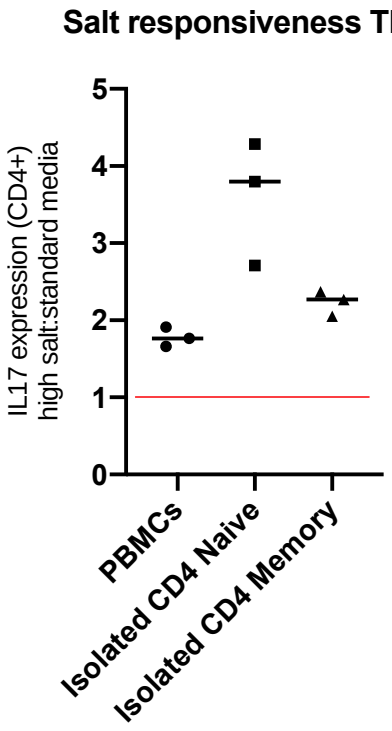

3.4.5 Sodium predominantly mediates the polarising effect of sodium chloride on IL-17 responses

To determine whether the polarising NaCl effect on IL-17 responses is mediated by sodium, chloride, osmolality, or tonicity, 7-day Th17 polarisation experiments were undertaken in the presence of the effective osmoles NaCl 0-80mM, mannitol 0-160mM, and sodium gluconate 0-80mM, and the ineffective osmole urea 0-80mM. Final supernatant osmolality was measured and its relationship with IL-17 responses was assessed for each osmole creating the hyperosmolar conditions.

Initial experiments compared IL-17 responses between hyperosmolar conditions created by NaCl, mannitol, and urea (Figure 3.9). There was a strong and positive correlation between hyperosmolality created by NaCl and all IL-17 responses (Figure 3.9). There was either no correlation or a negative correlation between hyperosmolality created by urea and IL-17 responses (Figure 3.9). There was no correlation between hyperosmolality created by mannitol and Tc17 polarisation and supernatant IL-17 concentration; and

there was a positive correlation between hyperosmolality created by mannitol and Th17 polarisation although the angle of the slope on the linear regression analysis (representing the magnitude of increase in Th17 polarisation for any given increase in osmolality created by that osmole) was less than it was with NaCl (Figure 3.9).

Figure 3.9: IL-17 responses according to hyperosmolar conditions created by NaCl, mannitol and urea

A. Th17 polarisation according to hyperosmolar conditions created by NaCl, mannitol and urea. Th17 polarisation plotted against measured final supernatant osmolality created by each of the osmoles; and summary of correlation and linear regression analysis.

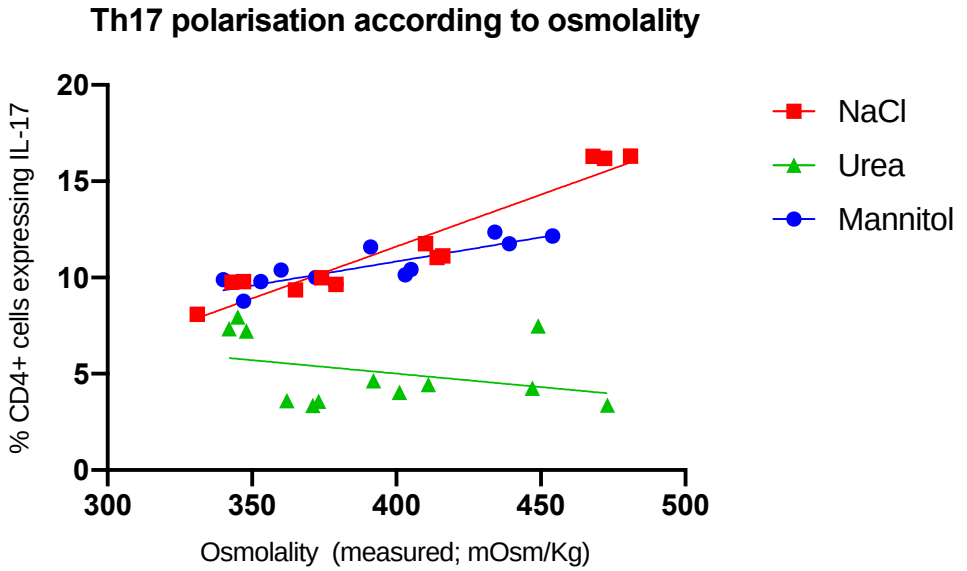

	Osmolality (measured; mOsm/Kg) vs. Th17 polarisation Mannitol	**Osmolality (measured; mOsm/Kg) vs. Th17 polarisation NaCl**	**Osmolality (measured; mOsm/Kg) vs. Th17 polarisation Urea**
Correlation analysis			
Spearman R	0.8252	0.8951	-0.3007
95% Confidence Interval	0.4623 to 0.9513	0.6495 to 0.9716	-0.7543 to 0.3473
P-value	**0.0016**	**0.0002**	0.3424
Linear Regression analysis			
Slope	0.02503	0.05391	-0.01396

95% Confidence interval	0.01397 to 0.03608	0.04182 to 0.06599	-0.04116 to 0.01325
R-squared	0.7179	0.9080	0.1155
P-value (slope significantly non-zero)	**0.0005**	**<0.0001**	0.2797
Equation (where Y is Th17 polarisation and X is osmolality)	Y = 0.02503*X + 0.8247	Y = 0.05391*X - 9.952	Y = -0.01396*X + 10.59

B. Tc17 polarisation according to hyperosmolar conditions created by NaCl, mannitol and urea. Tc17 polarisation plotted against measured final supernatant osmolality created by each of the osmoles; and summary of correlation and linear regression analysis.

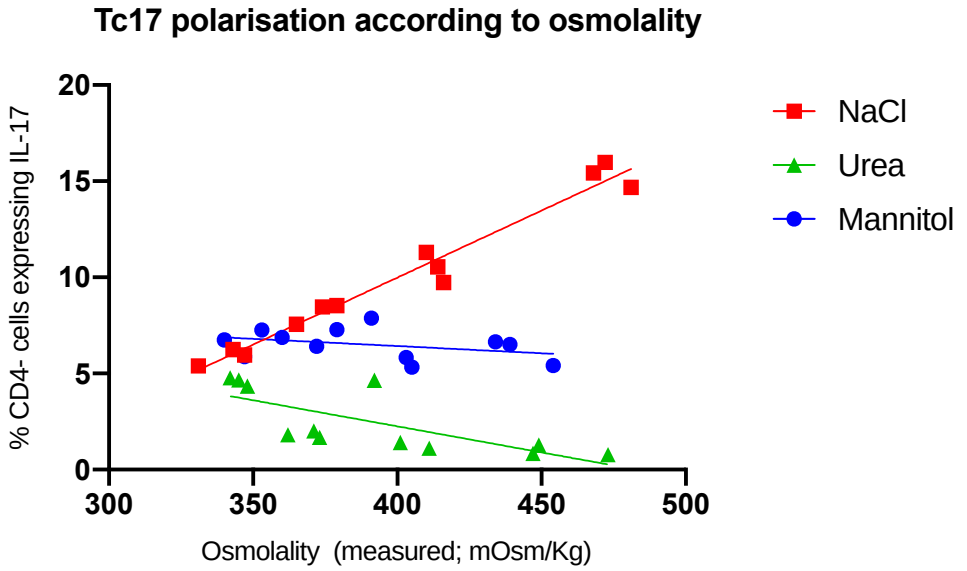

	Osmolality (measured; mOsm/Kg) vs. Tc17 polarisation Mannitol	**Osmolality (measured; mOsm/Kg) vs. Tc17 polarisation NaCl**	**Osmolality (measured; mOsm/Kg) vs. Tc17 polarisation Urea**
Correlation analysis			
Spearman R	-0.3986	0.9441	-0.9021
95% Confidence Interval	-0.7986 to 0.2455	0.8010 to 0.9851	-0.9735 to -0.6700
P-value	0.2010	**<0.0001**	**0.0002**
Linear Regression analysis			
Slope	-0.007522	0.06970	-0.02714
95% Confidence interval	-0.02100 to 0.005952	0.06052 to 0.07887	-0.04483 to -0.009446
R-squared	0.1340	0.9662	0.5388
P-value (slope significantly non-zero)	0.2419	**<0.0001**	**0.0066**

Equation (where Y is Th17 polarisation and X is osmolality)	Y = -0.007522*X + 9.432	Y = 0.06970*X - 17.90	Y = -0.02714*X + 13.10

C. Supernatant IL-17 concentration according to hyperosmolar conditions created by NaCl, mannitol and urea. Supernatant IL-17 concentration plotted against measured final supernatant osmolality created by each of the osmoles; and summary of correlation and linear regression analysis.

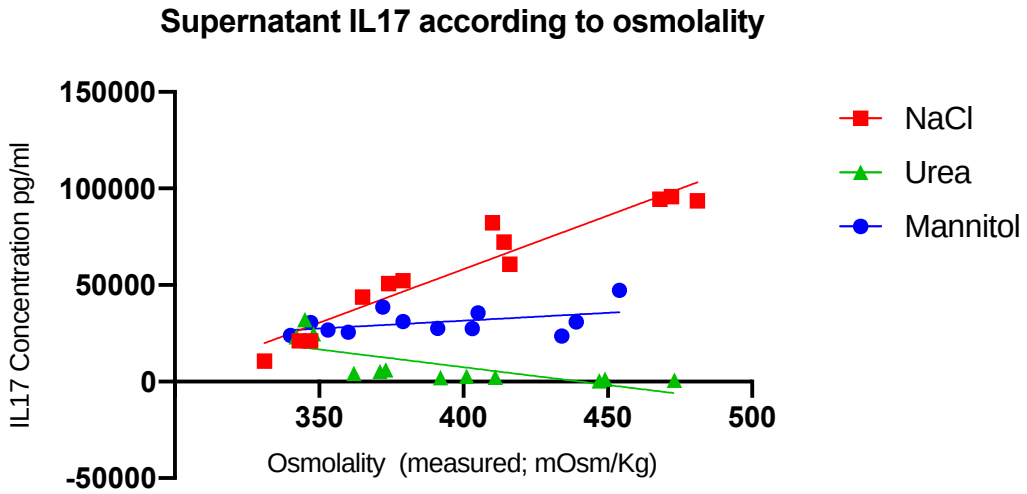

	Osmolality (measured; mOsm/Kg) vs. Supernatant IL-17 Mannitol	**Osmolality (measured; mOsm/Kg) vs. Supernatant IL-17 NaCl**	**Osmolality (measured; mOsm/Kg) vs. Supernatant IL-17 Urea**
Correlation analysis			
Spearman R	-0.3986	0.9441	-0.9021
95% Confidence Interval	-0.7986 to 0.2455	0.8010 to 0.9851	-0.9735 to -0.6700
P-value	0.2010	**<0.0001**	**0.0002**
Linear Regression analysis			
Slope	81.07	555.1	-184.1
95% Confidence interval	-33.37 to 195.5	440.0 to 670.3	-304.7 to -63.51
R-squared	0.1994	0.9202	0.5364
P-value (slope significantly non-zero)	0.1456	**<0.0001**	**0.0068**
Equation (where Y is Th17 polarisation and X is osmolality)	Y = 81.07*X - 873.0	Y = 555.1*X - 163835	Y = -184.1*X + 81083

Subsequent experiments compared IL-17 responses between hyperosmolar conditions created by NaCl, Na gluconate and mannitol (Figure 3.10). There

was a strong and positive correlation between both sodium containing osmoles (NaCl and Na gluconate) and all IL-17 responses (Figure 3.10). The angle of the slope on the linear regression analysis for NaCl and Na gluconate across all 3 parameters assessed (Th17 and Tc17 polarisation and supernatant IL-17 concentration) was similar (Figure 3.10). In these experiments, there was a correlation between hyperosmolar conditions created by mannitol and IL-17 responses but the angle of the slope in the linear regression analysis was less than that with sodium containing osmoles (Figure 3.10). Together, these experiments confirm previous data demonstrating that sodium is the predominant mediator of the effect of salt (sodium chloride) on IL-17 responses, although tonicity itself (mannitol) did promote IL-17 responses in some experiments.

Figure 3.10: IL-17 responses according to hyperosmolar conditions created by NaCl, Na gluconate, and mannitol

A. Th17 polarisation according to hyperosmolar conditions created by NaCl, Na gluconate, and mannitol. Th17 polarisation plotted against measured final supernatant osmolality created by each of the osmoles; and summary of correlation and linear regression analysis.

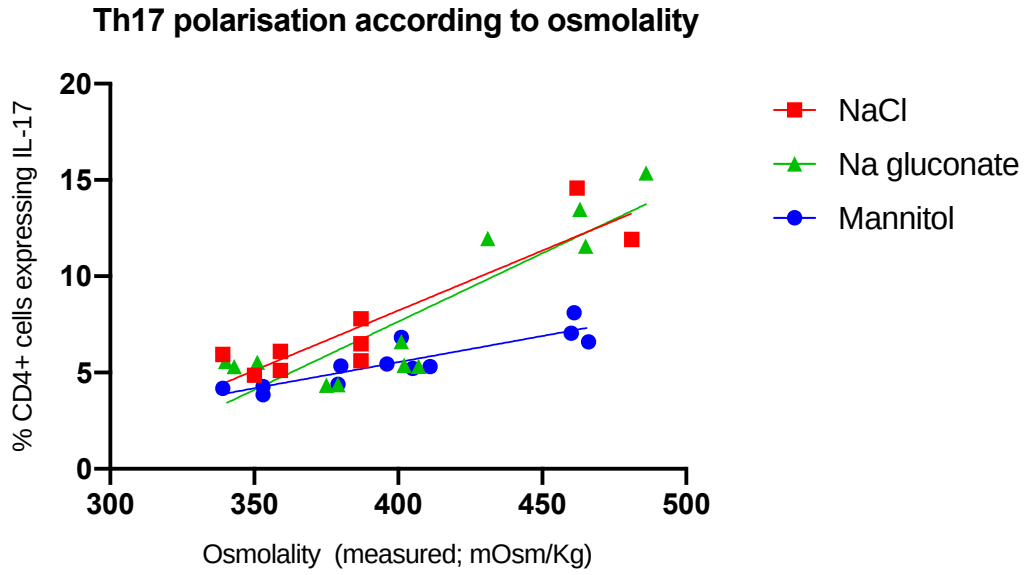

	Osmolality (measured; mOsm/Kg) vs. Th17 polarisation Mannitol	Osmolality (measured; mOsm/Kg) vs. Th17 polarisation NaCl	Osmolality (measured; mOsm/Kg) vs. Th17 polarisation Na gluconate
Correlation analysis			
Spearman R	0.8266	0.7746	0.6713
95% Confidence Interval	0.4658 to 0.9517	Insufficient pairs	0.1396 to 0.9025
P-value	**0.0182**	**0.0202**	**0.0182**
Linear Regression analysis			
Slope	0.02714	0.06223	0.07090
95% Confidence interval	0.01713 to 0.03716	0.03734 to 0.08712	0.04382 to 0.09798
R-squared	0.7848	0.8331	0.7729
P-value (slope significantly non-zero)	**0.0001**	**0.0006**	**0.0002**
Equation (where Y is Th17 polarisation and X is osmolality)	Y = 0.02714*X - 5.318	Y = 0.06223*X - 16.67	Y = 0.07090*X - 20.72

B. Tc17 polarisation according to hyperosmolar conditions created by NaCl, Na gluconate and mannitol. Tc17 polarisation plotted against measured final supernatant osmolality created by each of the osmoles; and summary of correlation and linear regression analysis.

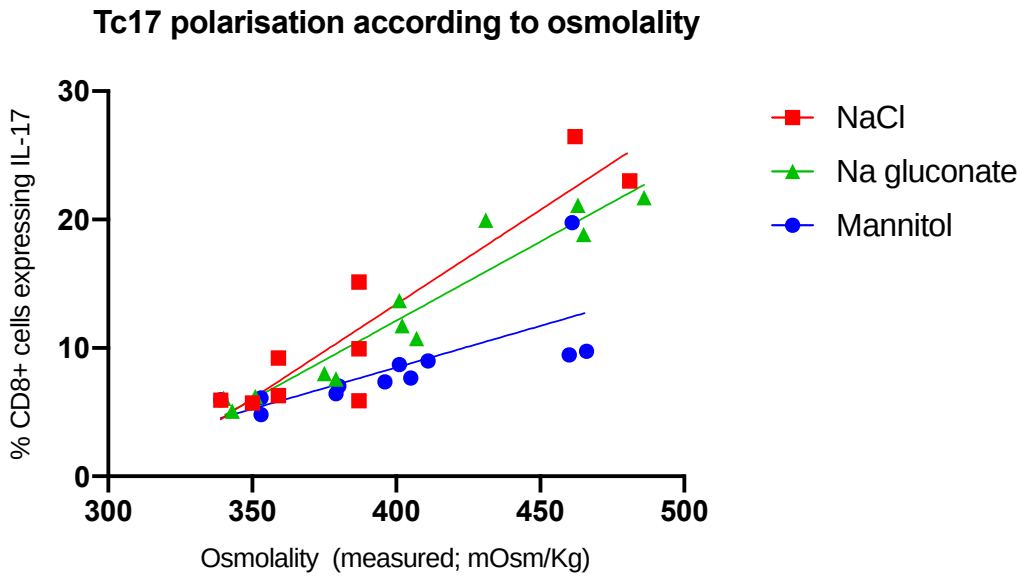

	Osmolality (measured; mOsm/Kg) vs. Tc17 polarisation Mannitol	Osmolality (measured; mOsm/Kg) vs. Tc17 polarisation NaCl	Osmolality (measured; mOsm/Kg) vs. Tc17 polarisation Na gluconate
Correlation analysis			
Spearman R	0.9737	0.7746	0.9371
95% Confidence Interval	0.9028 to 0.9931	Insufficient pairs	0.7782 to 0.9832
P-value	**<0.0001**	**0.0182**	**<0.0001**
Linear Regression analysis			
Slope	0.06471	0.1469	0.1231
95% Confidence interval	0.02190 to 0.1075	0.09167 to 0.2022	0.09772 to 0.1484
R-squared	0.5314	0.8496	0.9212
P-value (slope significantly non-zero)	**0.0072**	**0.0004**	**<0.0001**
Equation (where Y is Th17 polarisation and X is osmolality)	Y = 0.06471*X - 17.40	Y = 0.1469*X - 45.36	Y = 0.1231*X - 37.11

C. Supernatant IL-17 concentration according to hyperosmolar conditions created by NaCl, Na gluconate and mannitol. Supernatant IL-17 concentration plotted against measured final supernatant osmolality created by each of the osmoles; and summary of correlation and linear regression analysis.

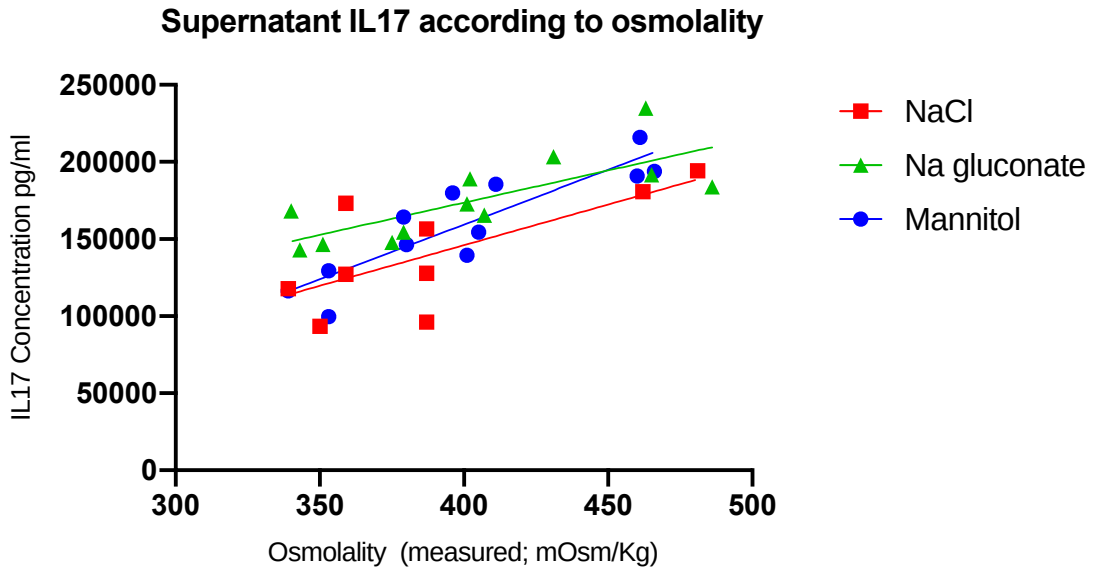

	Osmolality (measured; mOsm/Kg) vs. Supernatant IL-17 Mannitol	Osmolality (measured; mOsm/Kg) vs. Supernatant IL-17 NaCl	Osmolality (measured; mOsm/Kg) vs. Supernatant IL-17 Na gluconate
Correlation analysis			
Spearman R	0.8897	0.7065	0.7622
95% Confidence Interval	0.6338 to 0.9700	Insufficient pairs	0.3175 to 0.9321
P-value	**0.0002**	**0.0385**	**0.0055**
Linear Regression analysis			
Slope	709.4	527.3	417.9
95% Confidence interval	445.2 to 973.5	58.25 to 996.3	166.3 to 669.5
R-squared	0.7817	0.5024	0.5780
P-value (slope significantly non-zero)	**0.0001**	**0.0325**	**0.0041**
Equation (where Y is Th17 polarisation and X is osmolality)	Y = 709.4*X - 124300	Y = 527.3*X - 64877	Y = 417.9*X + 6469

3.4.6 Sodium channels and transporters are expressed on diverse immune cells

The mechanism by which sodium exerts its polarising effect on Th17 and Tc17 cells was investigated. I hypothesised that sodium entry in to T cells was required for this process. The presence of sodium transport mechanisms on immune cells was initially determined. The epithelial sodium channel (ENaC) and the sodium chloride cotransporter (NCC) were expressed on diverse immune cell subtypes (Figure 3.11). The pattern of expression was similar for both sodium transport mechanisms. Expression was highest on CD56+ (NK) cells, and expression was greater on naïve as opposed to memory cells. FACS plots also demonstrated high and low level expression of both ENaC and NCC (Figure 3.12). The proportion of expression that was high was also determined (Figure 3.13). High expression levels were most common on CD56+ (NK) cells, and more so on CD8 and naïve (CD45RA+) cells compared to CD4 and memory (CD45RA-) cells respectively.

Figure 3.11: αENaC and NCC expression on lymphocyte subtypes

αENaC expression was determined in 7 healthy controls, and NCC expression in 1 healthy control.

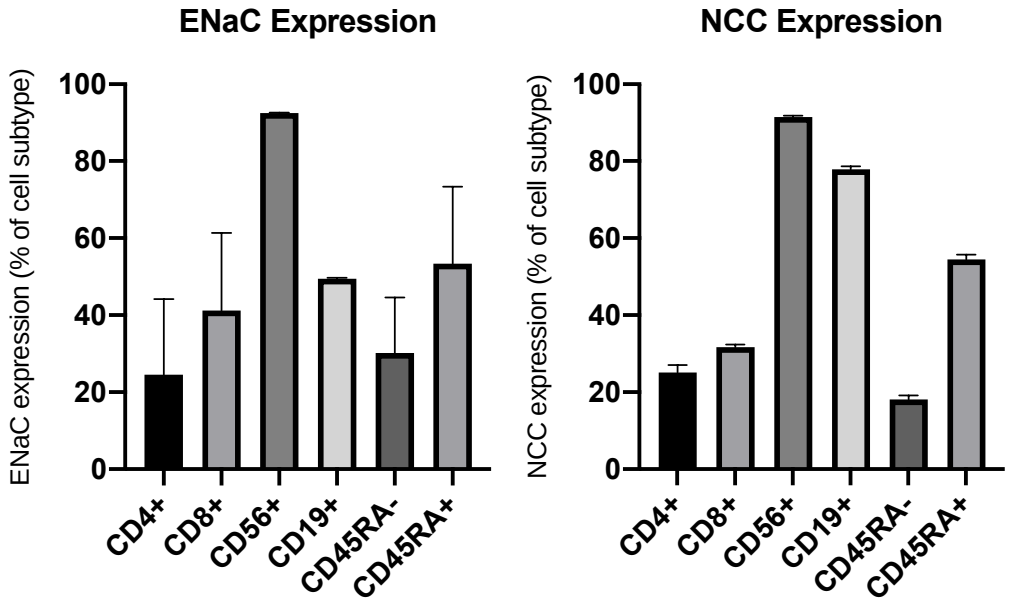

Figure 3.12: Representative FACS plots of high and low level ENaC expression

Example of high and low level expression of ENaC on CD8+ cells shown.

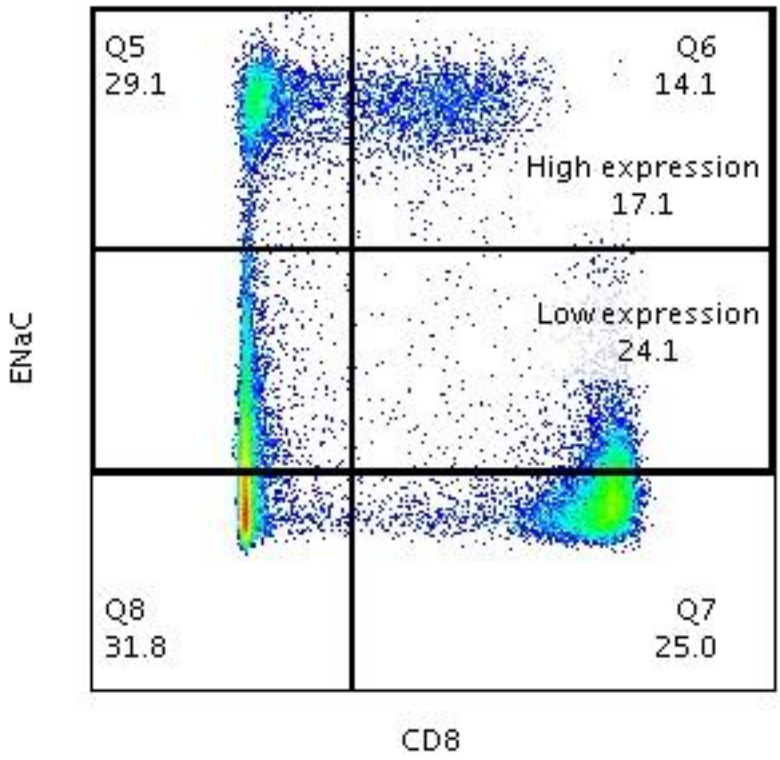

Figure 3.13: Expression levels of ENaC and NCC on lymphocyte subtypes

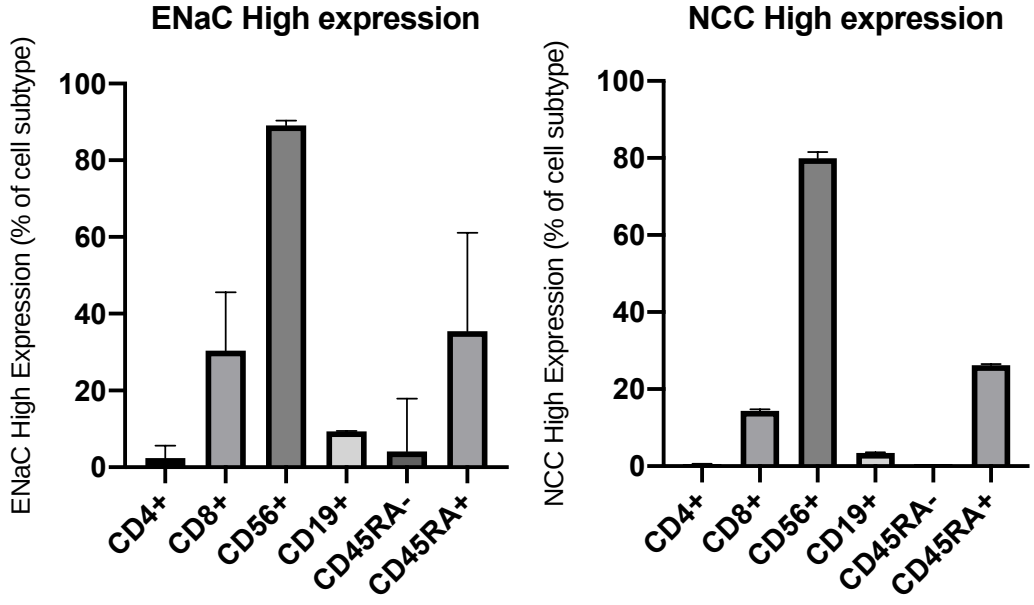

3.4.7 Sodium transport inhibition abrogates sodium chloride driven IL-17 responses

To investigate whether lymphocyte sodium transport inhibition reduced salt driven IL-17 responses, Th17 polarisation experiments were undertaken in the presence of sodium transporter inhibitors (NKCC inhibitor Furosemide; NCC inhibitor hydrochlorothiazide; and NCX inhibitor KB-R7943) and the ENaC inhibitor amiloride. The effect of inhibitors on cell viability and IL-17 responses are outlined in Figure 3.14, Figure 3.15, Figure 3.16, and Figure 3.17. The experiments are then summarised in Figure 3.18. These experiments demonstrated that amiloride and furosemide abrogated salt driven IL-17 responses; amiloride and furosemide both reduced Tc17 polarisation and this was associated with a reduction in supernatant IL-17 concentration with amiloride. HCT and KB-R7943 had no effect on IL-17 responses; KB-R7943 reduced cell viability significantly. Supernatant lFNγ concentrations were also measured in the experiments with amiloride added; like IL-17, there was a reduction in lFNγ when amiloride was added to culture conditions (Figure 3.19). The effect of amiloride on isolated naïve CD4+ (CD4+CD45RA+) cells and naïve CD8+ (CD8+CD45RA+) cells was also assessed. Amiloride reduced salt driven IL-17 expression in both isolated naïve CD4+ and CD8+ cells (Figure 3.20).

Figure 3.14: Effect of amiloride on cell viability, Th17 and Tc17 polarisation, and supernatant IL-17 concentration

12 experiments were performed in 9 healthy controls. Variables in standard media (+0mM NaCl), in high salt media (+40mM NaCl), and in high salt media + amiloride 20uM are plotted. Variables are compared between high salt media with and without amiloride 20uM present using a Wilcoxon test.

Viability (% lymphocytes alive): + 40mM NaCl 73% (69-77); + 40mM NaCl/amiloride 20uM 73% (67-77); median difference -1% (95% CI: -4.9, 1.3); p=0.24
Th17 polarisation: + 40mM NaCl 11.2% (7.1-15.1); + 40mM NaCl/amiloride 20uM 10.4% (8.5-13.7); median difference -0.4% (95% CI: -4, 1.3); p=0.62.

Tc17 polarisation: + 40mM NaCl 7.4% (3.8-11.3); + 40mM NaCl/amiloride 20uM 6.9% (4.0-8.7); median difference -0.6% (95% CI: -2.1, -0.09); p=0.043.
Supernatant IL-17 concentration: + 40mM NaCl 11288pg/ml (6420-26795); + 40mM NaCl/amiloride 20uM 4428pg/ml (2556-8825); median difference -4884pg/ml (95% CI: -14130, -3504); p=0.001.

ns – not significant (p>0.05), *p≤0.05, **p≤0.01, ***p≤0.001, ****p≤0.0001

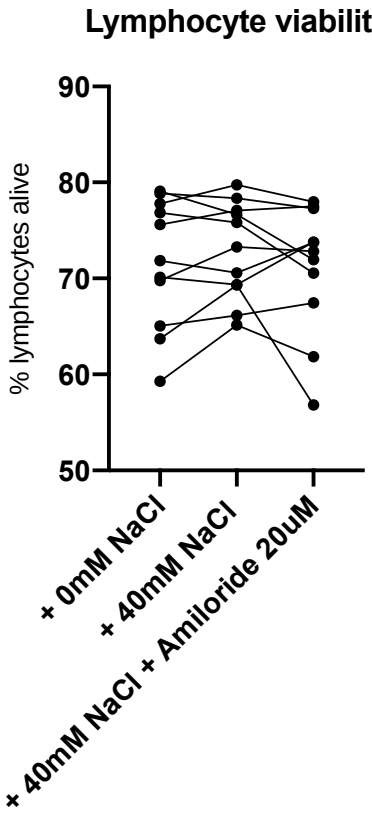

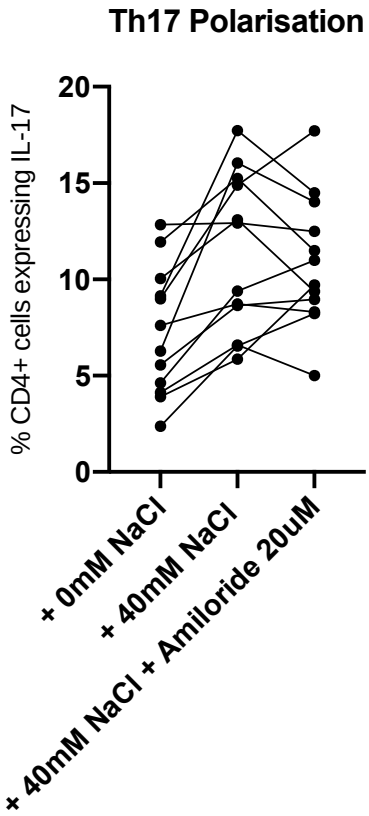

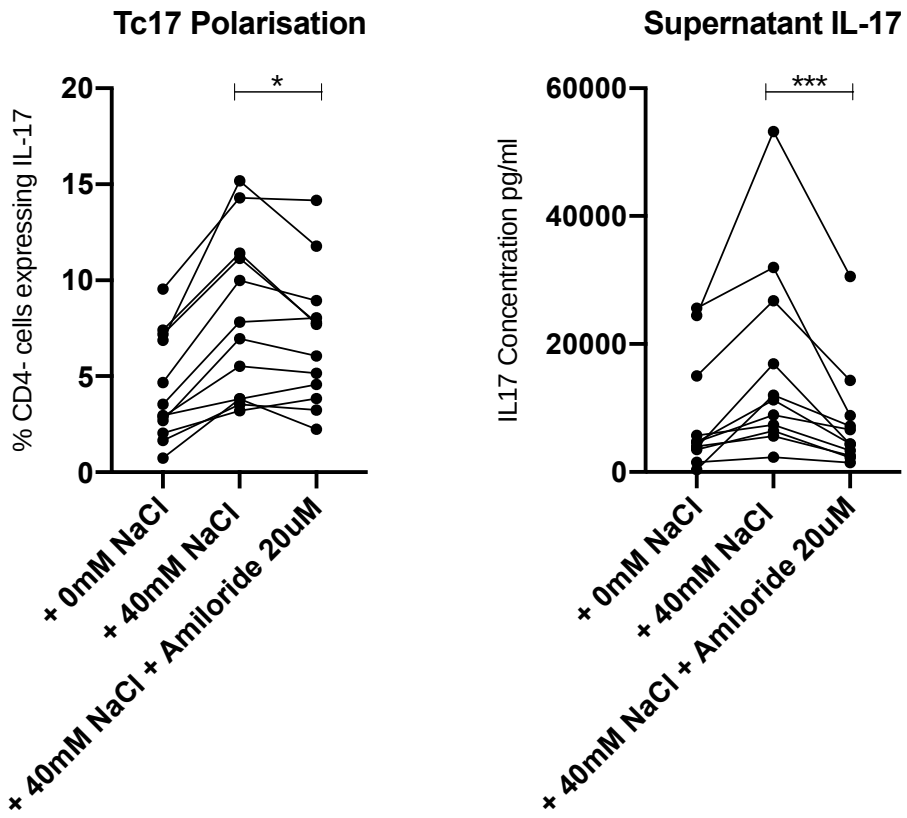

Figure 3.15: Effect of furosemide on cell viability, Th17 and Tc17 polarisation, and supernatant IL-17 concentration

13 experiments were performed in 11 healthy controls. Variables in standard media (+0mM NaCl), in high salt media (+40mM NaCl), and in high salt media + furosemide 10-20uM are plotted. Variables are compared between high salt media with and without furosemide 10-20uM using a Wilcoxon test.

Viability (% lymphocytes alive): + 40mM NaCl 73% (69-77); + 40mM NaCl/furosemide 10-20uM 73% (69-77); median difference 1% (95% CI: -0.15, 2.8); p=0.12

Th17 polarisation: + 40mM NaCl 8.6% (5.9-13.1); + 40mM NaCl/furosemide 10-20uM 7.1% (5.1-10.4); median difference -0.9% (95% CI: -2.4, -0.02); p=0.064.

Tc17 polarisation: + 40mM NaCl 5.5% (3.2-10.0); + 40mM NaCl/furosemide 10-20uM 3.6% (3.0-7.5); median difference -0.34% (95% CI: -2.1, -0.13); p=0.03.

Supernatant IL-17 concentration: + 40mM NaCl 11288pg/ml (6580-23830); + 40mM NaCl/furosemide 10-20uM 6269pg/ml (3644-19368); median difference -1251pg/ml (95% CI: -5608, -88); p=0.057.

ns – not significant (p>0.05), *p≤0.05, **p≤0.01, ***p≤0.001, ****p≤0.0001

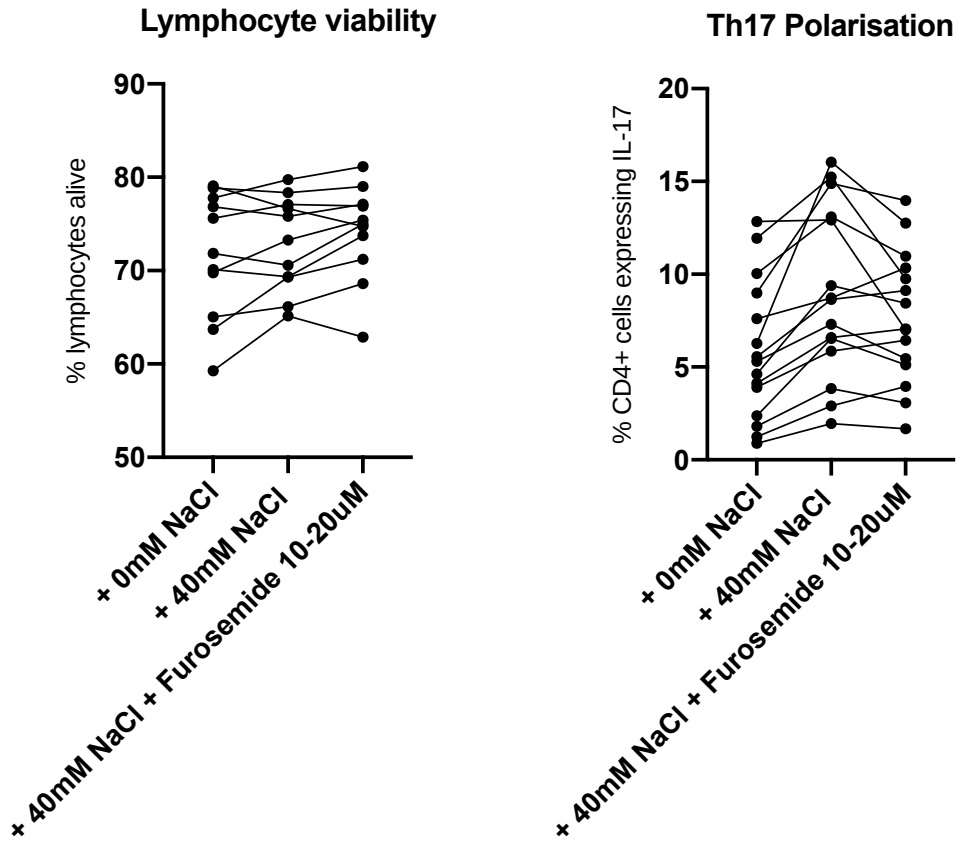

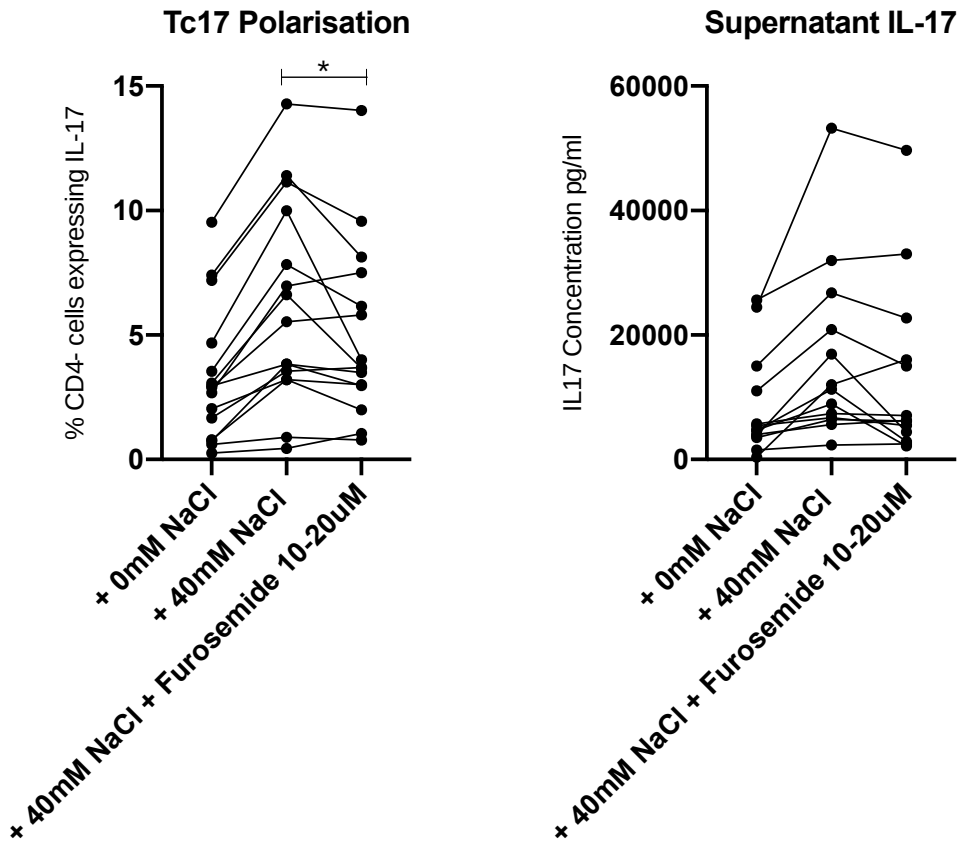

Figure 3.16: Effect of hydrochlorothiazide on cell viability, Th17 and Tc17 polarisation, and supernatant IL-17 concentration

11 experiments were performed in 9 healthy controls. Variables in standard media (+0mM NaCl), in high salt media (+40mM NaCl), and in high salt media + HCT 20uM plotted. Variables are compared between high salt media with and without HCT 20uM using a Wilcoxon test.

Viability (% lymphocytes alive): + 40mM NaCl 73% (69-77); + 40mM NaCl/HCT 20uM 74% (71-77); median difference 0.6% (95% CI: 0.09, 2.6); p=0.02
Th17 polarisation: + 40mM NaCl 9.3% (6.5-14.9); + 40mM NaCl/HCT 20uM 9.9% (7.3-11.1); median difference -1.2% (95% CI: -2.2, 0.6); p=0.24.
Tc17 polarisation: + 40mM NaCl 6.9% (3.8-11.1); + 40mM NaCl/HCT 20uM 7.1% (3.9-9.1); median difference 0.02% (95% CI: -1.3, 0.58); p=0.64.
Supernatant IL-17 concentration: + 40mM NaCl 11288pg/ml (6420-26795); + 40mM NaCl/HCT 20uM 12164pg/ml (6290-24953); median difference 907pg/ml (95% CI: -2106, 3412); p=0.64.

ns – not significant (p>0.05), *p≤0.05, **p≤0.01, ***p≤0.001, ****p≤0.0001

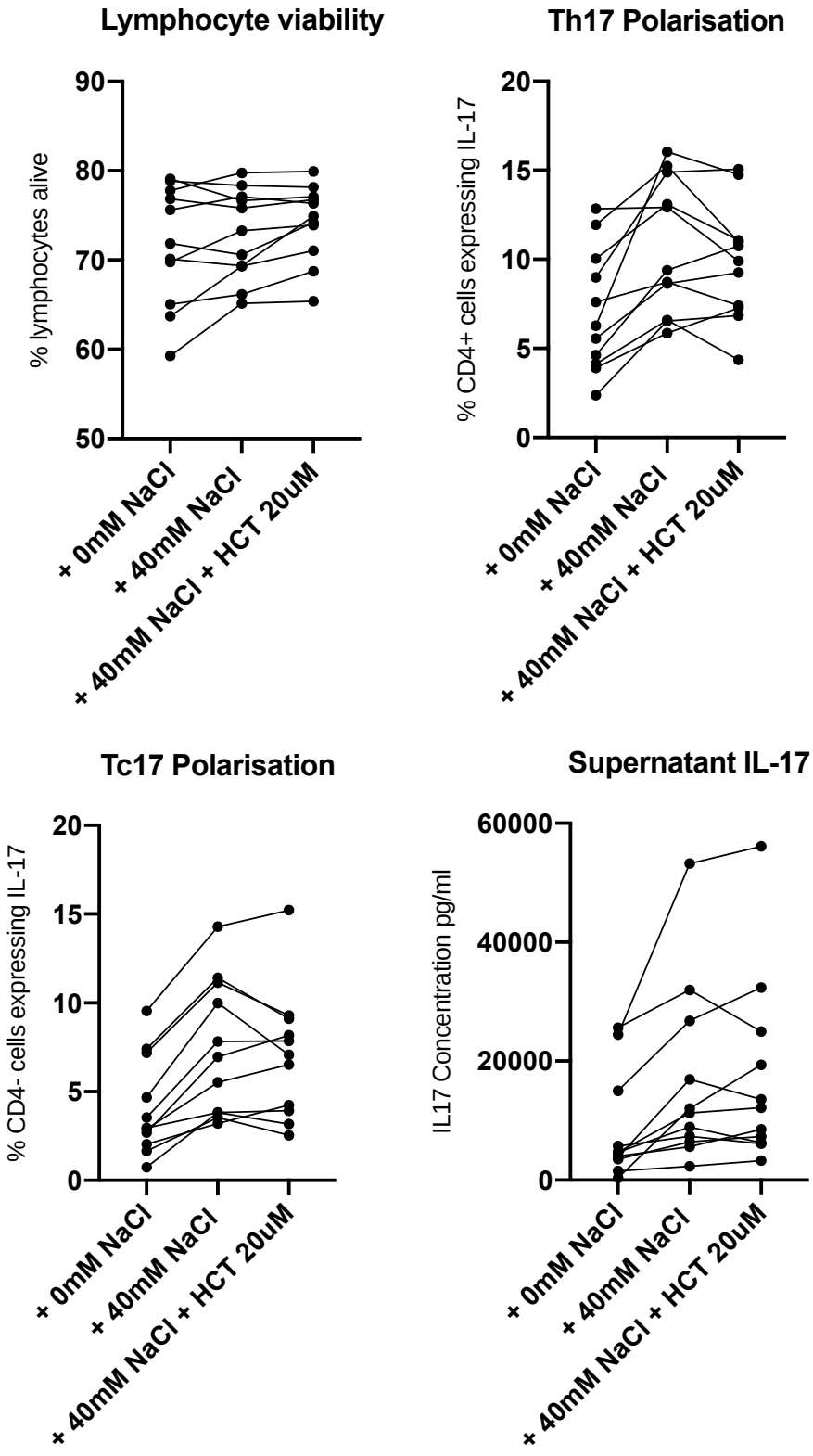

Figure 3.17: Effect of KB-R7943 on cell viability, Th17 and Tc17 polarisation, and supernatant IL-17 concentration

8 experiments were performed in 7 healthy controls. Variables in standard media (+0mM NaCl), in high salt media (+40mM NaCl), and in high salt media + KB-R7943 200nM are plotted. Variables are compared between high salt media with and without KB-R7943 200nM using a Wilcoxon test.

Viability (% lymphocytes alive): + 40mM NaCl 70% (60-78); + 40mM NaCl/KB-R7943 200nM 64% (43-75); median difference -7% (95% CI: -15, -1); p=0.0078
Th17 polarisation: + 40mM NaCl 7.7% (4.7-14.7); + 40mM NaCl/ KB-R7943 200nM 8.2% (7.1-13.2); median difference 0.3% (95% CI: -2.9, 2.6); p=0.84.
Tc17 polarisation: + 40mM NaCl 3.7% (2.4-11.1); + 40mM NaCl/ KB-R7943 200nM 4.8% (3.9-10.2); median difference 0.3% (95% CI: -1.3, 1.9); p=0.54.
Supernatant IL-17 concentration: + 40mM NaCl 14110pg/ml (9534-28198); + 40mM NaCl/KB-R7943 200nM 13073pg/ml (6109-22739); median difference -2674pg/ml (95% CI: -7862, 1274); p=0.12.

ns – not significant (p>0.05), *p≤0.05, **p≤0.01, ***p≤0.001, ****p≤0.0001

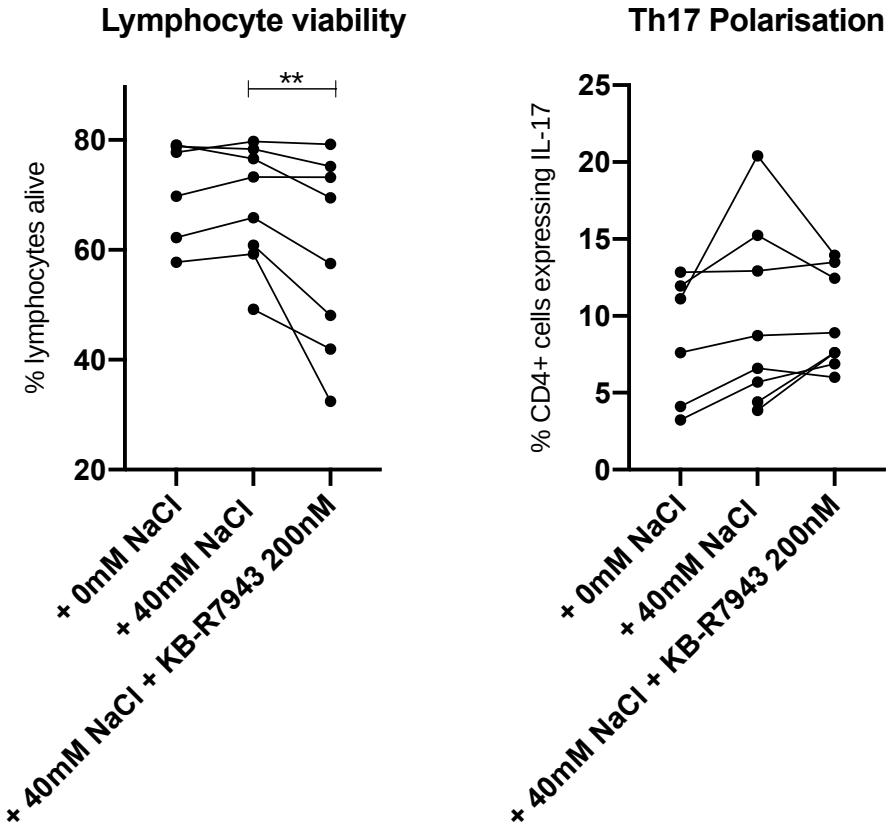

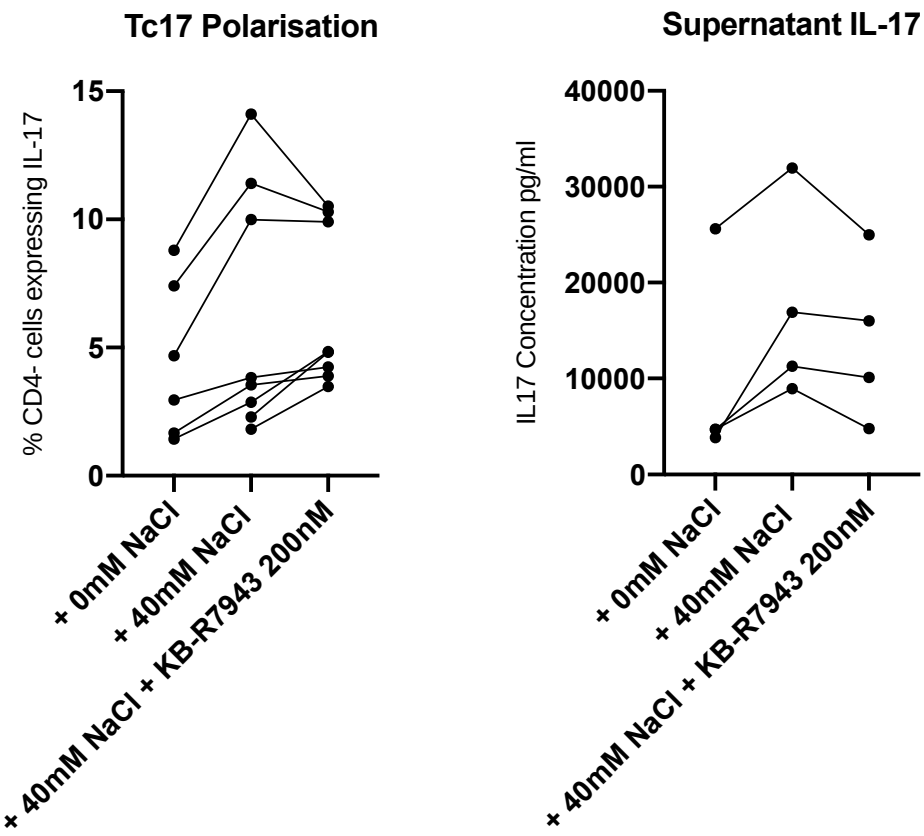

Figure 3.18: Summary of the effect of amiloride 20uM, furosemide 10-20uM, Hydrochlorothiazide 20uM, and KB-R7943 200nM on IL-17 responses

Variables (lymphocyte viability, Th17 and Tc17 polarisation, and supernatant IL-17 concentration) in the presence of inhibitor are expressed as a ratio to culture without the inhibitor present. Red lines drawn at ratio = 1 represent no difference between conditions.

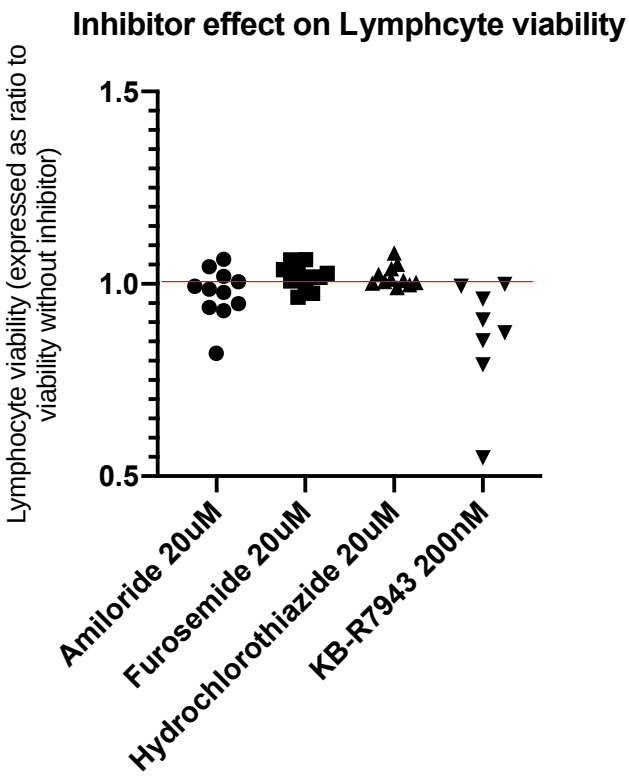
Inhibitor effect on Lymphcyte viability
Lymphocyte viability (expressed as ratio to viability without inhibitor)
1.5
1.0
0.5
Amiloride 20uM
Furosemide 20uM
Hydrochlorothiazide 20uM
KB-R7943 200nM

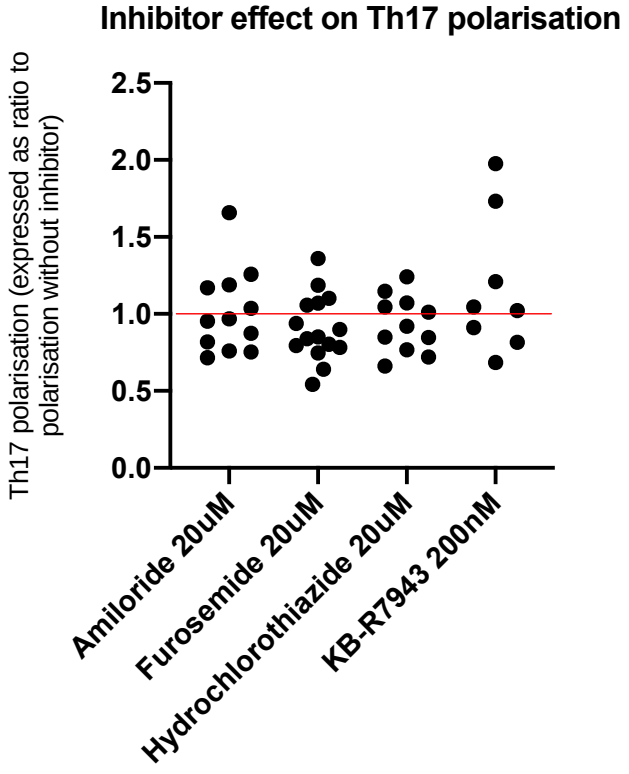
Inhibitor effect on Th17 polarisation
Th17 polarisation (expressed as ratio to polarisation without inhibitor)
2.5
2.0
1.5
1.0
0.5
0.0
Amiloride 20uM
Furosemide 20uM
Hydrochlorothiazide 20uM
KB-R7943 200nM

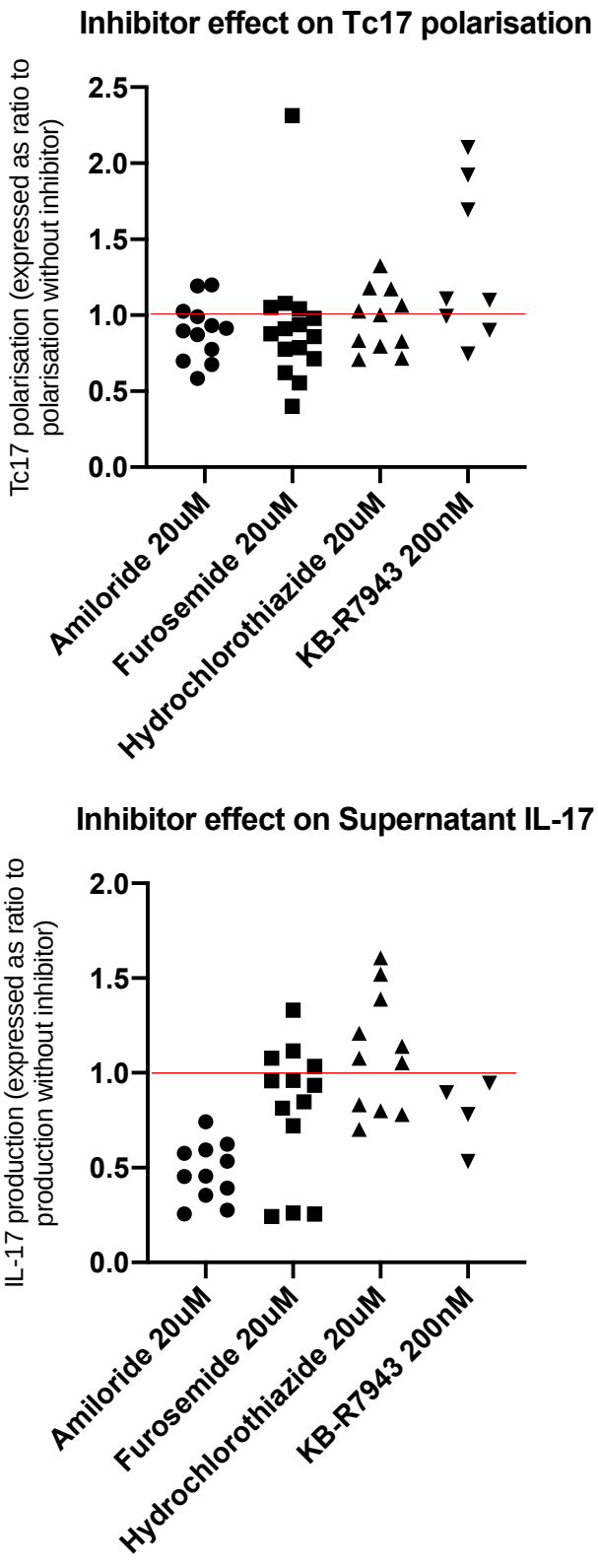

Figure 3.19: Effect of amiloride on supernatant IFNγ concentration

9 experiments were performed in 9 healthy controls. Supernatant IFNγ in standard media (+0mM NaCl), in high salt media (+40mM NaCl), and in high salt media +

amiloride 20uM are plotted. Supernatant IFNγ concentrations are compared between high salt media with and without amiloride 20uM using a Wilcoxon test.

Supernatant IFNγ concentration: + 40mM NaCl 30627pg/ml (23647-70161); + 40mM NaCl/amiloride 20uM 16722pg/ml (8403-63453); median difference -16717pg/ml (95% CI: -19956, -5367); p=0.020.

ns – not significant (p>0.05), *p≤0.05, **p≤0.01, ***p≤0.001, ****p≤0.0001

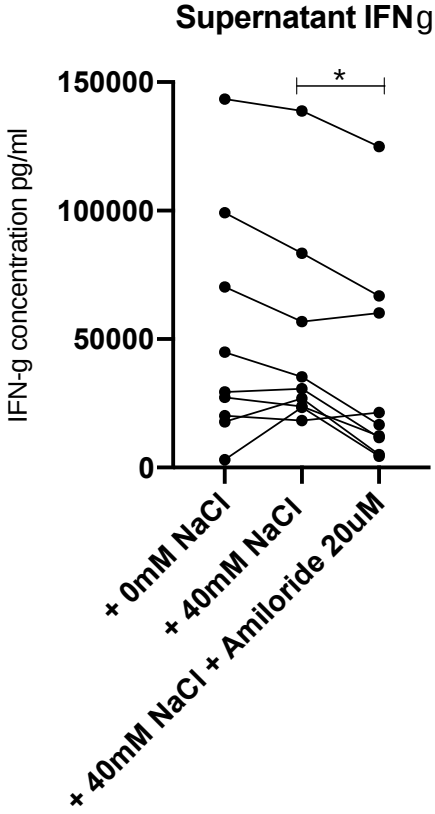

Figure 3.20: Effect of amiloride on IL-17 expression in isolated naïve CD4+ and CD8+ cells

Isolated naïve CD4 and CD8 population purity was confirmed prior to 7-day stimulation in the presence of Th17 polarising cytokines. Technical replicates (x2 for each condition) within an individual are shown.

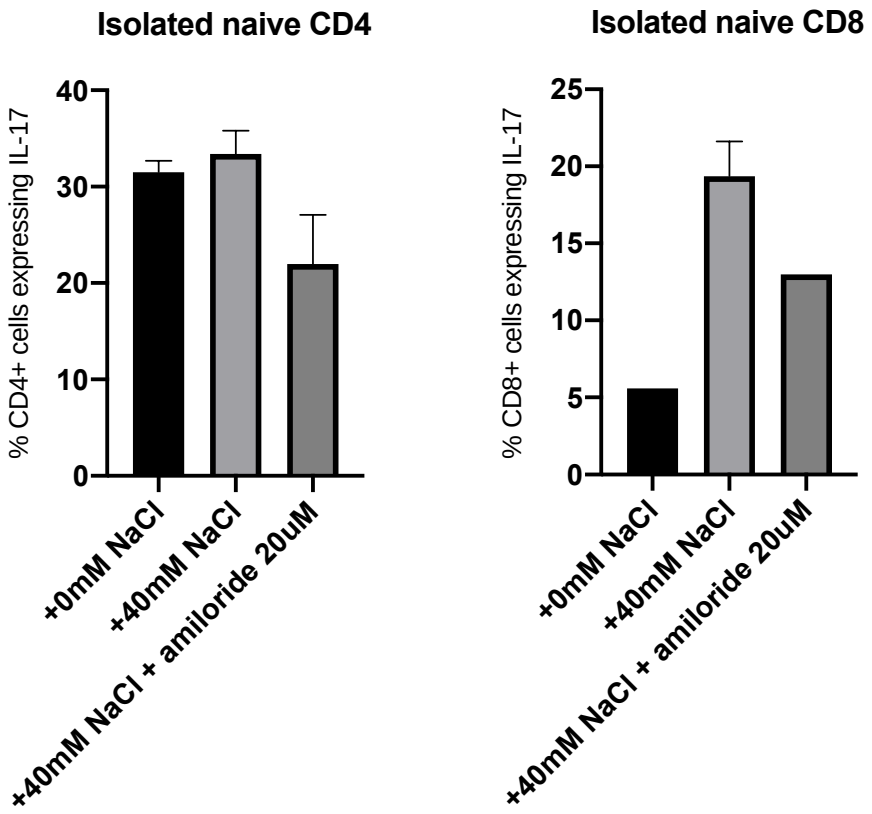

3.4.8 T cell activation in the presence of sodium is associated with an alteration in calcium flux

To investigate how sodium signals to intracellular pathways to exert its polarising effect, calcium flux after T cell activation was measured in the presence of NaCl. NaCl altered calcium flux after T cell activation with a dose dependent reduction in the peak X, peak Y, and area under the calcium flux curves (Figure 3.21).

Figure 3.21: Calcium flux in CD4+ cells after T cell activation in the presence of NaCl.

A. Representative calcium flux curves in CD4+ cells from a healthy control

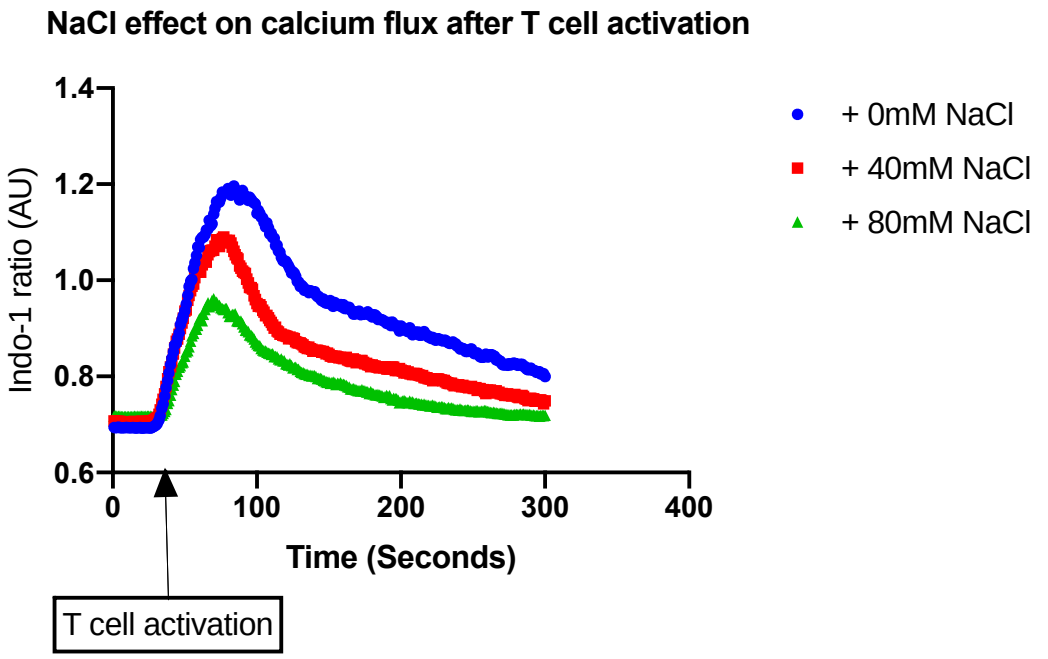

B. Peak X, Peak Y, and area under the calcium flux curves in CD4+ cells after T cell activation in the presence of NaCl 0-80mM. Experiments were undertaken in 6 healthy controls. Variables are compared with a Kruskall-Wallis test with Dunn's multiple comparison testing.

Peak X: +0mM NaCl 83.5 seconds (75.8-86.0); +40mM NaCl 74.0 seconds (65.5-77.5); +80mM NaCl 70.0 seconds (60.0-75.0); p=0.023

Peak Y: +0mM NaCl 1.20 AU (1.12-1.21); +40mM NaCl 1.10 AU (1.03-1.14); +80mM NaCl 0.97 (0.96-1.10); p=0.01

Area under curve: +0mM NaCl 271 AU (258-283); +40mM NaCl 252 (242-261); +80mM NaCl 243 (231-253); p=0.023

ns – not significant (p>0.05), *p≤0.05, **p≤0.01, ***p≤0.001, ****p≤0.0001

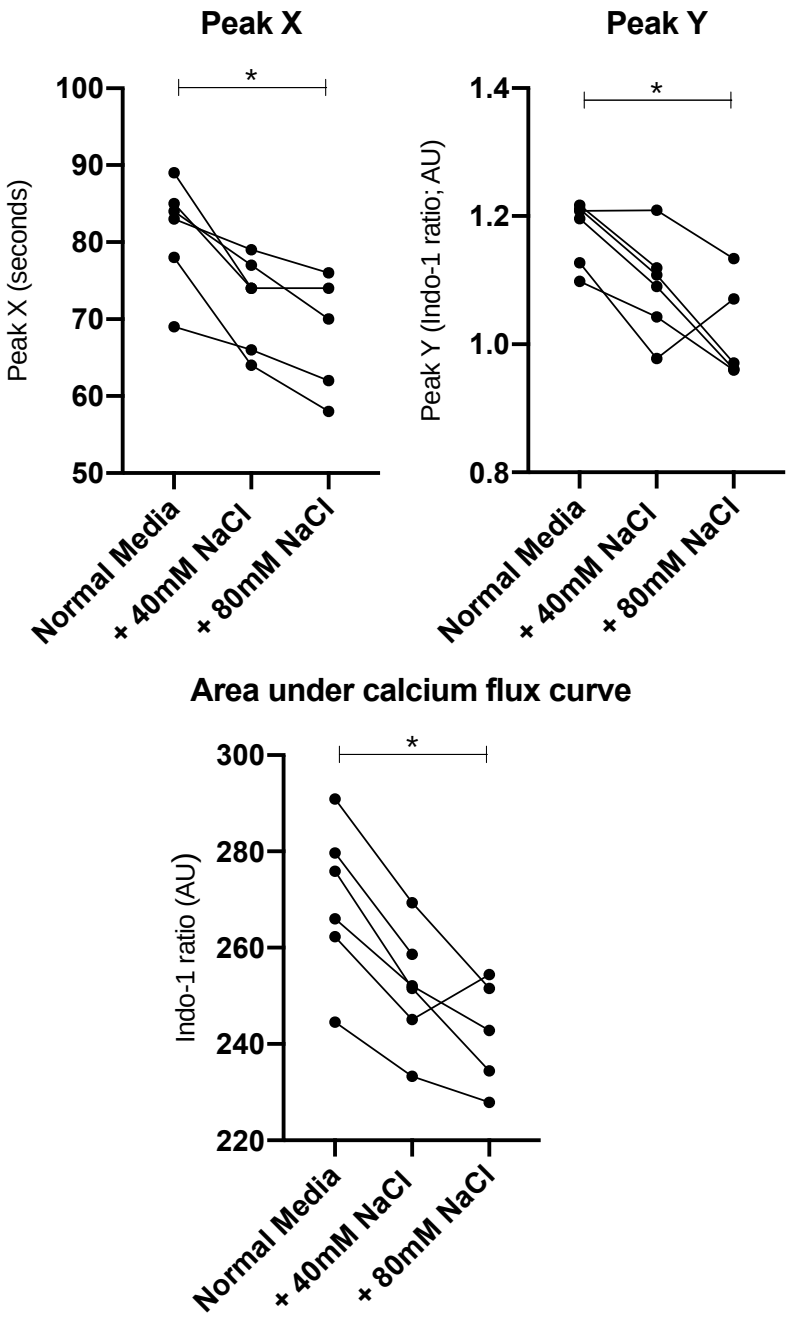

To confirm this effect was sodium mediated, experiments were repeated in the presence of Na gluconate, and mannitol. Like NaCl, Na gluconate also produced a dose dependent reduction in calcium flux, whereas mannitol had no effect (Figure 3.22).

Figure 3.22: Calcium flux in CD4+ cells after T cell activation in the presence of Na gluconate and mannitol

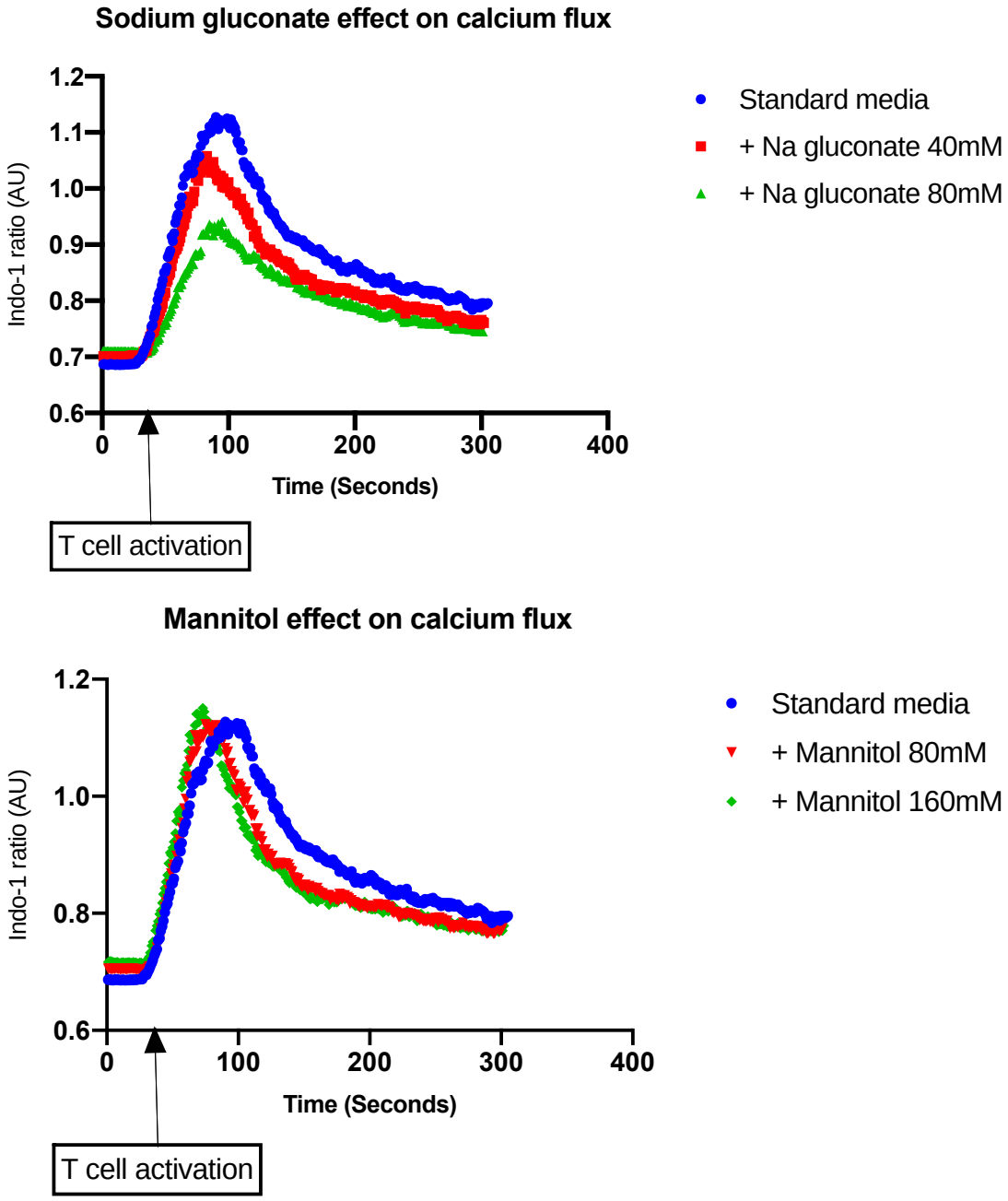

Next, the effect of sodium channel and transporter inhibitors on calcium flux was investigated. Amiloride increased calcium flux during T cell activation, whereas furosemide and HCT had no effect (Figure 3.23). This effect of amiloride was seen in standard media (Figure 3.23) and in media supplemented with NaCl (Figure 3.24).

Figure 3.23: Amiloride, furosemide, and HCT effect on calcium flux in CD4+ cells after T cell activation

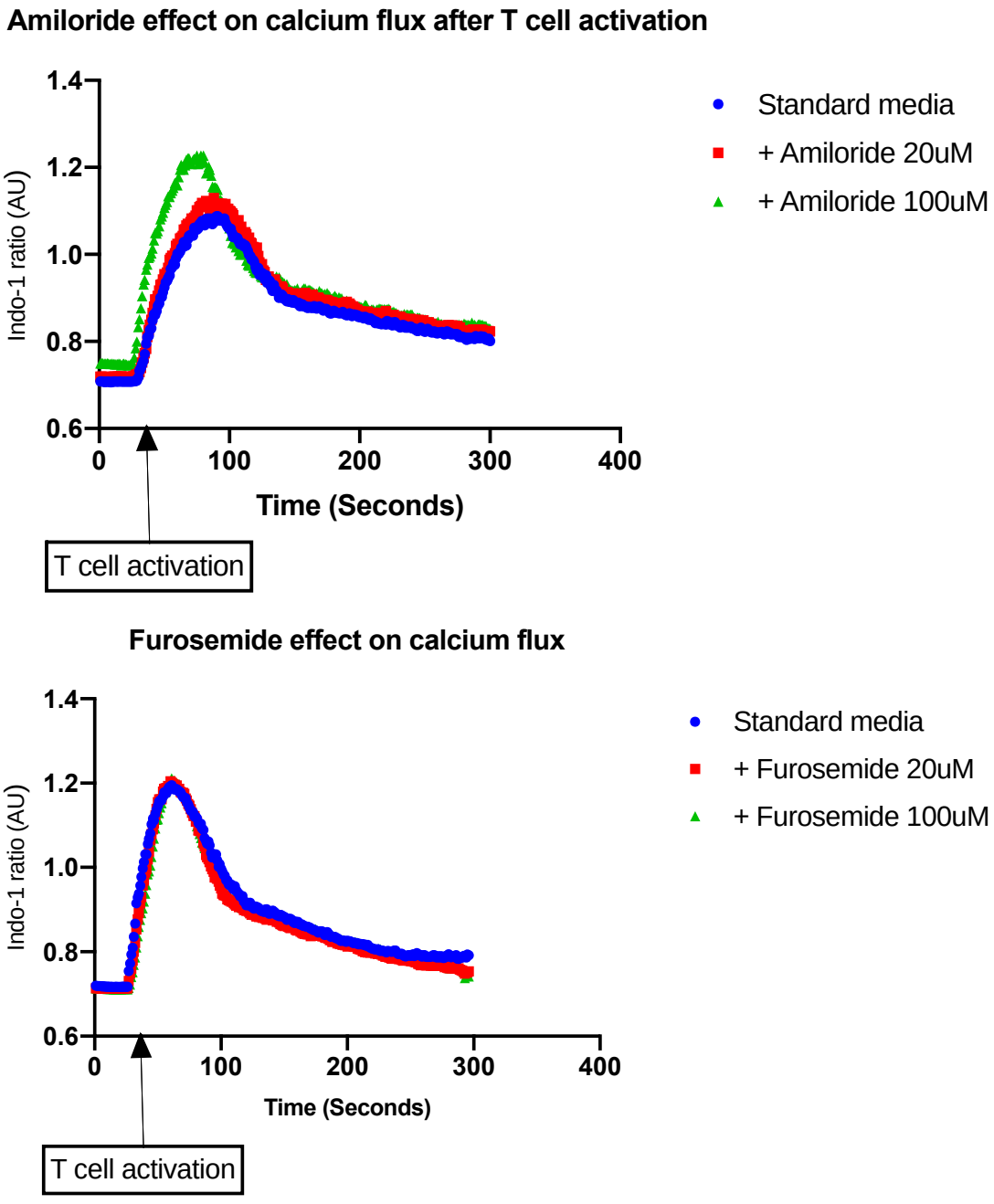

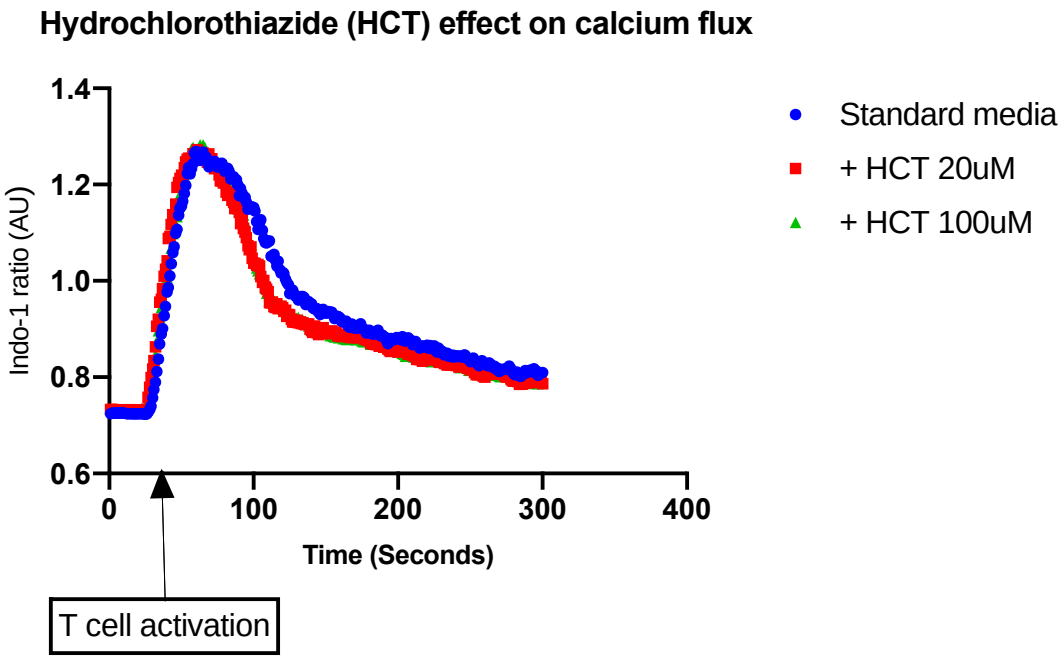

Figure 3.24: Effect of amiloride on calcium flux in CD4+ cells after T cell activation in high salt conditions

Experiments were replicated in 3 healthy controls. Representative curves from one experiment are shown.

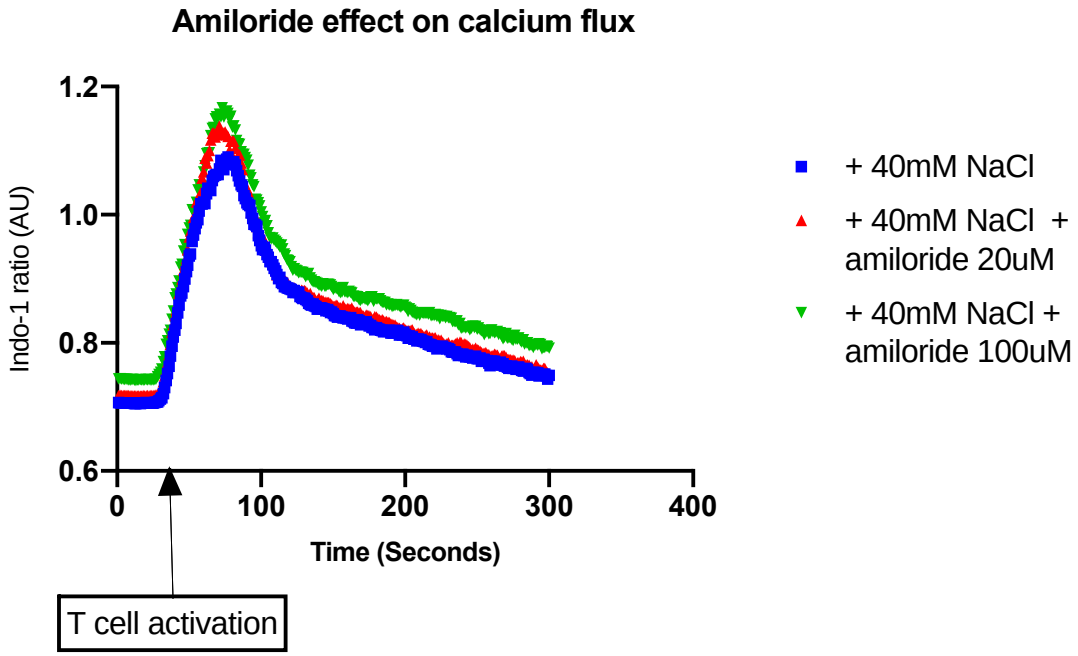

Together, these experiments demonstrate that sodium leads to an altered pattern of calcium flux in CD4+ cells after T cell activation with a dose

dependent reduction in calcium flux in to the cell. This effect is reversed when the ENaC inhibitor amiloride is added to activating conditions.

3.4.9 Extrapolating *in vitro* findings to patients with Pseudohypoaldosteronism type 1 (PHA1)

Having demonstrated that amiloride could reverse the polarising effect of sodium on *in vitro* IL-17 responses and the sodium effect on calcium flux during T cell activation, immunity was then investigated in 3 patients from a single family with autosomal recessive pseudohypoaldosteronism type 1 (AR PHA1) (Figure 3.25). All patients had an inactivating splice site mutation in the gene encoding the gamma subunit of ENaC (SCNN1G; c.318-1 G>A). Treatment and biochemical findings at the time of recruitment are outlined in Table 3.2. Serum electrolytes were largely within the laboratory reference ranges on treatment.

Figure 3.25: Family tree of patients with pseudohypoladosteronism type 1

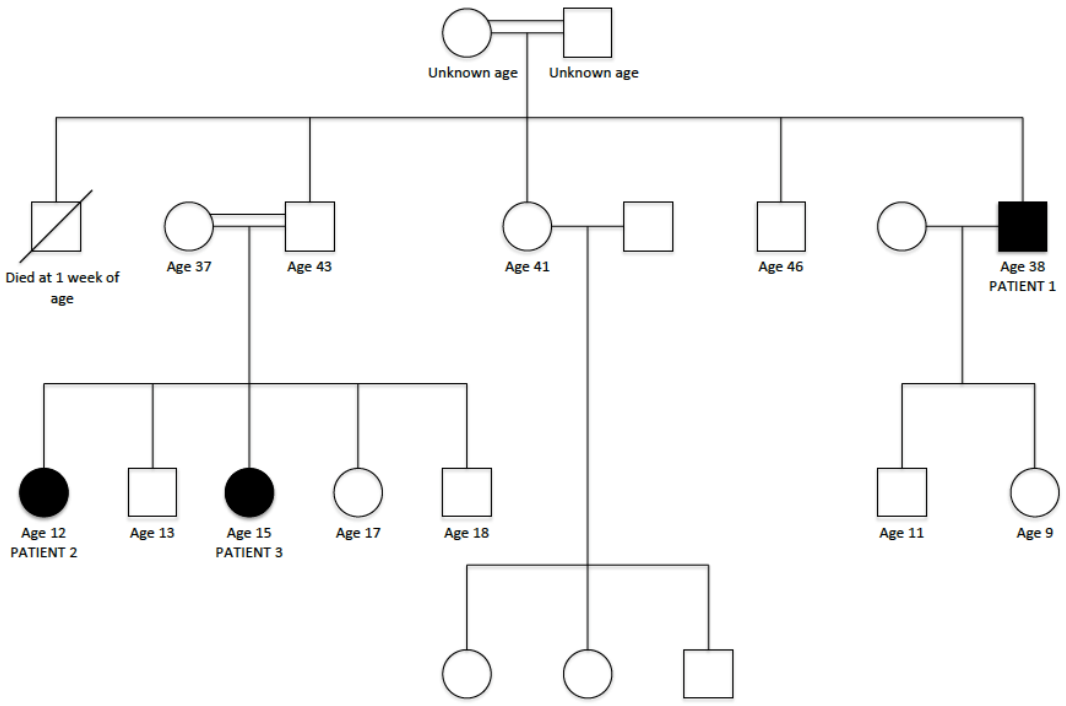

Table 3.2: Treatment and serum biochemistry at time of recruitment in PHA1 patients

	Patient 1	Patient 2	Patient 3
Treatment	NaCl and Na bicarbonate supplementation; sodium resonium	NaCl and Na bicarbonate supplementation; sodium resonium	NaCl and Na bicarbonate supplementation; sodium resonium
Na (mmol/l)	135	138	132
K (mmol/l)	5.5	4.5	5.2
Cl (mmol/l)	100	101	95
HCO3 (mmol/l)	24	24	21
Creatinine (umol/l)	75	45	75
cCa (mmol/l)	2.41	2.41	2.63
PO4 (mmol/l)	1.44	1.68	1.41
Mg (mmol/l)	0.76	0.89	0.95

Clinical features of altered immunity in each of the patients are summarised in Table 3.3. This confirmed previous findings in PHA1 patients of increased lower respiratory tract infections; however, all patients also had increased upper respiratory tract infections, one patient had recurrent viral and fungal infection, and all patients had contact allergies.

Table 3.3: Clinical features of altered immunity in patients with PHA1

LRTI – lower respiratory tract infection; URTI – upper respiratory tract infection; HSV – herpes simplex virus; HPV – human papilloma virus

	Patient 1	Patient 2	Patient 3
Demographic	38M	12F	15F
Bacterial infections	Recurrent parotitis LRTI as child Frequent admissions as child with febrile episodes of unclear source requiring intravenous antibiotics Recurrent URTI (4-6 in worst year; required intravenous antibiotics on 2 occasions)	Recurrent LRTI (>3 episodes requiring intravenous antibiotics) Recurrent URTI – predominantly otitis (largely winter; oral antibiotics); >6 in worst year	Recurrent LRTI (3-4 episodes requiring intravenous antibiotics) Recurrent URTI – predominantly throat (4-6 episodes)
Fungal Infections	Fungal skin infection and fungal nail infection	Nil	Nil
Viral (recurrent) Infections	Recurrent HSV	X2 episodes HPV	Nil
Autoimmune phenomena	Nil	Nil	Nil
Atopy	Hay fever and asthma	Eczema and hay fever	Nil
Allergy	Dust allergy (had patch test)	Allergy to peanuts and soap products	Contact allergy to metals

Initial immunological investigation is outlined in **Table 3.4**. CD19+ (B) cells as a percentage of lymphocytes were increased in all patients, and CD16/56+ (NK) cells were reduced in 2 of the 3 patients.

Next, the pattern of calcium flux during T cell activation was investigated in CD4+ cells. Similar to healthy control cells treated with amiloride, patients with PHA1 had altered calcium flux with increased calcium entry during T cell activation (

Figure 3.26). The addition of amiloride had no effect on calcium flux in PHA1 Patient 3; an increase in calcium flux was however seen with amiloride in PHA1 Patient 2 (**Figure 3.26**).

Table 3.4: Initial immunological investigation in patients with PHA1

Laboratory reference range (adult) and results for each patient are shown. Results outside reference range in bold.

NR – not recorded

	Normal Range	Patient 1	Patient 2	Patient 3
Haemoglobin (g/l)	110-150 (F); 135-170 (M)	156	145	148
White Cell Count (x10^9/l)	3.5-11	8.94	6.96	9.52
Neutrophil (x10^9/l)	1.7-7.5	4.4	3.51	6.57
Lymphocyte (x10^9/l)	1-4	3.64	2.31	1.91
Monocyte (x10^9/l)	0.2-1.5	0.79	0.55	0.91
Eosinophil (x10^9/l)	0-0.5	0.09	0.54	0.09
Basophil (x10^9/l)	0-0.1	0.03	0.04	0.04
Erythrocyte Sedimentation Rate (mm/hr)	0-20	21	2	19
C-Reactive Protein (mg/L)	0-5	4	1	2
Immunoglobulin A (g/l)	0.7-4	4	2.1	2.7
Immunoglobulin G (g/l)	7-16	13.1	12.1	13.8
Immunoglobulin M (g/l)	0.4-2.3	3.3	2	2.2
Total Immunoglobulin E (KUL)	0-120	NR	**706**	24
Complement C3 (g/l)	0.9-1.8	NR	1.14	1.78
Complement C4 (g/l)	0.1-0.4	NR	0.29	0.38
Lymphocyte (absolute; g/l)	1-2.8	**3.049**	2.021	1.412
CD3 (absolute; g/l)	0.7-2.1	2.004	1.214	0.941
CD4 (absolute; g/l)	0.3-1.4	1.133	0.698	0.479
CD8 (absolute; g/l)	0.2-0.9	0.749	0.361	0.393
CD19 (absolute; g/l)	0.1-0.5	**0.76**	**0.62**	0.447
CD16,CD56 (absolute; g/l)	0.09-0.6	0.139	0.171	**0.065**
CD3 (% of lymphocytes)	55-83	67	59	66
CD4 (% of lymphocytes)	28-57	37	35	34
CD8 (% of lymphocytes)	10-39	25	18	28

CD19 (% of lymphocytes)	6-19	**26**	**30**	**31**
CD16, CD56 (% of lymphocytes)	7-31	**5**	8	**4**
CD4/CD8	1-3.6	1.51	1.93	1.22

Figure 3.26: Lymphocyte calcium flux in patients with PHA1

A. Calcium flux (gated on PBMCs) in Patient 1 compared to a healthy control after stimulation with ionomycin.

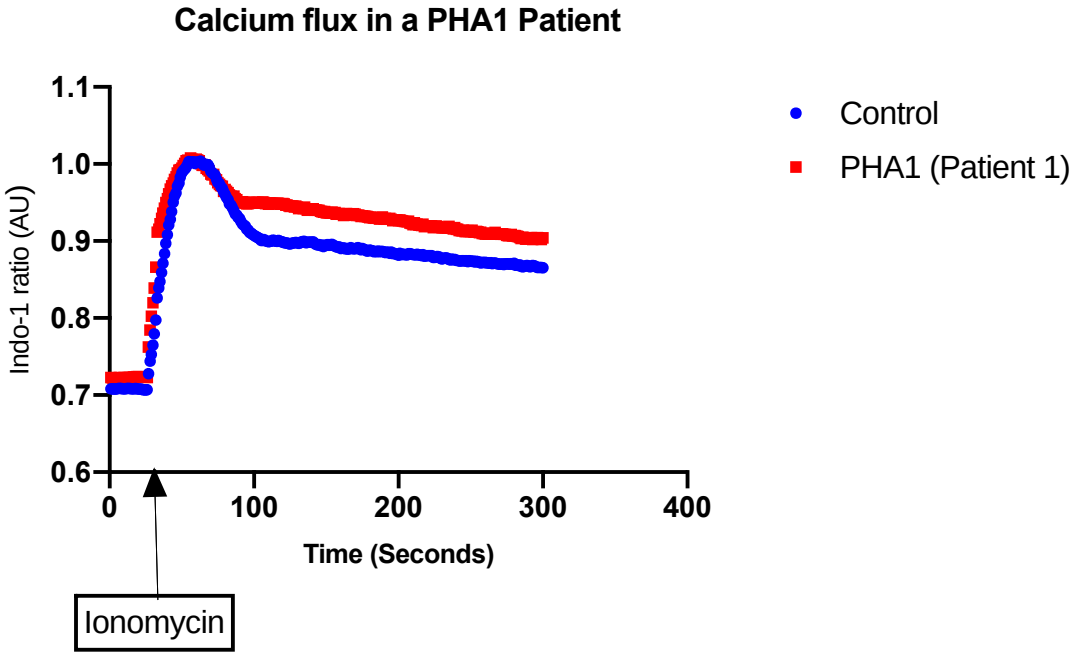

B. Calcium flux (gated on CD4+ cells) in Patient 2 and 3 after T cell stimulation (CD3/streptavidin) compared to the mean flux in 3 healthy controls analysed within the same experiment.

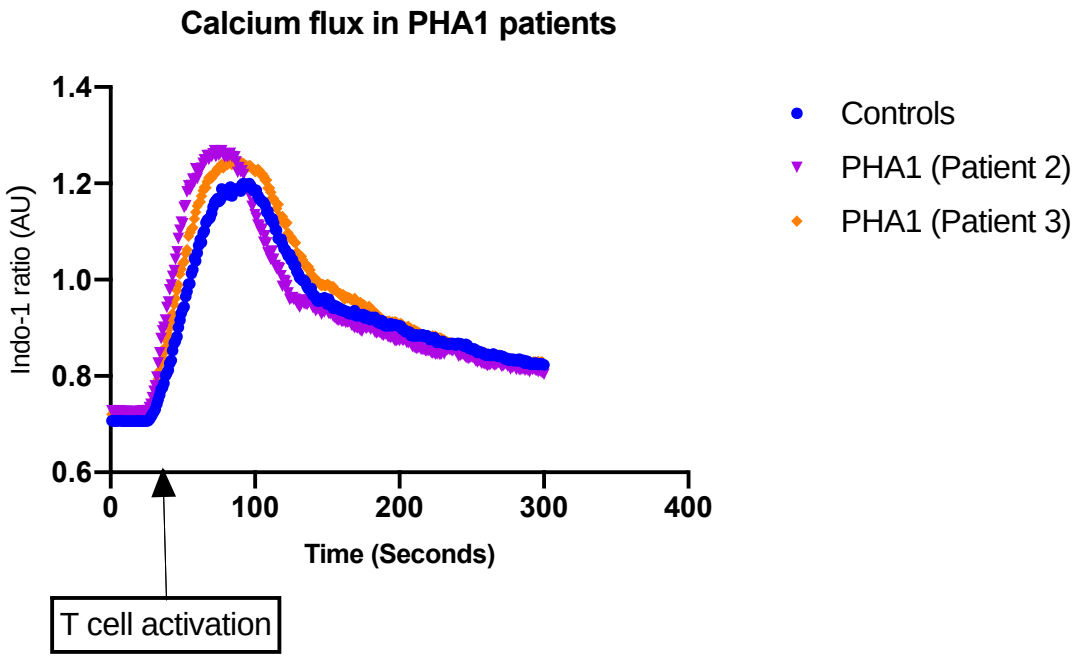

C. The effect of amiloride on calcium flux after T cell activation in PHA1 patients 2 and 3. Findings were consistent in technical duplicates.

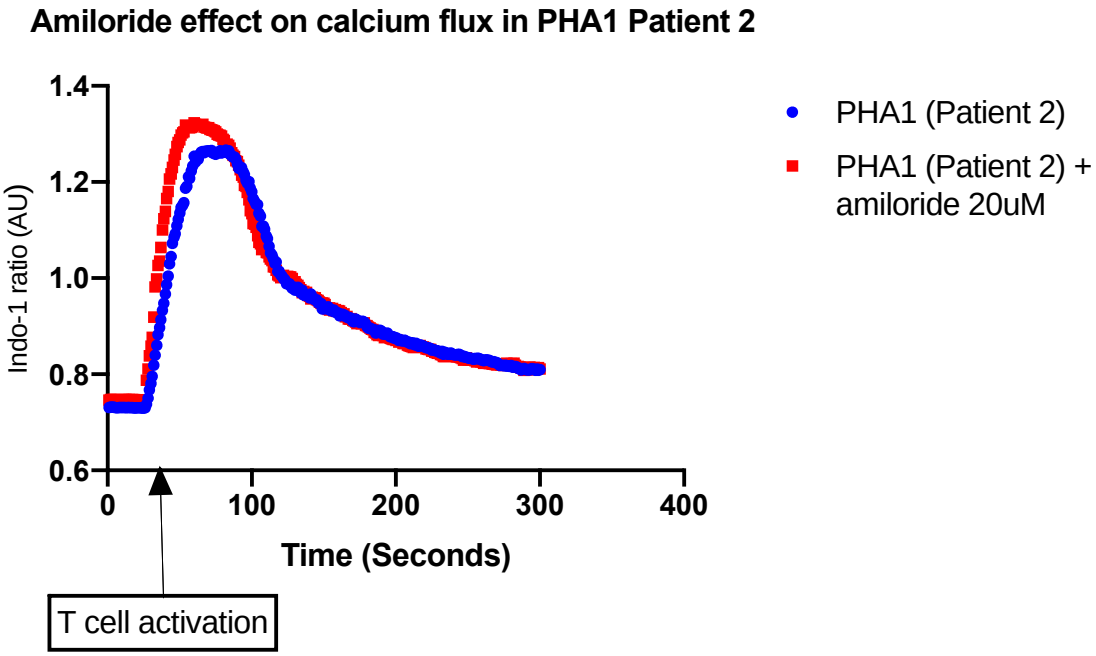

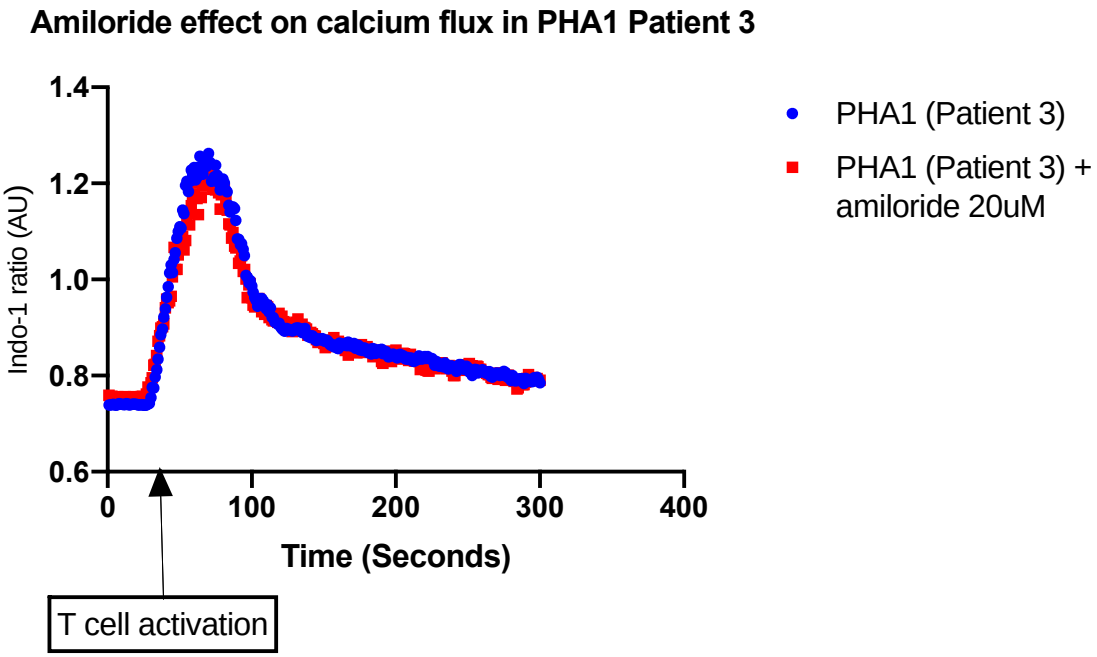

To determine if this led to an alteration in T cell responses: T cell activation and proliferation, and T cell IL-17 responses were assessed in PHA1 patients and compared to controls. T cell proliferation was not affected in PHA1 patients; T cell activation, as determined by CD25 expression after anti-CD3/28 stimulation was reduced in Patient 1 but not in patient 2 or 3 (Figure 3.27). Th17 and Tc17 polarisation in PHA1 patients were not different to healthy controls (Figure 3.28). Supernatant IL-17 and IFNγ concentrations were measured in experiments undertaken in Patient 1; supernatant IL-17 was reduced compared to controls (Figure 3.29). IL-17 responses were also upregulated by the addition of 40mM NaCl to culture conditions in PHA1 patients as they were in controls; however, amiloride did not abrogate IL-17 responses in the PHA1 patient in which this was tested (Figure 3.30).

Figure 3.27: T cell proliferation and activation in patients with PHA1

A. Ki67 expression in CD4+ cells after 72 hours stimulation with anti-CD3 and anti-CD28 in PHA1 patients and healthy controls. Healthy control Ki67 expression (% of CD4+ cells): 84% (69-88); PHA1 86% (67-87); p=0.99. Compared with Mann-Whitney test.

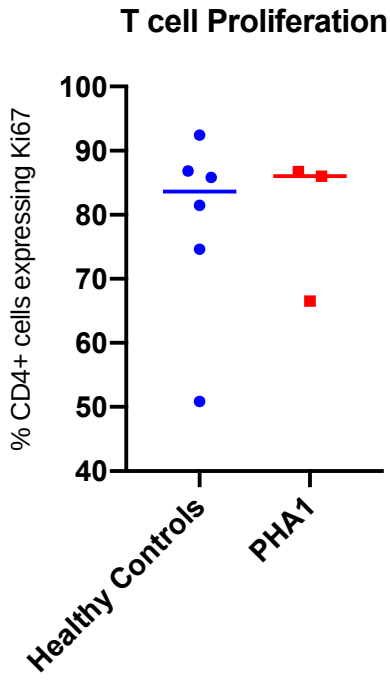

B. CD25 expression in CD4+ cells after 72 hours stimulation with anti-CD3 and anti-CD28 in PHA1 patients and healthy controls. Healthy control CD25 expression (% of CD4+ cells): 89% (85-94); PHA1 91% (62-93); p=0.67. Compared with Mann-Whitney test.

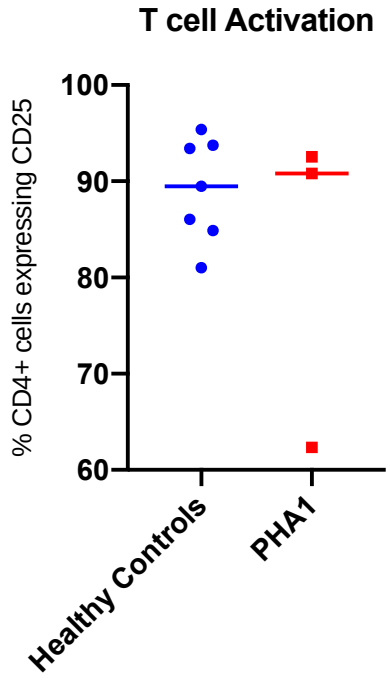

Figure 3.28: IL-17 responses in PHA1 patients and healthy controls

Experiments undertaken in 3 PHA1 patients (repeated in patient 1 twice) and in 26 healthy controls (HCs). 7-day culture undertaken with anti-CD3/28 and Th17 polarising cytokine stimulation as previously described.

Th17 polarisation (% CD4+ cells expressing IL-17) in PHA1 patients and HCs. HC 3.2% (2.5-6.3); PHA1 5.6% (2.9-10.1); p=0.30. Compared with Mann-Whitney test.

Tc17 polarisation (% CD4- cells expressing IL-17) in PHA1 patients and HCs. HC 1.5% (0.6-2.9); PHA1 3.6% (0.9-6.0); p=0.24. Compared with Mann-Whitney test.

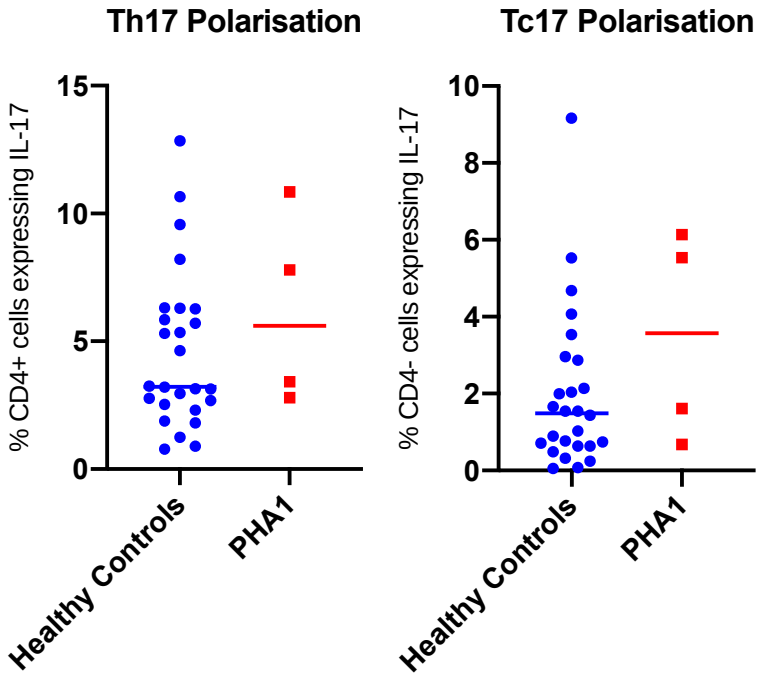

Figure 3.29: Supernatant IL-17 and IFNγ concentrations in PHA1 Patient 1 and healthy controls

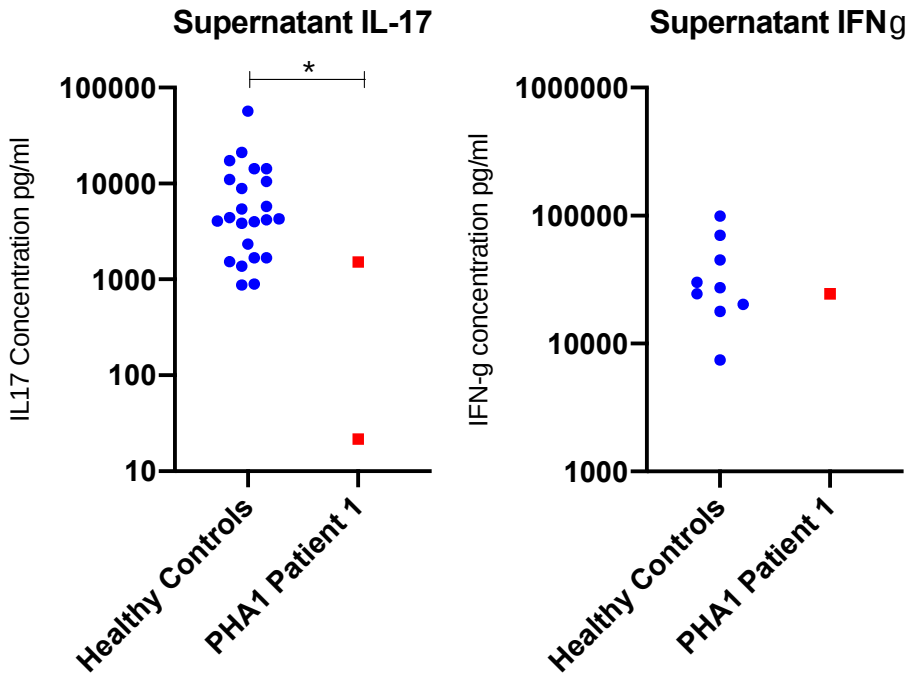

Figure 3.30: Salt responsiveness of IL-17 responses in PHA1 patients and controls, and the effect of amiloride on IL-17 responses in PHA1 patient 1

A. Th17 and Tc17 salt responsiveness in PHA1 patients (n=3, duplicated in PHA1 patient 1) and healthy controls (n=26). Th17 and Tc17 polarisation expressed in high salt media (+40mM NaCl) as a ratio with media without additional NaCl.

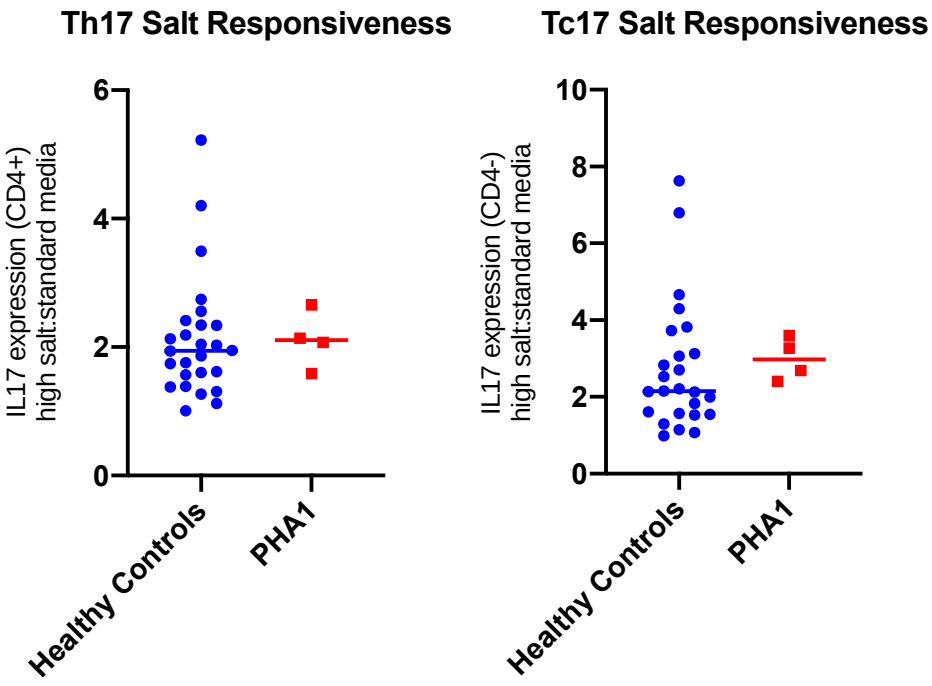

B. The effect of amiloride on IL-17 responses in PHA1 patient 1. Data points represent technical replicates. PBMCs stimulated for 7 days with anti-CD3/28 and Th17 polarising cytokines in media with and without +40mM NaCl and amiloride 20uM.

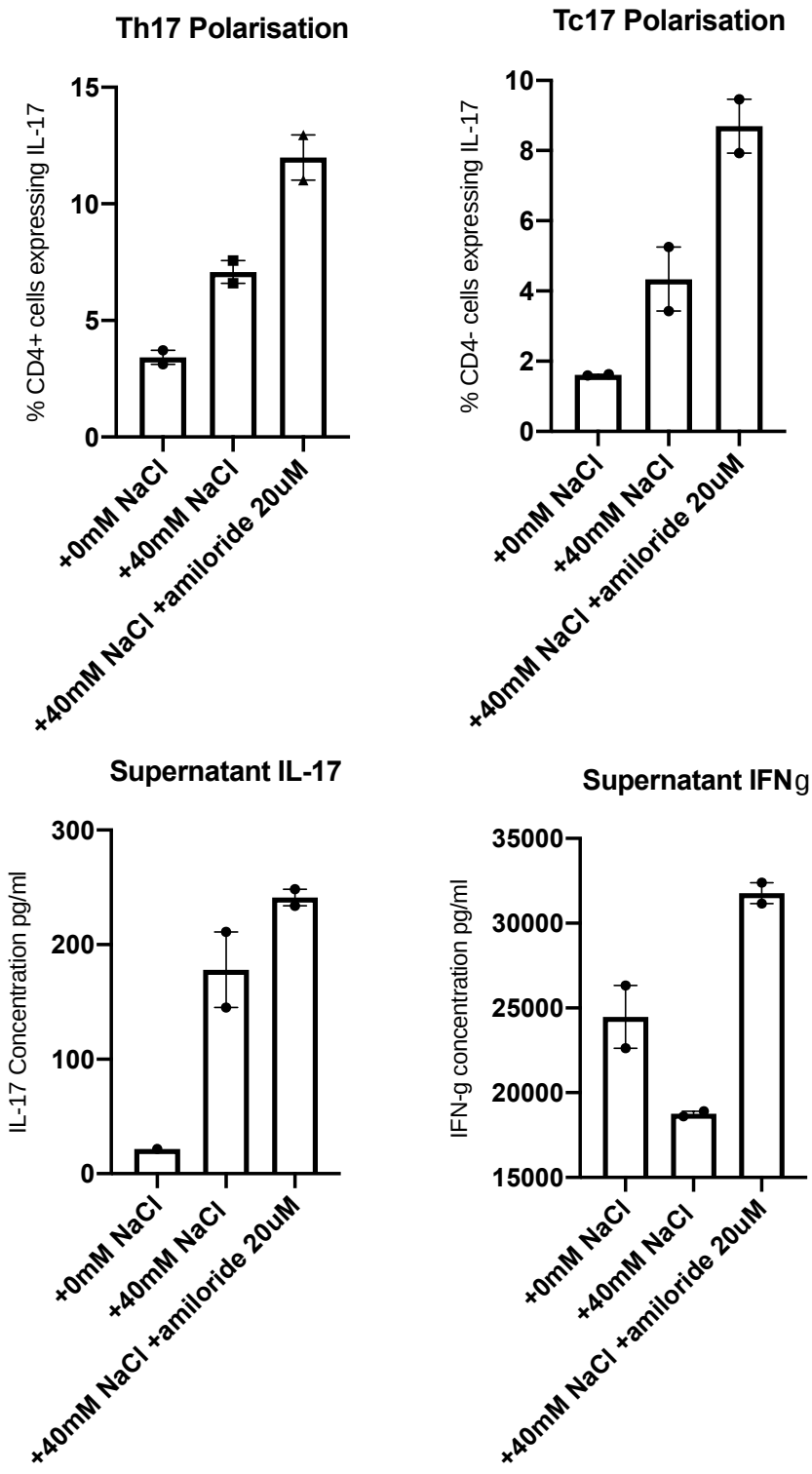

Cytokine stimulation assays were undertaken in Patient 1 who had evidence of reduced T cell activation in our assays. Table 3.5 demonstrates cytokine production in response to innate and T cell stimuli in Patient 1 and in a healthy control analysed within the same experiment. There was a widespread reduction in cytokine concentrations in Patient 1 compared to the healthy control tested; specifically, IFNγ and IL-17 concentrations were reduced in

patient 1 in response to multiple T cell stimuli, in particular PHA. There were also reduced cytokine concentrations in Patient 1 in response to innate stimuli.

Table 3.5: Whole blood cytokine stimulation assay results in Patient 1

Cytokine concentrations (IFN-γ, IL-17, TNF-α, IL-1β, IL-6, IL-10, and IL-12) are reported in response to innate and T cell stimuli and shown against healthy control concentrations analysed within the same experiment.

LPS – Lipopolysaccharide; ZYM – Zymosan; B-GLUC - Beta-glucan; MDP – Muramyldipeptide; aCD3 – anti human CD3; PMA-IONO – phorbol myristate acetate and ionomycin; PHA - phytohaemagglutinin

	IFN-γ (pg/ml)		**IL-17 (pg/ml)**	
	Healthy control	**Patient 1**	**Healthy control**	**Patient 1**
INNATE				
LPS	331	<5.4		
LPS/IL12	1425	1113		
IL18/IL12	8106	4477		
ZYM	628	20		
ZYM/IL12	1327	806		
B-GLUC	64	<5.4		
B-GLUC/IL12	2498	765		
IL15/IL12	744	141		
T CELL				
IL2	57	<5.4	6.2	<1.56
aCD3	942	938	200	72
aCD3+IL2	2200	2294	328	143
PMA-IONO	9640	7132	2045	702
PHA	238	57	398	55.2
PHA/IL12	1651	582		

	TNF-α (pg/ml)		**IL-6 (pg/ml)**		**IL-1β (pg/ml)**	
	Healthy control	**Patient 1**	**Healthy control**	**Patient 1**	**Healthy control**	**Patient 1**
INNATE						
LPS	4579	991	11143	3857	6172	524
LPS/IFNg	10702	3756				

ZYM	4406	2584	5059	3105	12150	7284
B-GLUC	1572	1202	6576	4500	2364	2070
PAM2	159	61	707	27	81	38
MDP	18	11	26	21	33	29
T CELL						
aCD3	1216	857	45	153	37	100
aCD3+IL 2	2656	1628	148	322	153	287
PHA	610	92	2312	245	117	24

	IL-10 (pg/ml)		**IL-12 (pg/ml)**	
	Healthy control	**Patient 1**	**Healthy control**	**Patient 1**
INNATE				
LPS	754	62	55	17
LPS/IFNg	154	68	420	135
ZYM	209	121		
B-GLUC	87	35		
PAM2	15	<0.53		
T CELL				
IL2	2.3	<0.52		
aCD3	535	154		
aCD3+IL2	1595	439		
PHA	298	39		

Cytokine concentrations in response to T cell stimuli in Patient 1 were then compared to a larger group of controls (n=42). The concentrations of IFNγ, IL-17, and TNFα in Patient 1 are plotted against concentrations in this larger control group (Figure 3.31). The lower 95% confidence limit of the median for IL-17, IFNγ, and TNFα concentrations in response PHA stimulation in controls were 202pg/ml, 97pg/ml, and 644pg/ml respectively. IL-17, IFNγ, and TNFα concentrations in Patient 1 were below these levels.

Figure 3.31: IFNγ, IL-17, and TNFα concentrations in PHA1 Patient 1 from whole blood cytokine stimulation assays plotted against concentrations in 42 healthy controls

Healthy control represented by _C (blue triangle) for each stimulating condition; patient 1 represented by _P (red circle) for each stimulating condition

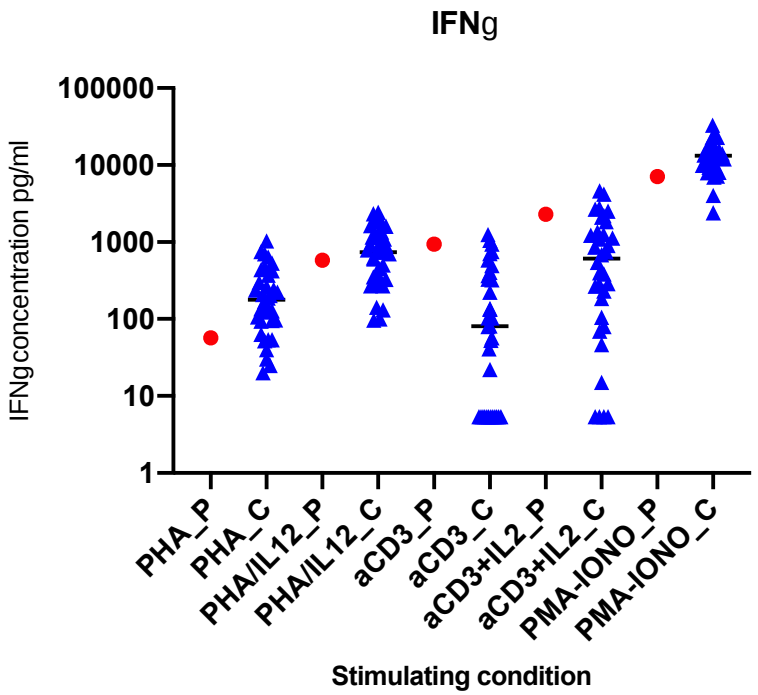
IFNg
IFNg concentration pg/ml
100000
10000
1000
100
10
1
PHA_P
PHA_C
PHA/IL12_P
PHA/IL12_C
aCD3_P
aCD3_C
aCD3+IL2_P
aCD3+IL2_C
PMA-IONO_P
PMA-IONO_C
Stimulating condition

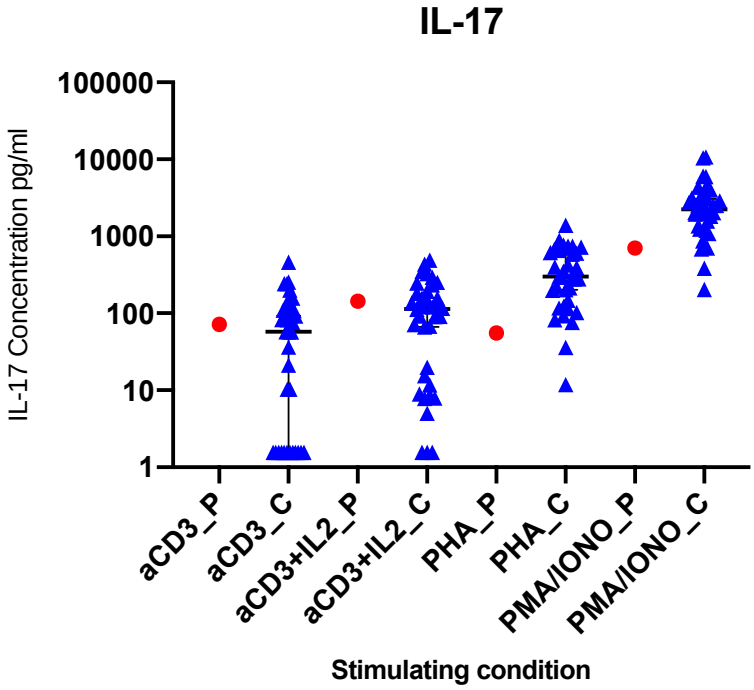
IL-17
IL-17 Concentration pg/ml
100000
10000
1000
100
10
1
aCD3_P
aCD3_C
aCD3+IL2_P
aCD3+IL2_C
PHA_P
PHA_C
PMA/IONO_P
PMA/IONO_C
Stimulating condition

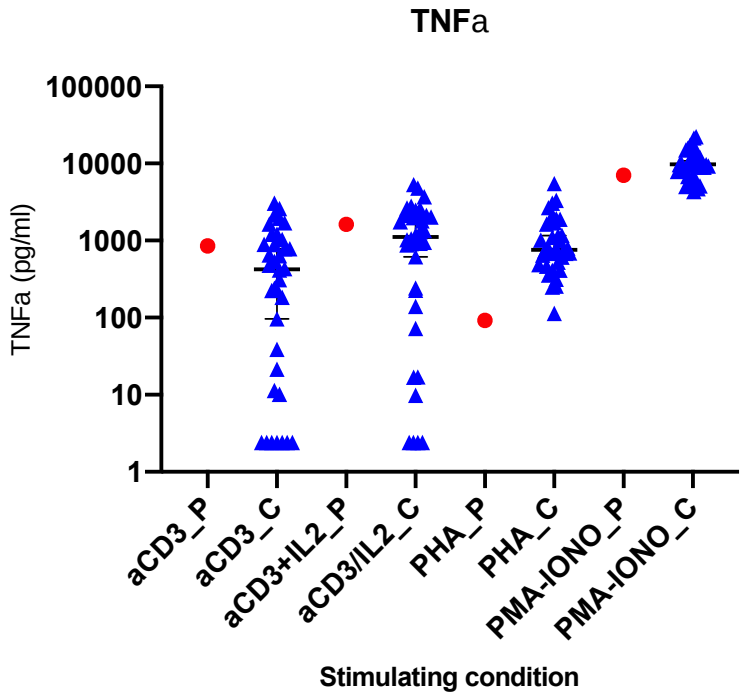

3.5 Discussion

In the initial part of this project, I investigated the effect and mechanism of the inflammatory effect of sodium chloride on *in vitro* IL-17 responses. Having established a 7-day Th17 polarisation assay using stimulated PBMCs, I then investigated the effect of sodium chloride on IL-17 expression in CD4+ (Th17) and CD4- (Tc17) cells. I confirmed previous data demonstrating the addition of 40mM NaCl to culture conditions augmented Th17 polarisation in controls, but also demonstrated this effect was seen in Tc17 cells. Tc17 cells are IL-17 expressing CD8+ cells, which are increasingly implicated in inflammatory disease, including psoriasis, multiple sclerosis, and type 1 diabetes[143]. They require the same cytokine polarising conditions as Th17 cells (I.e. IL-1, IL-6, IL-21, IL-23, and TGFβ) and like Th17 cells, express the pro-inflammatory cytokine IL-17[144]. They may also however co-express other cytokines, notably IFNγ and TNFα, and their immune function is thought to be due largely to the production of this array of inflammatory cytokines, as opposed to through direct cytotoxicity[143,144]. Tc17 cells do, however, show marked plasticity and readily convert to IFNγ expressing CD8+ (Tc1) cells, which possess potent

cytotoxic capabilities. Hence, sodium chloride promotes *in vitro* IL-17 responses in multiple cell types. I also demonstrated that NaCl increases IL-17 expression in both naïve and memory CD4+ cells; these data contradict the findings of the original research in to the effect of salt on IL-17 responses, which reported an effect solely on naïve CD4+ cells[52,53], but are consistent with more recent data which demonstrates salt may also affect memory T cell populations[59]. Naïve cells were more sodium responsive than memory cells and this may be due to the differential sodium channel expression between these subtypes, which was subsequently shown.

To determine the mechanism of NaCl induced inflammation I initially confirmed it was predominantly sodium that mediated its IL-17 polarising effect. This was done through adding alternative osmoles to 7-day culture conditions and correlating measured final supernatant osmolality created by each osmole to IL-17 responses. The ineffective osmole (i.e. one that readily diffuses across the cell membrane and therefore exerts limited tonic effect) urea produced no effect on IL-17 whereas both sodium chloride and sodium gluconate produced a similar inflammatory effect. The effective osmole mannitol had a subtle effect on IL-17 responses in one experiment, albeit not to the extent of sodium containing osmoles, as it has in previous studies[52]. This may be related to increased lymphocyte sodium entry (e.g. through NKCC1) which occurs as a protective mechanism to prevent excessive cell shrinkage in other cells when exposed acutely to hypertonicity regardless of the effective osmole creating the hypertonic conditions[145]. Efforts were made to measure lymphocyte sodium flux using a non-ratiometric sodium dye, but these were unsuccessful.

I then investigated which sodium channels and transporters mediate sodium entry into lymphocytes to exert its pro-inflammatory effect. In dendritic cells in mice, sodium entry is dependent on ENaC, and in T cells sodium entry has been shown to be dependent on NKCC1[49,142]. Consistent with ENaC and NKCC1 mediating the polarising sodium effect in human T cells, I demonstrated that amiloride and furosemide abrogated salt driven IL-17 responses. The inhibitory amiloride effect was specifically on T cells as

opposed to being via an effect on innate immunity, and there was a greater effect with both inhibitors on Tc17 than Th17 cells. Consistent with this Tc17 effect, amiloride reduced both supernatant IL-17 and IFNγ expression, although an inhibitory effect of amiloride on more widespread T cell activation or indeed on alternative sodium transport mechanisms (e.g. sodium-hydrogen exchanger 1) is also possible. Subsequent experiments showed that sodium alters the pattern of calcium flux during T cell activation and that this is reversed with amiloride. These findings of sodium altering calcium flux are consistent with the alteration in intracellular calcium in non-immune human cells that respond to sodium (e.g. osmoreceptors[146]), and the change in calcium signalling in response to sodium seen in mouse dendritic cells (albeit calcium flux reduced in response to sodium in our studies)[49]. Together, these data not only provide an improved understanding of the mechanisms of sodium driven IL-17 inflammation, but also suggests the use of commonly used diuretics may have an immunosuppressive effect and warrants further study.

I finally extrapolated these *in vitro* findings of amiloride sensitive pathways being involved in sodium driven T cell inflammation to patients with rare inherited mutations of one of the subunits of ENaC (resulting in AR PHA1). Whilst respiratory infection is recognised in this patient population and has been attributed to altered salt transport within the lungs, my investigation of immunity demonstrated an increase in bacterial infections both within the lower respiratory tract and elsewhere, and this was associated with other features of dysregulated immunity including fungal/viral infections and increased allergic disease. Similar to the effect observed when amiloride was added to healthy control cells, patients with PHA1 had an altered pattern of calcium flux during T cell activation; this altered calcium signalling is consistent with other ion channelopathies that lead to immunodeficiency[147,148]. This was associated with reduced T cell activation in one of the patients who also had reduced cytokine responses to T cell stimuli, specifically PHA, in whole blood assays. The reason for this specific defect to PHA and not other T cell stimuli is unknown. Cytokine stimulation assays are proposed in the other patients to see if this effect is consistent. There was no obvious change

in 7 day Th17 or Tc17 polarisation in any of the patients but supernatant IL-17 was reduced over 2 experiments in the one patient in which it was measured.

These findings provide the basis of future work that should be aimed at clarifying whether PHA1 patients represent a novel ion channelopathy leading to immunodeficiency. This work should aim to include: a larger cohort of AR PHA1 patients from multiple centres; an analysis of sodium flux in controls and AR PHA1 during T cell activation using patch clamp techniques; a broader assessment of innate and adaptive immune cell subsets (e.g monocyte and NK cell subsets, CD4 and CD8 subsets, and B cell subsets) in PHA1; and an assessment of the effect of amiloride on a wider range of innate and adaptive cytokine responses.

CONCLUSIONS

Sodium chloride increases IL-17 responses in both CD4+ (Th17) and CD4- (Tc17) cells. This effect is mediated predominantly by sodium and is associated with an altered pattern of calcium flux during T cell activation. Sodium channels and transporters are expressed on diverse immune cells and inhibition of ENaC and NKCC1 with amiloride and furosemide respectively abrogates Tc17 polarisation. Patients with inherited mutations in one of the genes that encode ENaC subunits suffer from recurrent infections affecting the upper and lower respiratory tract. Initial data suggests these patients may have a primary defect in T cell function potentially representing a novel ion channelopathy but this requires further study.

4 CHAPTER 4: INVESTIGATING IMMUNITY IN PATIENTS WITH INHERITED SALT LOSING TUBULOPATHY

4.1 Introduction

IL-17 is a pro-inflammatory cytokine produced by CD4+ (Th17) and CD8+ (Tc17) T cells. IL-17 responses provide protection from infection, particularly at epithelial surfaces, but are increasingly implicated in autoimmune disease[70]. Inherited defects in IL-17 immunity lead to Chronic Mucocutaneous Candidiasis (CMC), characterised by mucosal bacterial and fungal infection, often associated with other clinical features of dysregulated immunity including increased allergic disease. CMC is most commonly due to inherited mutations affecting the phosphorylation and activity of the cytokine signalling molecules Signal transducer and activator of transcription 1 and 3 (STAT1 and STAT3), which subsequently impacts Th17 polarisation[87,149].

Initial *in vitro* studies of the effect of salt on IL-17 responses demonstrated:

- Salt (NaCl) activates both Th17 and Tc17 cells;
- The pro-inflammatory effect of salt is predominantly mediated by sodium, as opposed to osmolality;
- Sodium channels and transporters are expressed on diverse immune cells and inhibition of amiloride sensitive channels abrogates sodium driven IL-17 responses;
- Alterations in calcium signalling during T cell activation may mediate inflammatory sodium responses.

These data confirm previous findings on how sodium impacts IL-17 immunity and expand on the mechanisms of sodium sensing and signalling for creation of its inflammatory effect.

The *in vivo* consequences of altering sodium balance on immunity have largely focused on salt loading and how this impacts inflammatory diseases in

animal models. Studies have shown that increased salt intake promotes IL-17 mediated inflammation and worsens autoimmune disease in models of multiple sclerosis, inflammatory bowel disease, and SLE[51,53,54,56,71]. However, the consequences of salt depletion on immunity are unexplored. Moreover, the evolutionary pressures linking immune function to sodium are unclear. Long-term salt restriction studies are logistically challenging and difficult to adhere to; therefore to understand the consequences of reduced sodium balance, I investigated immunity in patients with rare inherited Salt Losing Tubulopathies (SLTs).

Renal sodium handling involves the glomerular filtration of large amounts of sodium, which is then reabsorbed across the tubular epithelium, a process that is homeostatically controlled mainly in the distal nephron. This involves a number of different sodium transporters often functioning in concert with other ion transport mechanisms[118]. Inherited defects in renal sodium reabsorption due to mutations in genes encoding sodium or other ion transporters underlie SLT[117]. The commonest causes of SLT are defects in sodium reabsorption in the thick ascending limb (TAL) and distal convoluted tubule (DCT), leading to Bartter Syndrome (BS) and Gitelman Syndrome (GS) respectively. Defective reabsorption in the DCT is also a feature of the rarer EAST (Epilepsy, Ataxia, Sensorineural deafness, and Tubulopathy) Syndrome, which has a tubular phenotype indistinguishable from GS[129]. Together, these salt losing tubulopathies share a number of clinical and biochemical features including chronic salt depletion from renal salt wasting, in addition to hyperaldosteronism and hypokalaemic metabolic alkalosis, commonly with renal magnesium wasting and hypomagnesaemia. Patients may also have features not apparently related to volume depletion or electrolyte imbalance, including glucose intolerance, recurrent febrile episodes in childhood, and a link to autoimmunity in both BS and GS has been described[125,136,150–154]. These patients therefore provide a unique *in vivo* model of chronic salt depletion but an assessment of their immunity was previously unexplored.

4.2 Aims

i. Investigate whether patients with inherited SLT have clinical features of altered immunity.
ii. Understand the immunological causes of clinical features of altered immunity if present
iii. Determine the mechanisms by which immunity is altered in SLT patients, including investigating the effect of multiple ions on innate and adaptive immune responses

4.3 Brief Methods

SLT patients (GS, BS, and EAST syndrome) were recruited from 2 tertiary centres and they underwent structured history focused on clinical features of altered immunity (Appendix 8.1). This was also undertaken in age and sex matched healthy and disease controls and the prevalence of clinical features of altered immunity compared between the groups. Serum biochemical abnormalities were compared between SLT patients and disease controls, and a subset of SLT patients underwent ^{23}Na-MRI of the lower limb to assess interstitial sodium stores. An infection score based on the diagnostic criteria for patients with inherited defects in IL-17 mediated immunity was created, compared between groups, and correlated to biochemical parameters in SLT patients.

Initial immunological investigations were undertaken in NHS laboratories and included a standard work-up of patients presenting with clinical features suggesting immunodeficiency. I then undertook a more detailed immunological analysis in the UCL research laboratory. Lymphocyte subsets, T cell proliferation and activation, and antigen specific antibody responses were assessed. The urinary microbial community in SLT patients was determined with urine sediment cultures and compared to controls. The following immunological parameters were then analysed in SLT patients and compared to control cohorts:

i. CD4 subsets.

PBMCs were isolated and stimulated with PMA and ionomycin in the presence of brefeldin A for 4 hours prior to analysis of Th1, Th2, and Th17 subsets with FACS.

Next, I investigated the effect of altering extracellular ions on CD4 subset balance. Healthy control PBMCs were stimulated for 3 days with anti-CD3 and anti-CD28, and CD4 subsets were analysed with FACS. Experiments were undertaken in standard media, and in media supplemented with NaCl (+0-40mM), KCl (+0-2mM), and $MgCl_2$ (0-1mM) used alone and in combination.

ii. Th17 and Tc17 polarisation.

PBMCs were isolated and stimulated for 7 days with anti-CD3, anti-CD28 in the presence of cytokines required for optimal IL-17 expression (IL-1, IL-6, IL-21, IL-23, and TGFβ). On day 7, supernatants were collected, and cells were restimulated with PMA and ionomycin in the presence of brefeldin A and Th17 and Tc17 cell polarisation was determined with FACS. Supernatant IL-17 concentrations were measured by ELISA.

In SLT patients, these experiments were undertaken in standard conditions and in media supplemented with NaCl 40mM as in the experiments described in 2.2.1. In control cells these experiments were repeated in the presence of NaCl (+0-40mM), KCl (+0-2mM), and $MgCl_2$ (+0-1mM) used alone and in combination, in addition to experiments with additional aldosterone and angiotensin II.

iii. STAT1 and STAT3 phosphorylation

PBMCs were isolated and stimulated for 15 minutes with IL-6, IL-21, and IFNα. Cells were fixed immediately, then phosphorylation of STAT1 and STAT3 were measured with FACS.

iv. Calcium flux during T cell activation

PBMCs were isolated and loaded with the ratiometric calcium dye indo-1. Cells were then incubated with biotinylated anti-CD3 and baseline intracellular calcium concentrations were analysed with FACS. CD3 was then cross-linked with the addition of streptavidin and calcium flux in to the cell determined. Calcium flux in SLT patients was compared to controls.

v. Expression of components of the intracellular pathway that mediates salt driven IL-17 responses

Lymphocyte SGK1 expression was measured by western blot; NFAT5 expression was measured by quantitative PCR; and IL-23 receptor expression on CD4+ cells determined by FACS.

vi. Innate cytokine responses

Whole blood was stimulated with a variety of innate stimuli and cytokine responses (TNFα, IL-1β, lL-6, IL-10, IL-12, and IFN-γ) measured by multiplex bead array. Experiments were performed by Dr. Rainer Doffinger, Cambridge University Immunology Department.

vii. Monocyte subsets and function

PBMCs were isolated and stained for CD14 and CD16 to determine classical, intermediate, and non-classical subsets. Cells were also stimulated for 4 hours with LPS in the presence of brefeldin A and IFN-γ expression in CD14+ cells was determined by FACS. Stimulation in healthy controls was undertaken in standard conditions and in media supplemented with NaCl, KCl, $MgCl_2$, and aldosterone.

viii. NK subsets and function

PBMCs were isolated and stained for CD45, CD3, CD56, and CD16. The proportion of lymphocytes that were NK cells (CD45+CD3-CD56+CD16+) was determined as was the proportion of CD45+CD3-CD56+ cells expressing

CD16 (the Fc receptor - for recognition and activation by antibody coated cells). Cells were then stimulated for 4 hours with IL-12 and IL-18 in the presence of brefeldin A and NK cell expression of IFN-γ analysed with FACS. In healthy controls stimulation was undertaken in standard conditions and in media supplemented with 40mM NaCl.

4.4 Results

4.4.1 SLT and control cohorts

Immunity was investigated in 47 patients with genotyped SLT[140]. 23 (49%) patients had BS, 22 (47%) patients had GS, and 2 (4%) patients had EAST syndrome (**Table 4.1**). Median age was 35 (28-43) years and 26 (55.3%) patients were female. Biochemical findings at the time of recruitment were typical of SLT, with hypokalaemic metabolic alkalosis and frequent hypomagnesaemia (**Table 4.2**). Consistent with other BS and GS cohorts, BS types 1,2, and 4 had worse renal function and less marked hypokalaemia, hypomagnesaemia and alkalosis than other SLT subtypes[155].

Immunity was compared to age and sex matched healthy (n=24) and disease controls (n=22). Disease controls included patients attending the Tubular Disorders Clinics, but who had no evidence of a significant salt wasting phenotype. Conditions included: proximal tubulopathy = 7; monogenic hypertension = 5 (familial hyperkalaemic hypertension = 3; *STX16* mutation = 2); distal renal tubular acidosis/nephrocalcinosis = 3; isolated renal magnesium wasting = 1; hyperparathyroidism = 1; tubulointerstitial nephritis = 2; medullary sponge kidney = 1; diabetes insipidus = 1; non renal hypokalaemia = 1. The biochemical features of SLT patients were not seen in disease controls; biochemical parameters were not measured in healthy controls but presumed to be normal (**Table 4.3**). Renin or aldosterone was elevated in 24 (96%) of the 25 SLT patients in whom they were measured.

Table 4.1: Demographic data and genotype of salt losing tubulopathy patients

Patient number	Age	Sex	Diagnosis	Gene Affected	Nucleotide Change	Protein Change	Status
1	36	M	Bartter (type 1)	SLC12A1	c.1215G>A	p.(=)	Homozygous
2	26	F	Bartter (type 1)	SLC12A1	c.1316G>A	p.Arg439Gln	Homozygous
3	18	M	Bartter (type 1)	SLC12A1	c.450-451del; c.967G>A	Asp150Glufs*4; Glu323Lys	Compound heterozygous
4	17	M	Bartter (type 1)	SLC12A1	c.1316G>A	p.Arg439Gln	Homozygous
5	19	M	Bartter (type 2)	KCNJ1	Not available		
6	18	F	Bartter (type 2)	KCNJ1	Not available		
7	33	M	Bartter (type 2)	KCNJ1	Not available		
8	41	F	Bartter (type 2)	KCNJ1	c.89G>A	p.Cys30Tyr	Homozygous
9	28	M	Bartter (type 3)	CLCNKB	Not available		
10	31	M	Bartter (type 3)	CLCNKB	Whole gene deletion		Homozygous
11	41	F	Bartter (type 3)	CLCNKB	Whole gene deletion		Homozygous
12	32	F	Bartter (type 3)	CLCNKB	c.887G>A; c.1929+1G>A	p.gly296asp	Compound heterozygous
13	34	M	Bartter (type 3)	CLCNKB	c.887G>A; c.1929+1G>A	p.gly296asp	Compound heterozygous
14	31	M	Bartter (type 3)	CLCNKB	c.1897del	p.Leu633*	Homozygous
15	30	M	Bartter (type 3)	CLCNKB	c.875G>T	p.Cys292Phe	Homozygous
16	23	M	Bartter (type 3)	CLCNKB	c.1395del	p.Tyr466Metfs*13	Homozygous
17	2	F	Bartter (type 3)	CLCNKA; CLCNKB	Partial Deletion both genes		Heterozygous
18	59	F	Bartter (type 3)	CLCNKB	Partial Deletion		Homozygous
19	39	M	Bartter (type 3)	CLCNKB	Whole gene deletion		
20	34	M	Bartter (type 3)	CLCNKB	Not available		
21	24	F	Bartter (type 3)	CLCNKB	Whole gene deletion		Homozygous
22	33	M	Bartter (type 3)	CLCNKB	c.1783C>T	p.Arg595*	Homozygous
23	18	F	Bartter (type 4a)	BSND	c.125G>A; c.139G>A	p.Ser42Asn; p.Gly47Arg	Compound heterozygous

24	27	M	EAST	KCNJ10	c.194G>C	p.Arg65Pro	Homozygous
25	25	F	EAST	KCNJ10	c.194G>C	p.Arg65Pro	Homozygous
26	52	F	Gitelman	SLC12A3	c.1000C>T; c.2221G>A	p.Arg334Trp; p.Gly741Arg	Compound heterozygous
27	37	F	Gitelman	SLC12A3	c.2221G>A; c.2581C>T	p. Gly741Arg; p.Arg861Cys	Compound heterozygous
28	35	M	Gitelman	SLC12A3	c.1825del; ex1_ex8del	p.Glu609Argfs*2	Compound heterozygous
29	85	M	Gitelman	SLC12A3	c.961C>T; c.2883+1G>T	p.Arg321Trp; p.?	Compound heterozygous
30	57	F	Gitelman	SLC12A3; WNK4	c.111T>A; c.1510C>T	p.Tyr37*; p.Gln504*	SLC12A3 heterozygous, WNK4 heterozygous
31	41	F	Gitelman	SLC12A3	c.1196_1202dup; c.2221G>A	p.Ser402*; p.Gly741Arg	Compound heterozygous
32	64	F	Gitelman	SLC12A3	c.1928C>T; ex14del	p.Pro643Leu	Compound heterozygous
33	52	M	Gitelman	SLC12A3	c.1664C>T; c.2882+1G>T	p.Ser555Leu	Compound heterozygous
34	36	F	Gitelman	SLC12A3	c.1261T>C; c.1930del	p.Cys421Arg; p.Gln644Serfs*28	Compound heterozygous
35	47	M	Gitelman	SLC12A3	c.1028T>A	p.Met343Lys	Homozygous
36	33	F	Gitelman	SLC12A3	c.237_238dup	p.Arg80Profs*35	Homozygous
37	68	F	Gitelman	SLC12A3	c.1046C>T; c.1055C>A	p.Pro349Leu; p.Thr352Lys	Compound heterozygous
38	39	M	Gitelman	SLC12A3	c.2576T>C; c.2965G>A	p.Leu859Pro; p.Gly989Arg	Compound heterozygous
39	40	F	Gitelman	SLC12A3	Not available		
40	62	M	Gitelman	SLC12A3	c.1046C>T; c.1055C>A	p.Pro349Leu; p.Thr352Lys	Compound heterozygous
41	31	F	Gitelman	SLC12A3	Not available		
42	35	F	Gitelman	SLC12A3	Not available		
43	58	F	Gitelman	SLC12A3	c.910A>C; c.2883+1G>T	p.Thr304Pro	Compound heterozygous
44	39	F	Gitelman	SLC12A3	c.2368+1del; ex6del		Compound heterozygous

45	67	F	Gitelman	SLC12A3	c.427A>G; c.2221G>A	p.Met143Val; p.Gly741Arg	Compound heterozygous
46	43	F	Gitelman	SLC12A3	c.1664C>T; c.2882+1G>T	p.Ser555Leu	Compound heterozygous
47	31	F	Gitelman	SLC12A3	c.1964G>A; c.2221G>A	p. Arg655His; p.Gly741Arg	Compound heterozygous

Table 4.2: Serum biochemistry in Salt Losing Tubulopathy (SLT) Cohort.

Values reported are mean (standard deviation). Variables are compared between BS types 1,2, and 4 ('antenatal BS/loop phenotype'), BS type 3 ('classical BS/mixed loop and distal tubule phenotype'), and GS/EAST syndrome ('distal tubule phenotype') with a one-way analysis of variance.

	Whole SLT cohort n=47	Bartter syndrome types 1,2, and 4 n=9	Bartter syndrome type 3 n=14	Gitelman and EAST syndrome n=24	P-value
Na (mmol/l)	140 (3)	141 (4)	140 (3)	140 (3)	0.68
K (mmol/l)	3.3 (0.6)	3.7 (0.6)	2.9 (0.6)	3.4 (0.5)	**0.0045**
Cl (mmol/l)	95 (4)	99 (2)	91 (4)	96 (3)	**<0.0001**
HCO3 (mmol/l)	28 (4)	25 (3)	30 (4)	28 (3)	**0.014**
Creatinine (umol/l)	94 (79)	166 (140)	103 (63)	62 (14)	**0.0016**
cCa (mmol/l)	2.43 (0.13)	2.41 (0.12)	2.41 (0.14)	2.45 (0.12)	0.59
PO4 (mmol/l)	1.11 (0.20)	1.19 (0.25)	1.13 (0.21)	1.06 (0.16)	0.20
Mg (mmol/l)	0.70 (0.17)	0.79 (0.18)	0.75 (0.16)	0.64 (0.16)	**0.05**

Table 4.3: Serum biochemistry in Salt Losing Tubulopathy patients and disease controls.

Values reported are median (IQR) and compared with Mann-Whitney test.

	Salt Losing Tubulopathy	Disease Control	P-value
Na (mmol/l)	140 (138-142)	141 (138-142)	0.54
K (mmol/l)	3.3 (2.9-3.8)	4.3 (4.1-4.5)	**<0.0001**
Cl (mmol/l)	95 (91-99)	103 (102-104)	**<0.0001**
HCO3 (mmol/l)	29 (26-30)	24 (22-25)	**<0.0001**
Creatinine (umol/l)	71 (57-88)	81 (62-120)	0.21
cCa (mmol/l)	2.42 (2.37-2.51)	2.39 (2.36-2.43)	0.09
PO4 (mmol/l)	1.08 (1.00-1.23)	1.10 (0.87-1.16)	0.42
Mg (mmol/l)	0.70 (0.58-0.79)	0.87 (0.79-0.92)	**0.0004**

4.4.2 SLT patients have reduced sodium stores

Whether sodium stores (e.g. in muscle and skin) are altered in SLT is unknown. Total body sodium depletion was suggested in SLT by low/normal blood pressure; mean systolic and diastolic blood pressures were 117 ± 12mmHg and 74 ± 7.4mmHg respectively. To measure sodium stores directly, ^{23}Na-MRI was established and optimised using peritoneal dialysis patients as salt loaded positive controls (**Figure 4.1**). After optimisation, four SLT patients underwent ^{23}Na-MRI imaging of the lower limb, which confirmed reduced sodium stores in the skin compared to age matched healthy controls (**Figure 4.2**). Hence, in addition to reduced extracellular potassium and magnesium, SLT patients also have compartments where extracellular sodium concentrations are reduced.

Figure 4.1: ^{23}Na-MRI images demonstrating increased skin and muscle sodium storage in a dialysis patient compared to an age matched healthy control (HC)

Representative ^{23}Na-MRI images of the lower limb from a dialysis patient and a HC. Phantoms of known sodium concentration (0-80mM) are imaged alongside the lower limb.

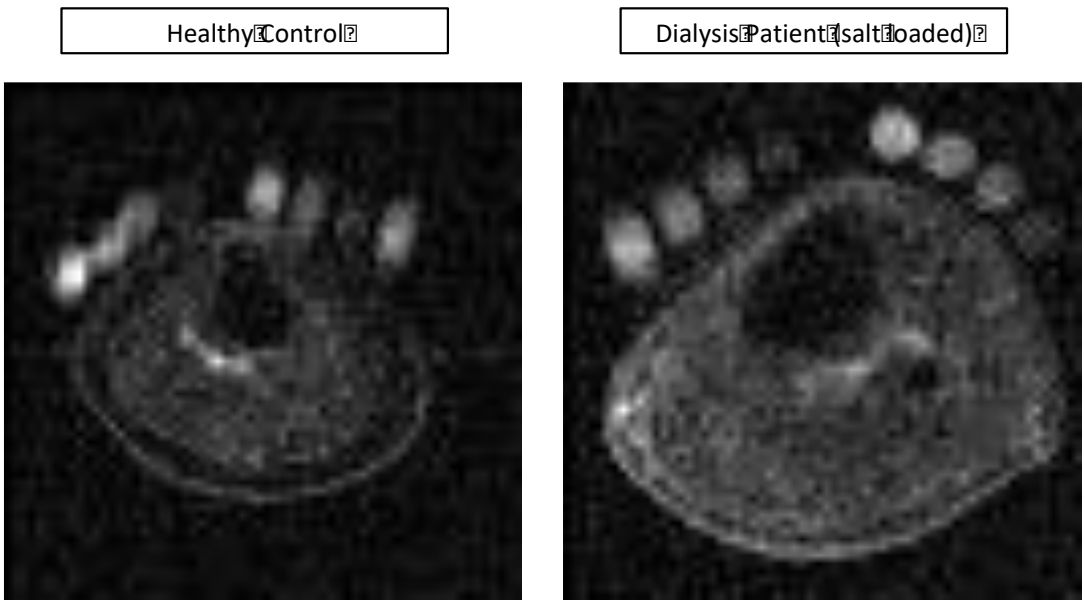

Figure 4.2: **^{23}Na-MRI images demonstrating reduced skin sodium stores in Salt Losing Tubulopathy (SLT) patients compared to age matched healthy controls (HC).**

ns – not significant (p>0.05), *p≤0.05, **p≤0.01, ***p≤0.001, ****p≤0.0001

HC – healthy control; SLT – salt losing tubulopathy

A. Representative ^{23}Na-MRI images of the lower limb from a SLT patient and a HC. Phantoms of known sodium concentration (0-80mM) are imaged alongside the lower limb (red arrows).

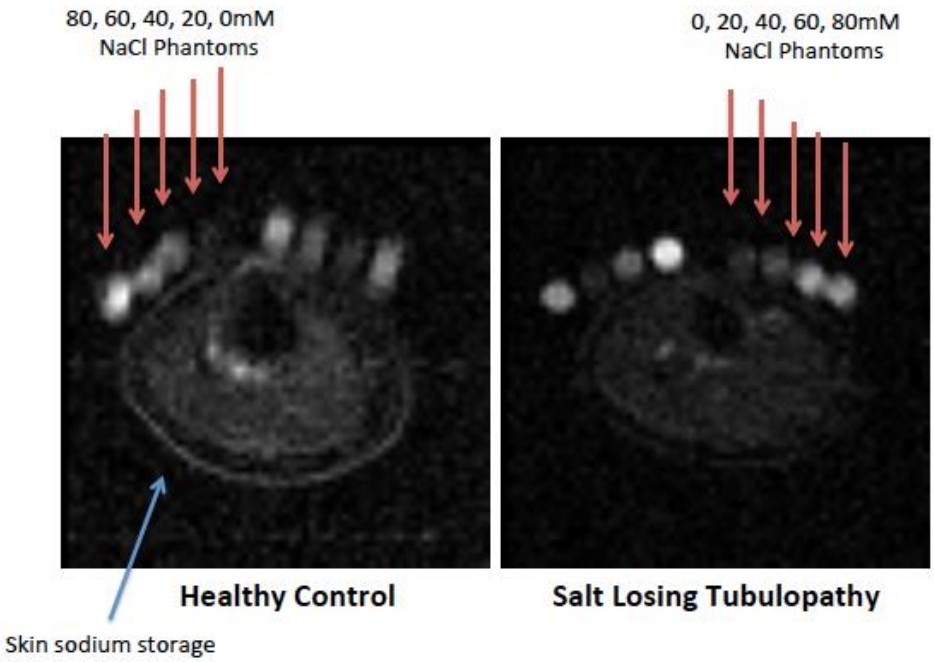

B. Skin and muscle sodium concentrations (median; IQR plotted) as determined by ^{23}Na-MRI in SLT patients (n=4) and age matched healthy controls (n=4). Skin sodium: HC 17.4 (14.0-18.6) AU, SLT 10.8 (7.1-12.9) AU, p=0.029; Muscle sodium: HC 16.3 (15.9-22.1) AU, SLT 16.3 (10.7-20.6) AU, p=0.69. Compared with Mann-Whitney test.

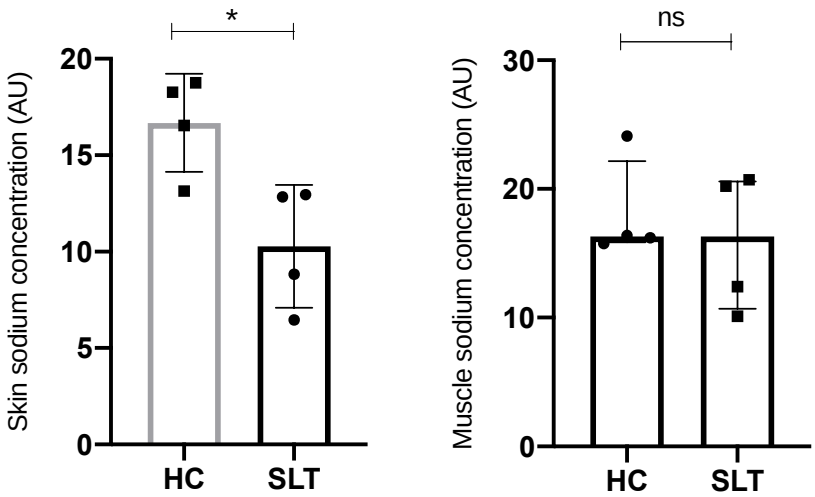

4.4.3 SLT patients have clinical features of immunodeficiency

SLT patients and controls underwent structured clinical history focused on features of dysregulated immunity. These features were compared between

SLT patients and healthy and disease (non-salt losing tubular disease) controls (**Table 4.4**). SLT patients reported increased bacterial (skin abscess, upper respiratory and urinary tract infections) and fungal (mucocutaneous candidiasis; **Figure 4.3**) infections. Viral infections were not different between the groups. In addition, SLT patients reported an increased prevalence of eczema/dermatitis and allergic disease to a variety of antigens. Moreover, autoimmune phenomena were reported in 14 (29.8%) SLT patients: psoriasis n=5; hypothyroidism n= 2: autoimmune hepatitis n=1; vitiligo n= 2; Raynauds n= 2; and sicca symptoms/Sjögren's syndrome n= 2. Hence, SLT patients have clinical features to suggest altered immunity, features that have not been fully appreciated in this patient population before.

Table 4.4: Clinical features of dysregulated immunity in patients with Salt Losing Tubulopathy (SLT) compared to healthy and disease controls.

Prevalence of each clinical feature is reported and number and percentage. SLT patients are compared to healthy controls and disease controls with a Fisher's exact test.

	Salt Losing Tubulopathy N =47	Healthy Controls N=24	Disease Controls N=22	P-value (SLT vs. healthy controls)	P-value (SLT vs. disease controls)
Demographic					
Age (median; IQR)	35 (28-43)	34 (31-45.5)	42 (22-53)	>0.99	>0.99
Sex (n female; %)	26 (55.3)	15 (62.5)	11 (50)	0.56	0.68
Bacterial Infections					
Any bacterial infection	37 (78.7)	8 (33.3)	11 (50.0)	**0.0003**	**0.024**
Abscess	10 (21.3)	2 (8.3)	0 (0.0)	0.2	**0.024**
Pneumonia	8 (17.0)	3 (12.5)	2 (9.1)	0.73	0.48
Recurrent Upper Respiratory Tract Infection (URTI)*	23 (48.9)	3 (12.5)	4 (18.1)	**0.0037**	**0.018**
Recurrent Urinary Tract	17 (36.2)	0 (0.0)	4 (18.1)	**0.0003**	0.17

Infection (UTI)**					
Other severe/recurrent bacterial infection*/****	12 (25.5)	2 (8.3)	5 (22.7)	0.11	>0.99
Fungal Infections					
Any fungal infection	25 (53.2)	12 (50.0)	7 (31.8)	0.8	0.12
Recurrent vaginal (>=2 episodes) **or oral candidiasis**	18 (38.3)	3 (12.5)	5 (22.7)	**0.029**	0.27
Fungal fingernail infection	6 (12.8)	7 (29.2)	0 (0.0)	0.11	0.17
Other severe/recurrent fungal infection***	8 (17.0)	3 (12.5)	2 (9.1)	0.74	0.48
Viral Infections					
Any recurrent viral infection (>=2 episodes**) or severe viral infection**	14 (33.3)	9 (37.5)	5 (21.7)	0.79	0.57
Recurrent varicella zoster virus (VZV)	1 (2.3)	1 (4.2)	2 (9.1)	>0.99	0.27
Recurrent human papilloma virus (HPV)	9 (21.4)	3 (12.5)	2 (9.1)	0.51	0.3
Recurrent Herpes simplex virus (HSV)	6 (14.2)	5 (20.8)	1 (4.5)	0.51	0.41
Other severe/recurrent viral infection****	1 (2.4)	1 (4.2)	3 (13.6)	>0.99	0.11
Atopy					
Any atopic disease	23 (48.9)	11 (45.8)	11 (50.0)	>0.99	>0.99
Asthma	8 (17.0)	5 (20.8)	4 (18.1)	0.75	>0.99
Eczema/dermatitis	15 (31.9)	2 (8.3)	4 (18.1)	**0.039**	0.26

Hay fever/non-allergic rhinitis	16 (34.0)	6 (25.0)	7 (31.8)	0.59	>0.99
Allergy					
Any allergic disease	28 (59.6)	3 (12.5)	10 (45.4)	**0.0001**	0.31
Contact/environmental allergy	17 (36.2)	2 (8.3)	3 (13.6)	**0.012**	0.08
Food allergy	8 (17.1)	0 (0.0)	3 (13.6)	**0.045**	>0.99
Drug allergy	12 (25.5)	1 (4.2)	6 (27.2)	**0.048**	>0.99
Angioedema/urticaria unexplained	5 (10.6)	0 (0.0)	0 (0.0)	0.16	0.17

*inc. tonsilitis, otitis, adenitis and sinusitis; >=3 in worst year; or tonsilitis requiring tonsillectomy; or URTI requiring admission for intravenous antibiotics

**>=3 in worst year in females; or any UTI in childhood; or any UTI in male

***requiring antibiotic treatment or admission

**** **Other severe/recurrent bacterial infection in salt losing tubulopathy:** recurrent dental infection (1); necrotizing gingivitis (1); appendicitis/diverticulitis (3); recurrent adenitis (1); skin (empitigo/cellulitis/wound) (3); recurrent gastroenteritis (2); lymphangitis (1); pelvic (1); septicaemia (staph) (1); recurrent mastitis (1);

***** **Other severe/recurrent fungal infection in salt losing tubulopathy:** skin (7); fungal UTI (1)

****** **Other severe/recurrent viral infection in salt losing tubulopathy:** herpetic stomatitis (1)

Figure 4.3: Recurrent fungal toenail affecting all toes in a patient with Bartter syndrome type 3

4.4.4 SLT patients have an altered urinary microbial community

Given the increased prevalence of mucosal microbial infections in SLT, urine sediment cultures to investigate potential differences in the urinary microbial communities of SLT patients and healthy controls were performed (summarised in **Table 4.5**; full list of organisms in Appendix 8.4). There were altered bacterial constituents with an increase in the presence of *Corynebacterium sp.* in SLT compared to controls. There was no difference in microbial diversity or burden between groups.

To determine whether alterations in extracellular sodium concentration directly affect microbial growth, strains of *E. coli, S. aureus, C. albicans* and *C. amycolatum* were cultured in media supplemented with NaCl. NaCl had no

effect on the growth of the bacteria tested, whereas there was a dose-dependent reduction in the size of *Candida* colonies with additional NaCl (

Figure 4.4). A direct effect of altered extracellular sodium may therefore contribute to mucosal fungal infection; however, the lack of an effect on bacterial growth is consistent with a defect in immunity underlying the altered microbiome and increased urinary infection rate observed in SLT.

Table 4.5: Urinary microbial community in Salt Losing Tubulopathy (SLT) patients and healthy controls (HC).

* reported as median (IQR) CFU/ml across all isolates or across isolates of a specific genus, and compared between SLT and HC with the Mann-Whitney test.

**reported as number (%) of patients with genus present in culture, and compared between SLT and HC with the Fisher's exact test.

***Corynebacterium species isolated in salt losing tubulopathy: *Corynebacterium amycolatum* = 1; *Corynebacterium aurimucosum* = 2; *Corynebacterium coyleae* = 1; *Corynebacterium singular* = 2; *Corynebacterium tuberculostearicum* = 1.

	Salt Losing Tubulopathy N =14	**Healthy Controls N =12**	**P-value**
Demographic			
Age (median; IQR)	33 (30-42)	31 (25-42)	0.64
Male (n;%)	7 (50)	6 (50)	0.99
Microbial diversity			
Number of microbial isolates per subject (median; IQR)	4 (2-4)	3 (2-4)	0.84
Microbial burden*			
All isolates CFU/ml (median; IQR)	66 (3.2-3000)	24 (5-2400)	0.59
Staphylococcus CFU/ml (median; IQR)	36 (3-800)	15 (2-42)	0.24
Streptococcus CFU/ml (median; IQR)	1450 (27-4900)	2400 (78-422400)	0.73
Enterococcus CFU/ml (median; IQR)	60 (5-2000)	20 (5-3200)	0.99
Microbial constituents**			
Citrobacter (n; %)	0 (0.0)	1 (8.3)	0.46
Corynebacterium (n; %)***	7 (50.0)	1 (8.3)	**0.0357**
Staphylococcus (n; %)	10 (71.4)	9 (75.0)	0.99

Streptococcus (n; %)	4 (28.6)	5 (41.7)	0.68
Escherichia (n; %)	2 (14.3)	3 (25.0)	0.99
Lactobacillus (n; %)	1 7.1)	1 (8.3)	0.99
Enterococcus (n; %)	7 (50.0)	4 (33.3)	0.45
Aerococcus (n; %)	1 (7.1)	0 (0.0)	0.99
Facklamia (n; %)	0 (0.0)	1 (8.3)	0.46
Klebsiella (n; %)	2 (14.3)	1 (8.3)	0.99

Figure 4.4: Microbial culture (serial dilutions neat, 10^{-1}, 10^{-2}, 10^{-3}) in tryptone soya agar media, with and without additional NaCl (+0-160mM)

1. <u>*Candida albicans*</u>. Demonstrates reduction in colony size with additional NaCl

A. No additional NaCl **B. +40mM NaCl**

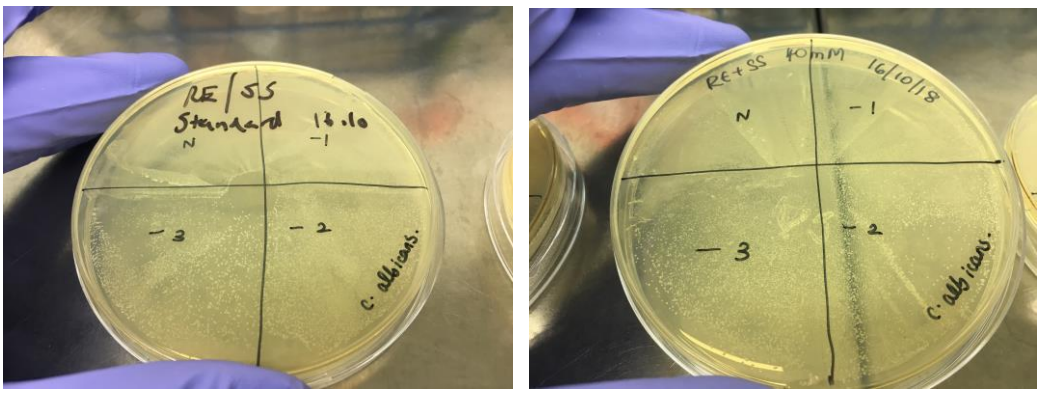

C. +80mM NaCl **D. +160mM NaCl**

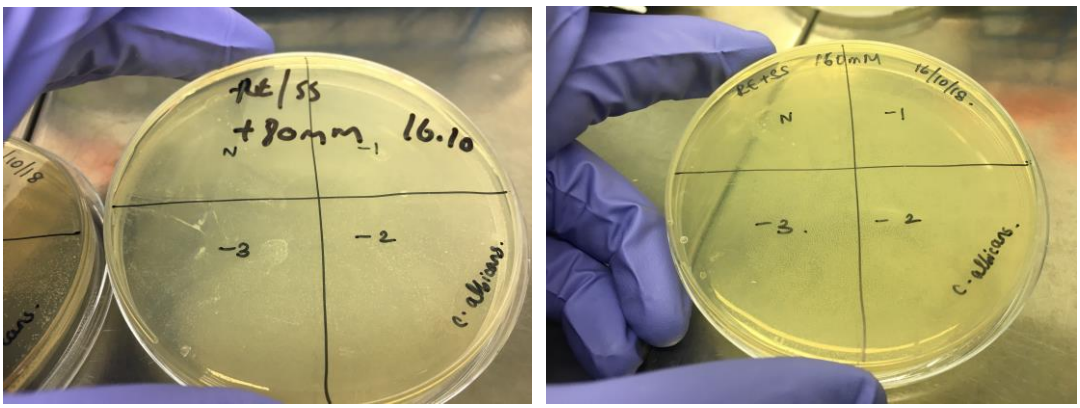

2. <u>*Corynebacterium amycolatum*</u>. Demonstrates no effect of NaCl on growth

A. No additional NaCl **B. +40mM NaCl**

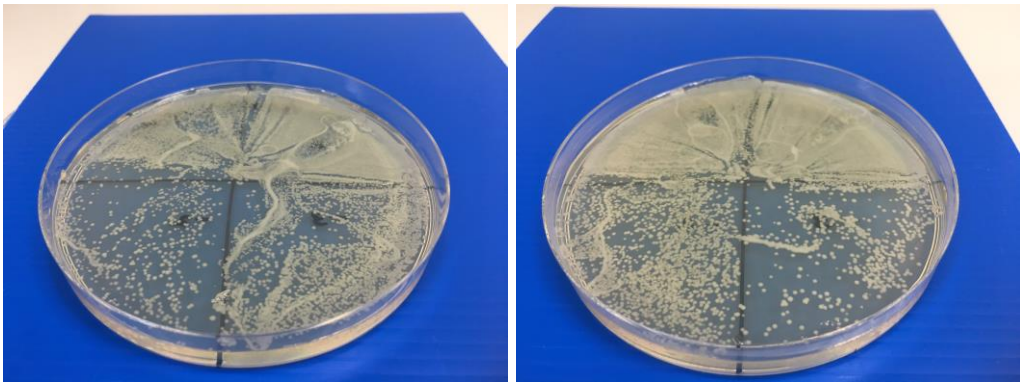

C. +80mM NaCl **D. +160mM NaCl**

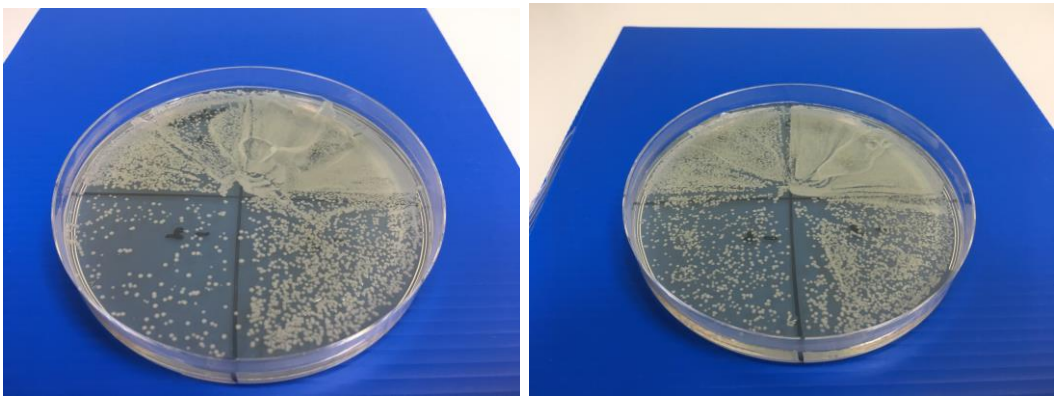

4.4.5 Initial immunological analysis of SLT patients suggests a quantitative defect in NK cells

Immunological analysis of SLT patients is summarised in **Table 4.6**. Total IgE level was elevated in 10 (33.3%) of 30 patients in whom it was measured, and CD16+CD56+ NK (Natural Killer) cells were reduced in 13 (40.6%) of 32 patients (**Figure 4.5**). Otherwise parameters tested, including leucocyte count/differential and lymphocyte (CD3, CD4, CD8, CD19) subsets, were within laboratory reference ranges.

T cell proliferation and activation, determined as the percentage of CD4+ cells expressing Ki67 and CD25 respectively after 72 hours of anti-CD3 and anti-CD28 stimulation, were no different in SLT patients compared to controls

(**Figure 4.6** and **Figure 4.7**). Analysis of antigen specific antibody responses demonstrated SLT patients had protective levels of varicella zoster and pneumococcal immunoglobulin G, similar to the healthy adult population (Figure 2E). Initial immunological analysis of SLT patients therefore demonstrated a reduction in NK cell number, with mild-moderate increases in total IgE (albeit not to the levels seen in Hyper-IgE syndrome[141]), but no other gross defect in adaptive immunity.

Table 4.6: Initial immunological analysis of patients with Salt Losing Tubulopathy (SLT).

Median (IQR) values within the SLT cohort are given, along with the clinical laboratory reference range and the number of values for each variable recorded.

	Normal Range	Number of values	Salt Losing Tubulopathy (median; IQR)
Haemoglobin (g/l)	110-150 (F); 135-170 (M)	46	140.5 (129.5-153.5)
White Cell Count (x10^9/l)	3.5-11	46	8.6 (6.8-10.5)
Neutrophil (x10^9/l)	1.7-7.5	46	5.4 (4.0-6.7)
Lymphocyte (x10^9/l)	1-4	46	2.5 (2.1-3.0)
Monocyte (x10^9/l)	0.2-1.5	46	0.6 (0.5-0.8)
Eosinophil (x10^9/l)	0-0.5	46	0.1 (0.1-0.2)
Basophil (x10^9/l)	0-0.1	46	0.1 (0.1-0.1)
Erythrocyte Sedimentation Rate (mm/hr)	0-20	32	9.0 (7.0-31.3)
C-Reactive Protein (mg/L)	0-5	36	2.0 (1.0-5.0)
Immunoglobulin A (g/l)	0.7-4	34	2.3 (1.5-3.2)
Immunoglobulin G (g/l)	7-16	34	11.3 (9.5-14.9)
Immunoglobulin M (g/l)	0.4-2.3	34	1.1 (0.8-1.8)
Total Immunoglobulin E (KUL)	0-120	30	55.0 (26.8-170.8)
Complement C3 (g/l)	0.9-1.8	32	1.4 (1.2-1.7)
Complement C4 (g/l)	0.1-0.4	32	0.3 (0.2-0.3)
Lymphocyte (absolute; g/l)	1-2.8	32	2.1 (1.6-2.6)
CD3 (absolute; g/l)	0.7-2.1	32	1.6 (1.2-1.9)
CD4 (absolute; g/l)	0.3-1.4	32	1.0 (0.8-1.2)
CD8 (absolute; g/l)	0.2-0.9	32	0.5 (0.4-0.6)
CD19 (absolute; g/l)	0.1-0.5	32	0.2 (0.2-0.4)

CD16, CD56 (absolute; g/l)	0.09-0.6	32	0.1 (0.1-0.2)
CD3 (% of lymphocytes)	55-83	32	77.0 (69.0-81.8)
CD4 (% of lymphocytes)	28-57	32	46.0 (44.0-54.8)
CD8 (% of lymphocytes)	10-39	32	24.0 (18.3-28.0)
CD19 (% of lymphocytes)	6-19	32	11.0 (9.0-15.8)
CD16, CD56 (% of lymphocytes)	7-31	32	7.5 (5.0-11.0)
CD4/CD8 (ratio)	1-3.6	32	2.0 (1.6-3.0)

Figure 4.5: Abnormalities on initial immunological work-up of SLT patients

A. Total Immunoglobulin E (IgE) levels in SLT. Red line depicts upper limit of normal at 120 KUL; 10/30 (33%) SLT patients had IgE > 120 KUL.

B**.** NK cells expressed as a proportion of lymphocytes in SLT. Red line depicts lower limit of normal at 7%; 13/32 (40.6%) SLT patients had NK cells < 7%.

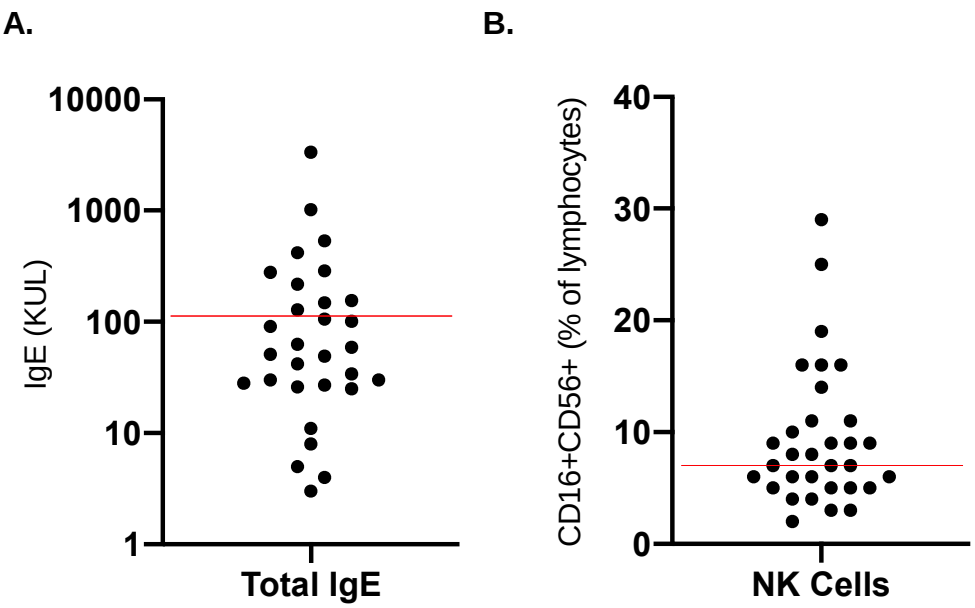

Figure 4.6: T cell proliferation assessment in SLT patients and controls

ns – not significant (p>0.05), *p≤0.05, **p≤0.01, ***p≤0.001, ****p≤0.0001

HC – healthy control; SLT – salt losing tubulopathy

A. T cell proliferation analysis (summary data with median (IQR) plotted) demonstrating percentage of CD4+ cells expressing Ki67 after 72 hours anti-

CD3/anti-CD28 stimulation: HC 83.6% (68.7-88.2) and SLT 76.2% (70.4-85.6), p=0.48. Compared with Mann-Whitney test.

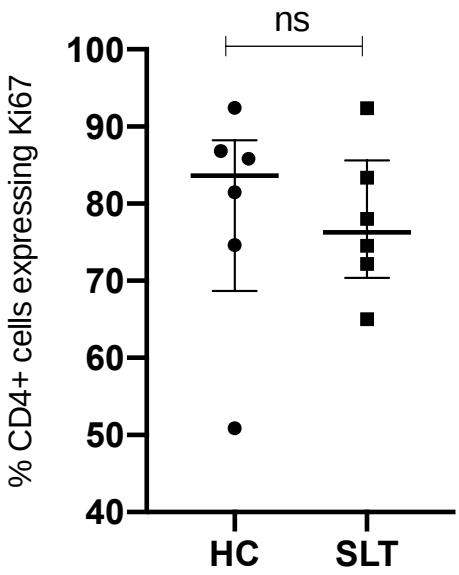

B. Representative FACS plots (CD4 and Ki67 staining) of T cell proliferation analysis in a HC and SLT patient after cell stimulation with anti-CD3/anti-CD28 for 72 hours

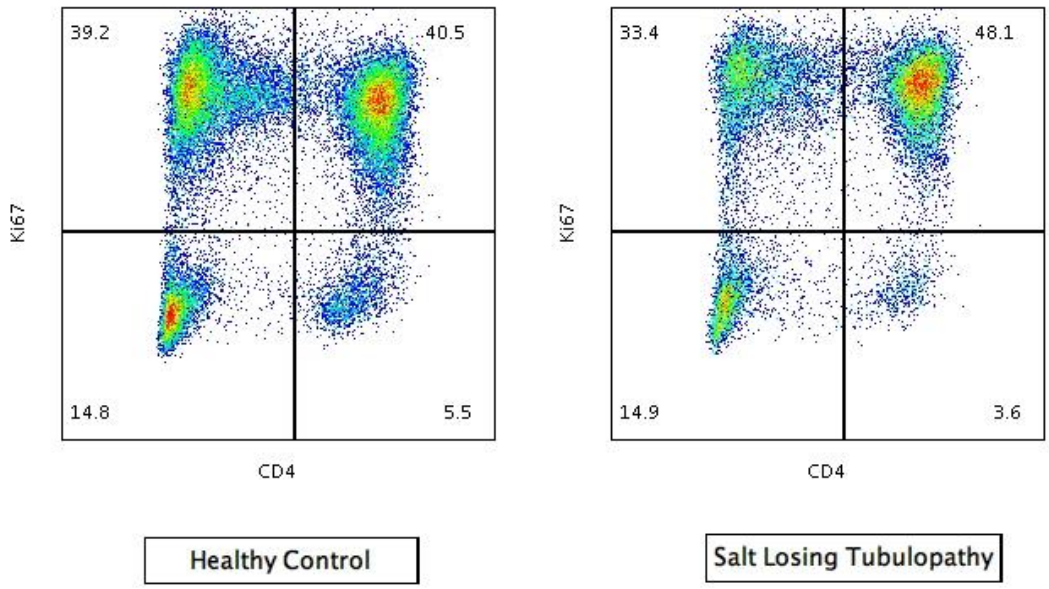

Figure 4.7: **T cell activation assessment in SLT patients and controls**

ns – not significant (p>0.05), *p≤0.05, **p≤0.01, ***p≤0.001, ****p≤0.0001

HC – healthy control; SLT – salt losing tubulopathy

A. T cell activation analysis (summary data with median (IQR) plotted) demonstrating percentage of CD4+ cells expressing CD25 after 72 hours anti-CD3/anti-CD28 stimulation: HC 89.5% (84.9-95.4), SLT 89.1% (87.3-93.5), p=0.99. Compared with Mann-Whitney test.

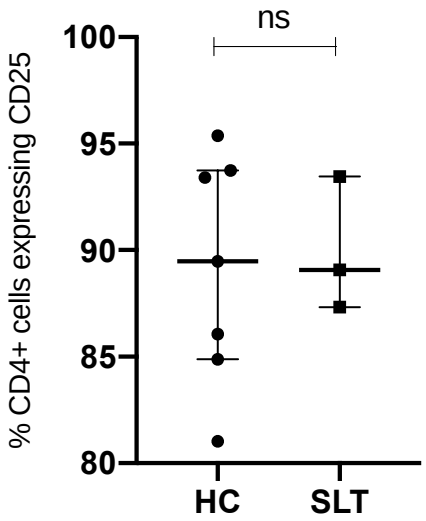

B**.** Representative FACS plots (CD4 and CD25 staining) of T cell activation analysis in a HC and SLT patient after cell stimulation with anti-CD3/anti-CD28 for 72 hours

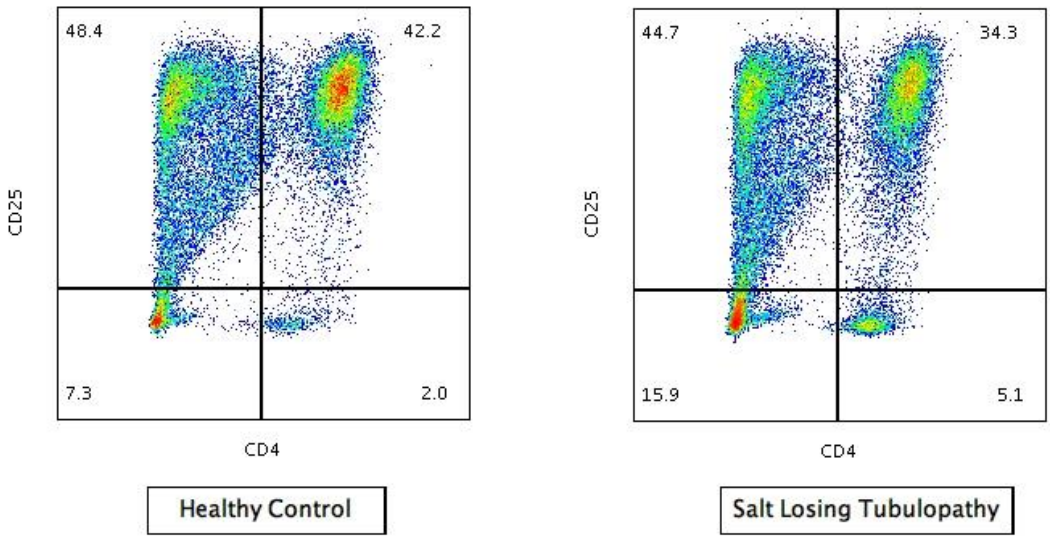

Figure 4.8: Antigen specific immunoglobulin responses in SLT patients

Varicella zoster and pneumococcal specific immunoglobulin G levels in SLT patients; levels are consistent with healthy adult population as per assay interpretation data.

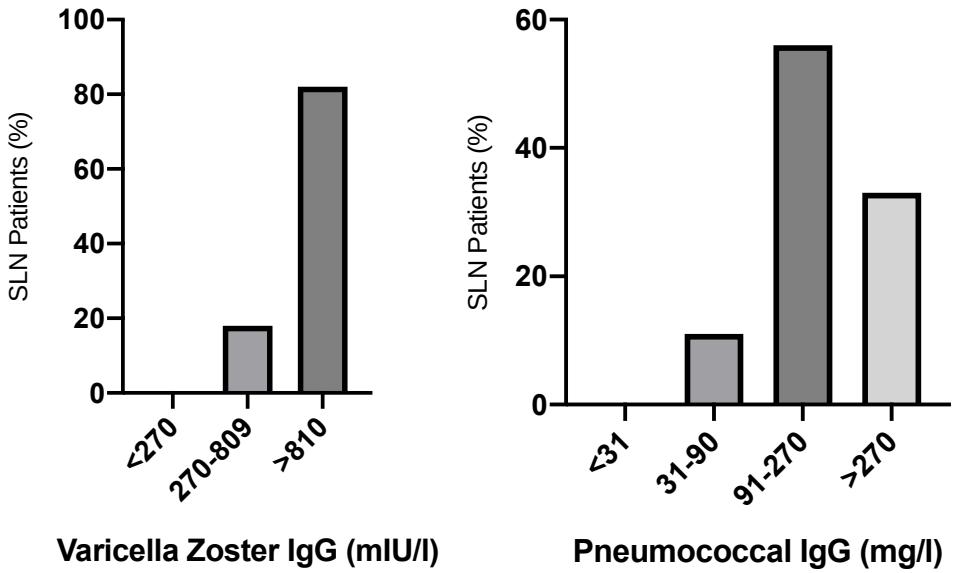

4.4.6 Circulating Th17 cells are reduced in SLT patients

Given the clinical findings in SLT of increased mucosal infection, and the known effect of salt on Th17 responses, CD4+ T cell subsets were assessed in SLT and compared these to healthy and disease controls. Analysis of IFNγ, IL-4, and IL-17 expression in CD4+ cells, representative of Th1, Th2, and Th17 cells respectively, demonstrated a significant reduction of Th17 cells in SLT, whilst Th1 and Th2 cells were not different between groups (**Figure 4.9**).

When CD4 subsets were expressed as a ratio of one cell subtype to another within each subject, there was a difference in the ratio of Th2:Th17 cells between SLT patients and controls, although individual group differences were not significant in multiple comparison testing (**Figure 4.10**). This imbalance in CD4 subsets with a reduction in Th17 cells and increase in Th2 cells is consistent with the observed findings of increased infection in the SLT cohort, and the increased prevalence of allergy and associated increase in total IgE.

Figure 4.9: CD4 subset analysis in Salt Losing Tubulopathy (SLT) patients and controls.

HC – healthy control; SLT – salt losing tubulopathy; DC – disease control

A. IFNγ, IL-4, and IL-17 expression in CD4+ cells after 4 hours stimulation with phorbol myristate acetate (PMA) and ionomycin in SLT patients, healthy controls (HC) and disease controls (DC). Cytokine expression is reported as percentage of CD4+ cells; median (IQR) values within each group are plotted. Groups are compared with the Kruskall-Wallis test with Dunn's multiple comparison testing.

IFNγ expression (Th1 cells): HC 1.9% (1.5-4.0), SLT 1.3% (1.0-3.7), DC 0.9% (0.5-8.9), p=0.53.

IL-4 expression (Th2 cells): HC 2.8% (0.8-4.8), SLT 3.0% (1.7-3.3), DC 2.5% (0.7-3.0), p=0.52.

IL-17 expression (Th17 cells): HC 1.4% (0.9-2.2), SLT 0.7% (0.3-1.4), DC 1.0% (0.8-1.4), p=0.038.

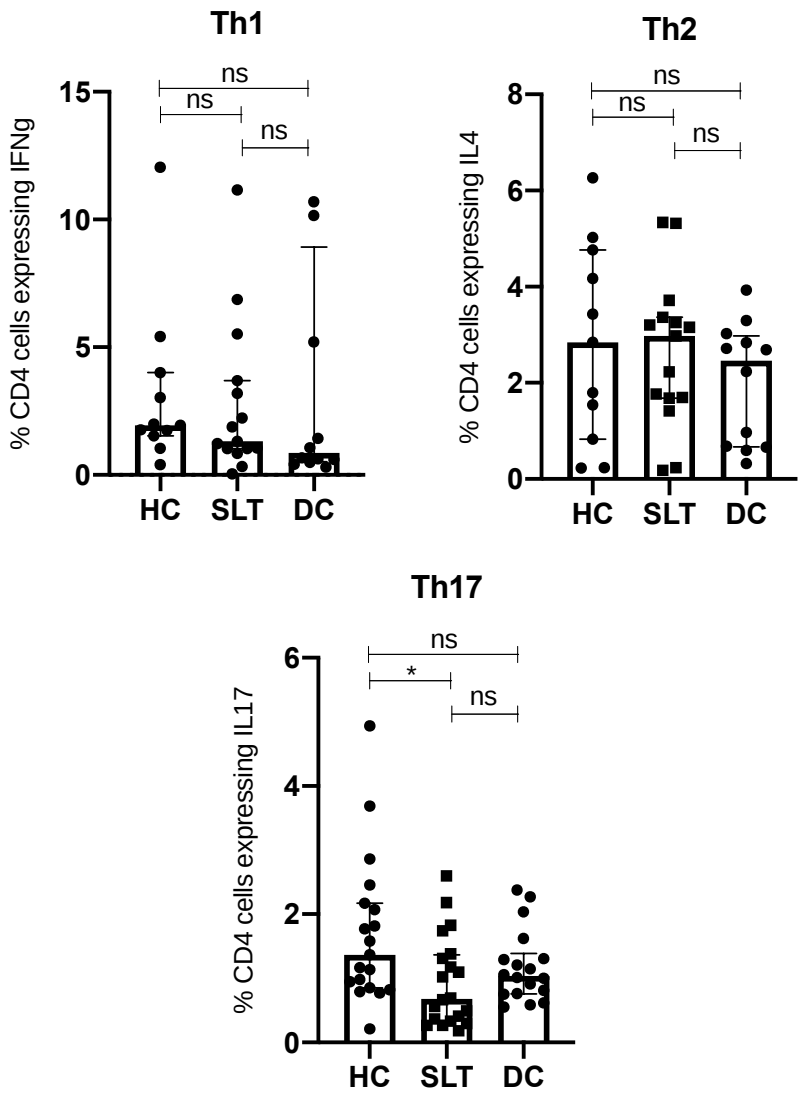

B. Representative FACS plots of IFNγ, IL-4, and IL-17 expression in CD4+ cells in a SLT patient and HC

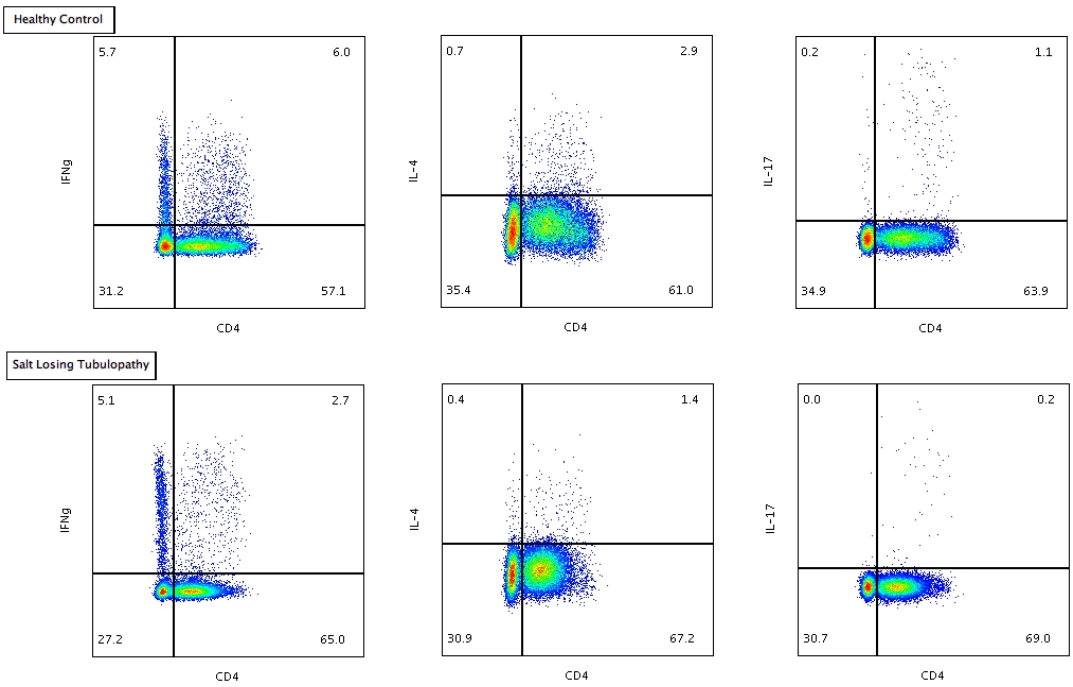

Figure 4.10: Balance of Th1, Th2 and Th17 cells in SLT patients and controls

Ratio of IFNγ, IL-4, and IL-17 expression in each subject in SLT patients, HC, and DC. Median (IQR) values within each group are plotted. Groups are compared with the Kruskall-Wallis test with Dunn's multiple comparison testing.

IFNγ:IL-4 (Th1:Th2): HC 1.2 (0.4-2.9), SLT 0.7 (0.3-3.9), DC (1.0 (0.4-3.9), p=0.82.

IFNγ:IL-17 (Th1:Th17): HC 1.8 (0.8-7.0), SLT 3.3 (1.6-8.3), DC 1.0 (0.5-7.8), p=0.40.

IL-4:IL-17 (Th2:Th17): HC 1.9 (0.4-3.2), SLT 3.4 (1.2-6.6), DC 1.4 (0.7-2.5), p=0.05.

HC – healthy control; SLT – salt losing tubulopathy; DC – disease control

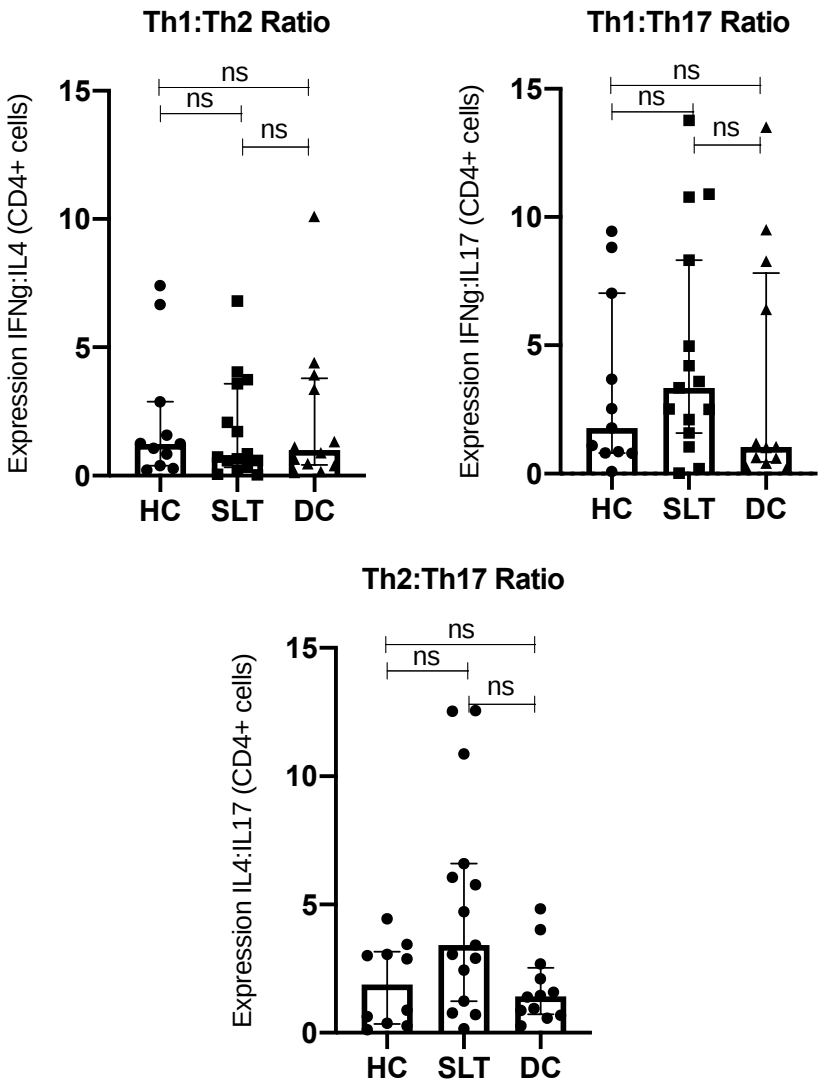

4.4.7 Th17 and Tc17 polarisation are reduced in SLT patients

To further investigate IL-17 responses, PBMCs were cultured under optimal Th17 polarising conditions for 7 days. IL-17 expression in CD4+ and CD4- cells, representing Th17 and Tc17 polarisation respectively, were reduced in SLT patients compared to both healthy and disease controls (**Figure 4.11**). Supernatant IL-17 concentrations were reduced in SLT patients compared to healthy controls (**Figure 4.12**). Together with the CD4+ cell subset analysis, these data confirm SLT patients have reduced IL-17 responses.

Figure 4.11: Th17 and Tc17 polarisation in Salt Losing Tubulopathy (SLT) patients, healthy controls (HC) and disease controls (DC).

A. IL-17 expression in CD4+ cells (Th17): HC 3.2% (2.5-6.3), SLT 1.6% (0.8-2.0), DC 2.6% (2.1-3.5), p=0.0001. Groups compared with the Kruskall-Wallis test with Dunn's multiple comparison testing.

B. IL-17 expression in CD4- cells (Tc17): HC 1.5% (0.6-3.0), SLT 0.6% (0.3-1.1), DC 1.9% (1.1-2.2), p=0.0005. Groups compared with the Kruskall-Wallis test with Dunn's multiple comparison testing.

C. Representative FACS plots of IL-17 expression in CD4+ cells in a HC and 2 SLT patients.

ns – not significant (p>0.05), *p≤0.05, **p≤0.01, ***p≤0.001, ****p≤0.0001

SLT – salt losing tubulopathy; HC – healthy control; DC – disease control; PBMCs – peripheral blood mononuclear cells

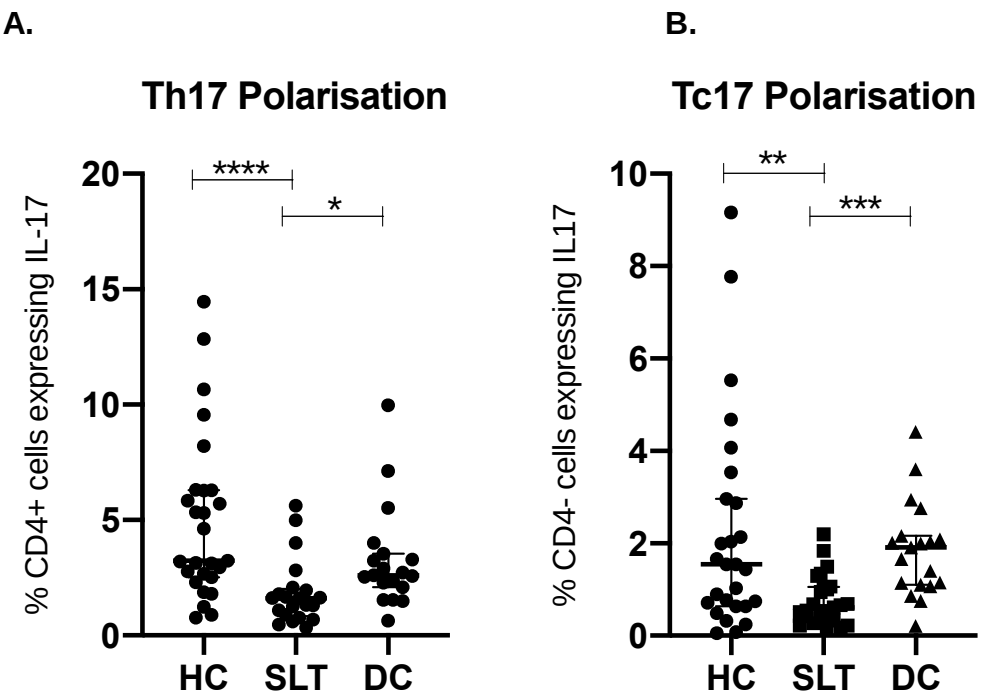

C.

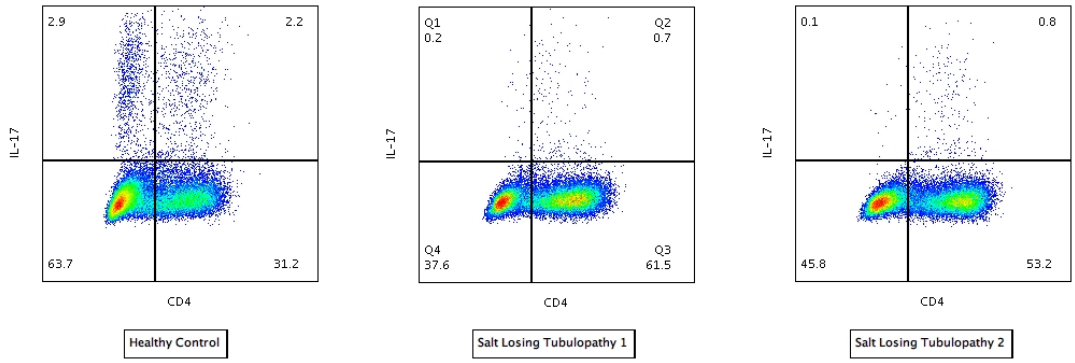

Figure 4.12: Supernatant IL-17 concentrations in SLT patients and controls

Supernatant IL-17 concentrations: HC 4287pg/ml (1681-10487), SLT 1117pg/ml (249-3709), DC 951pg/ml (503-3768), p=0.0012.

ns – not significant (p>0.05), *p≤0.05, **p≤0.01, ***p≤0.001, ****p≤0.0001

SLT – salt losing tubulopathy; HC – healthy control; DC – disease control; PBMCs – peripheral blood mononuclear cells

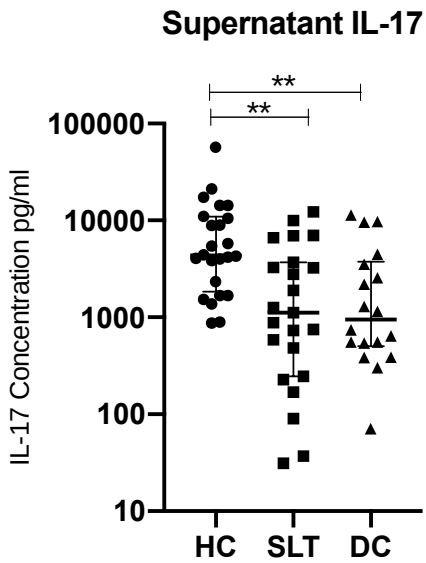

4.4.8 The clinical phenotype in SLT patients is consistent with an IL-17 defect, but STAT1 and STAT3 phosphorylation are normal

Reduced IL-17 responses underlie CMC, which is commonly due to mutations in STAT1 or STAT3 and may be part of the Hyper-IgE syndrome. To assess

whether the infections suffered by SLT patients were consistent with an IL-17 defect, we devised a scoring system based on the infection related components of the Hyper-IgE syndrome diagnostic criteria (Table 2.1), and applied this to SLT patients and controls[141]. IL-17 related infection scores were higher in SLT patients than both control groups (**Figure 4.13**); moreover, the clinical phenotype of SLT patients was similar to patients with STAT1 and STAT3 mutations (

Table 4.7). We then assessed STAT1 and STAT3 phosphorylation in SLT patients, but these were normal demonstrating STAT1 and STAT3 signalling defects are not the cause of defective IL-17 responses (

Figure 4.14).

Figure 4.13: IL-17 related infection score in SLT patients and controls

HC 1.0 (0.0-2.8); SLT 5.0 (1.0-8.0); DC 0.0 (0.0-2.3), p=0.0006. Median (IQR) scores plotted in each group. Groups compared with Kruskall-Wallis test with Dunn's multiple comparison testing.

ns – not significant (p>0.05), *p≤0.05, **p≤0.01, ***p≤0.001, ****p≤0.0001
SLT – salt losing tubulopathy; HC – healthy control; DC – disease control

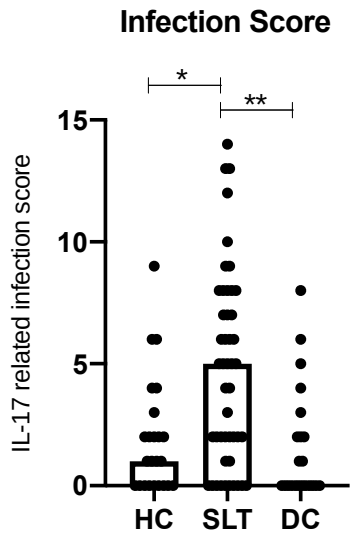

Table 4.7: Clinical features in the Salt Losing Tubulopathy cohort in this study and in cohorts of patients with inherited defects in IL-17 mediated immunity due to mutations in STAT1 and STAT3.

Study Reference	**Salt Losing Tubulopathy Cohort in this study**	**Autosomal Dominant Hyper-IgE Syndrome in the USIDNET Registry.** Gernez et al. J Allergy Clin Immunol Pract 2018.[86]	**Heterozygous STAT1 gain-of-function mutations underlie an unexpectedly broad clinical phenotype.** Toubiana J et al. Blood 2016.[89]
Location	United Kingdom	North America	International (62% European)
Genetic cause of chronic mucocutaneous candiasis	NA	STAT3 deficiency (Autosomal Dominant Hyper-IgE Syndrome)	STAT1 gain-or-function
Number of patients in cohort	47	85	274
Demographics	Median age 35 (time of study); 55.3% female	59% male; 62.4% Caucasian	Median age 22 (time of study); M:F ratio 1.03
Bacterial Infections			
Any bacterial infection	79%		74%
Abscess	21%	74%	28% (recurrent skin infections including cellulitis, abscess, and paronychia)

Lower Respiratory Tract Infection	17%	72%	47%
Upper respiratory tract infection	49%	48.8% sinusitis; 42.7% otitis; 11.7% tonsillectomy	44%
Urinary Tract Infection	36%	2.4% pyelonephritis	2.9% recurrent pyelonephritis
Other severe bacterial infection	6.4% appendicitis/diverticulitis; 6.5% skin infection; 4.3% recurrent gastroenteritis; 2.1% sepsis	18.2% cellulitis, 7.3% sepsis, 6.1% meningitis, 5.8% lymphadenitis	2.9% severe gastroenteritis, 2.6% sepsis, 6% mycobacterial diseases.
Fungal Infections			
Recurrent oral/vaginal candidiasis	38%	21%	98% chronic mucocutaneous candidiasis (93% oral thrush, glossitis, and/or chelitis; 56% oesophageal/genital)
Fingernail fungal infection	13%	28%	56%
Other fungal infection	15 % fungal skin infection		10% invasive fungal infections.
Viral Infections			
Any recurrent or severe viral infection	33%	7.4% herpes.	38% at least 1 systemic or atypical viral infection, or recurrent mucocutaneous viral infection
Recurrent VZV	2%		12% shingles and 7% severe chicken-pox
Recurrent HPV	21%		12% moluscum contagiosum or warts
Recurrent HSV	14%		32% recurrent mucocutaneous viral infection HSV or VZV)
Other viral infection			8% severe systemic viral infection
Atopic disease			
Asthma	17%	39%	
Eczema	32%	57%	
Allergic disease			
Any allergic disease	60%	65%	
Contact and environmental allergy (inc wasp stings, dust, dander pollens)	36%	18%	
Food allergy	17%	37%	

Drug allergy	26%	43%	
Angioedema/hives unexplained	11%	8.5% anaphylaxis, 15.9% urticaria	
Other features			
Malignancy		7% malignancy (lymphoma 3, thyroid 1, brain 1, squamous cell carcinoma 1)	
Autoimmune	30%		37% autoimmune manifestation (largely thyroid disease, 22%)

Figure 4.14: Phosphorylation of STAT1 and STAT3 in Salt Losing Tubulopathy (SLT) patients

SLT – salt losing tubulopathy; HC – healthy control; DC – disease control

A. Phosphorylation of STAT1 after stimulation with IFNα in SLT patients (expressed as ratio of up-regulation of pSTAT1 in SLT compared to HC; red line drawn at ratio of 1 representing no difference between SLT and HC).

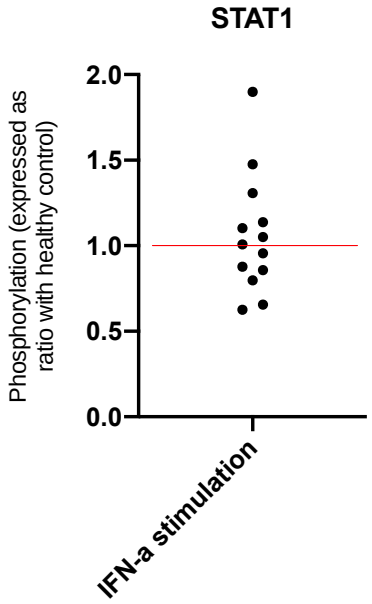

B. Representative histograms of up-regulation of pSTAT1 after stimulation with IFNα in a SLT patient and a HC (red – unstimulated; blue – stimulated).

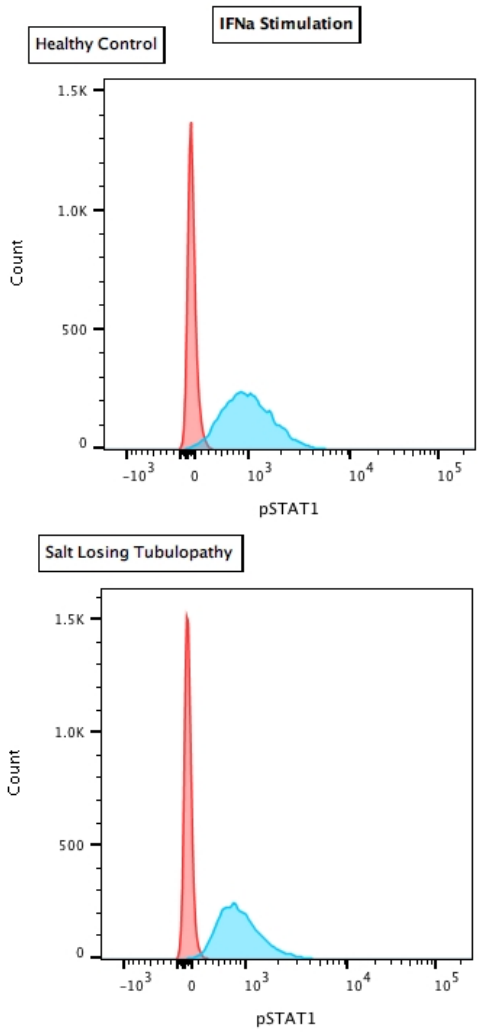

C. Phosphorylation of STAT3 after stimulation with IL-6 and IL-21 in SLT patients (expressed as ratio of up-regulation of pSTAT3 in SLT compared to HC; red line drawn at ratio of 1 representing no difference between SLT and HC).

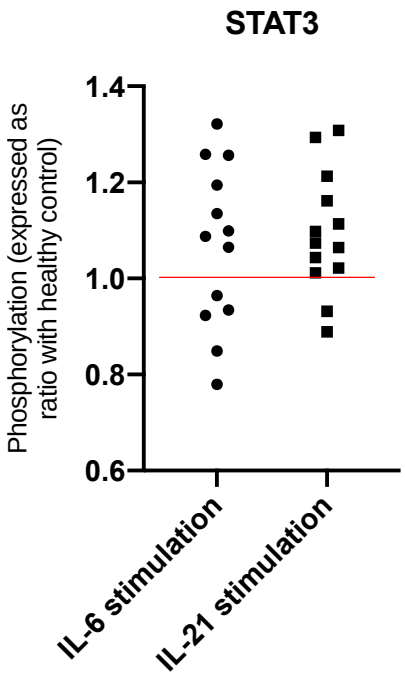

D. Representative histograms of up-regulation of pSTAT3 after stimulation with IL-6 and IL-21 in a SLT patient and a HC (red – unstimulated; blue – stimulated).

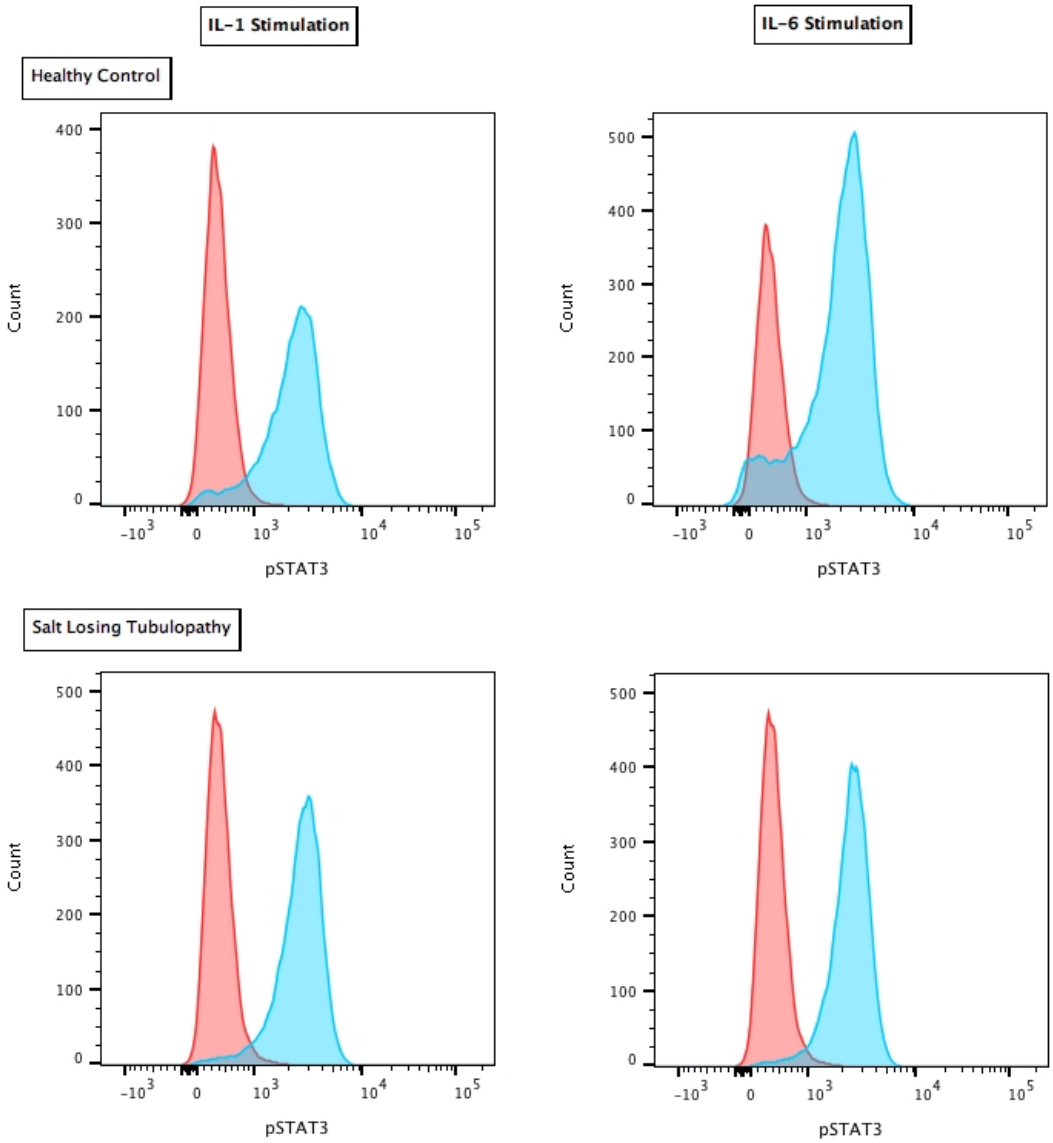

4.4.9 Reduced IL-17 responses in SLT patients are not due to altered ion channel or transporter activity on immune cells

Mutations in a number of different ion channels expressed on immune cells lead to immunodeficiency, largely as a result of associated changes in calcium signalling during leucocyte activation[156]. The commonest defective sodium transporter in our SLT cohort was the sodium chloride cotransporter (NCC, SLC12A3). As demonstrated in 3.4.6, NCC is expressed on diverse immune cell subtypes in healthy controls and NCC inhibition with hydrochlorothiazide (HCT; 20uM) has no effect on wildtype *in vitro* IL-17 responses or calcium flux during T cell activation (Figure 3.16, Figure 3.23).

NCC expression and calcium flux were also assessed in lymphocytes in GS. NCC was expressed on diverse lymphocytes in GS as it was in controls (**Figure 4.15**). This is consistent with the NCC transporter defect in GS being functional as opposed to being due to reduced cell surface expression. Moreover, SLT patients had a normal pattern of calcium flux during T cell activation (**Figure 4.16**). Given these data, reduced IL-17 responses in SLT are not likely to be due to primary perturbations of NCC function or secondary dysregulation of intracellular calcium signalling in immune cells.

Figure 4.15: NCC expression on lymphocytes in Gitelman Syndrome patients

NCC expression is demonstrated on CD4+, CD8+, CD45+CD3-CD56+, CD45RA-, and CD45RA+ cells; reported as percentage of cell type expressing NCC in 2 GS patients (median;IQR plotted). The pattern of expression is consistent with healthy control NCC expression (NCC expression in one healthy control demonstrated).

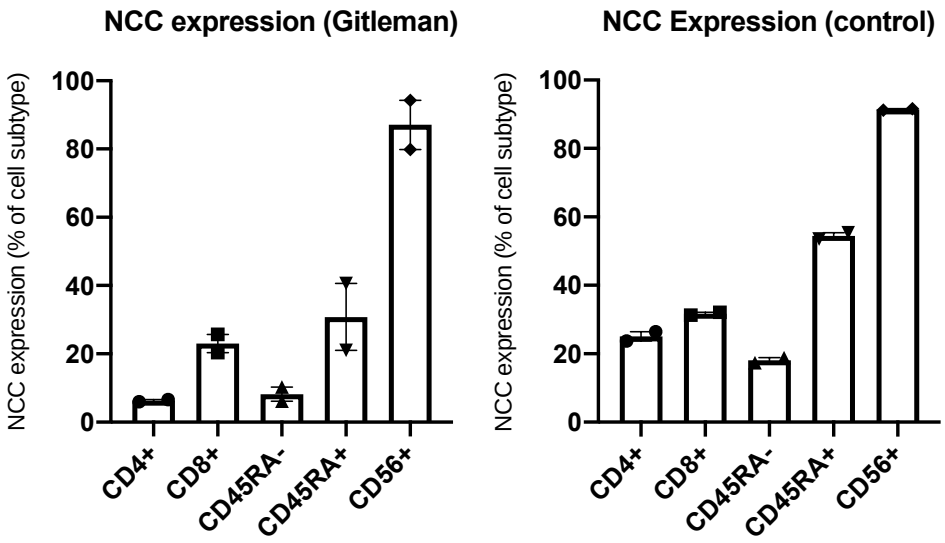

Figure 4.16: Calcium flux after T cell activation in Gitelman Syndrome

HC – Healthy Control; GS – Gitelman Syndrome

A. Area under the calcium flux curve (as determined using the ratiometric calcium dye Indo-1 gated on CD4+ cells) after T cell activation with anti-CD3: HC 275.9AU (265.9-279.9); Gitelman Syndrome (GS) 277.8AU (257.5-280.5), p=0.94. Compared with Mann-Whitney test.

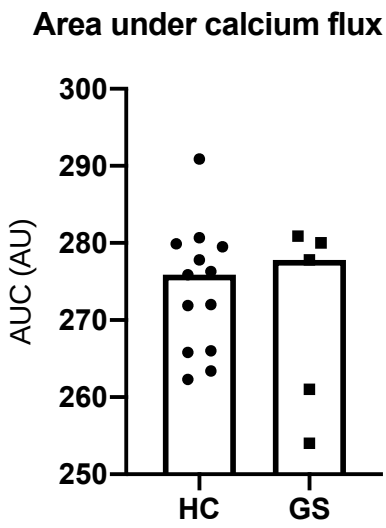

B. Representative calcium flux curves in CD4+ cells after T cell activation in a healthy control and 2 patients with GS.

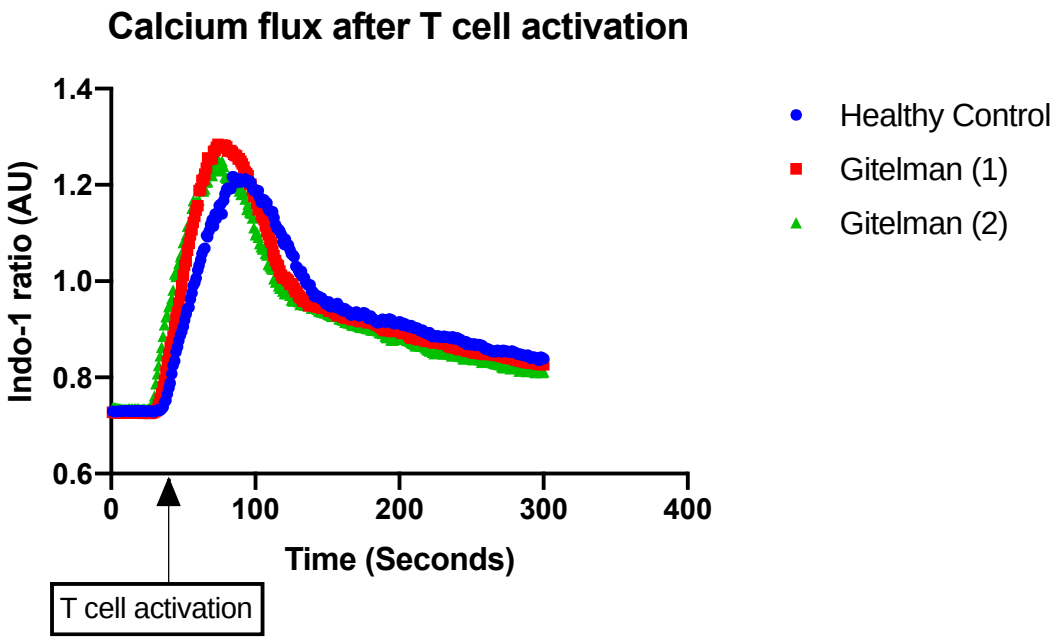

4.4.10 Multiple ions influence IL-17 responses and alterations in the *in vivo* extracellular ionic environment may explain altered immunity in SLT

I hypothesised that reduced IL-17 responses in SLT were due to their altered *in vivo* ionic environment of reduced extracellular sodium, potassium, and

magnesium. Therefore, the effect of altering extracellular sodium, potassium and magnesium concentrations, individually and in combination, on the balance of CD4+ subsets after non-specific T cell stimulation and on IL-17 responses in cells cultured under optimal polarising conditions were assessed.

4.4.10.1 Effect of altering extracellular ions on CD4 subset balance

PBMCs were stimulated with anti-CD3 and anti-CD28 for 72 hours in different ionic environments and the expression of IFNγ, IL-4, and IL-17 in CD4+ cells were measured. The addition of NaCl (0-40mM), KCl (0-2mM), and $MgCl_2$ (0-1mM) resulted in a dose-dependent reduction in the ratio of expression of IFNγ:IL-17 and IL-4:IL-17 in CD4+ cells (**Figure 4.17**). The addition of each of the ions had no effect on cell viability, there was no consistent effect on IFNγ:IL-4 expression, and combining multiple ions further attenuated the reduced IL-4:IL-17 expression ratio previously found (**Figure 4.17**). It may therefore be that SLT patients have an extracellular ionic environment which favours Th2 over Th17 responses, as we had found in our CD4 subset analysis and consistent with their clinical phenotype.

Figure 4.17: Effect of altering extracellular ions during T cell activation on CD4 subset balance

A. Cell viability with the addition of ions to culture conditions (expressed as ratio to cell viability in normal media; red line drawn at ratio of 1 represents no difference to normal media).

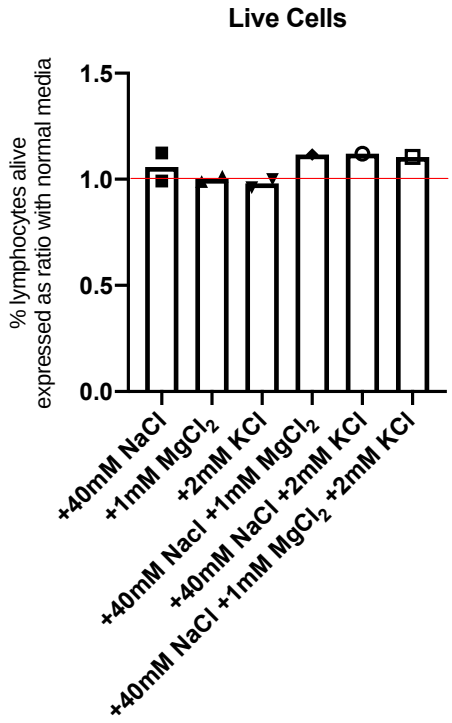

B. Effect of NaCl (0-40mM), KCl (0-2mM), and $MgCl_2$ (0-0.8mM) during T cell activation on the ratio of expression of IFNγ:IL-17 in CD4+ cells, representative of Th1:Th17 cells; data shown represents dose-response in a healthy control.

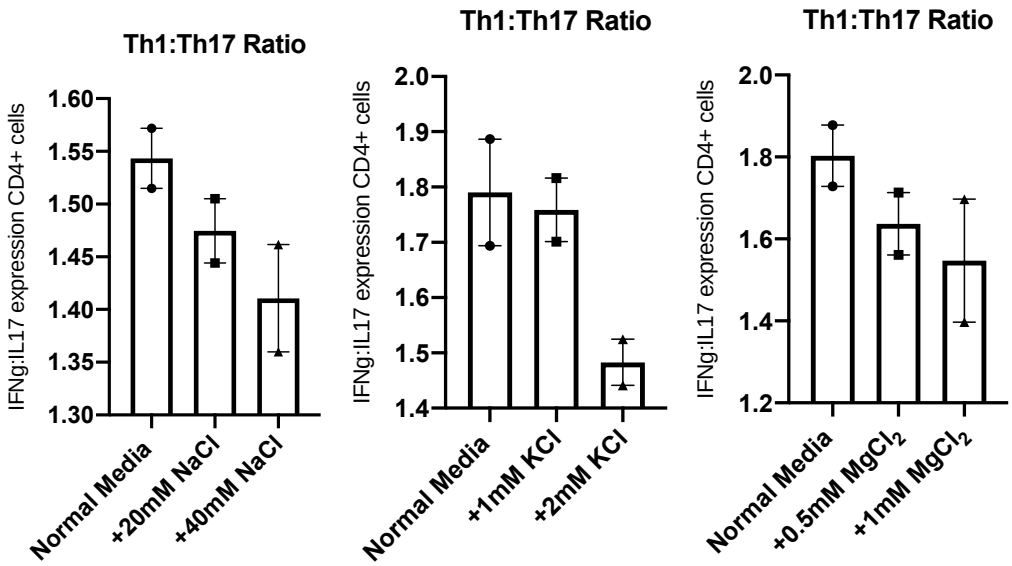

C. Effect of NaCl (0-40mM), KCl (0-2mM), and $MgCl_2$ (0-0.8mM) during T cell activation on the ratio of expression of IL-4:IL-17 in CD4+ cells, representative of Th2:Th17 cells; data shown represents dose response in a healthy control.

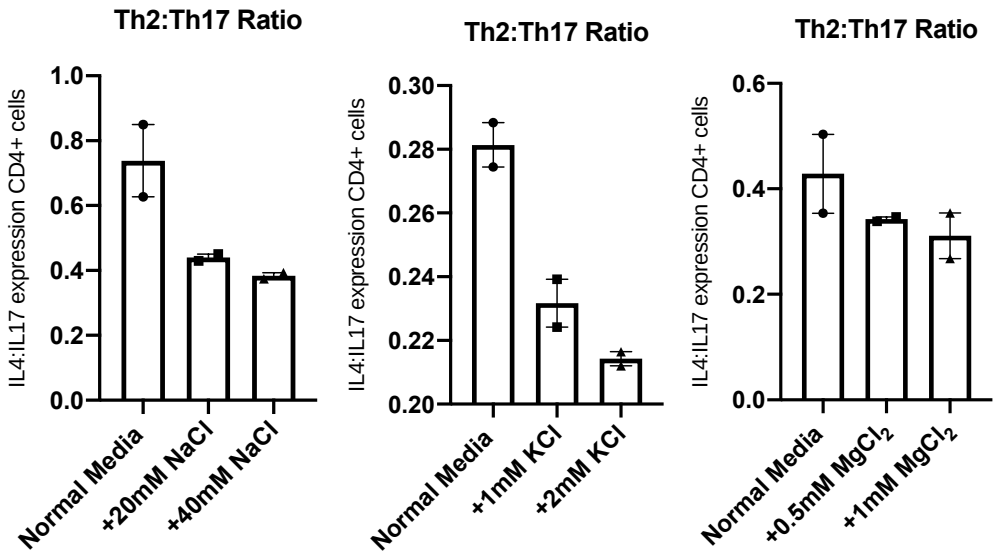

D. Representative FACS plots of the effect of +40mM NaCl on the expression of IFNγ, IL-4, and IL-17 in CD4+ cells.

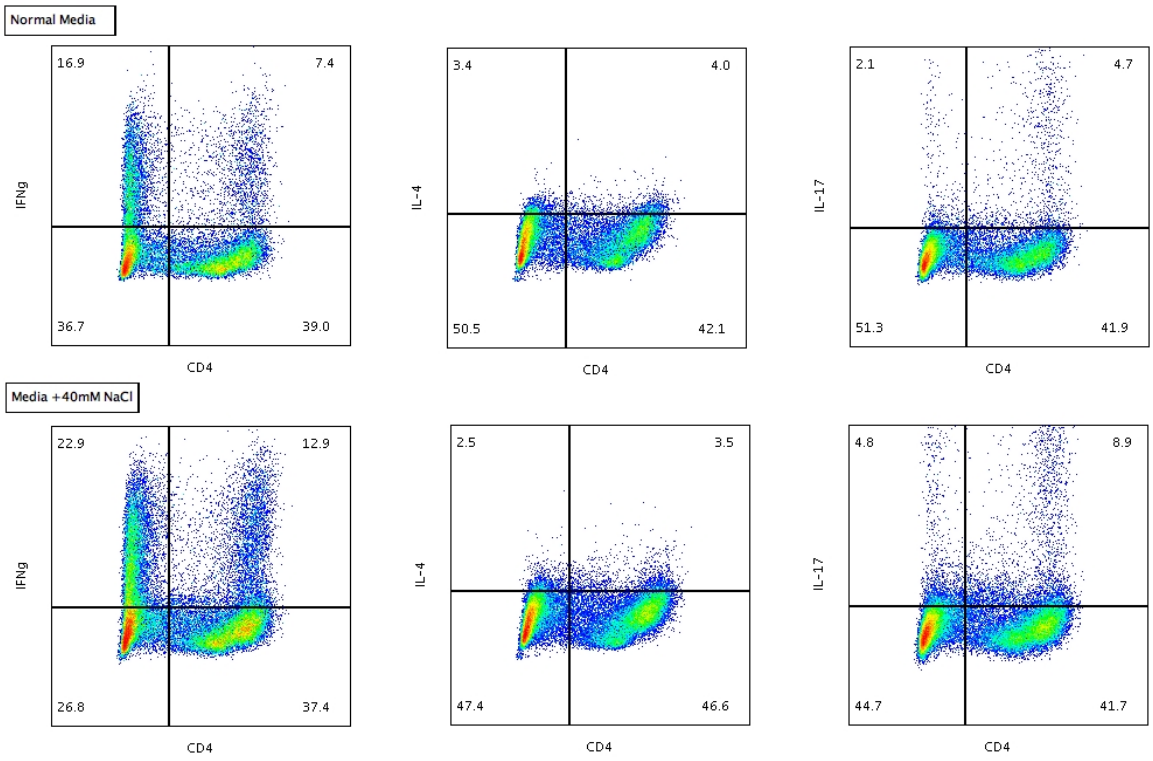

E. CD4+ subset balance after T cell activation in the presence of NaCl (40mM), KCl (2mM), and $MgCl_2$ (1mM) used alone and in combination. Data represents subset balance reported as a ratio to standard conditions in 2 healthy controls (median, IQR plotted). Red line drawn at ratio of 1 represents no difference in subset balance in the presence of ions.

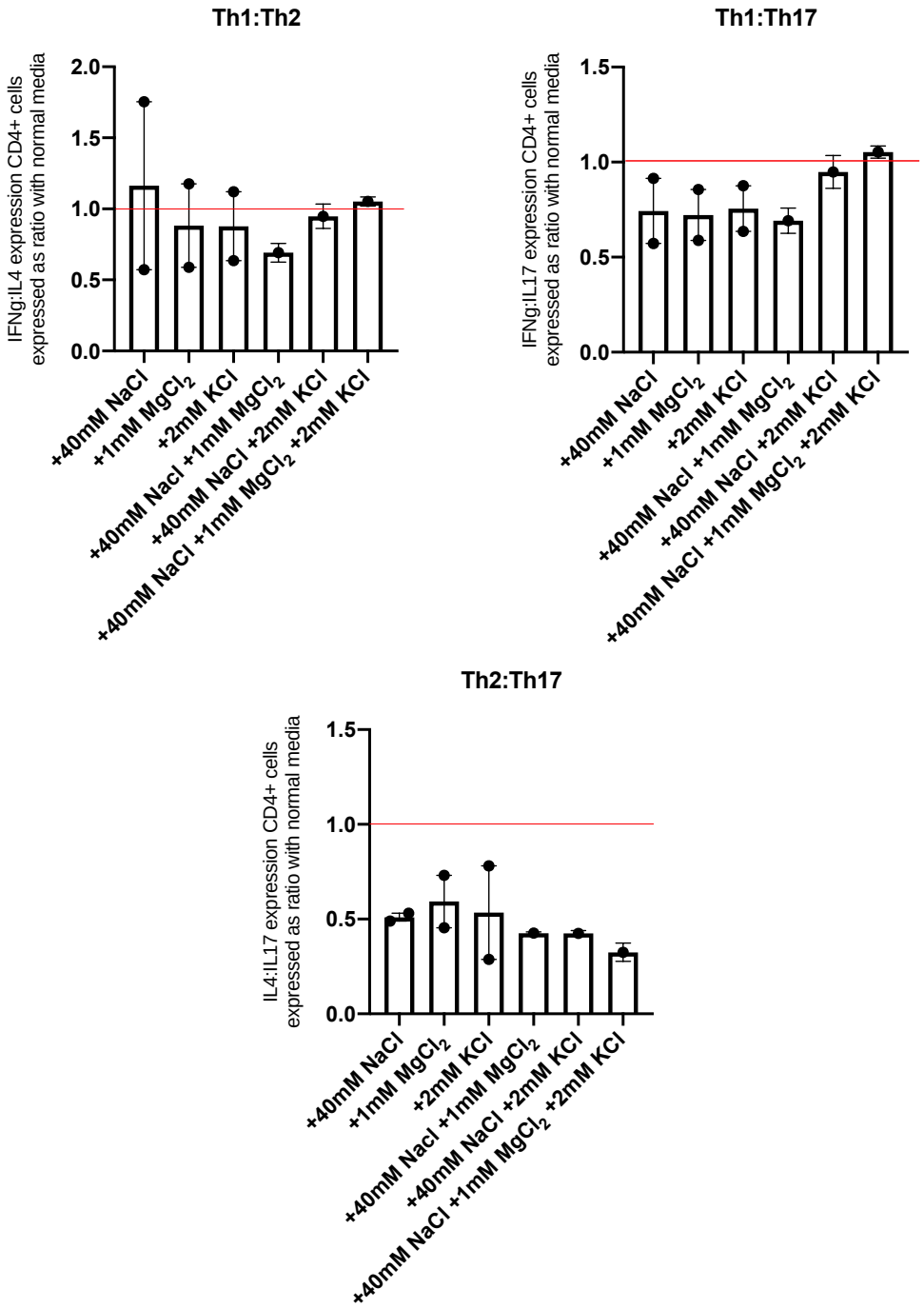

To determine whether magnesium and potassium alter calcium flux during T cell activation, in a similar manner as it had been shown that sodium does, calcium flux was measured in CD4+ cells activated in the presence of $MgCl_2$ and KCl. There was a dose-dependent reduction in calcium flux when $MgCl_2$ and KCl were added to activating conditions (Figure 4.18).

Figure 4.18: Calcium flux after T cell activation in the presence of $MgCl_2$ and KCl

Experiments were replicated in 3 healthy controls. Representative curves from one experiment are shown.

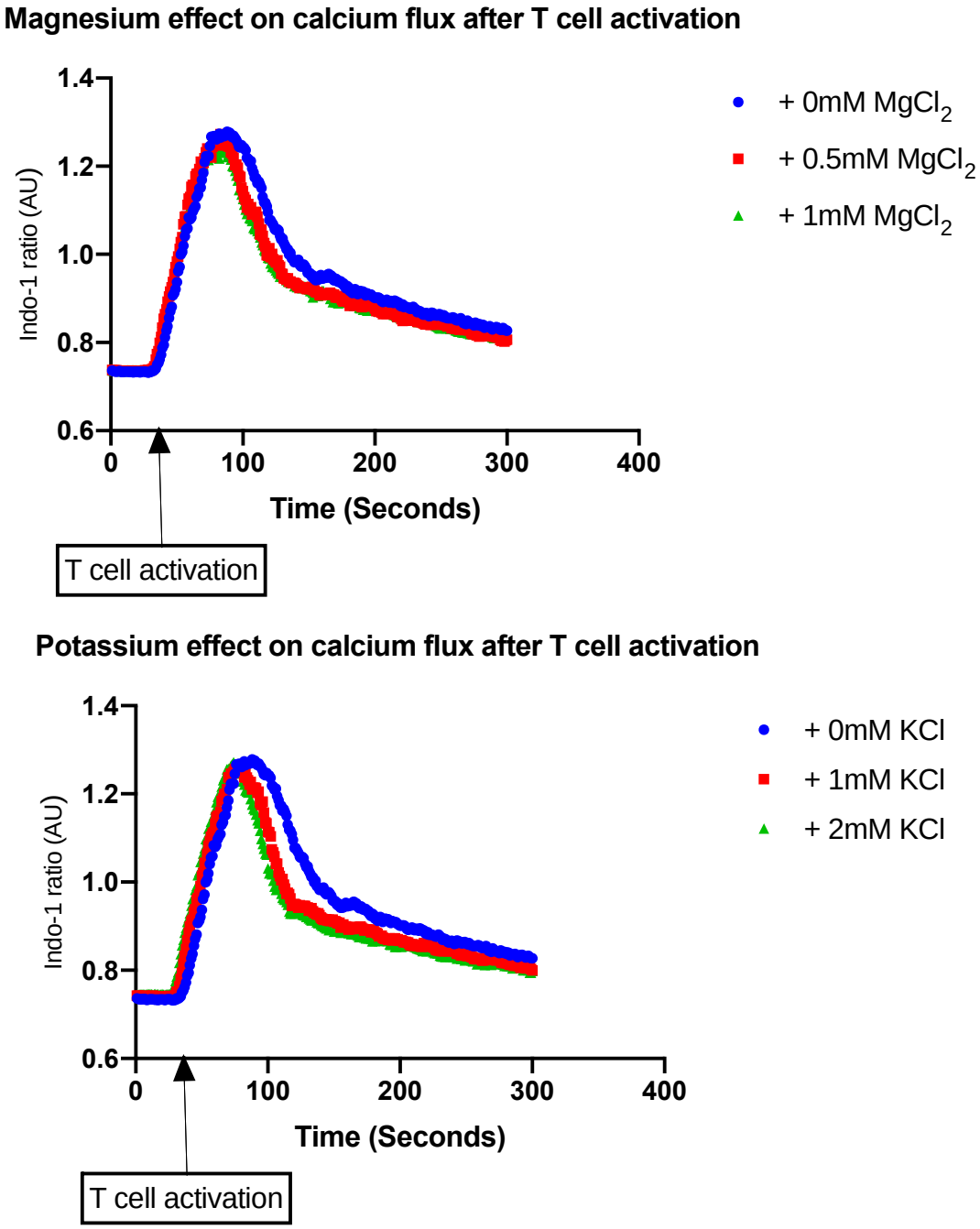

4.4.10.2 Effect of altering extracellular ions and RAAS components on Th17 and Tc17 polarisation

The effect of altering extracellular ionic concentrations on 7-day IL-17 responses in healthy control cells was then assessed. As demonstrated in 3.4.2, there is a dose dependent increase in Th17 and Tc17 polarisation with the addition of NaCl (0-40mM) to culture conditions. Altering potassium and magnesium within a clinically relevant range was also investigated given the extracellular changes in these ions in SLT patients. Like NaCl, adding KCl (0-2mM) and $MgCl_2$ (0-0.8mM) to culture conditions also increased Th17 and Tc17 polarisation in a dose-dependent manner (**Figure 4.19**).

Both angiotensin II and aldosterone have been shown to impact immunity, and SLT patients have an activated RAAS. Their effect on IL-17 responses was therefore investigated. Angiotensin II added to culture conditions increased IL-17 responses (**Figure 4.20**) whereas aldosterone had no effect. SLT patients therefore have an extracellular ionic environment that reduces IL-17 responses, and this environment may impact IL-17 expression in multiple cell types. Angiotensin II may serve as a compensatory immune mechanism for salt loss.

Figure 4.19: Effect of altering extracellular ion concentration on Th17 and Tc17 polarisation

A. Increase in Th17 polarisation with additional NaCl (p=0.03), KCl (p=0.008), and $MgCl_2$ (p=0.0017) added to cultures conditions. Data represents median (IQR) values in 2 or 3 healthy controls. Conditions compared with one-way analysis of variance.

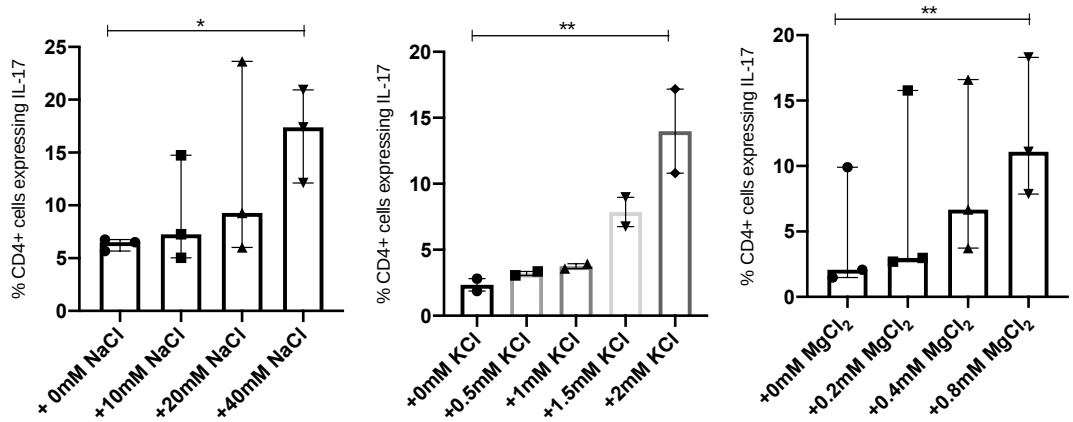

B. Increase in Tc17 polarisation with additional NaCl (p=0.02), KCl (p=0.008), and $MgCl_2$ (p=0.0017) added to cultures conditions. Data represents median (IQR) values in 2 or 3 healthy controls. Conditions compared with one-way analysis of variance.

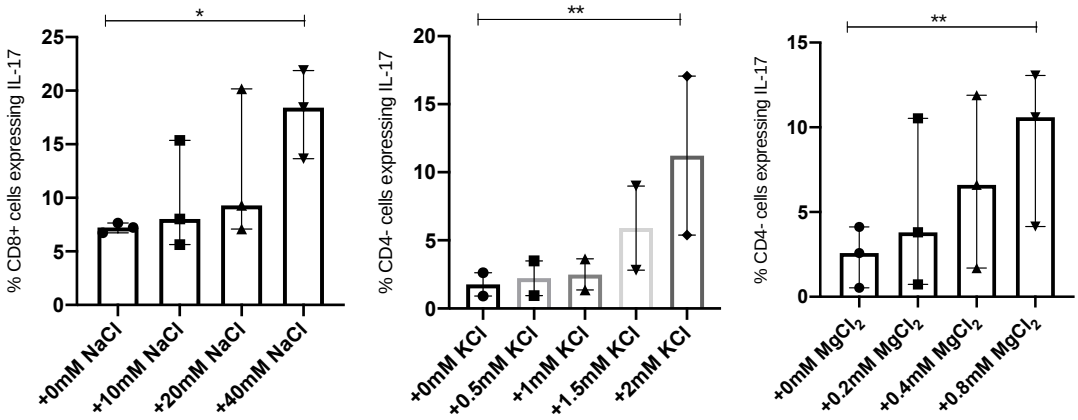

Figure 4.20: Effect of angiotensin II on IL-17 responses

IL-17 expression in CD4+ and CD4- cells (expressed as median fluorescence intensity) in PBMCs stimulated in optimal Th17 polarising conditions with and with angiotensin II (0.1-1uM).

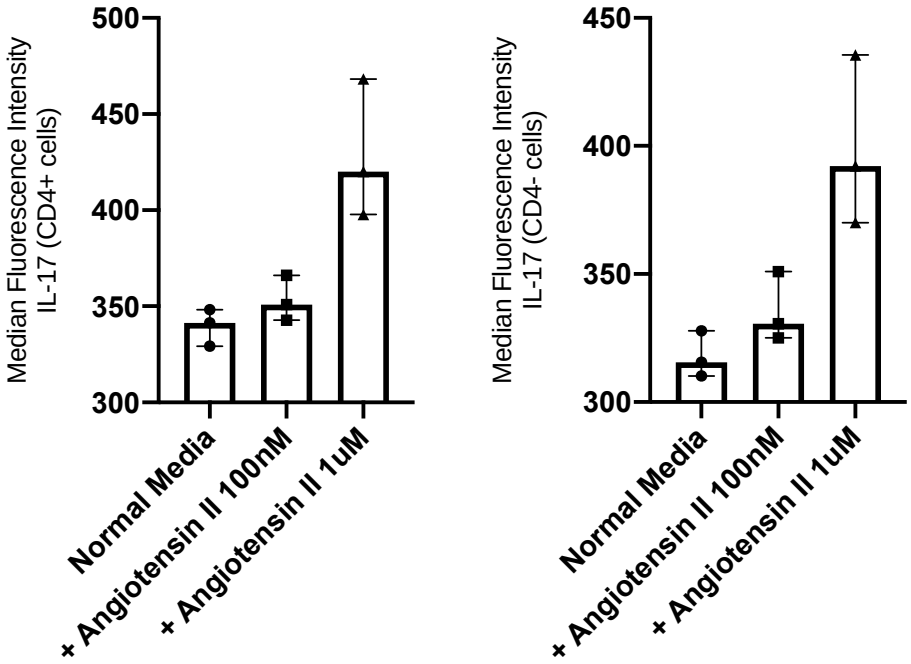

4.4.10.3 Correlation of serum biochemical parameters and IL-17 related infections in SLT patients

Serum biochemical parameters and blood pressure in SLT were then correlated with their IL-17 related infection score. In support of a predominant effect of salt depletion on immunity, the serum creatinine (and hence salt accumulation as renal function deteriorates) inversely correlated with infection score (Pearson r -0.30 (95% CI -0.54, -0.01), p=0.043), whilst there was no correlation of infection score with serum magnesium or potassium (**Figure 4.21**). Similarly, there was an inverse correlation of mean arterial blood pressure (Spearman r -0.37 (-0.61, -0.08), p=0.012) and diastolic blood pressure systolic (Spearman r -0.41 (-0.63, -0.12), p=0.0055) with infection score; systolic blood pressure did not correlate (Spearman r -0.24 (-0.51, 0.06) p=0.11). Aligned with their differences in renal function, there was a difference in infection score between SLT types with infection score highest in patients with GS and EAST syndrome (most preserved renal function), and lowest in patients with BS types 1,2 and 4 (**Figure 4.21**).

Figure 4.21: IL-17 related infection score according to serum biochemical parameters and disease subtypes in Salt Losing Tubulopathy (SLT) patients

ns – not significant (p>0.05), *p≤0.05, **p≤0.01, ***p≤0.001, ****p≤0.0001

A. Correlation of serum biochemical parameters to IL-17 related infection score in SLT patients; analysed with Pearson correlation.

	Pearson r	95% Confidence Interval	R squared	P value
Infection Score vs. Na (mmol/l)	-0.1654	-0.4321 to 0.1278	0.02737	0.2664
Infection Score vs. K (mmol/l)	-0.09249	-0.3728 to 0.2033	0.008554	0.541
Infection Score vs. Cl (mmol/l)	-0.2305	-0.4908 to 0.06760	0.05313	0.1277
Infection Score vs. HCO3 (mmol/l)	0.0489	-0.2449 to 0.3345	0.002391	0.7469
Infection Score vs. Creatinine (umol/l)	-0.2963	-0.5377 to -0.009975	0.08779	**0.0432**
Infection Score vs. cCa (mmol/l)	-0.1446	-0.4203 to 0.1556	0.0209	0.3434
Infection Score vs. PO4 (mmol/l)	-0.239	-0.4950 to 0.05510	0.05713	0.1096
Infection Score vs. Mg (mmol/l)	-0.04587	-0.3450 to 0.2617	0.002104	0.773

B. Serum creatinine plotted against IL-17 related infection score in SLT patients;

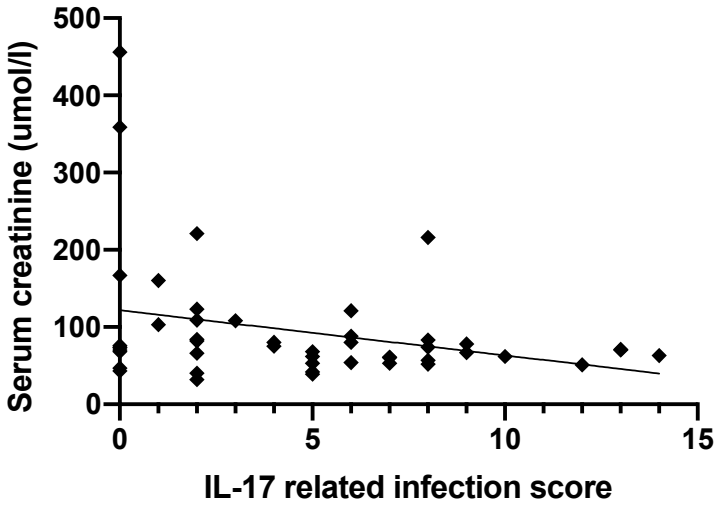

C**.** Infection score according to SLT type; groups compared with the Kruskall-Wallis test with Dunn's multiple comparison testing.

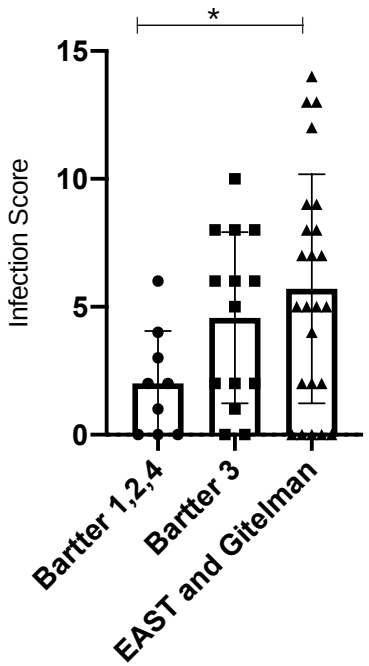

4.4.11 The intracellular pathway which mediates salt-driven IL-17 inflammation is intact in SLT patients

The intracellular pathway by which sodium increases Th17 polarisation includes the up-regulation of SGK1, NFAT5, and the IL23-receptor (IL-23R)[52,53]. Whether this pathway was intact in SLT patients was assessed. SLT lymphocyte expression of SGK1 (**Figure 4.22**) and NFAT5 (**Figure 4.23**) were not reduced compared to healthy controls, neither was IL-23R expression on CD4+ cells; IL23-R expression was in fact increased in non CD4 lymphocytes in SLT patients (
Figure 4.24).

Figure 4.22: SGK1 expression in SLT patients and controls

ns – not significant (p>0.05), *p≤0.05, **p≤0.01, ***p≤0.001, ****p≤0.0001

HC – healthy control; SLT – salt losing tubulopathy; AU – arbitrary units

A. Relative lymphocyte SGK1 expression: relative intensity HC = 1.07 AU (0.73-1.2), SLT = 1.09 AU (0.80-1.31), p=0.70; median (IQR) expression plotted; compared with Mann-Whitney test.

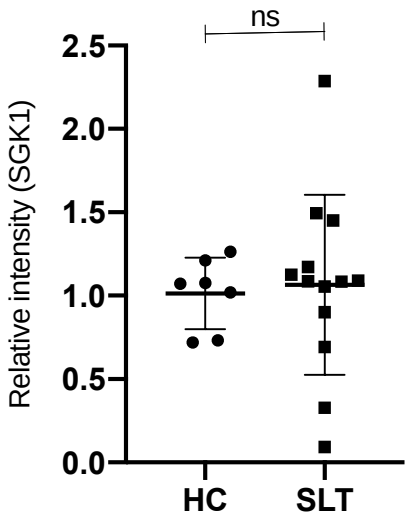

B. Representative western blot of SGK1 expression in HC and SLT**.**

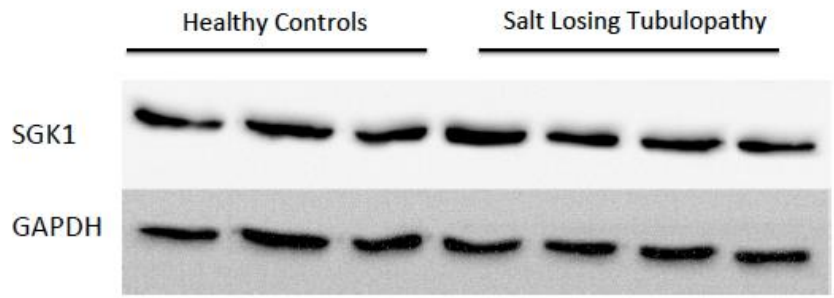

Figure 4.23: NFAT5 expression in SLT patients and controls

Relative lymphocyte NFAT5 expression: HC 1.01 AU (0.70-1.95), SLT 1.10 AU (0.76-1.62), p=0.85; median (IQR) expression plotted; compared with Mann-Whitney test

ns – not significant (p>0.05), *p≤0.05, **p≤0.01, ***p≤0.001, ****p≤0.0001

HC – healthy control; SLT – salt losing tubulopathy; AU – arbitrary units

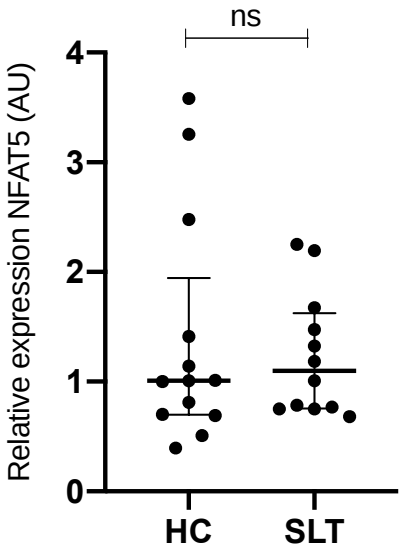

Figure 4.24: IL23-R expression in SLT patients and controls

A. IL-23 receptor expression on unstimulated CD4+ cells: HC 0.42% (0.34-1.01), SLT 0.79% (0.73-2.60), p=0.07; median (IQR) expression plotted; compared with Mann-Whitney test.

B. IL-23 receptor expression on unstimulated CD4- cells: HC 3.34% (2.26-6.56), SLT 9.67% (5.64-10.65), p=0.02; median (IQR) expression plotted; compared with Mann-Whitney test.

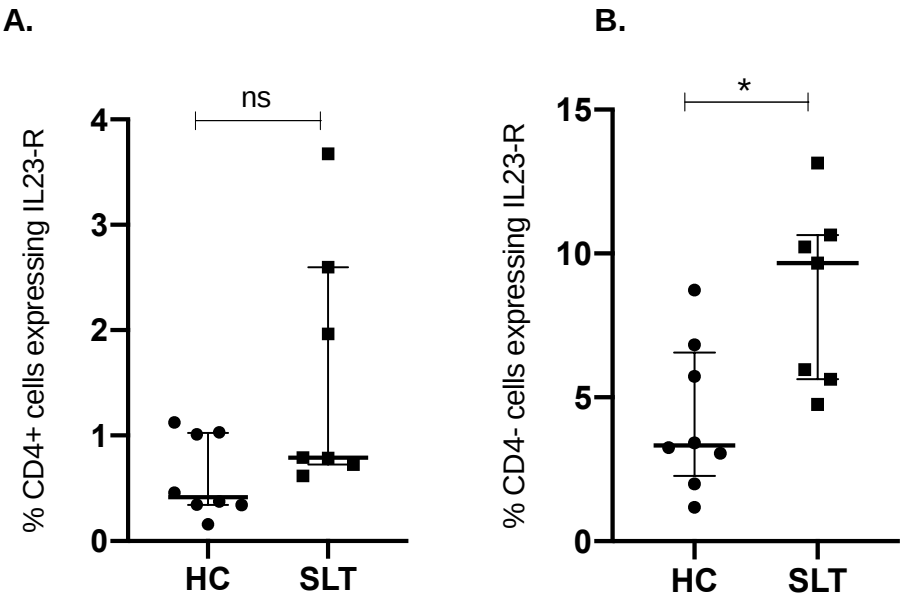

C. Representative FACS plots of IL23 receptor (IL23-R) expression on CD4+ cells in a SLT patient and HC

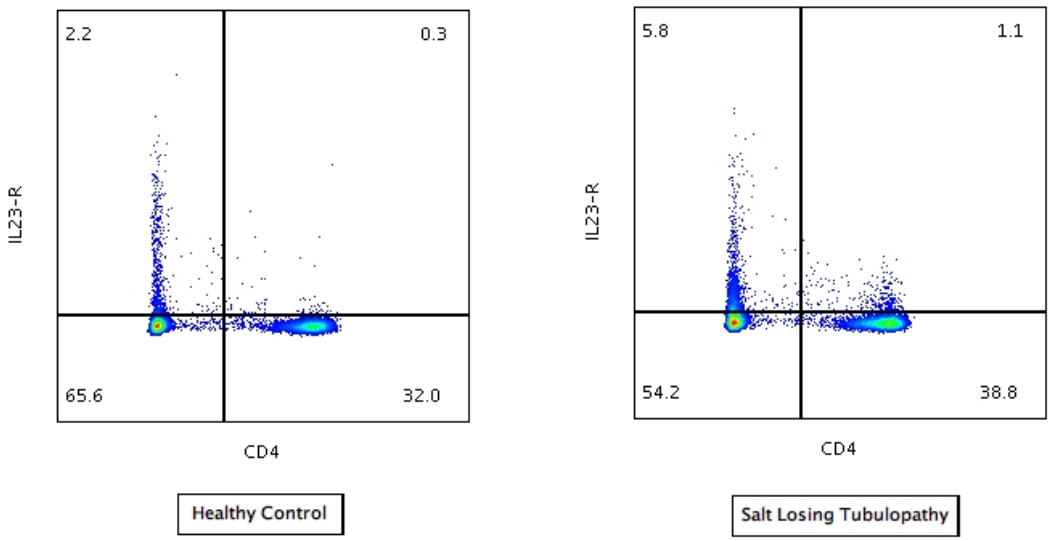

4.4.12 Th17 polarisation defects can be rescued by the addition of salt to culture conditions

Given the preservation of this salt pathway, I hypothesised that *in vitro* IL-17 responses could be rescued in SLT patients by supplementing culture conditions with salt. Indeed, the addition of 40mM NaCl to culture conditions upregulated IL-17 responses in SLT cells such that Th17 and Tc17 polarisation were equivalent to healthy and disease control cell polarisation under standard conditions (**Figure 4.25**). Salt responsiveness of *in vitro* IL-17 responses in SLT patients was no different to controls (**Figure 4.26**). These data demonstrate that salt supplementation ameliorates IL-17 response defects in SLT *in vitro*, but whether this is feasible and effective *in vivo* is unknown.

Figure 4.25: Salt rescue of *in vitro* IL-17 responses in Salt Losing Tubulopathy (SLT) patients

A. Th17 polarisation in HC (n=27) and SLT (n=25) in standard media, and in SLT patients in media supplemented with 40mM NaCl: HC +0mM NaCl 3.2% (2.5-6.3); SLT +0mM NaCl 1.6% (0.8-2.0); SLT +40mM NaCl 3.1% (2.4-5.3); p=<0.0001; Median (IQR) IL-17 expression plotted (CD4+ cells); compared with one-way analysis of variance with Dunn's multiple comparison testing.

B. Tc17 polarisation in HC (n=27) and SLT (n=25) in standard media, and in SLT patients in media supplemented with 40mM NaCl: HC +0mM NaCl 1.5% (0.6-3.0); SLT +0mM NaCl 0.6% (0.3-1.1); SLT +40mM NaCl 1.6% (0.9-3.1); p=0.0007; Median (IQR) IL-17 expression plotted (CD4- cells); compared with one-way analysis of variance with Dunn's multiple comparison testing.

ns – not significant (p>0.05), *p≤0.05, **p≤0.01, ***p≤0.001, ****p≤0.0001

HC – healthy control; SLT – salt losing tubulopathy

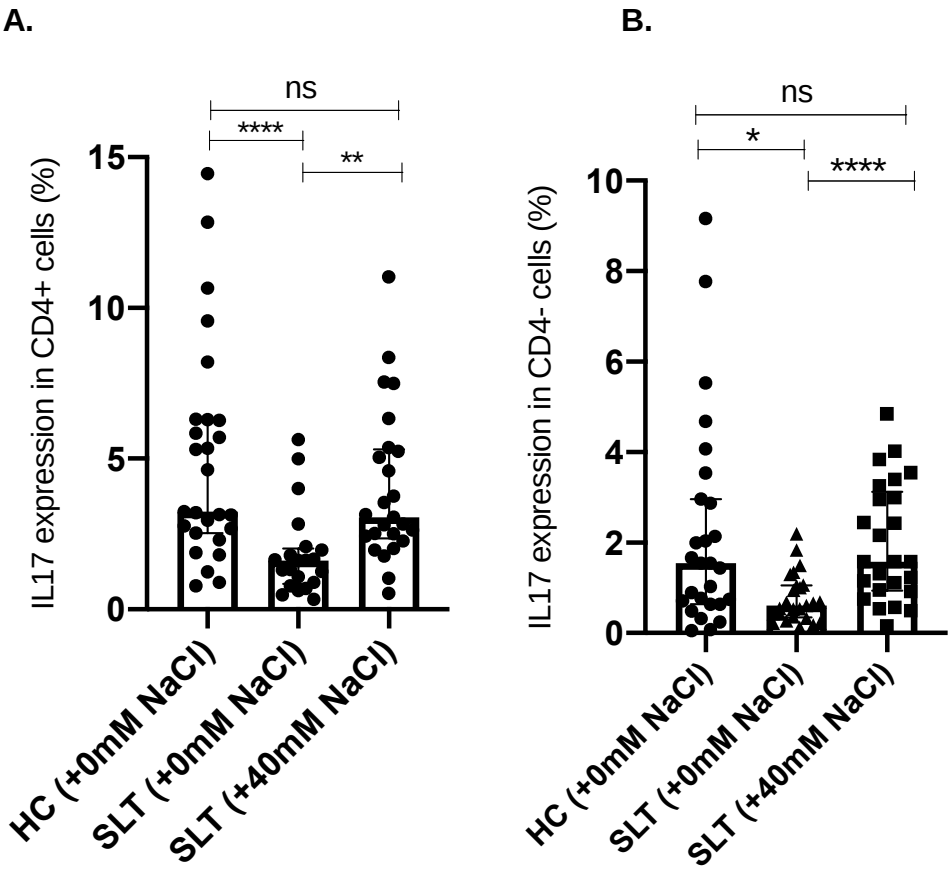

Figure 4.26: Salt responsiveness of IL-17 responses in SLT patients and controls

A. Salt responsiveness (readout in media supplemented with NaCl 40mM expressed as ratio to readout in normal media) of Th17 cells in SLT patients and controls (red line drawn at ratio of 1 demonstrating no difference between high salt media and normal media);

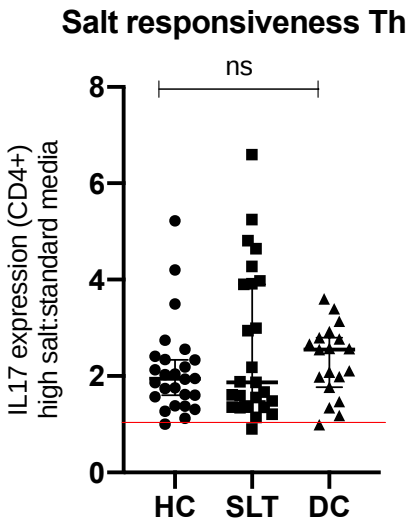

B. Salt responsiveness (readout in media supplemented with NaCl 40mM expressed as ratio to readout in normal media) of Tc17 cells in SLT patients and controls (red line drawn at ratio of 1 demonstrating no difference between high salt media and normal media).

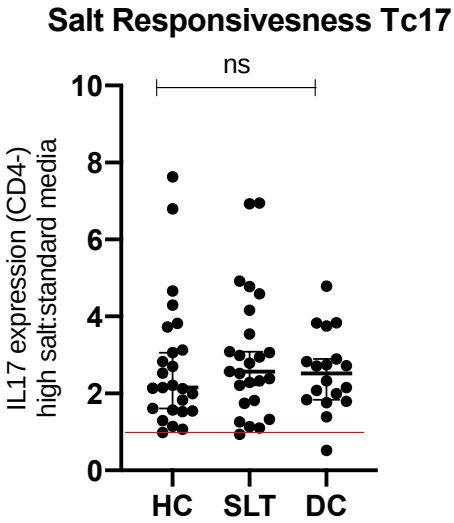

4.4.13 SLT patients do not have defective innate immune responses

Polarisation of Th17 cells requires antigen presentation by antigen presenting cells in the presence of Th17 polarising cytokines produced by innate immune cells. Defective IL-17 responses can therefore be a consequence of impaired innate immunity. Innate immune responses in SLT patients were assessed by measuring cytokine production to a range of stimuli in whole blood assays. These demonstrated no reduction in innate responses; indeed, production of

several innate cytokines (e.g. IL-1, IL-6, and TNFα) was increased in SLT patients compared to controls (**Table 4.8**). Reduced innate immune responses are therefore not the cause of reduced IL-17 responses and increased infection in SLT patients.

Table 4.8: Whole blood cytokine stimulation assays to assess innate cytokine responses in Salt Losing Tubulopathy patients.

Experiments undertaken by University of Cambridge Immunology Department. Cytokine concentrations (TNF-α, IL-1β, IL-6, IL-10, IL-12, and IFN-γ) are reported as median (IQR) and compared between SLT patients (n= 13) and healthy controls (n=42) using the Mann-Whitney test.

LPS – Lipopolysaccharide; ZYM – Zymosan; B-GLUC - Beta-glucan; MDP – Muramyldipeptide.

	TNF-α (pg/ml)			IL-6 (pg/ml)			IL-1β (pg/ml)		
Stimulation	**Salt Losing Tubulopathy**	**Healthy Control**	**P-value**	**Salt Losing Tubulopathy**	**Healthy Control**	**P-value**	**Salt Losing Tubulopathy**	**Healthy Control**	**P-value**
IFNg	2.4 (2.4-2.4)	2.4 (2.4-2.4)	0.09	1.4 (1.4-16.9)	1.4 (1.4-1.4)	0.06	7.1 (1.5-33.2)	1.08 (1.08-2.92)	**0.0007**
LPS	3166 (1669-5083)	1420 (928-2654)	**0.0091**	20733 (16734-28187)	14128 (10436-18901)	**0.0025**	7047 (3361-9777)	3344 (2141-4708)	**0.0017**
LPS/IFNg	8584 (6225-12665)	4945 (2937-6201)	**0.0006**	26489 (18107-32192)	15717 (11840-23041)	**0.0038**	11197 (6561-16324)	8832 (5805-11057)	0.06
ZYM	2588 (2051-4714)	1740 (1352-2722)	**0.0079**	8370 (6529-12742)	5033 (3406-6608)	**0.0057**	18009 (9639-21308)	8880 (7192-11562)	**0.0061**
ZYM/IFNg	3328 (2432-6574)	2137 (1496-2696)	**0.0006**	5636 (3113-6686)	2358 (1424-3117)	**0.0049**	20704 (7319-26839)	8741 (6584-12962)	**0.004**
B-GLUC	1482 (951-2532)	1107 (500-1630)	**0.029**	12239 (10664-20716)	11562 (6427-14381)	0.17	4026 (2126-6700)	2675 (1570-3984)	0.051
B-GLUC/IFNg	2408 (900-4286)	1539 (940-2223)	0.09	7368 (1011-12052)	3456 (1982-5628)	0.16	8458 (2217-11370)	3630 (2229-5578)	**0.032**
PAM2	229 (137-827)	73 (34-166)	**0.0007**	5771 (2518-9729)	1035 (608-3297)	**0.0004**	581 (177-1367)	151 (56-325)	**0.0023**
MDP	58.8 (21-163)	13 (7.2-24.9)	**0.0023**	236 (50-1977)	16.1 (7.6-139)	**0.0027**	65 (22-298)	14 (6.6-50)	**0.0089**

	IL-10 (pg/ml)			IL-12 (pg/ml)		
Stimulation	**Salt Losing Tubulopathy**	**Healthy Control**	**P-value**	**Salt Losing Tubulopathy**	**Healthy Control**	**P-value**
IFNg	0.52 (0.52-0.52)	0.52 (0.52-0.52)	0.53	5.1 (5.1-5.1)	5.1 (5.1-5.1)	0.24
LPS	771 (521-997)	882 (589-1207)	0.42	33.3 (7.3-40.5)	7.9 (5.1-25.9)	**0.02**
LPS/IFNg	265 (129-335)	227 (117-365)	0.95	322 (198-428)	139 (61-218)	**0.0011**
ZYM	140 (76-262)	162 (72-237)	0.98	10.9 (6.4-44.2)	5.1 (5.1-18.2)	0.07
ZYM/IFNg	31 (8-87)	37 (9.7-60.7)	0.95	80 (46-113)	49 (15-113)	0.1
B-GLUC	102 (29-149)	51 (20-79)	**0.04**	5.1 (5.1-15.8)	5.1 (5.1-5.1)	0.22
B-GLUC/IFNg	10 (0.8-34)	3.8 (0.8-7.6)	0.18	18.2 (5.1-54)	10.6 (5.1-24.9)	0.27
PAM2	42 (28-100)	16.2 (7.2-51.2)	**0.02**			

	IFN-γ (pg/ml)		
Stimulation	**Salt Losing Tubulopathy**	**Healthy Control**	**P-value**
IL12	5.4 (5.4-5.4)	5.4 (5.4-5.4)	0.99
LPS	5.4 (5.4-5.4)	5.4 (5.4-5.4)	0.18
LPS/IL12	420.7 (155.8-1161)	277.7 (138.3-572.8)	0.35
IL18	5.4 (5.4-5.4)	5.4 (5.4-5.4)	0.89
IL18/IL12	4587 (2792-10970)	391.1 (216-730)	0.28
ZYM	5.4 (5.4-23.0)	5.4 (5.4-17.2)	0.69
ZYM/IL12	477.4 (107-866.9)	391.1 (216-730)	0.88
B-GLUC	5.4 (5.4-9.25)	5.4 (5.4-5.4)	0.27
B-GLUC/IL12	370 (50.25-1060)	269.6 (94.2-557.1)	0.93

IL15	5.4 (5.4-5.4)	5.4 (5.4-5.4)	0.25
IL15/IL12	43.1 (9.6-173.2)	42.55 (19.28-148.1)	0.98

4.4.14 Monocyte analysis in SLT patients

Monocyte responses were then assessed in more detail to try and explain these altered innate responses in SLT patients. There was, however, no difference in monocyte subsets (classical, intermediate, and non-classical) or in monocyte expression of TNFα in SLT patients compared to controls in the experiments undertaken (

Figure 4.27). The effect of altering extracellular ionic concentrations and aldosterone on monocytes was then assessed. Additional 40mM NaCl, 2mM KCl, 1mM $MgCl_2$, and aldosterone (10-100nM) to stimulating conditions had no effect on monocyte TNFα expression (**Figure 4.28**). The increased innate cytokine responses in SLT patients are hence unexplained.

Figure 4.27: Monocyte analysis in Salt Losing Tubulopathy (SLT) patients.

A. Classical (CD14+CD16-), intermediate (CD14+CD16+) and non-classical (CD14-CD16+) monocyte subsets in SLT patients and HCs; compared with Mann-Whitney test; no significant differences in populations.

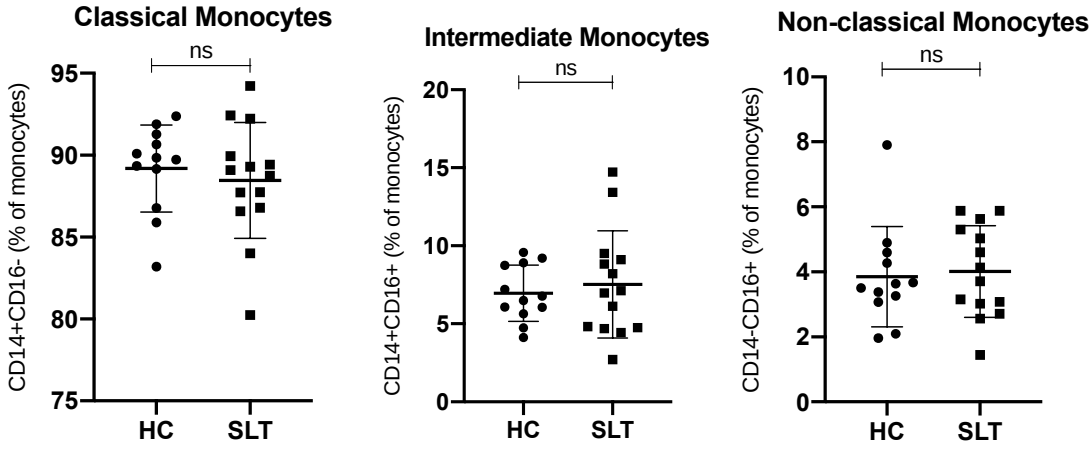

B. Representative FACS plots of CD14 and CD16 staining in a HC and SLT patient

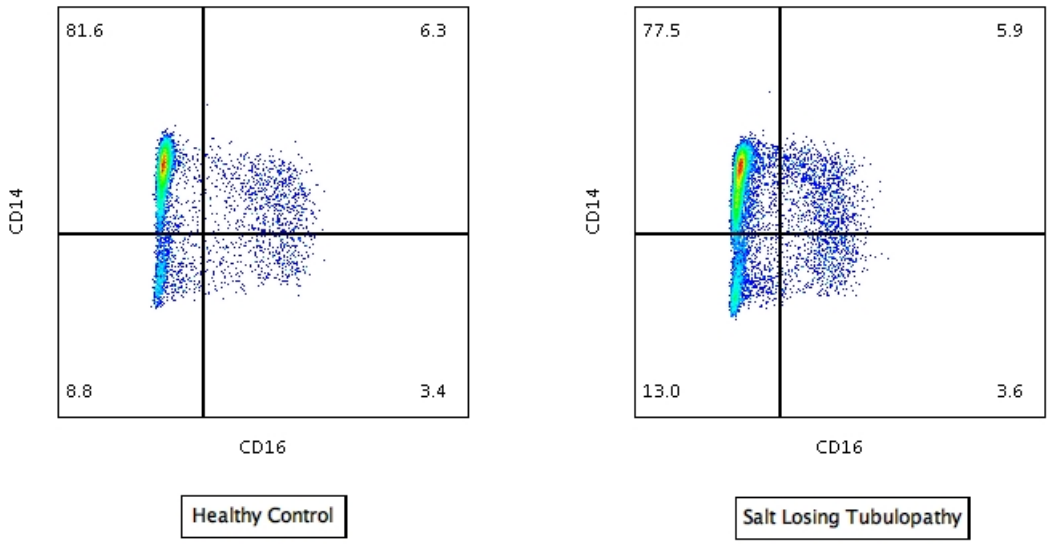

C. Proportion of Lipopolysaccharide (LPS) stimulated CD14+ cells expressing TNFα in SLT and HCs; compared with Mann-Whitney test; no significant differences in TNFα expression.

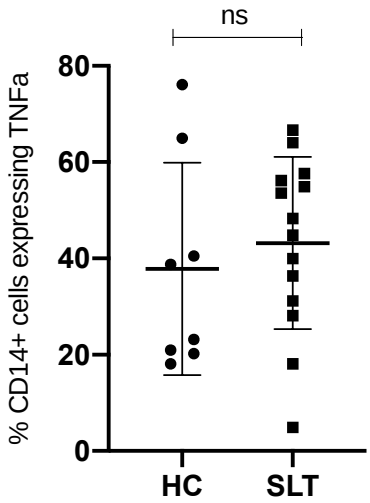

D. Representative FACS plots of TNFα expression in CD14+ cells in a HC and SLT patient.

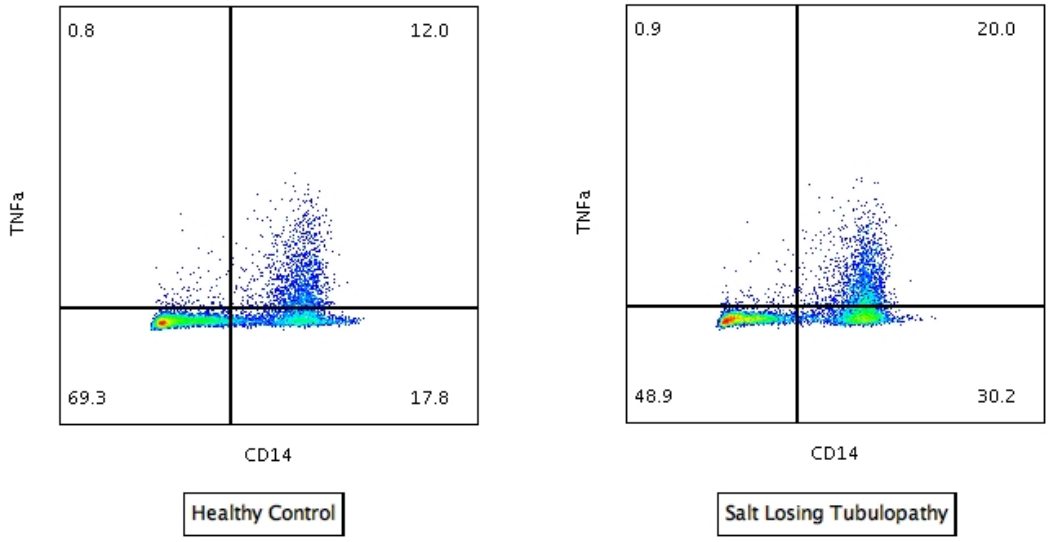

Figure 4.28: **Effect of altering extracellular ions on monocyte function**
Effect of altering extracellular ionic concentration on TNFα expression in CD14+ cells; expressed as ratio of TNFα expression in supplemented media compared to standard conditions (red line drawn at ratio of 1 represents no difference with addition of ions).

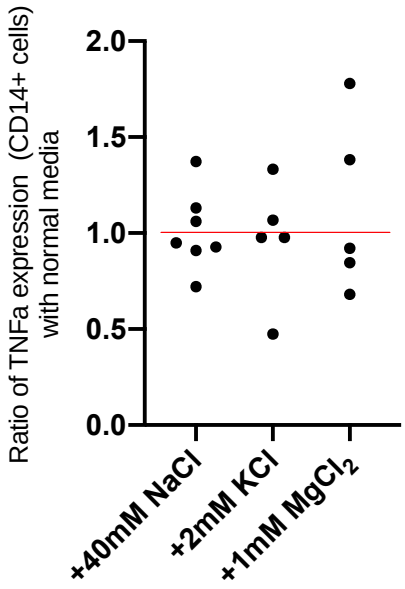

4.4.15 Further analysis of NK cells in SLT patients

Given the findings of a reduction in NK cell numbers on initial immunological assessment (**Figure 4.5**), an additional investigation of NK cells in SLT patients was undertaken to further characterise NK cell subsets and assess NK cell function. In this analysis, CD45+CD3-CD56+CD16+ (NK) cells accounted for 10.2% (5.9-13.8) of lymphocytes in healthy controls and 6.9% (3.9-10.0) in SLT patients (p=0.1, **Figure 4.29**). 8 (50%) SLT patients had NK cells of less than 7% of lymphocytes, but so did 5 (29%) controls (p=0.3). The proportion of CD56+ cells, however, expressing CD16 (the Fc receptor) was reduced in SLT patients (**Figure 4.29**). To assess NK cell function, PBMCs were stimulated with IL-12 and IL-18 for 4 hours and NK cell expression of IFNγ determined. IFNγ expression was no different between SLT and controls (**Figure 4.29**).

Whilst the effect of extracellular sodium has been assessed in large parts of the immune system, its effect on NK cells has not. NK cells were therefore stimulated in the presence of additional NaCl (+40mM). Adding NaCl to stimulating conditions increased in the proportion of lymphocytes expressing CD56, but IFNγ expression by CD56+ cells was reduced (**Figure 4.30**). The effect of NaCl on CD16 expression was not determined.

Figure 4.29: Analysis of Natural Killer (NK) cells in Salt Losing Tubulopathy (SLT) patients.

A. NK cells (CD45+CD3-CD56+CD16+ cells) expressed as a proportion of lymphocytes (CD45+ cells) in SLT patients and HCs: HC 10.2% (5.9-13.8), SLT 7.0% (4.0-10.1), p=0.11; median (IQR) values plotted; compared with Mann-Whitney test.
B. Ratio of CD56+CD16+ to CD56+CD16- cells in SLT patients and HCs: HC 18.0 (13.7-24.8), SLT 11.4 (7.5-16.7), p=0.01; median (IQR) values plotted; compared with Mann-Whitney test.
C. IFNγ expression by CD45+CD3-CD56+ cells after 4 hours IL-12 and IL-18 stimulation in SLT patients and controls: HC 28.0% (23.9-38.0), SLT 32.8% (23.0-47.5), p=0.72; median (IQR) values plotted; compared with Mann-Whitney test.

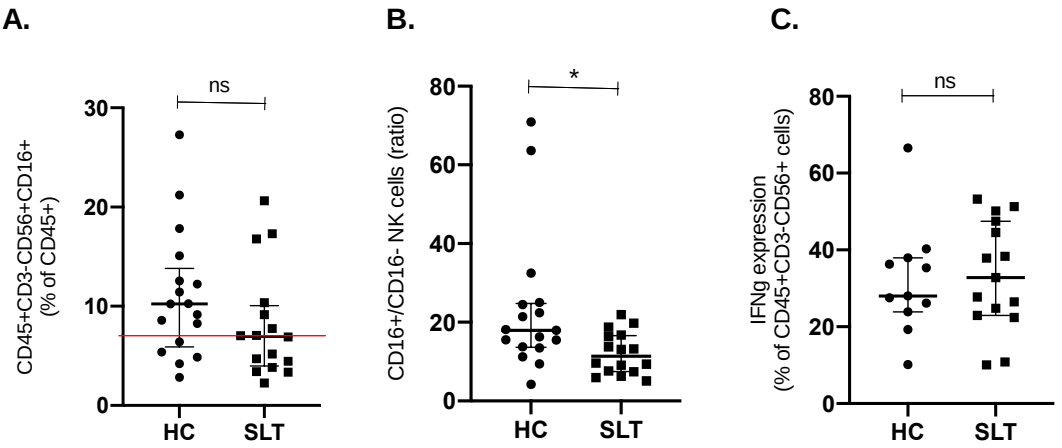

D. Representative FACS plots of CD56 and CD16 staining in a SLT patient and HC (gated on single CD45+CD3-CD56+ cells, therefore CD56 gate distinguishes CD56 bright from dim); SLT patients had reduced CD16 staining on CD56+ cells, as shown.

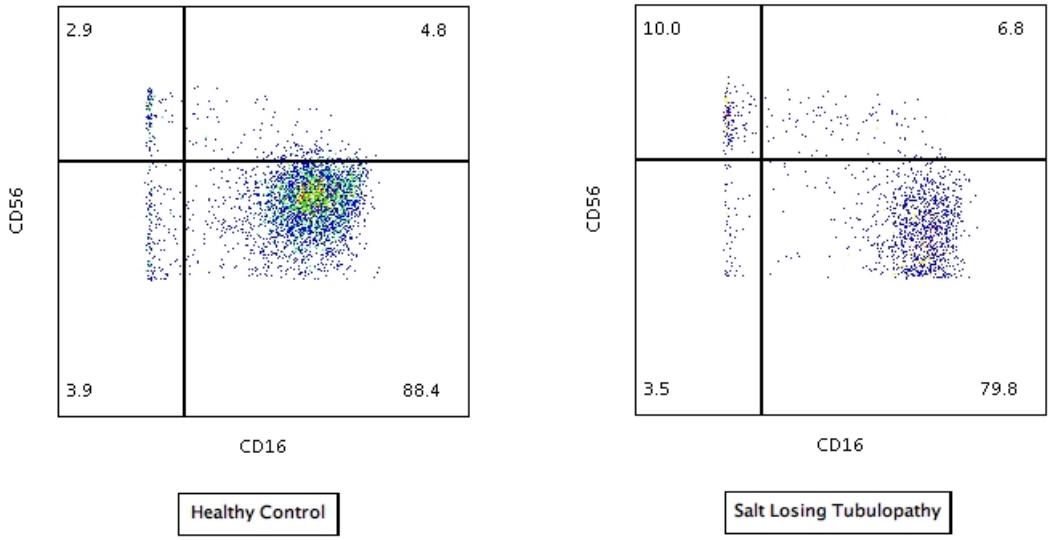

Figure 4.30: The effect of NaCl on NK responses

ns – not significant (p>0.05), *p≤0.05, **p≤0.01, ***p≤0.001, ****p≤0.0001

SLT – salt losing tubulopathy; HC – healthy control

A. NK cells, expressed as a proportion of lymphocytes (CD45+ cells), after stimulation (IL-12 and IL-18) in the presence of +40mM NaCl: normal media 8.7% (6.4-14.5), and high salt media 10.0% (6.8-15.5), p=0.008; change in individual subjects plotted; compared with Wilcoxon test.

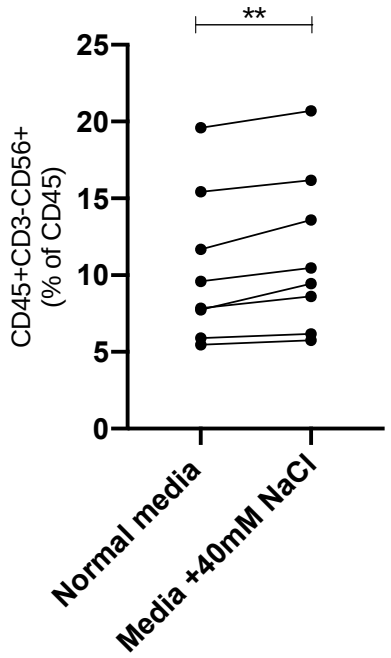

B. IFNγ expression by NK cells after stimulation (IL-12 and IL-18) in the presence of +40mM NaCl: normal media 31.8% (21.0-37.6), and high salt media 17.6% (12.0-20.6), p=0.008; change in individual subjects plotted; compared with Wilcoxon test.

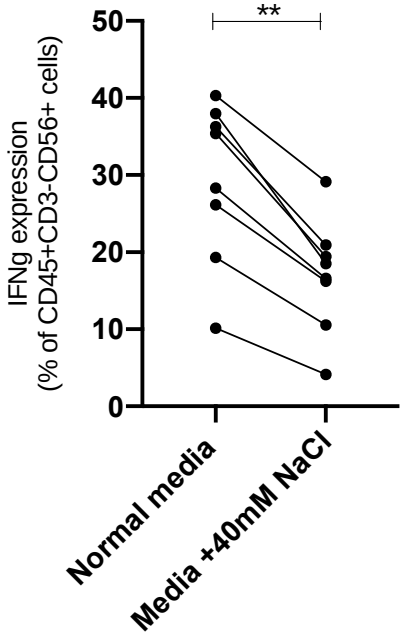

C. Representative FACS plots of IFNγ expression by NK cells after stimulation in the presence and absence of +40mM NaCl

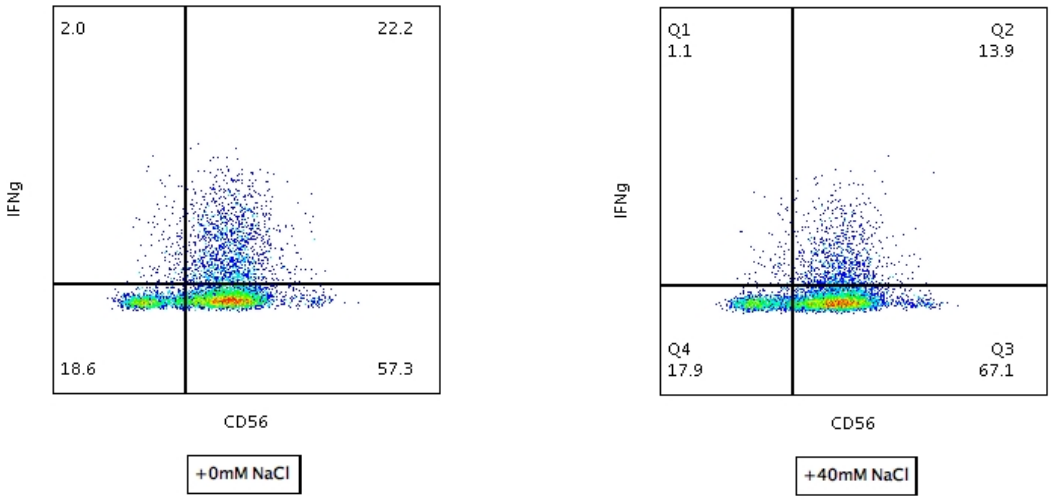

4.5 Discussion

Novel findings from long-term sodium balance studies have demonstrated a third compartment of osmotically inactive sodium stored at interstitial sites in the muscle and skin. Visualisation and measurement of sodium stores with magnetic resonance imaging (^{23}Na-MRI) has demonstrated that sodium concentrations at these sites increase with age and in disease states that result in sodium loading such as heart failure and chronic kidney disease[36,37,39–41]. In SLT, adaptive mechanisms such as increased salt appetite and enhanced reabsorption of sodium in unaffected nephron segments are upregulated to prevent catastrophic sodium loss[127]. Whilst SLT patients waste sodium, how this affects sodium stores or if this impacts on total body sodium balance in the long term was unknown. Using ^{23}Na-MRI, I demonstrated that renal sodium stores are reduced in SLT patients compared to controls. This alteration in extracellular sodium combined with reduced serum potassium and magnesium concentrations mean immune cells in SLT patients are exposed to a unique combination of altered extracellular ionic cues, which I propose impacts immune function.

The presentation of SLT may be through the identification of biochemical abnormalities incidentally on blood tests performed for other reasons or be with an array of relatively non-specific symptoms. These include cramps,

weakness, dizziness, and fatigue, and such symptoms have been traditionally attributed directly to electrolyte derangement. However, there are no consistent data demonstrating correlation between symptom burden and electrolyte abnormalities, and symptoms are often persistent and disabling even when serum electrolytes are within normal range. Moreover, some recognised clinical features, such as recurrent febrile episodes in childhood in GS, theoretically cannot be explained by a direct electrolyte effect. My data demonstrating immunodeficiency in SLT potentially provide an explanation for these symptoms. Moreover, an association between SLT and autoimmunity (e.g. autoimmune thyroid disease, Sjögren's syndrome, autoimmune hepatitis, and vasculitis) is recognised[136,150,151,153,154]; findings in our cohort confirm this association and our demonstration of dysregulated immunity may explain the cause for this link.

Th17 cells are pro-inflammatory, and provide protection against extracellular bacterial and fungal infections, particularly at mucosal surfaces[157]. Polarisation requires stimulation by IL-1β, IL-6, and TGF-β, while full maturation requires IL-21 and IL-23. Th17 cells secrete various cytokines including IL-17, which induces release of other pro-inflammatory cytokines and chemokines and is important for neutrophil recruitment. Defective IL-17 responses may be inherited and result in CMC syndrome, or may be acquired in patients with thymoma[82] (production of neutralizing antibodies to IL-17) or in patients taking anti-IL-17 monoclonal antibodies for the treatment of autoimmune disease[83]. I demonstrate that the primary cause for immunodeficiency in SLT patients is reduced IL-17 responses and the mucosal nature of bacterial and fungal infections in SLT is consistent with the phenotype of patients with inherited IL-17 defects (

Table 4.7). CMC is most commonly due to STAT1 phosphorylation abnormalities[87], but these were absent in SLT patients, as were alterations in STAT3 mediated cytokine signalling[85,141].

Immunodeficiency as a result of altered ionic flux in immune cells is largely described in humans from inherited ion channelopathies that result in

impaired store operated calcium entry (SOCE) during T cell activation[158]. This may be due to Calcium-release activated calcium current (CRAC) channel mutations leading to impaired calcium release from the endoplasmic reticulum (e.g. Stromal interaction molecule 1 [STIM1] mutations) or impaired extracellular calcium entry across the plasma membrane (e.g. Calcium release-activated calcium modulator 1 [ORAI1] mutations)[147,159–163]. Impaired SOCE also can occur due to a magnesium channel defect, Magnesium Transporter 1 (MAGT1) mutation, which results in X-linked immunodeficiency with magnesium defect, EBV viraemia and neoplasia (XMEN) syndrome[148,164]. Moreover, in mice, impaired SOCE due to deletion of ORAI1 or STIM1 impairs Th17 polarisation[165,166], and sodium has been shown to exert its proinflammatory effect through alterations in calcium signalling[49]. In SLT patients, I demonstrate that calcium flux is unaffected after T cell activation. Although I have shown the presence of sodium transporters on diverse immune cells, this unaltered calcium flux, alongside the lack of an effect of sodium chloride cotransporter inhibition on Th17 polarisation, and the inclusion of patients with multiple ion channel/transporter mutations in our cohort make reduced function of channel/transporter activity on immune cells an unlikely reason for altered immunity.

What makes SLT patients unique is their characteristic extracellular ionic environment, directly and indirectly related to renal salt wasting. In the light of recent evidence highlighting the effect of sodium on IL-17 responses[51–56], and on previous evidence demonstrating an effect of other extracellular ions (e.g. magnesium) on immunity[167], I hypothesised that reduced IL-17 responses are due to the altered ionic environment *in vivo* in SLT patients. I demonstrated that the addition of sodium, potassium and magnesium, within a clinically relevant range, promoted both a reduction in the ratio of Th2:Th17 polarisation during 3-day T cell stimulation experiments, and an increase in Th17 and Tc17 polarisation during 7-day experiments in culture conditions optimal for IL-17 production. I demonstrate therefore that the extracellular ionic environment typically found in SLT patients is inhibitory to protective IL-17 responses. These experiments confirm previous data demonstrating sodium promotes IL-17 responses[51–56], but also highlight a potential role of

sodium impacting Th2 and NK responses, and suggest an influence of other cations on Th17 polarisation. I also provide evidence for the first time that sodium depletion affects immunity and leads to IL-17 mediated immunodeficiency.

Given this proposal of ionic changes altering immunity in SLT, I lastly tested whether manipulation of the extracellular ionic environment *in vitro* could be used to augment SLT IL-17 responses, as I had shown in controls. I demonstrated that the intracellular pathway that mediates sodium driven Th17 polarisation is intact in SLT patients and that Th17 polarisation could be rescued with the addition of NaCl to culture conditions. This raises the possibility that increased salt supplementation and better correction of extracellular ionic concentrations *in vivo* in SLT patients may improve IL-17 responses and mitigate infection risk and warrants further study. Moreover, these data suggests that manipulation of the extracellular ionic environment may provide a therapeutic strategy in IL-17 mediated inflammatory diseases.

I did not assess all CD4+ subtypes and any effect on regulatory T cells or T follicular helper cells, both of which may be affected by sodium[57,58,60], in SLT patients was unexplored. I measured calcium flux during T cell activation but was unable to measure sodium flux in patients or controls. SLT patients have an activated renin-angiotensin-aldosterone system, albeit largely as a consequence of salt wasting, and whilst I assessed the effect of aldosterone and angiotensin II on Th17 polarisation, I did not assess the direct effect of renin, which has been shown to have an independent immunomodulatory role[112]. However, despite the compensatory effect of angiotensin II on IL-17 responses, the net effect in SLT patients is an immunodefective phenotype. I also did not assess the impact of altered prostaglandin E2, which is known to affect immunity[126] and which is increased in some patients with BS types 1, 2, and 4. Finally, I did not investigate the *in vivo* location of the effect of sodium and other ions on immunity, which remains an important unknown from this and other studies on the effect of salt on immunity.

Conclusions

I describe a novel immunodeficiency in SLT patients, who have increased mucosal bacterial and fungal infections, alongside other clinical features of dysregulated immunity including autoimmune phenomena, dermatitis and allergic disease. These clinical features are associated with impaired IL-17 responses, which I propose are due to sodium wasting and the unique extracellular ionic environment found in SLT patients. I highlight the role of multiple extracellular ions on immune cell activation states and demonstrate that SLT IL-17 responses may be rescued *in vitro* by salt. The manipulation of the extracellular ionic environment may therefore be of therapeutic benefit in SLT patients to mitigate infection risk.

5 CHAPTER 5: INVESTIGATION AND TARGETING OF SODIUM BALANCE IN INFLAMMATORY KIDNEY DISEASES

5.1 Introduction

In the previous sections, I have demonstrated that sodium promotes inflammatory immune responses *in vitro*, and that patients with chronic salt wasting have dampened IL-17 responses, which is associated with clinical features of immunodeficiency. In the last section of my research, I attempt to translate these findings to inflammatory kidney diseases. Specifically, I investigate whether altering salt intake affects the development of an animal model of inflammatory kidney disease, and also whether alterations in sodium balance may be of therapeutic potential in patients with inflammatory kidney diseases, in whom abrogating IL-17 and other inflammatory responses may be clinically useful.

Autoimmune kidney diseases (AIKD) are a common cause of End Stage Kidney Disease (ESKD), particularly in younger patients. Over 60,000 people are currently undergoing renal replacement therapy (RRT) in the UK and kidney transplantation offers the best treatment for ESKD[168]. Whilst short-term outcomes have improved in these conditions, relapse in AIKD is frequent and immune-mediated allograft injury remains the commonest cause of transplant failure. Longer-term morbidity in both AIKD and kidney transplant recipients is often the result of prolonged immunosuppression, in particular through infection, cardiovascular disease and cancer. The development of therapeutic strategies in which immunosuppression can be minimised without an associated increase in immune mediated kidney injury is therefore of clinical importance.

A number of different cell subtypes that have been shown to be salt responsive contribute to immune mediated kidney injury in native AIKD and chronic allograft rejection, including Th17 and T follicular helper (TfH) cells.

For example, Th17 cells are implicated in the development of ANCA-associated glomerulonephritis[90,91], Lupus Nephritis[92], IgA Nephropathy[93], and Primary Sjögren's Syndrome associated tubulointerstitial nephritis[94,95] in the native kidney setting, and in acute and chronic kidney transplant rejection[97]. Through activation of these inflammatory cells, high salt diets in animal models worsen extra renal autoimmune disease (**Table 1.1**), but the effect of altering salt intake on inflammatory kidney disease is largely untested. Moreover, whilst *increasing* salt intake in healthy volunteers and patients with autoimmune disease has been shown to have an inflammatory effect on the immune system (**Table 1.3**), the immunological effect of *reducing* salt intake, which is of much greater translational importance, is unknown.

5.2 Aims

i. to investigate whether *in vitro* IL-17 responses in patients with AIKD and KTRs on maintenance immunosuppression are sodium responsive
ii. to determine if *in vitro* TfH responses in healthy controls are sodium responsive
iii. to investigate whether a high salt diet affects the development of inflammatory kidney disease in an animal model of crescentic glomerulonephritis
iv. to determine the feasibility of a short term low salt intervention in healthy controls and kidney transplant recipients (KTRs), and investigate its effect on sodium stores and immune responsiveness

5.3 Brief Methods

Patients with native AIKD and KTRs on maintenance immunosuppression were recruited from the Royal Free Hospital, London. PBMCs were isolated and cultured for 7 days in optimal IL-17 polarising conditions in standard media and in media supplemented with +40mM NaCl, as had been done in healthy controls earlier in the research project. The effect of NaCl on IL-17

responses (Th17 and Tc17 polarisation, and supernatant IL-17 concentration) was compared between standard and high salt conditions, and salt responsiveness of these responses was compared between AIKD patients, KTRs, and controls.

To investigate the effect of sodium on TfH responses, healthy control PBMCs were isolated and stimulated for 72 hours with anti-CD3/anti-CD28 in standard media and in media supplemented with +40mM NaCl. TfH polarisation (% of CD4+ cells expressing CXCR5) and IL-21 expression by TfH cells were compared between standard and high salt conditions.

The nephrotoxic nephritis model was used to investigate the effect of a high salt diet on the development of inflammatory kidney disease. This model involves the injection of nephrotoxic serum containing antibodies targeting glomerular antigens resulting in a crescentic glomerulonephritis and associated tubular injury. 2 experiments were undertaken, initially with the induction of severe glomerular disease and subsequently with a model of milder disease and more prolonged salt loading prior to disease induction. In both experiments the development of disease was compared between animals fed a standard diet to those fed a high salt (4% NaCl chow; 1% NaCl drinking water). Variables compared included proteinuria, serum creatinine, kidney histological scores, and Th17 cells infiltrating the kidney.

Lastly, to investigate whether a low salt diet may be of therapeutic potential, pilot interventional studies were undertaken in healthy controls and subsequently KTRs. Both healthy controls and KTRs underwent a 1-week low salt diet, with a planned intake of <2.5g salt/day. Clinical and physiological parameters, sodium intake and stores (as determined by lower limb ^{23}Na-MRI), and T cell responses (T cell subsets) were assessed prior to and immediately after intervention, and at 1-4 weeks thereafter, when back on standard diet. The safety, feasibility, and tolerability of the intervention were determined, as was its effect on sodium stores and immune responsiveness by comparing variables across these assessment time points.

5.4 Results

5.4.1 Sodium chloride increases *in vitro* IL-17 responses in patients with native autoimmune kidney disease and kidney transplant recipients on *in vivo* immunosuppression

The effect of NaCl on *in vitro* IL-17 responses was assessed in 9 patients with native AIKD (aged 69 (56-69.5) years; 7 (78%) female). 5 patients had AAV, 3 patients pSS TIN, and 1 patient LN. All patients were immunosuppressed at the time of PBMC sampling with a median creatinine of 100µmol/l (73-122) (**Table 5.1**). As in healthy controls, sodium chloride (+40mM NaCl added to culture conditions) increased IL-17 responses in AIKD patients despite maintenance *in vivo* immunosuppression (**Figure 5.1**).

Table 5.1: Demographic and clinical data of patients with native AIKD in whom IL-17 responses were assessed

AAV – ANCA-associated vasculitis; LN – lupus nephritis; pSS TIN – Primary Sjogren's Syndrome Tubulointerstitial Nephritis; MMF – mycophenolate mofetil.

Patient	Age	Sex	Diagnosis	Creatinine	Induction Therapy	Maintenance Therapy
1	69	F	AAV	90	Methylprednisolone; Cyclophosphamide i/v	Prednisolone 2mg/day; Azathioprine 50mg/day
2	69	F	AAV	83	Methylprednisolone; Rituximab; Cyclophosphamide i/v	Rituximab 6 monthly; MMF 500mg/day
3	56	M	AAV	121	Methylprednisolone; Rituximab; Plasma Exchange	Rituximab 6 monthly
4	68	F	AAV	122	Methylprednisolone; 1. Cyclophosphamide i/v. 2. MMF	Rituximab 6 monthly
5	69	M	AAV	141	Methylprednisolone; Rituximab; Cyclophosphamide i/v	Azathioprine 50mg/day
6	38	F	LN	100	Prednisolone; Rituximab; Cyclophosphamide	MMF 500mg/day, prednisolone 5mg/day

7	75	F	pSS TIN	100	Prednisolone	MMF 1g/day
8	70	F	pSS TIN	62	Nil	Hydroxychloriquine 200mg/day
9	56	F	pSS TIN	63	Nil	MMF 500mg/day, Hydroxychloroquine 800mg/day

Figure 5.1: The effect of NaCl on IL-17 responses in patients with AIKD (n=9) on maintenance immunosuppression

ns – not significant (p>0.05), *p≤0.05, **p≤0.01, ***p≤0.001, ****p≤0.0001

A. Th17 polarisation in unsupplemented media and in media supplemented with 40mM NaCl. Th17 cells as a percentage of CD4+ cells: +0mM NaCl 5.6% (1.9-9.5); +40mM NaCl 12.4% (6.0-17.2), median difference 4.9% (2.9-6.4), p=0.0039. Compared with Wilcoxon test.

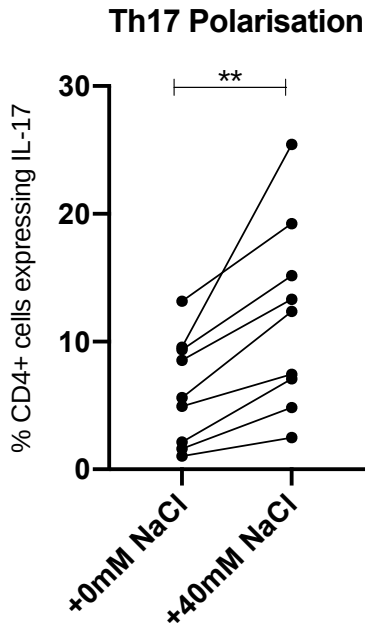

B. Tc17 polarisation in unsupplemented media and in media supplemented with 40mM NaCl. Tc17 cells as a percentage of CD8+ cells: +0mM NaCl 3.9% (0.8-6.3); +40mM NaCl 7.7% (1.5-14.1), median difference 3.1% (0.8-8.9), p=0.03. Compared with Wilcoxon test.

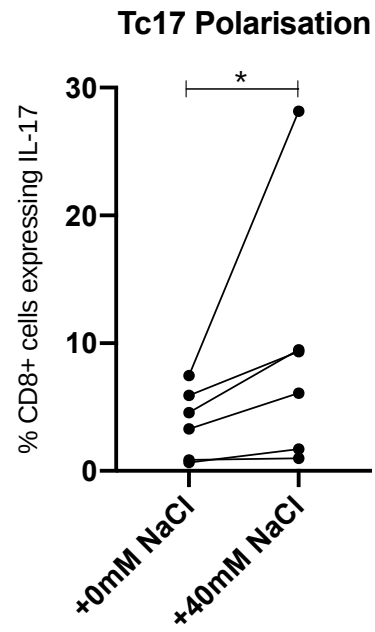

C. Supernatant IL-17 in cells stimulated in unsupplemented media and in media supplemented with 40mM NaCl. IL-17 concentration: +0mM NaCl 5640pg/ml (3908-14545); +40mM NaCl 19213pg/ml (8065-35096), median difference 12145pg/ml (4157-18986), p=0.0078. Compared with Wilcoxon test.

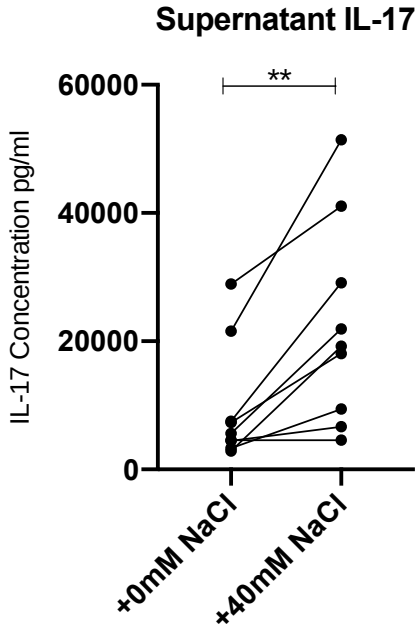

D. Representative FACS plots of IL-17 expression in CD4+ (Th17) cells and CD8 (Tc17) cells after stimulation in standard media and in media supplemented with 40mM NaCl in a patient with pSS (56 year old female; patient 9) on maintenance MMF

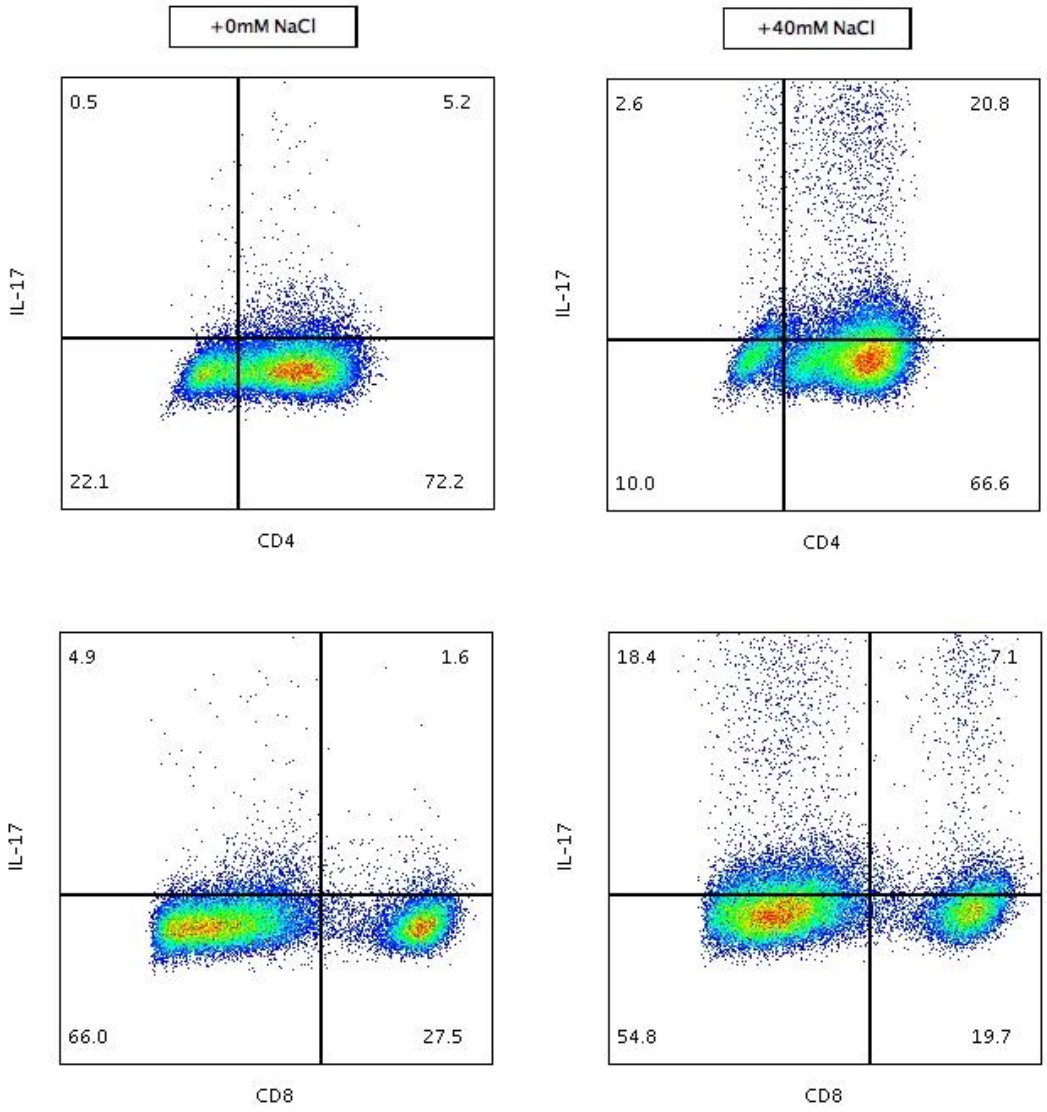

The effect of NaCl on IL-17 responses was also assessed in 14 kidney transplant recipients (aged 56 (42-64) years; 7 (50%) female). All patients were on immunosuppression and > 1 year post transplantation at the time of PBMC isolation, with median creatinine 109µmol/l (91-168) (**Table 5.2**). As in healthy controls and AIKD patients, the addition of +40mM NaCl to culture conditions increased IL-17 responses in kidney transplant recipients on maintenance immunosuppression (**Figure 5.2**).

Table 5.2: Demographic and clinical data of kidney transplant recipients in whom IL-17 responses were assessed

CFHR5 – complement factor H related protein 5; MMF – mycophenolate mofetil; PKD – polycystic kidney disease; ANCA – antineutrophil cytoplasmic antibody

Patient number	Age	Sex	Cause of ESKD	Transplant details	Immunosuppression (current)	Tacrolimus Level (ng/ml)	Cyclosporin Level (ng/ml)	Creatinine (umol/l)	Na (mmol/l)
1	70	F	CFHR5 Nephropathy	Deceased donor transplant	Tacrolimus; MMF 750mg/day	11.6		92	137
2	31	F	Medullary cystic kidney disease	Deceased donor transplant	Tacrolimus; MMF 1.5g/day	7.5		91	143
3	64	F	PKD	Deceased donor transplant	Tacrolimus; MMF 500mg/day	3.4		91	142
4	57	M	Unclear/small kidneys	Deceased donor transplant	Tacrolimus; 1.5g/day	6.2		172	140
5	43	F	Unclear/small kidneys	Deceased donor transplant	Cyclosporin; MMF 750mg/day		46	120	139
6	60	M	Unclear/small kidneys	Deceased donor transplant	Tacrolimus; MMF 500mg/day	8.7		133	137
7	30	M	Reflux nephropathy	ABO incompatible Live	Tacrolimus; MMF 2g/day	4.1		368	135
8	40	F	ANCA vasculitis	Live	Tacrolimus; Cepteva 720mg/day	4		84	141
9	44	F	Reflux nephropathy	Deceased donor transplant	Tacrolimus; azathioprine 75mg/day	6		102	136

10	77	F	Diabetes	Deceased donor transplant	Tacrolimus; MMF 1g/day	5.2		115	136
11	44	M	ANCA vasculitis	Deceased donor transplant	Tacrolimus	5.6		223	137
12	55	M	Tuberculosis	Deceased donor transplant	Tacrolimus; MMF 750mg/day	7.8		74	140
13	65	M	Diabetes	Deceased donor transplant	Sirolimus			96	137
14	59	M	PKD	Deceased donor transplant	Tacrolimus; MMF 1g/day	6.4		167	141

Figure 5.2: The effect of NaCl on IL-17 responses in kidney transplant recipients (n=14) on maintenance immunosuppression

ns – not significant (p>0.05), *p≤0.05, **p≤0.01, ***p≤0.001, ****p≤0.0001

A. Th17 polarisation in unsupplemented media and in media supplemented with 40mM NaCl. Th17 cells as a percentage of CD4+ cells: +0mM NaCl 6.0% (4.4-12.5); +40mM NaCl 16.7% (8.4-20.1), median difference 6.1% (-0.6-12.3), p=0.0134. Compared with Wilcoxon test.

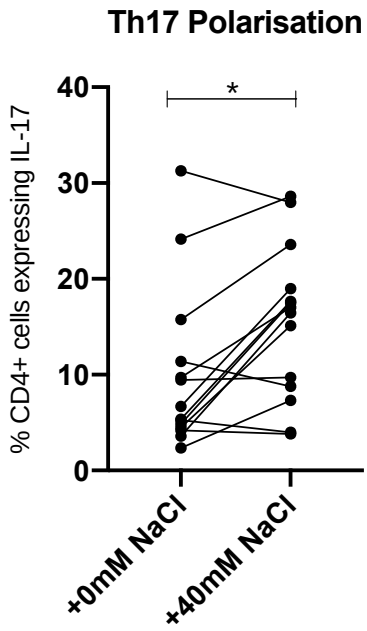

B. Tc17 polarisation in unsupplemented media and in media supplemented with 40mM NaCl. Tc17 cells as a percentage of CD8+ cells: +0mM NaCl 3.3% (1.8-5.6); +40mM NaCl 12.9% (6.1-17.4), median difference 9.0% (3.5-12.3), p=0.0017. Compared with Wilcoxon test.

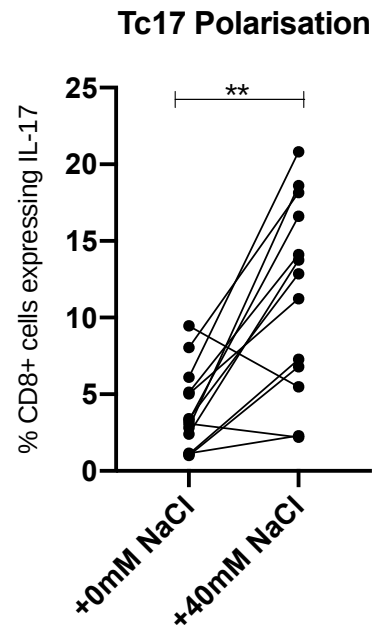

C. Supernatant IL-17 in cells stimulated in unsupplemented media and in media supplemented with 40mM NaCl. IL-17 concentration: +0mM NaCl 1888pg/ml (732-4636); +40mM NaCl 4761pg/ml (1432-9821), median difference 1594pg/ml (330-4925), p=0.0046. Compared with Wilcoxon test.

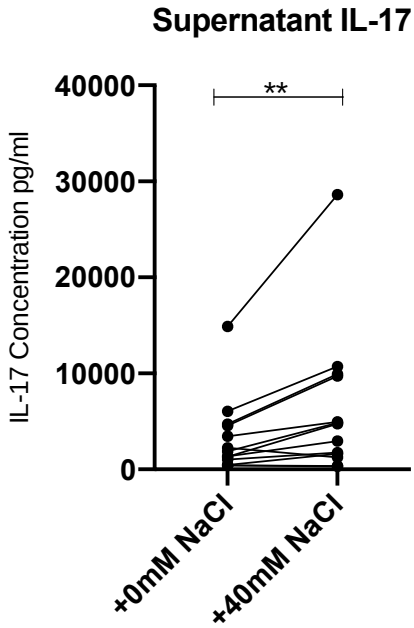

D. Representative FACS plots of IL-17 expression in CD4+ (Th17) cells and CD8 (Tc17) cells after stimulation in standard media and in media supplemented with

40mM NaCl in a transplant recipient (55 year old male; patient 12) on maintenance immunosuppression with tacrolimus and MMF

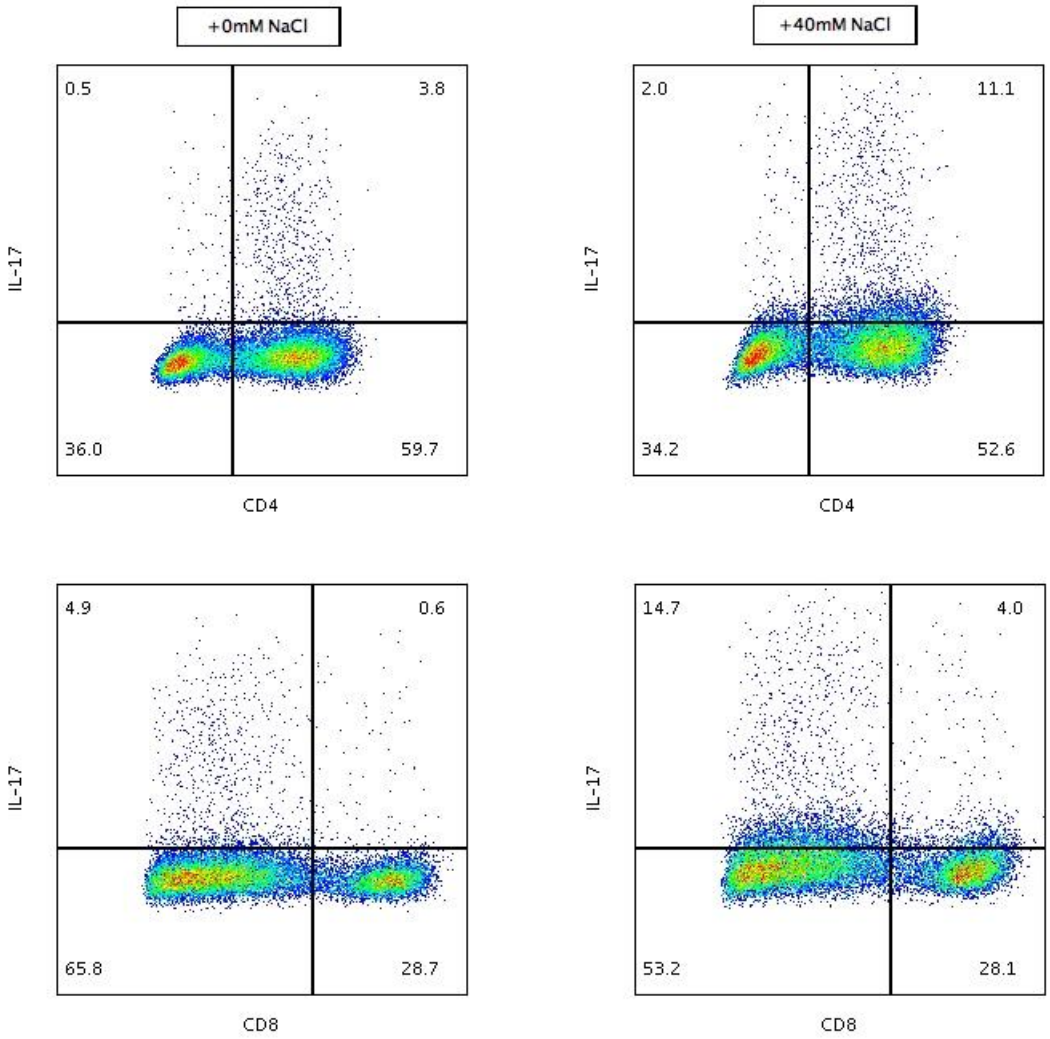

5.4.2 Salt responsiveness of IL-17 responses is not different in AIKD patients and kidney transplant recipients on immunosuppression compared to healthy controls

Salt responsiveness of IL-17 responses was determined in AIKD patients, KTRs and healthy controls. This was determined by expressing each IL-17 readout (Th17 and Tc17 cell polarisation, and supernatant IL-17 concentration) as a ratio of that in high salt culture conditions (+40mM NaCl) to that in standard conditions (+0mM NaCl). IL-17 salt responsiveness, as

determined by Th17 and Tc17 polarisation and supernatant IL-17 concentration over a 7-day culture were not different in AIKD patients or KTRs compared to healthy controls despite the presence of *in vivo* immunosuppression (**Figure 5.3**).

Figure 5.3: Salt responsiveness of IL-17 responses in healthy controls, patients with AIKD, and KTRs.

Red lines drawn at ratio of 1 (i.e. no difference between normal and high salt condition).

A. Salt responsiveness of Th17 polarisation: HC ratio 1.6 (1.3-2.3), AIKD ratio 2.2 (1.5-2.8), KTR ratio 1.6 (0.9-3.3); p=0.49. Compared with Kruskal-Wallis test

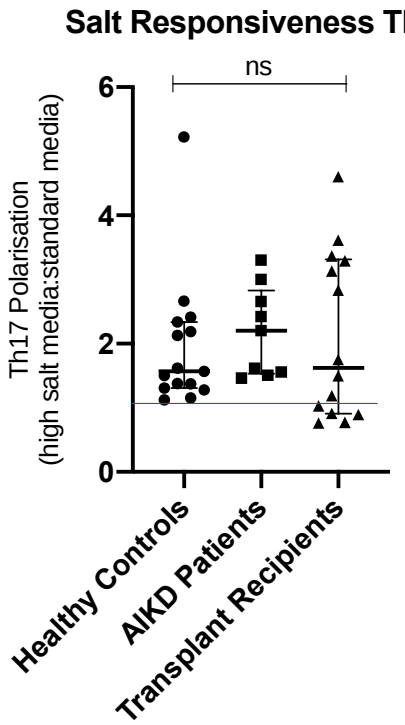

B. Salt responsiveness of Tc17 polarisation: HC ratio 2.1 (1.6-2.5), AIKD ratio 2.0 (1.5-2.9), KTR ratio 3.4 (2.1-6.2); p=0.17. Compared with Kruskal-Wallis test

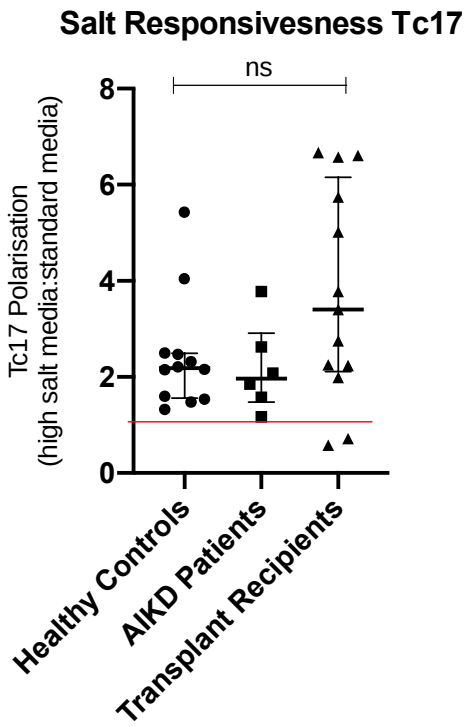

C. Salt responsiveness of supernatant IL-17 concentrations: HC ratio 1.8 (1.6-2.2), AIKD ratio 2.5 (1.5-3.9), KTR ratio 1.9 (1.1-2.4); p=0.33. Compared with Kruskal-Wallis test

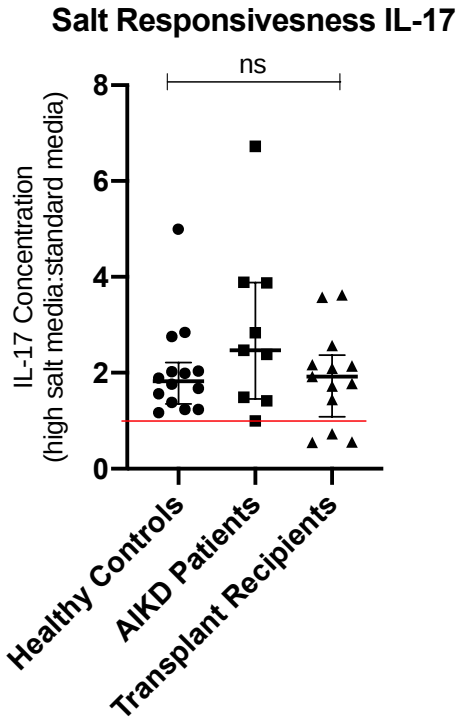

5.4.3 T follicular helper (TfH) cell responses were not affected by NaCl

Given their important role in the production of pathogenic auto- and allo-antibodies in native and transplant inflammatory kidney disease respectively, the effect of NaCl on TfH responses was then assessed. Healthy control PBMCs were stimulated for 72 hours with anti-CD3/anti-CD28 with and without +40mM NaCl added to culture conditions. The proportion of CD4+ cells expressing CXCR5 (TfH cells) and IL-21, as well as the proportion of CD4+CXCR5+ (TfH) cells expressing IL-21, were determined.

Experiments were undertaken in 7 healthy controls. The addition of NaCl in these experiments reduced cell viability, and there was no change in TfH cells as a proportion of CD4+ cells (**Figure 5.4**). There was also no significant change in IL-21 expression in CD4+ cells or in CD4+CXCR5+ (TfH) cells with the addition of NaCl (**Figure 5.4**).

Figure 5.4: The effect of NaCl on TfH responses in healthy controls (n=7)

ns – not significant (p>0.05), *p≤0.05, **p≤0.01, ***p≤0.001, ****p≤0.000

A. Cell viability after 3-day anti-CD3/28 stimulation: +0mM NaCl 55% (50-65), +40mM NaCl 47% (42-60), median difference -7% (-8, -5), p=0.02. Compared with Wilcoxon test.

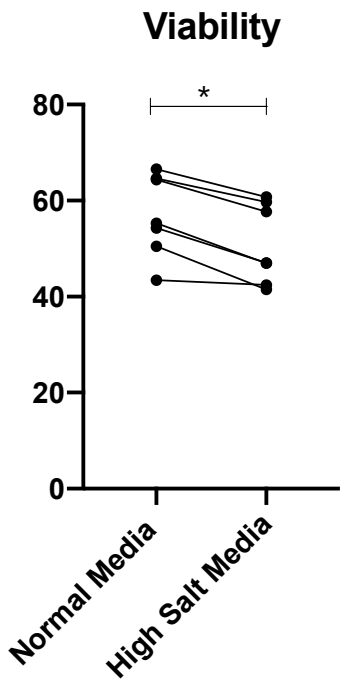

B. TfH polarisation (CD4+CXCR5+ cells) in unsupplemented media and in media supplemented with 40mM NaCl. TfH cells as a percentage of CD4+ cells: +0mM NaCl 11.1% (9.9-17.3); +40mM NaCl 16.7% (11.4-19.3), median difference 0.7% (-0.4-1.9), p=0.38. Compared with Wilcoxon tes**t.**

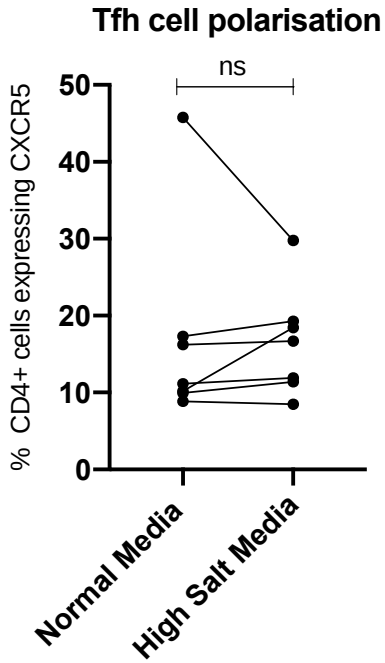

C. IL-21 expression by CD4+ cells in unsupplemented media and in media supplemented with 40mM NaCl. IL-21 expression by CD4+ cells: +0mM NaCl 33.7% (13.4-44.9); +40mM NaCl 41.9% (28.2-49.1), median difference 11.3% (-3.0-11.6), p=0.078. Compared with Wilcoxon tes**t.**

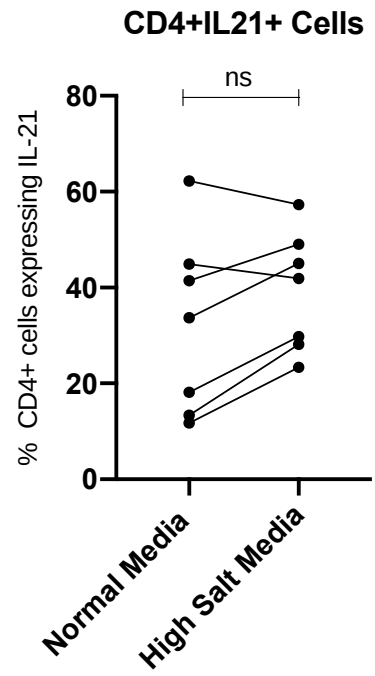

D. IL-21 expression by TfH cells in unsupplemented media and in media supplemented with 40mM NaCl. IL-21 expression by TfH cells: +0mM NaCl 57.6% (37.2-63.7); +40mM NaCl 61.7% (51.6-65.5), median difference 4.8% (0.5-10.9), p=0.16. Compared with Wilcoxon tes**t.**

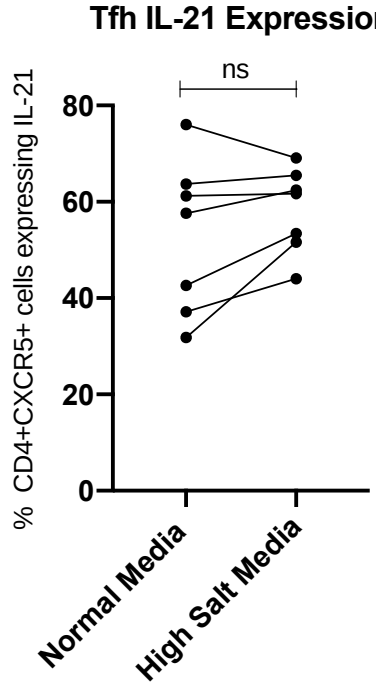

E. Representative FACS plots of CXCR5 (top panel) and IL21 (middle panel) expression by CD4+ cells, and IL-21 expression in CD4+CXCR5+ (TfH) cells (bottom panel). Gating determined by FMO.

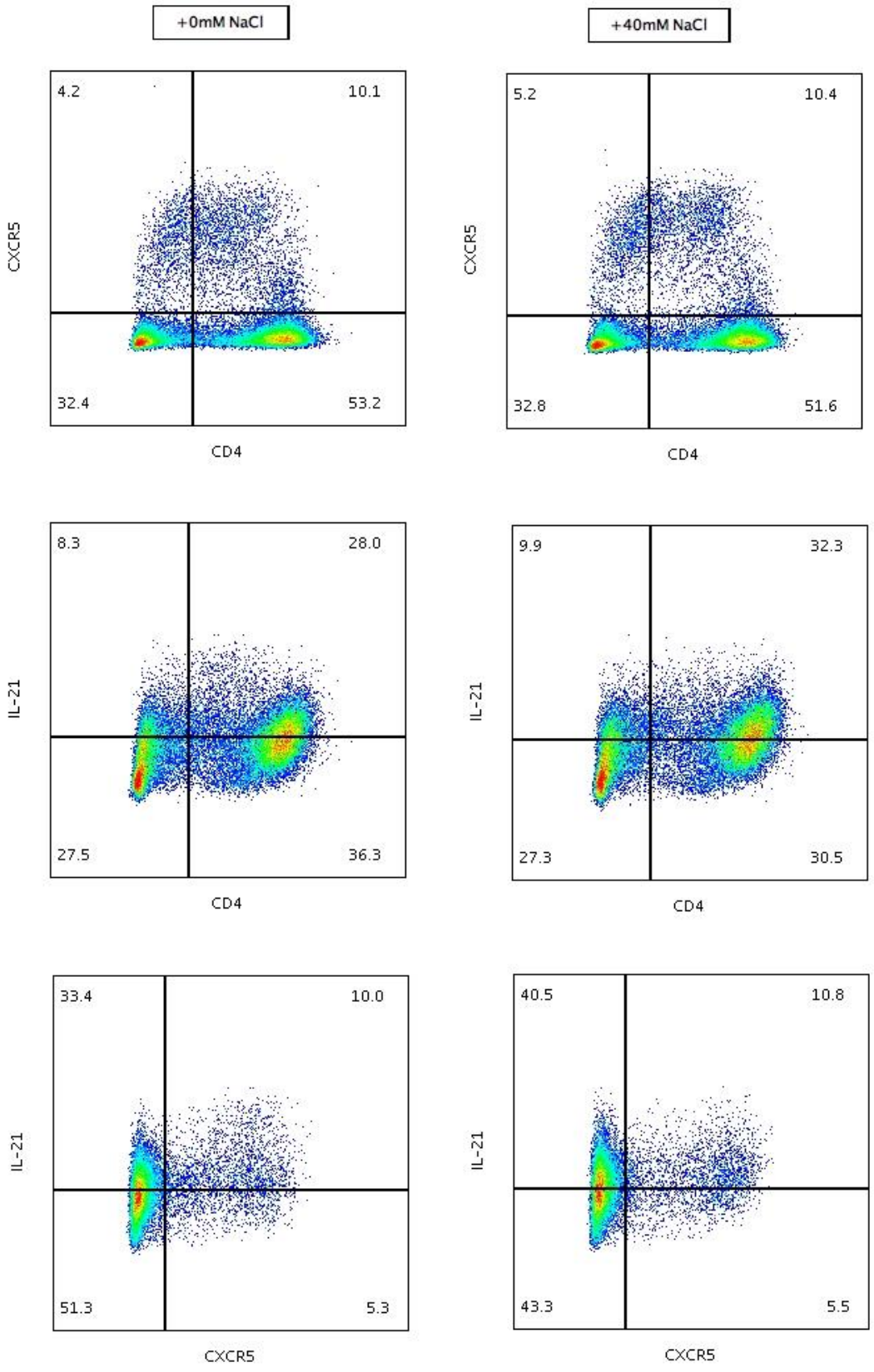
+0mM NaCl
+40mM NaCl
4.2
10.1
32.4
53.2
5.2
10.4
32.8
51.6
CXCR5
CD4
8.3
28.0
27.5
36.3
9.9
32.3
27.3
30.5
IL-21
33.4
10.0
51.3
5.3
40.5
10.8
43.3
5.5
CXCR5

5.4.4 Altering dietary salt intake did not affect the development of an animal model of glomerulonephritis

The effect of altering dietary salt intake on inflammatory kidney disease was investigated using the nephrotoxic nephritis (NTN) model of glomerulonephritis. This was done in 2 experiments.

5.4.4.1 Experiment 1

In experiment 1, mice were preimmunised with sheep IgG/CFA 5 days prior to the induction of disease. 8 mice fed a standard diet were compared to 8 mice fed a high salt diet (4% NaCl chow; 1% NaCl drinking water), starting at the time of pre-immunisation.

Clinical outcomes

1 mouse died prior to sacrifice on day 7 (standard diet group). Although not formally quantified, a number of the other mice in both groups demonstrated signs of severe illness (reduced movement, generalised oedema).

Urinalysis

Proteinuria according to urine dipstick is outlined in **Table 5.3**; urine volume and quantified proteinuria are outlined in **Figure 5.5**. Urine volume was non-significantly higher in the high salt diet group; proteinuria was not different between groups.

Table 5.3: Dipstick proteinuria (animal experiment 1)

*mouse died in metabolic cage

Mouse number	Standard Diet	High Salt Diet
1	3+*	Trace
2	2+	1+
3	4+	3+

4	+	1+
5	3+	Trace
6	3+	Trace
7	3+	4+
8	3+	4+

Figure 5.5: Urine volume (24 hour) and proteinuria in NTN mice on a standard and high salt diet (animal experiment 1)

Proteinuria is demonstrated as measured urine protein concentration, and as absolute amount of protein/24 hours, and as a ratio with urine creatinine to account for urine volume.

A. Urine volume (24 hour): Standard diet 1.0ml (0.87-2.7); High Salt diet 5.0ml (0.7-6.4); p=0.19. Compared with Mann-Whitney test.

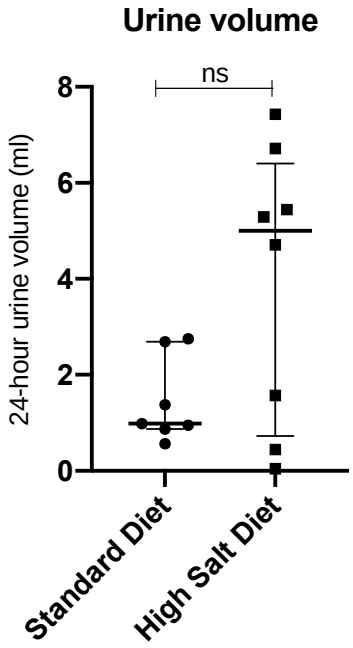

B. Urine protein concentration: Standard diet 55mg/ml (25-121); High Salt diet 22mg/ml (7-112); p=0.38. Compared with Mann-Whitney test.

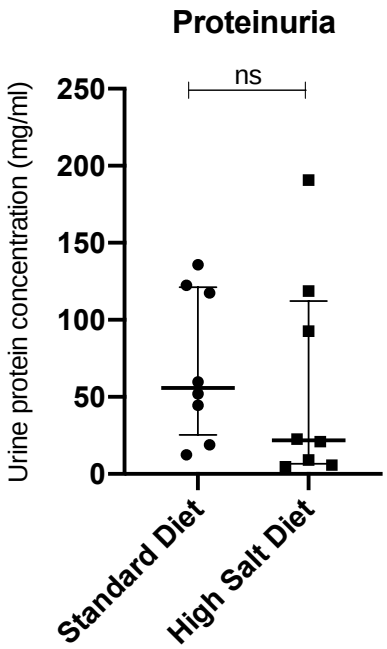

C. Proteinuria (mg/24 hours): Standard diet 102mg (18-187), High Salt diet 52mg (22-140), p=0.9. Compared with Mann-Whitney Test.

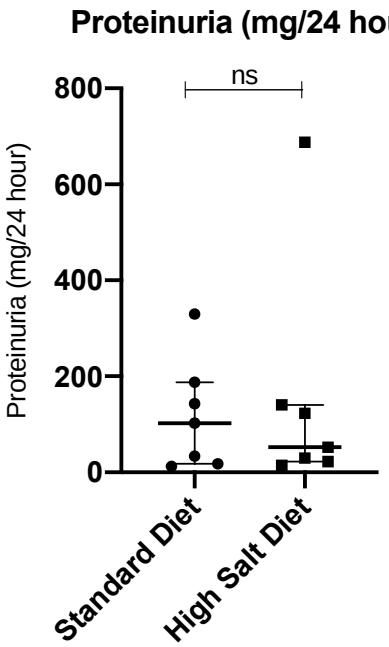

D. Urine protein:creatinine ratio: Standard diet 0.031mg/mmol (0.008-0.045); High Salt diet 0.017mg/mmol (0.004-0.077); p=0.87. Compared with Mann-Whitney test.

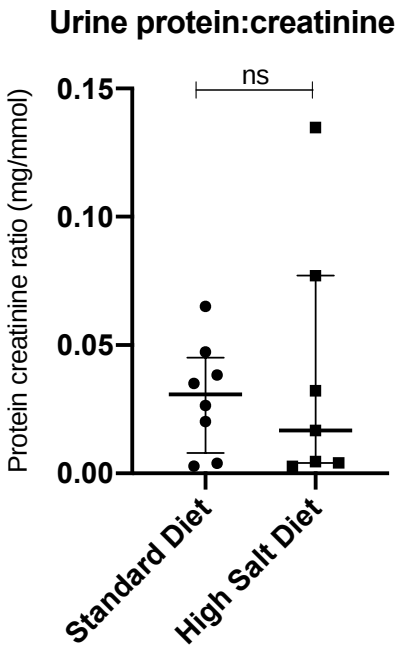

Serum biochemistry

There was no difference in serum sodium and creatinine between groups (**Figure 5.6**).

Figure 5.6: Serum sodium and creatinine in NTN mice on a standard and high salt diet (animal experiment 1)

A. Serum sodium: Standard diet 151mmol/l (145-156); High Salt Diet 158mmol/l (144-165); p=0.59. Compared with Mann Whitney test.

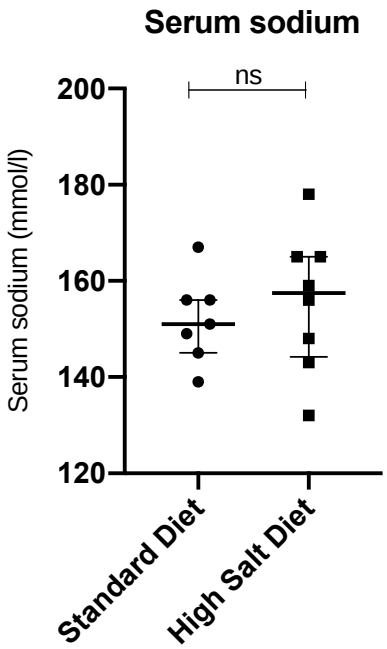

B. Serum creatinine: Standard diet 12.8µmol/l (9.6-37.6); High Salt Diet 13.7µmol /l (4.4-25.3); p=0.67. Compared with Mann Whitney test.

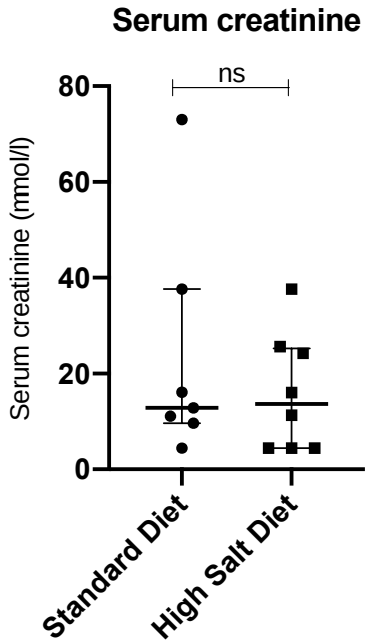

Kidney Histology

There was variability in histological disease severity within each group. Overall, there was no difference between groups in histological scores (**Figure 5.7**).

Figure 5.7: Kidney histology scores in NTN mice on a standard and high salt diet (animal experiment 1)

A. Sum of components of the histological score in each mouse in the standard and high salt diet groups. Median (IQR) score in each group demonstrated. Groups compared with a Mann-Whitney test.

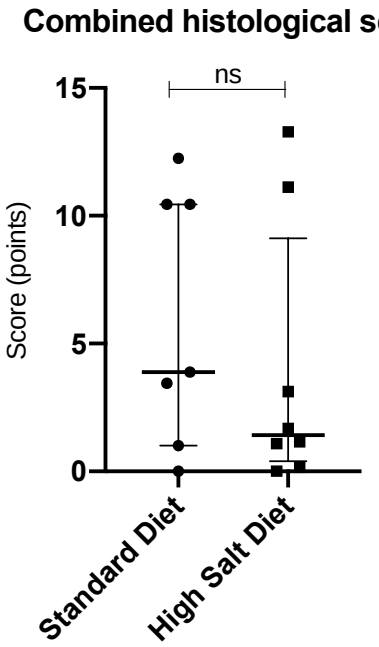

B. Individual components of the histological score in each mouse in the standard and high salt diet groups. Median (IQR) score in each group demonstrated. Groups compared with a Mann-Whitney test.

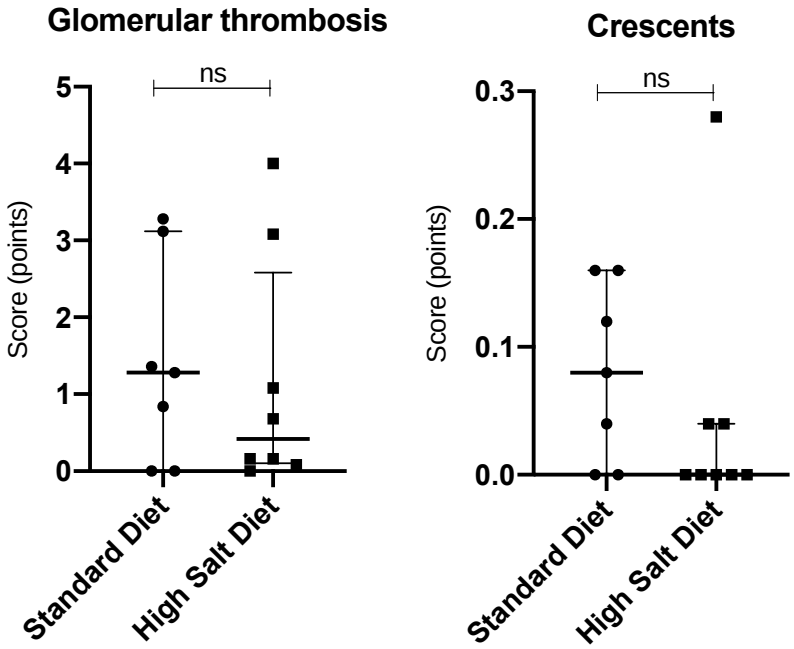

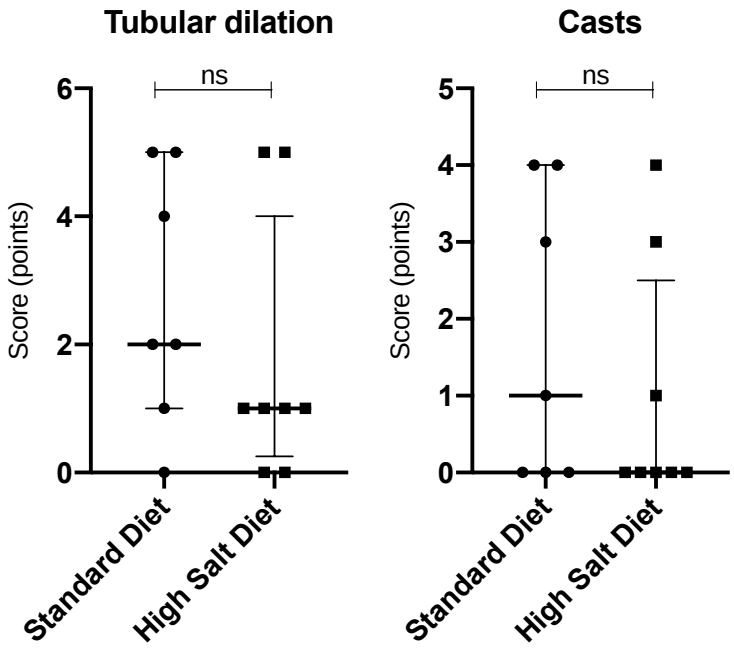

C. Period acid Schiff stained kidney (x40 magnification) sections from 2 mice within the normal salt diet group highlighting variability in histology within each group.

Image 1: demonstrates relatively normal glomeruli (single arrows) and tubules (double arrows).

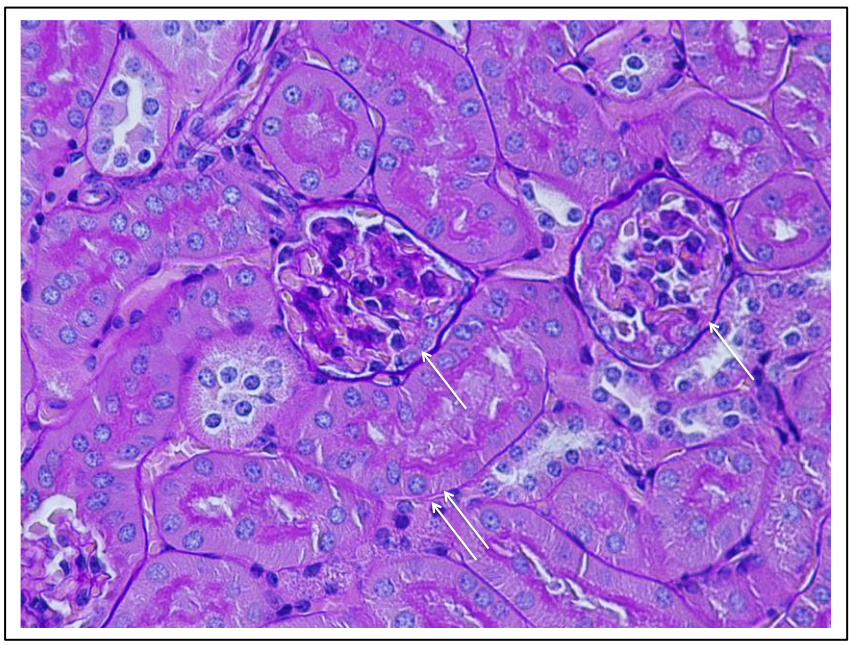

Image 2: demonstrates thrombosed glomeruli (single arrows) and surrounding tubules are dilated with tubular casts (double arrows).

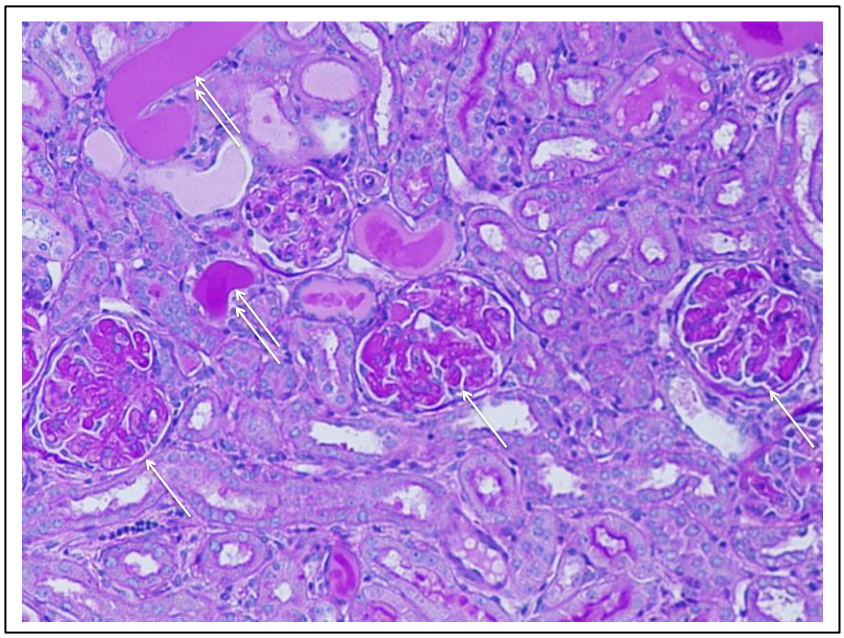

Lymphocytes infiltrating the kidney were unable to be analysed in experiment 1 due to cell death during processing.

5.4.4.2 Experiment 2

Given the severity of disease in the standard diet (‘control’) group In experiment 1, a subsequent experiment was undertaken in which milder disease was induced and in which mice in the high salt group underwent a more prolonged period of salt loading prior to the induction of disease. In this experiment, mice did not undergo preimmunisation with sheep IgG/CFA and the high salt diet started 2 weeks prior to the induction of disease. 7 mice fed a standard diet were compared to 7 mice fed a high salt diet (4% NaCl chow; 1% NaCl drinking water). Disease was assessed at 13 days after induction in 3 mice from each group and at 14 days after induction in 4 mice from each group.

Clinical outcomes

1 mouse died prior to sacrifice on day 13 (high salt diet group). Although not formally quantified, clinical signs of severe illness (reduced movement, generalised oedema) were less frequently present compared to experiment 1.

There was an increase in mouse weight across the duration of the experiment, the magnitude of which was not different between groups (**Figure 5.8**).

Figure 5.8: Mouse weights in animal experiment 2

A. Mouse weight at the start of the experiment (commencement of diet) and at the end of the experiment (time of sacrifice): start median 32g (30-32.5), end median 32g (32-33.5), p=0.002. Compared with Wilcoxon test. Blue - standard diet; Red – high salt diet

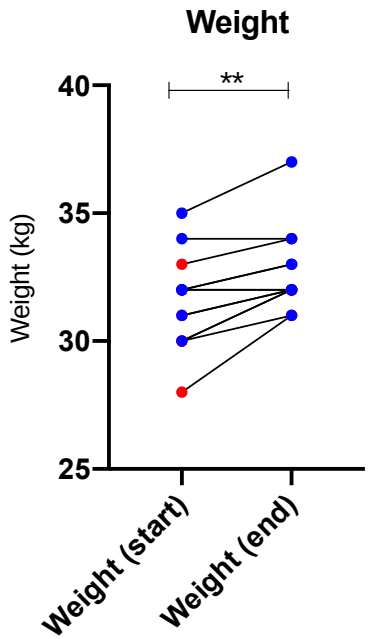

B. Weight change during experiment (weight end/weight start): standard diet ratio 1.032 (1.023-10.39), high salt diet ratio 1.049 (1.023-1.077), p=0.31. Compared with Mann-Whitney test.

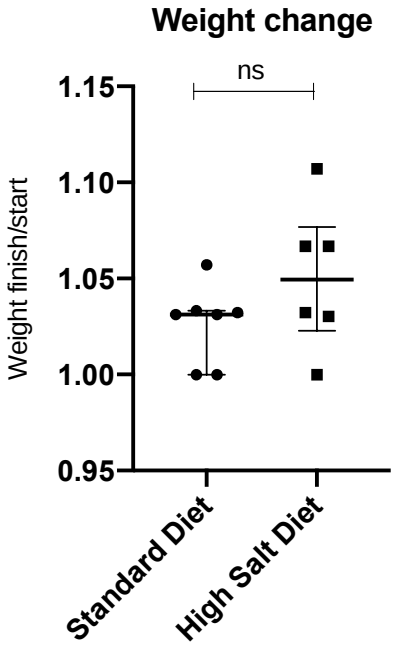

Urinalysis

Proteinuria according to urine dipstick is outlined in **Table 5.4**; urine volume and quantified proteinuria are outlined in **Figure 5.9**. Urine volume was significantly higher in the high salt diet group; proteinuria was not different between groups.

Table 5.4: Dipstick proteinuria (animal experiment 2)

*mouse died in metabolic cage

Mouse number	Standard Diet	High Salt Diet
1	4+	Negative
2	2+	Trace
3	3+	Negative
4	4+	3+
5	4+	Unknown*
6	Trace	2+
7	2+	3+

Figure 5.9: Urine volume (24 hour) and proteinuria in NTN mice on a standard and high salt diet (animal experiment 2)

Proteinuria is demonstrated as measured urine concentration, and as absolute amount of protein/24 hours accounting for urine volume.

A. Urine volume (24 hour): Standard diet 1.4ml (0.94-1.7); High Salt diet 6.8ml (5.2-8.6); p=0.0012. Compared with Mann-Whitney test.

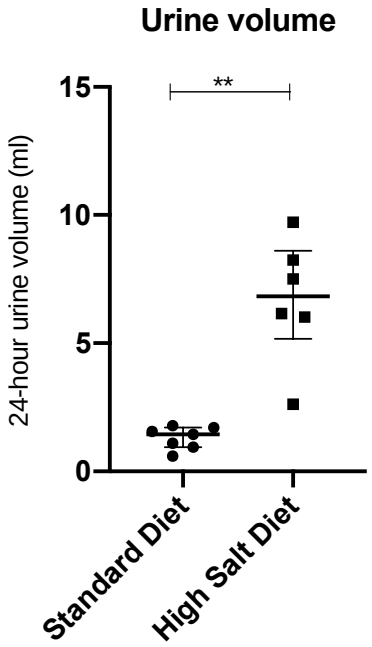

B. Urine protein concentration: Standard diet 6.6mg/ml (2.8-16.5); High Salt diet 1.0mg/ml (0.4-6.0); p=0.051. Compared with Mann-Whitney test.

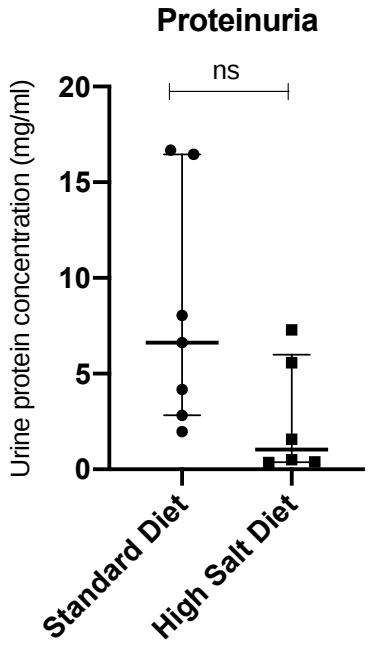

C. Proteinuria (mg/24 hours): Standard diet 9.6mg (3.0-22.9), High Salt diet 4.7mg (4.4-28.3), p=0.84. Compared with Mann-Whitney Test.

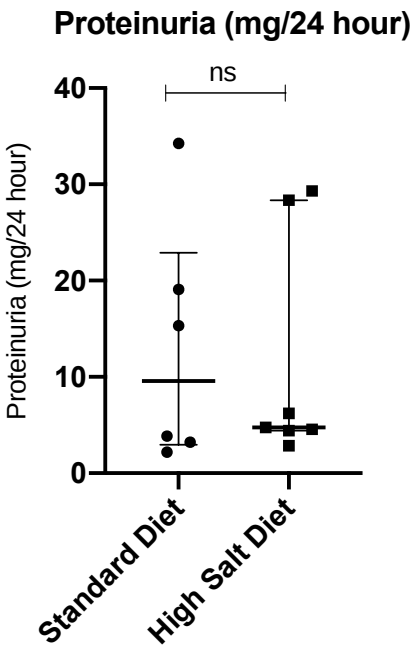

Serum biochemistry

Serum creatinine was higher in the standard diet group compared to the high salt diet group (**Figure 5.10**).

Figure 5.10: Serum creatinine in NTN mice on a standard and high salt diet (animal experiment 2)

Standard diet 11.8µmol/l (11.4-14.5), high salt diet 9.75µmol/l (8.65-10.4), p=0.0047. Compared with Mann-Whitney Test.

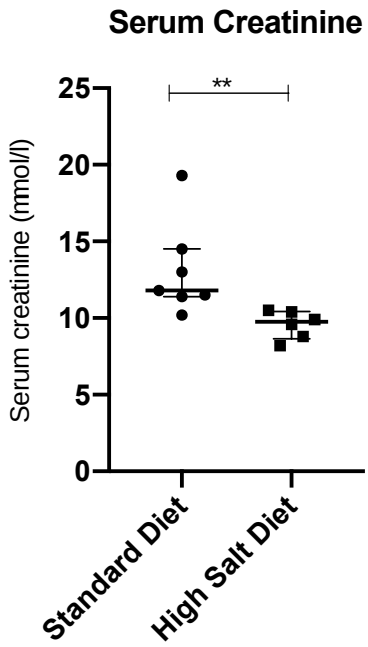

Kidney Histology

There were no differences in histological scores between groups (**Figure 5.11**).

Figure 5.11: Kidney histology scores in NTN mice on a standard and high salt diet (animal experiment 2)

A. Sum of components of the histological score in each mouse in the standard and high salt diet groups. Median (IQR) score in each group demonstrated. Groups compared with a Mann-Whitney test.

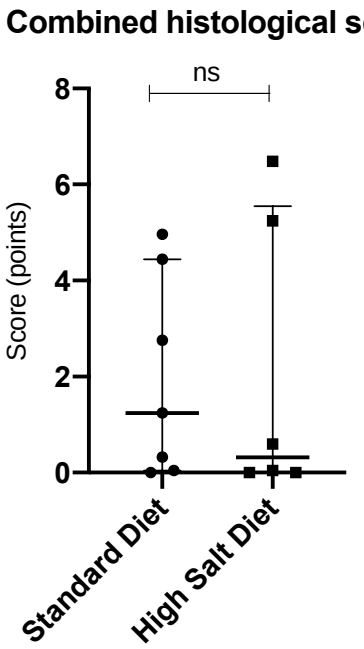

B. Individual components of the histological score in each mouse in the standard and high salt diet groups. Median (IQR) score in each group demonstrated. Groups compared with a Mann-Whitney test. No crescents were present in any of the mice therefore this component of score not shown.

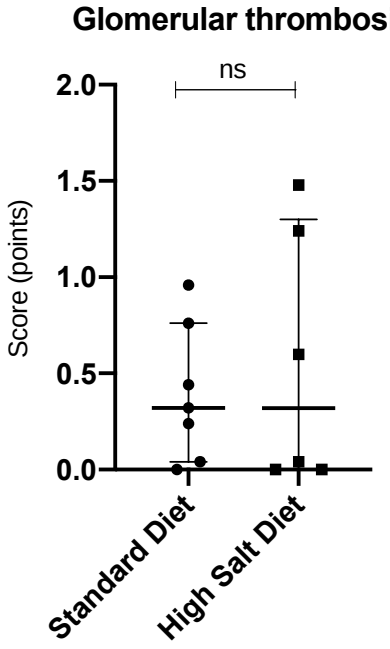

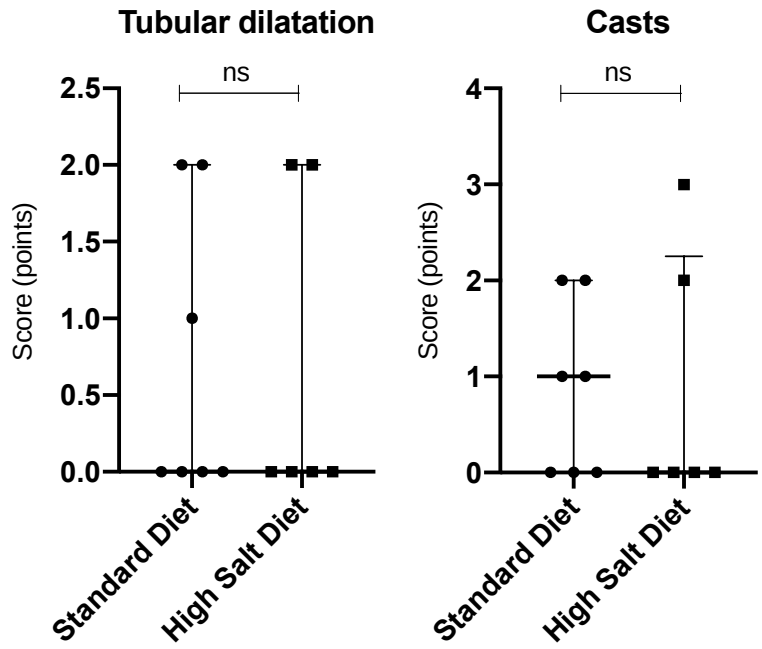

FACS analysis of IL-17 expressing lymphocytes in the kidney

Analysis of IL-17 expressing cells (IL-17 expression in all lymphocytes, IL-17 expression in CD4+ [Th17] cells, and IL-17 expression in CD4- [Tc17] cells) in the kidney of NTN mice was undertaken over 2 days for logistical reasons. 3 mice from each group were analysed on day 1, and the remaining 4 mice from the standard diet group and the remaining 3 mice from the high salt diet group analysed on day 2. The results from analysis on each of these days are presented separately. There was no difference in infiltrating IL-17 expressing cells between groups in the analysis from day 1, whilst there was a trend to an increase in infiltrating Th17 cells in the standard diet group in the analysis from day 2 (**Figure 5.12**).

Figure 5.12: Infiltrating IL-17 expressing cells in the kidneys of NTN mice on a standard and high salt diet (animal experiment 2)

Lines drawn represent median.

A. IL-17 expression in renal lymphocytes in standard and high salt diet NTN mice. Compared with Mann-Whitney test.

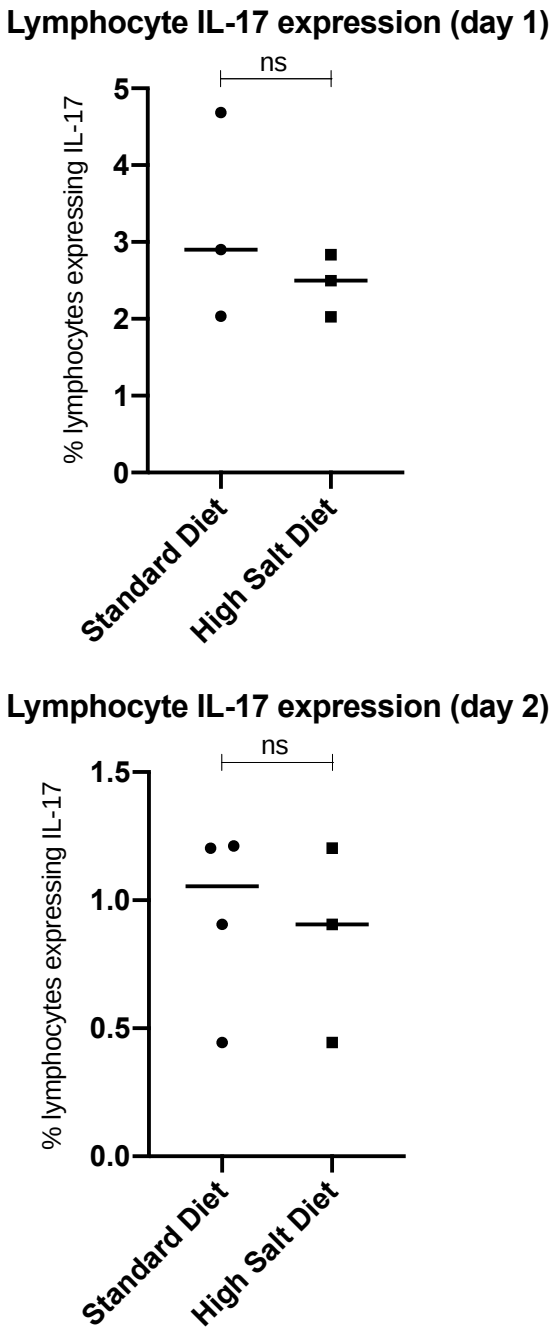

B. Kidney Th17 cells in standard and high salt diet NTN mice. Compared with Mann-Whitney test.

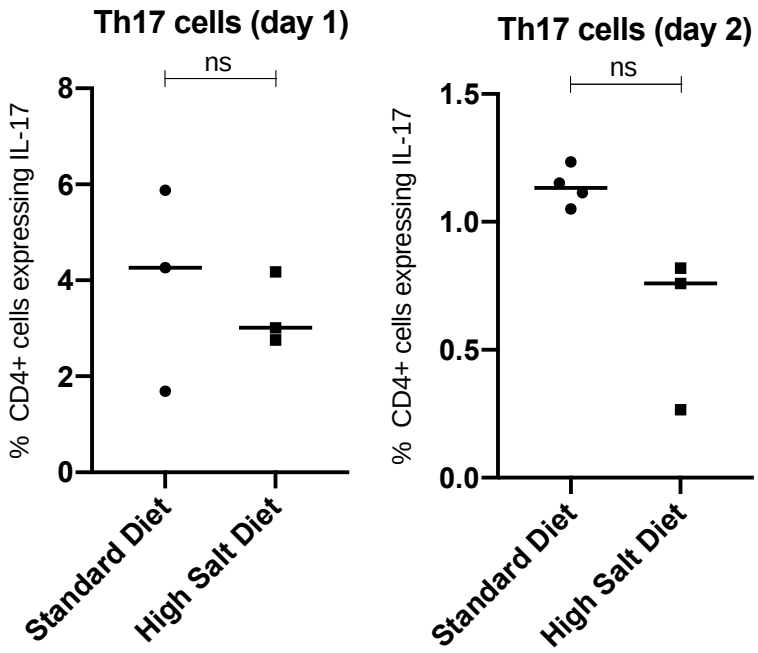

C. Kidney Tc17 cells in standard and high salt diet NTN mice. Compared with Mann-Whitney test.

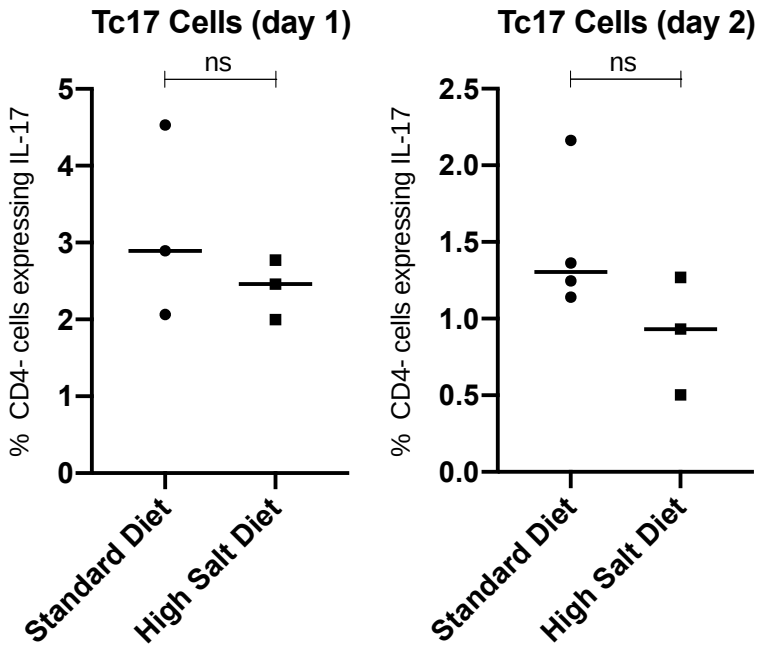

5.4.5 Dietary salt restriction is feasible in healthy controls but does not alter Th17 and Treg cells

A pilot study in healthy controls was undertaken to make an initial assessment of the feasibility of using dietary salt restriction as a therapeutic intervention in immunological disease. In this investigation, 9 volunteers (median age 34 (31.5-41.5) years, 6 (66.7%) female) underwent dietary salt restriction targeting a salt intake of <2.5g/day for one week. Clinical and physiological parameters, an assessment of salt intake, as well as Th17 and Treg cells, were assessed prior to the low salt diet, at the end of the low salt diet, and at 10-14 days thereafter when back on standard diet. The dietary intervention was tolerated by all subjects without side effects.

Salt intake assessment

Salt intake decreased significantly with intervention. Median salt intake questionnaire scores were 91 (69.5-99.1), 0 (0-5), and 60.25 (26.8-91.9) pre-low salt, post-low salt, and after 2 weeks back on standard diet respectively ($p<0.0001$).

Physiological parameters

Parameters at each assessment time point are outlined in **Table 5.5**. Weight reduced after intervention compared baseline and this was reflected in a reduction in total body water on body composition analysis. There was no difference in the proportion of body water that was extracellular, neither were there significant changes in systolic blood pressure, diastolic blood pressure, or pulse.

Table 5.5: Physiological parameters in healthy controls (n=9) undergoing low salt dietary intervention for 1 week

Median (IQR) values reported. Each parameter compared with one-way analysis of variance.

	Pre-low salt	Post-low salt	2 weeks back on normal diet	P-value
Weight (kg)	66.9 (61-82)	65.8 (60.3-80.2)	66.2 (60.3-80.1)	0.0024
Total body water (L)	35.2 (32.8-52.7)	35.2 (32.6-51.4)	36.1 (31.8-51.7)	0.0392
Extracellular water/total body water	0.375 (0.373-0.378)	0.375 (0.368-0.376)	0.374 (0.371-0.379)	0.19
Systolic blood pressure (mmHg)	117 (113-122)	114 (108-117)	115 (109-128)	0.77
Diastolic blood pressure (mmHg)	75 (69-79)	76 (65-79)	77 (70-79)	0.83
Pulse rate (beats per minute)	66 (55-70)	67 (58-81)	66 (62-75)	0.99

T cell subset analysis

There were no differences in Th17, Tc17, or Treg cells across the intervention periods, neither was there a difference in the ratio of Th17:Treg cells (**Figure 5.13**).

Figure 5.13: Analysis of T cell subsets in healthy controls undergoing dietary salt restriction

A. Th17 cells (% of CD4+ cells) pre low salt diet, after intervention, and at 2-4 weeks back on standard diet: Pre 1.8% (1.1-4.3), Post 1.7% (1.3-3.1), 2-4 weeks 1.9% (1.2-2.9), p=0.99. Compared with Friedman test.

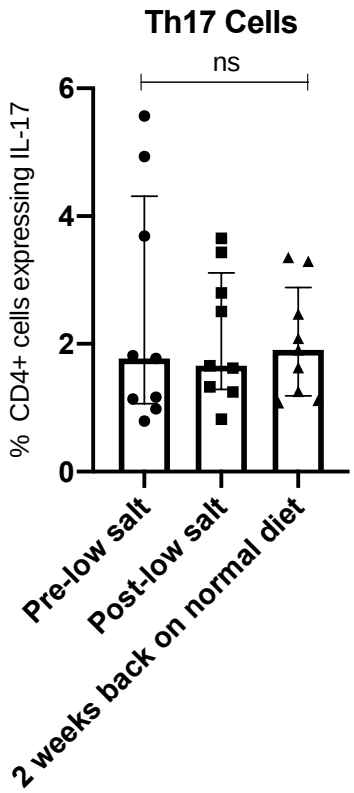

B. Tc17 cells (% of CD4- cells) pre low salt diet, after intervention, and at 2-4 weeks back on standard diet: Pre 0.3% (0.2-0.8), Post 0.4% (0.2-0.5), 2-4 weeks 0.2% (0.1-0.3), p=0.6. Compared with Friedman test.

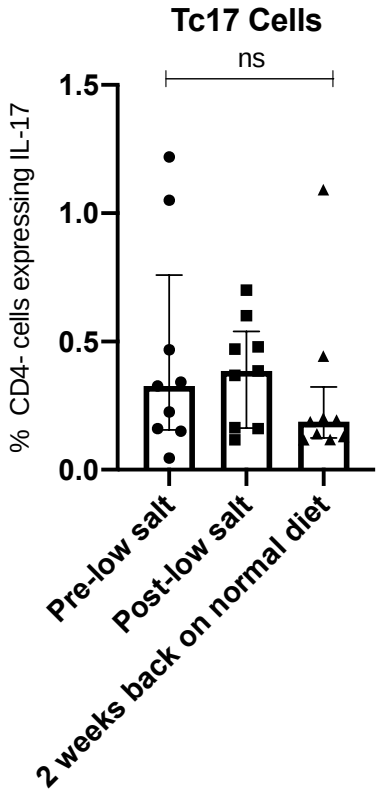

C. Treg cells (% of CD4+ cells) pre low salt diet, after intervention, and at 2-4 weeks back on standard diet: Pre 6.7% (5.9-8.7), Post 6.0% (4.2-7.3), 2-4 weeks 6.2% (5.0-7.0), p=0.97. Compared with Friedman test.

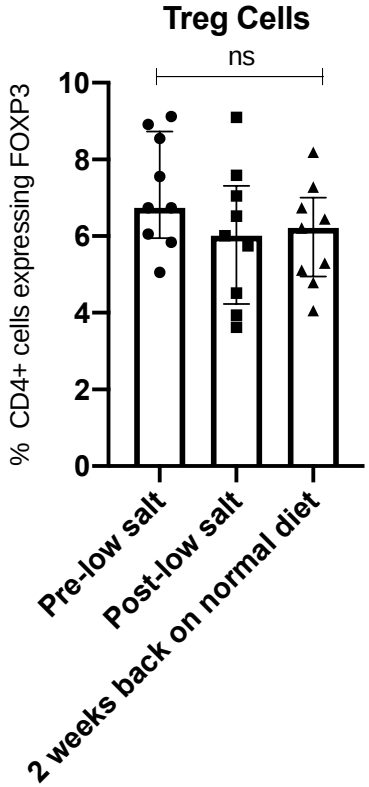

D. Ratio of Th17:Treg cells pre low salt diet, after intervention, and at 2-4 weeks back on standard diet: Pre 0.20 (0.16-0.58), Post 0.41 (0.16-0.57), 2-4 weeks 0.34 (0.19-0.51), p=0.28. Compared with Friedman test.

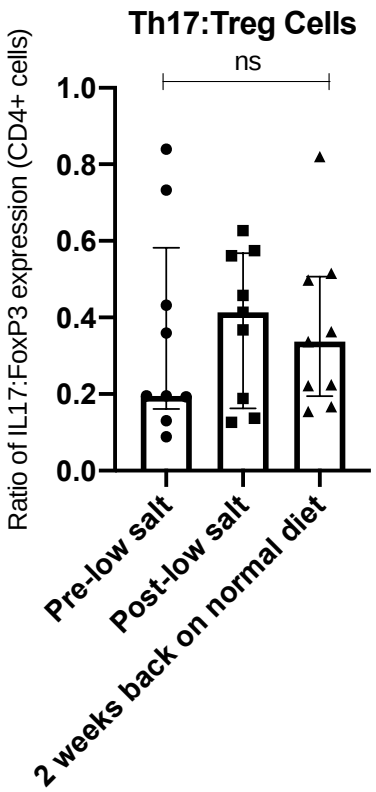

5.4.6 Prospective cohort study of immune responses to sodium minimisation through dietary salt restriction in kidney transplant recipients (KTRs)

A prospective cohort study was undertaken to determine the feasibility, safety and tolerability of a low salt diet intervention in KTRs, and to investigate its effect on immune responsiveness. The study was suspended after recruitment of 7 (out of a target of 10) patients due to the outbreak of Covid-19 in the UK. Reported below are the data on the 7 patients recruited to date.

5.4.6.1 Study Cohort

7 KTRs underwent low salt intervention (aged 48 (36-57) years; 6 (86%) male; (**Table 5.1**). KTRs were median 2815 (476-4920) days post-transplant at the time of enrolment with creatinine 136 (93-174) µmol/l.

Table 5.6: KTR cohort enrolled in pilot study

IgA – immunoglobulin A; ADPKD – autosomal dominant polycystic kidney disease; ANCA – anti neutrophil cytoplasmic antibody; HTN – hypertension; CVA – cerebrovascular accident; DVT – deep vein thrombosis; DM – diabetes mellitus; BCC – basal cell carcinoma; MMF – mycophenolate mofetil; eGFR – estimated Glomerular Filtration Rate

Patient Number	Age	Sex	Renal Diagnosis	Other diagnoses	Medications	Time since transplant (days)	Transplant details	Serum creatinine (µmol/l)	eGFR (ml/min / 1.73m^2)
1	30	M	IgA Nephropathy	HTN	Tacrolimus, minoxidil, ramipril, omacor, MMF, aspirin	1127	Live related	136	55
2	36	M	Reflux Nephropathy		Tacrolimus, ramipril, allopurinol, MMF.	2815	Live related	189	36
3	66	M	ADPKD	HTN, L CVA, DVT, post transplant DM	Tacrolimus, aspirin, MMF, irbesartan.	2835	Cadaveric (non-heart beating donor)	148	42
4	47	F	ANCA Vasculitis	gout, hyperthyroidism	Tacrolimus, MMF 1g/day, bisoprolol, lansoprazole, aspirin, mirtazapine, oestrogen gel	476	Live unrelated	117	45
5	48	M	Reflux Nephropathy	anterior uveitis; recurrent BCC	Irbesartan, azithromycin, tacrolimus, pregabilin, lansoprazole, prednisolone 5mg/day.	4920	Live related	93	79

6	48	M	Alport’s syndrome	HTN	Citalopram, tacrolimus, cholecalciferol, irbesartan, lansoprazole, MMF, prednisolone 5, tamsulosin, atorvastatin, tolterodine	5049	Cadaveric	174	37
7	57	M	Alport’s syndrome	recurrent UTI, osteoporosis	Eplerenone, prednisolone 2, MMF, bisoprolol, alfacalcidol, aspirin, tacrolimus, sodium bicarbonate, cholecalciferol, pravastatin	448	Live unrelated	69	>90

5.4.6.2 Feasibility, safety, and tolerability of intervention

All patients completed the 1-week low salt intervention and no side effects were reported. Responses to the post intervention questionnaire suggested the dietary intervention was feasible and well tolerated (**Table 5.7**).

Table 5.7: Post intervention questionnaire designed to assess tolerability of the low salt diet intervention

The low salt diet was easy to adhere to for 1 week	Strongly disagree	Disagree	Neither agree nor disagree	Agree	Strongly agree
Responses (n; %)	0 (0)	1 (14)	1 (14)	3 (43)	2 (29)
The low salt diet stopped me doing things I wanted to do	Strongly disagree	Disagree	Neither agree nor disagree	Agree	Strongly agree
Responses (n; %)	0 (0)	2 (29)	1 (14)	3 (43)	1 (14)
The low salt diet changed the amount of money I spent on food	Strongly disagree	Disagree	Neither agree nor disagree	Agree	Strongly agree
Responses (n; %)	0 (0)	2 (29)	0 (0)	3 (43)	2 (29)
If agree/strongly agree	Spent more	Spent less			
Responses (n; %)	0 (0)	5 (100)			
I had more energy on the low salt diet than my normal diet	Strongly disagree	Disagree	Neither agree nor disagree	Agree	Strongly agree
Responses (n; %)	0 (0)	0 (0)	5 (71)	2 (29)	0 (0)
I felt less fatigued on the low salt diet than my normal diet	Strongly disagree	Disagree	Neither agree nor disagree	Agree	Strongly agree
Responses (n; %)	0 (0)	0 (0)	5 (71)	2 (29)	0 (0)
I felt happier on the low salt diet than my normal diet	Strongly disagree	Disagree	Neither agree nor disagree	Agree	Strongly agree
Responses (n; %)	0 (0)	0 (0)	5 (71)	2 (29)	0 (0)
I would find it easy to continue a diet of this low salt content in the longer term	Strongly disagree	Disagree	Neither agree nor disagree	Agree	Strongly agree
Responses (n; %)	0 (0)	3 (43)	0 (0)	4 (57)	0 (0)
Having participated in the study, I am more aware of the salt content of different foods	Strongly disagree	Disagree	Neither agree nor disagree	Agree	Strongly agree
Responses (n; %)	0 (0)	0 (0)	1 (14)	3 (43)	3 (43)
After the study, I am likely to reduce the amount of salt in my diet	Strongly disagree	Disagree	Neither agree nor disagree	Agree	Strongly agree
Responses (n; %)	0 (0)	0 (0)	2 (29)	4 (57)	1 (14)

I would be willing to undertake changes in lifestyle if these were beneficial for my transplant outcome	Strongly disagree	Disagree	Neither agree nor disagree	Agree	Strongly agree
Responses (n; %)	0 (0)	0 (0)	0 (0)	2 (29)	5 (71)
I would prefer to undertake changes in lifestyle than take additional medications to improve my transplant outcome	Strongly disagree	Disagree	Neither agree nor disagree	Agree	Strongly agree
Responses (n; %)	0 (0)	0 (0)	1 (14)	1 (14)	5 (71)
Do you have any further comments on participating in the study:	"I suppose the hardest thing was keeping track. So perhaps a handout to help people document their food intake." "I'm grateful to the study for increasing my awareness of my regular salt intake, and for helping make me aware of how easy it is to reduce it. I'm aware that this is in any case beneficial to the kidney because of reduced blood pressure, and I plan to make changes to reduce it from now on."				

There was a trend to a reduction in serum sodium with intervention; there were no significant changes in renal function or other serum biochemical parameters (**Table 5.8**).

Table 5.8: Renal function and serum biochemical parameters at pre and post intervention

Median (IQR) for each variable reported. Compared with Wilcoxon test.

	Pre-low salt	**Post-low salt**	**P-value**
Sodium (mmol/l)	139 (139-141)	136.5 (136-138)	0.0625
Potassium (mmol/l)	4.9 (4.1-5.1)	4.8 (4.4-5.5)	0.19
Bicarbonate (mmol/l)	23 (19-25)	23 (22-24)	0.69
Chloride (mmol/l)	104 (101-105)	101 (100-103)	0.25
Magnesium (mmol/l)	0.78 (0.69-0.79)	0.79 (0.71-0.84)	0.38
Urea (mmol/l)	8.2 (5.0-13.9)	5.9 (5.3-12.0)	0.53
Creatinine (µmol/l)	142 (111-179)	149 (109-181)	0.21

5.4.6.3 Salt intake and physiological parameters

Salt intake, as determined by a validated food questionnaire (Appendix 8.2), reduced significantly during the intervention period (**Figure 5.14**). There were no associated significant changes in systolic or diastolic blood pressure, or weight with intervention (**Figure 5.14**).

Figure 5.14: Changes in salt intake and physiological parameters with low salt diet intervention

A. Salt intake score, as determined by food intake questionnaire, pre and post low salt diet: Pre 90 (42-103), Post 12.5 (6.5-16), median difference -76 (-93, -30), p=0.016. Compared with Wilcoxon test. Red line drawn ad score of 65 which signifies excess salt intake

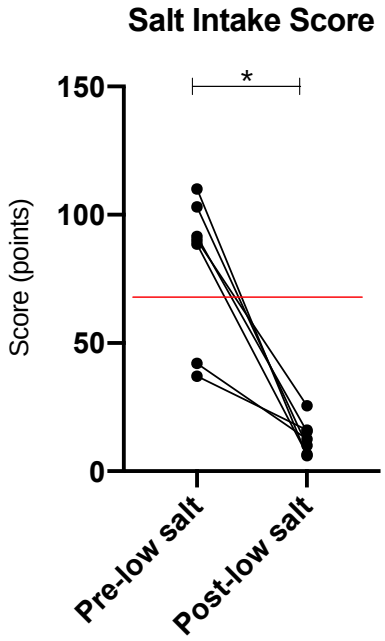

B. Physiological parameters (weight, systolic and diastolic blood pressure) pre and post low salt diet. Compared with Wilcoxon test.

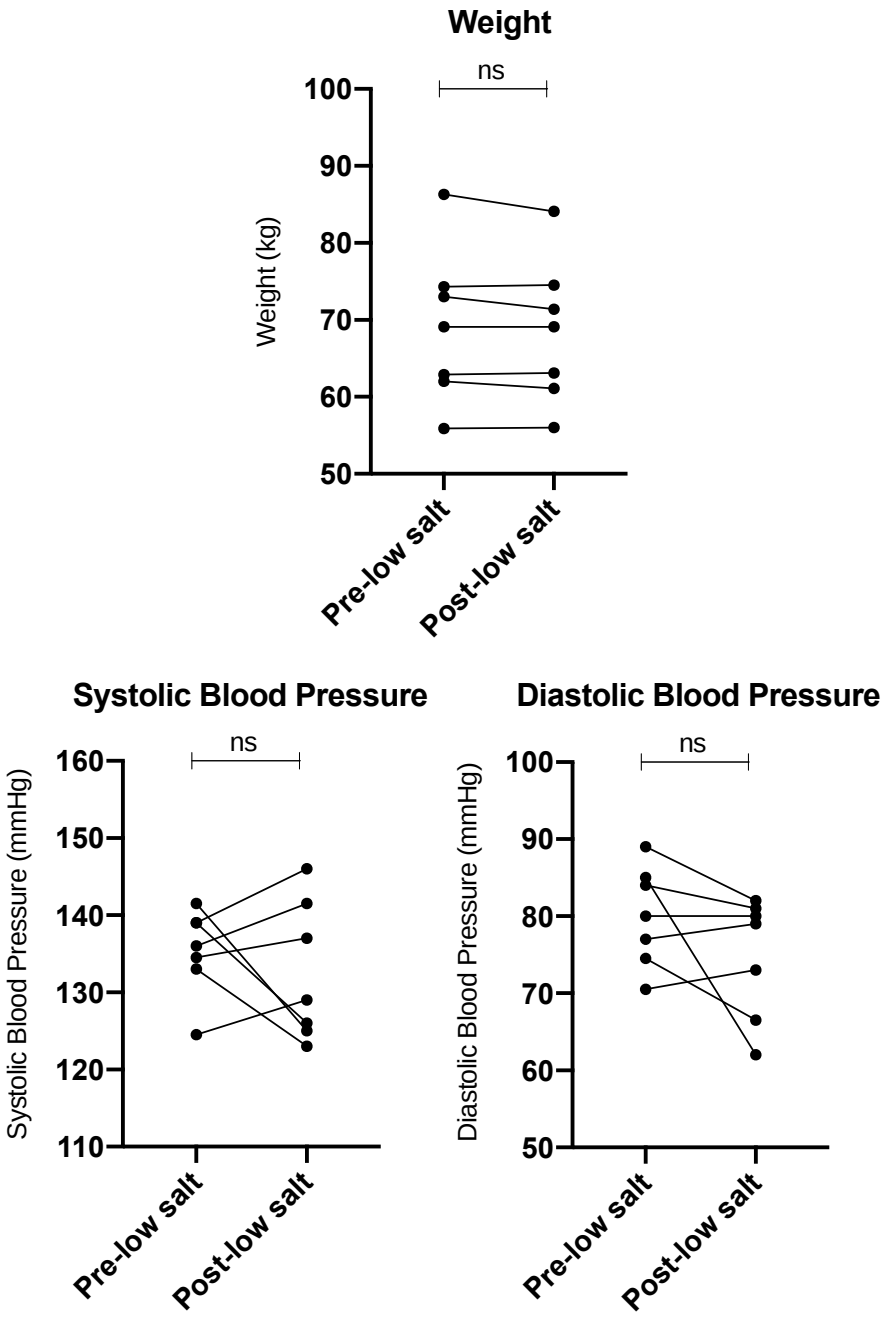

5.4.6.4 Sodium stores as determined by ^{23}Na-MRI

Paired ^{23}Na-MRI scans were undertaken in 5 patients to assess the effect of low salt dietary intervention on sodium stores. There was no difference in muscle sodium stores with intervention; 4 (80%) patients had a reduction in skin sodium storage but this did not reach statistical significance (**Figure 5.15**).

Figure 5.15: Muscle and skin sodium stores quantified by 23Na-MRI pre and post low salt diet in KTRs (n=5)

Mean sodium concentrations in each compartment as quantified over three ^{23}Na-MRI scans for each patient plotted. AU – arbitrary units.

A. Skin sodium concentration pre and post low salt intervention: Pre 18AU (12-22), Post 10AU (8-19), median difference -2.3AU (-9, -0.5), p=0.13. Compared with Wilcoxon test.

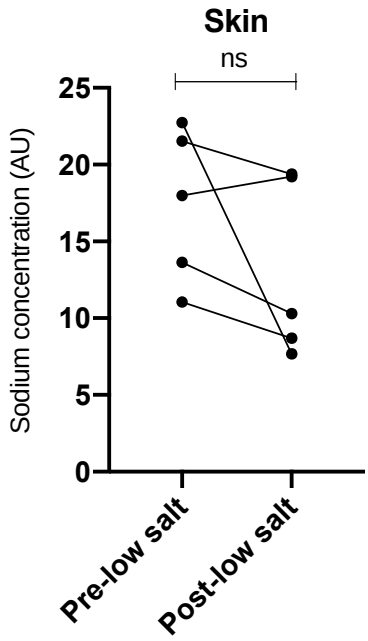

B. Muscle sodium concentration (in 4 different muscle groups) pre and post low salt intervention. Mean sodium concentration as quantified over three ^{23}Na-MRI scans for each patient plotted. Compared with Wilcoxon test.

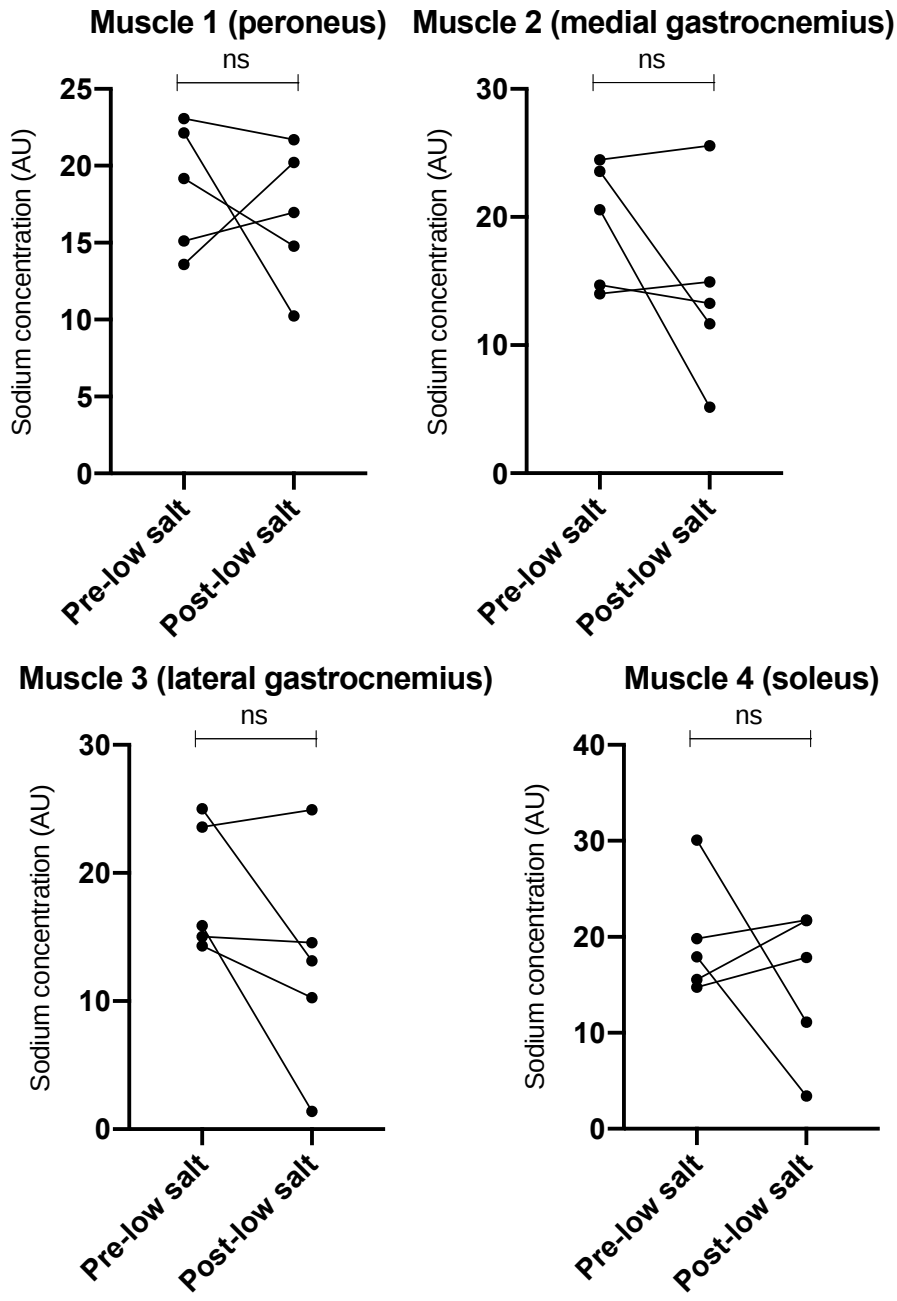

C. Representative ^{23}Na-MRI images of a KTR (patient 6) pre (left panel) and post (right panel) low salt intervention

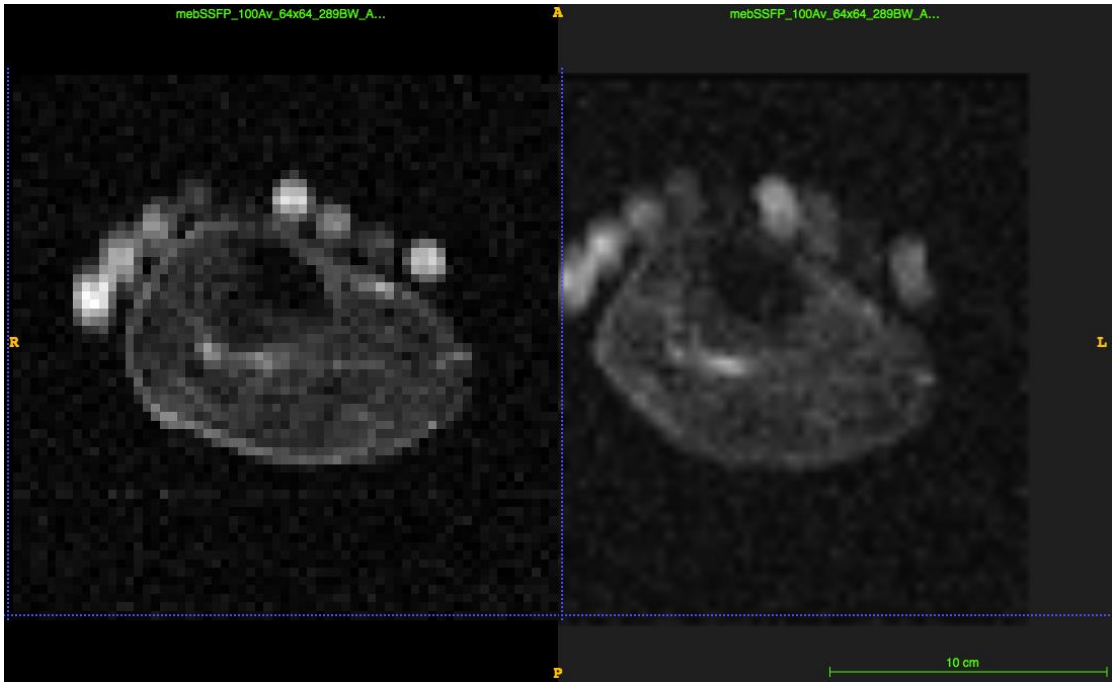

5.4.6.5 Immune responses

i. Leucocyte differential, C-reactive protein and total immunoglobulins

There were no changes in the leucocyte count or differential, C-reactive protein, or total immunoglobulins with intervention (**Table 5.9**).

Table 5.9: Leucocyte count and differential, C-reactive protein, and total immunoglobulins pre and post low salt diet in KTRs (n=7)

Median (IQR) values reported. Compared with Wilcoxon test.

	Pre-low salt	Post-low salt	P-value
White Cell Count ($x10^9$/l)	7.7 (5.6-10.4)	7.0 (5.5-9.9)	0.63
Neutrophil ($x10^9$/l)	5.5 (3.6-7.6)	4.0 (3.6-7.0)	0.44
Lymphocyte ($x10^9$/l)	1.3 (1.2-1.9)	1.6 (1.2-2.1)	0.99
Monocyte ($x10^9$/l)	0.65 (0.47-0.80)	0.67 (0.53-0.79)	0.87
Eosinophil ($x10^9$/l)	0.1 (0.04-0.18)	0.19 (0.04-0.32)	0.25
Basophil ($x10^9$/l)	0.04 (0.02-0.06)	0.04 (0.03-0.06)	0.75
C-Reactive Protein (mg/L)	1.5 (1-2.25)	1.0 (1.0-3.0)	0.99
Immunoglobulin A (g/l)	1.6 (1.15-1.98)	1.60 (1.23-1.98)	0.99
Immunoglobulin	12.5 (8.8-14.1)	12.3 (8.8-14.4)	0.99

G (g/l)			
Immunoglobulin M (g/l)	1.1 (0.5-1.3)	1.1 (0.5-1.3)	0.99

ii. T cell subset analysis

The proportion of CD4+ expressing IFNγ, IL-4, and IL-17 (representing Th1, Th2, and Th17 cells respectively) and CD4- cells expressing the same cytokines (representing Tc1, Tc2, and Tc17 cells) were determined in 4 subjects at each of the 3 assessment time points (T1 – pre low salt intervention; T2 – post low salt intervention; T3 – 2-4 weeks back on standard diet after completion of intervention). There were no significant differences in T cell subtypes with intervention, either when individual cell subtypes were compared (**Figure 5.16**, **Figure 5.17**), or when cells were expressed as a ratio to each other (**Figure 5.18**, **Figure 5.19**).

Figure 5.16: Th1, Th2, and Th17 cells pre low salt (T1), post low salt (T2), and at 2-4 weeks back on standard diet (T3) in KTRs (n=4)

Compared with Friedman test.

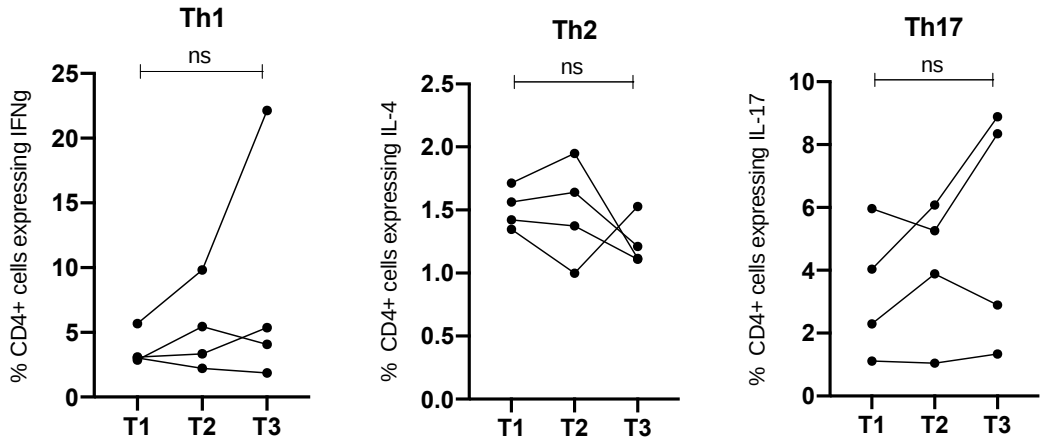

Figure 5.17: Tc1, Tc2, and Tc17 cells pre low salt (T1), post low salt (T2), and at 2-4 weeks back on standard diet (T3) in KTRs (n=4)

Compared with Friedman test.

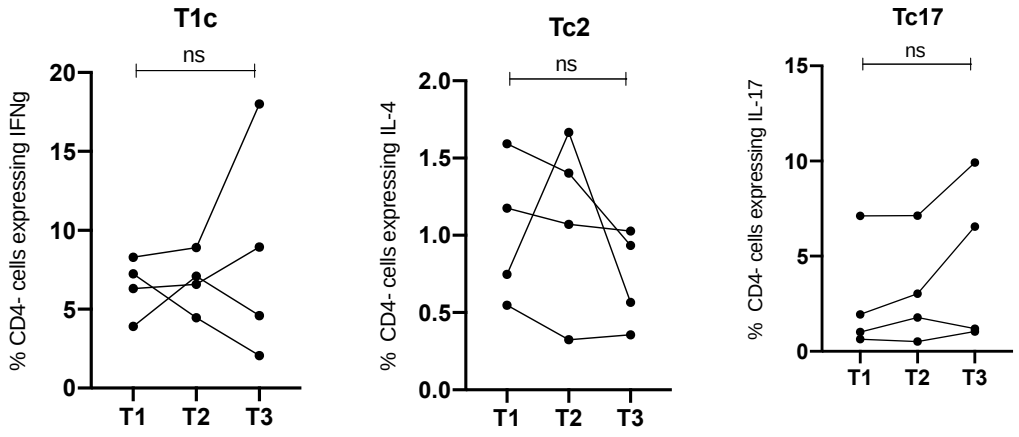

Figure 5.18: Th1, Th2, and Th17 cells (expressed as a ratio to each other) pre low salt (T1), post low salt (T2), and at 2-4 weeks back on standard diet (T3) in KTRs (n=4)

Compared with Friedman test.

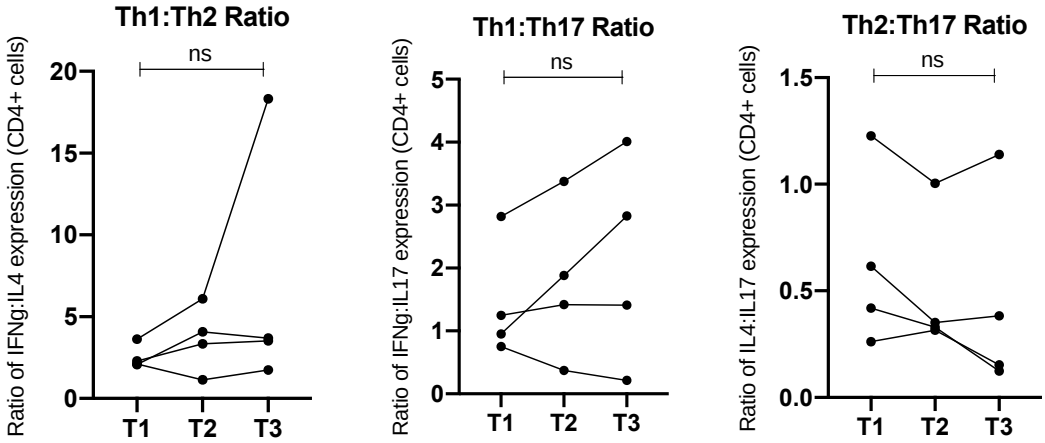

Figure 5.19: Tc1, Tc2, and Tc17 cells (expressed as a ratio to each other) pre low salt (T1), post low salt (T2), and at 2-4 weeks back on standard diet (T3) in KTRs (n=4)

Compared with Friedman test.

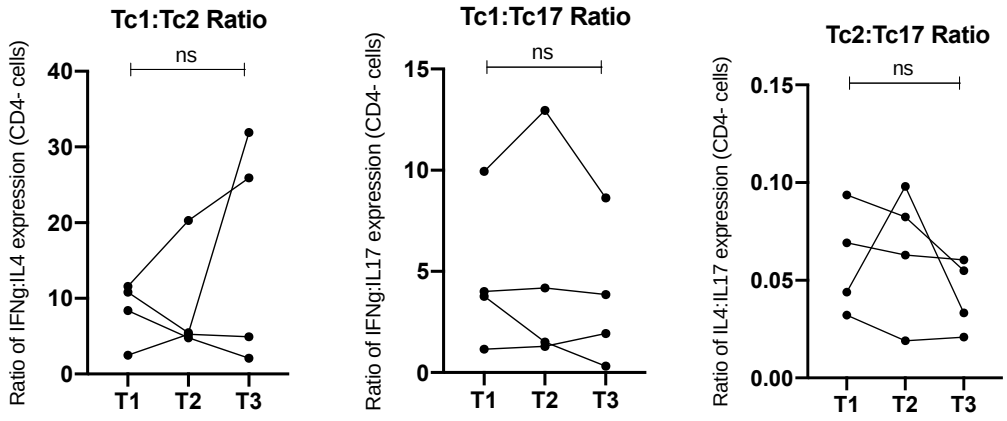

iii. TfH Responses

TfH responses were assessed in 3 KTRs. PBMCs were stimulated for 72 hours with anti-CD3/anti-28 and TfH polarisation and IL-21 expression by TfH cells were determined. The low salt diet intervention had no effect on TfH responses (**Figure 5.20**).

Figure 5.20: TfH polarisation and iL-21 expression by TfH cells pre low salt (T1), post low salt (T2), and at 2-4 weeks back on standard diet (T3) in KTRs (n=3)

Compared with Friedman test.

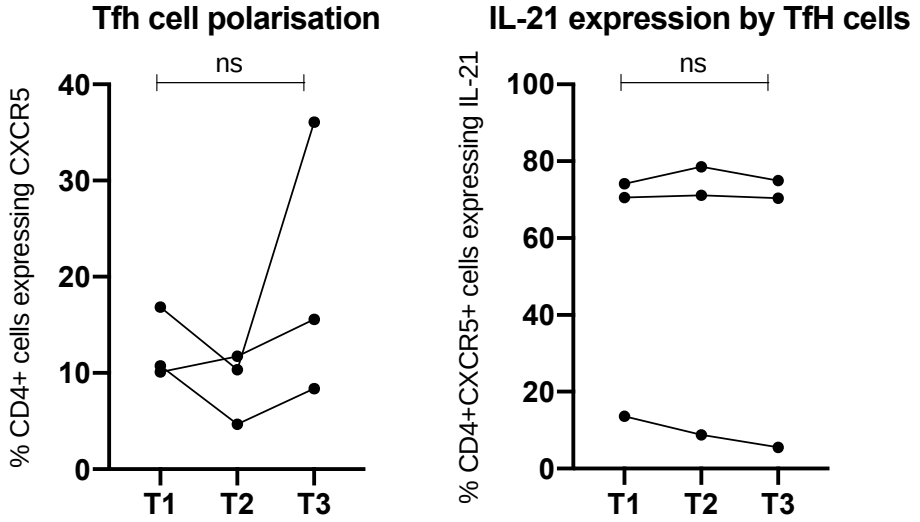

5.5 Discussion

In the final part of this project, I investigated the impact of extracellular sodium on immune responsiveness in the setting of inflammatory kidney disease and kidney transplantation. This was undertaken with a view to the potential use of strategies to alter sodium balance as immunomodulatory therapies in these conditions. Such strategies are required due to the high burden of morbidity associated with current immunosuppression regimens, and their lack of efficacy in preventing chronic immune mediated native and allograft kidney injury.

In initial experiments, the salt responsiveness of Th17 and Tc17 polarisation in AIKD patients and KTRs were determined. Despite the presence of *in vivo* immunosuppression, *in vitro* IL-17 salt responsiveness in patients was no different to healthy controls suggesting that current immunosuppressive regimens do not impact the inflammatory effect of NaCl on T cells. Larger numbers of patients would be required to investigate subgroups of patients on different regimens alongside the use of immunosuppressive drugs *in vitro* to determine if immunosuppressive drugs have differential effects on sodium driven inflammation. Most KTRs however, and some AIKD patients, are managed with calcineurin inhibitor based regimens; intracellular pathways that mediate NaCl induced inflammation include upregulation of NFAT5, SGK1, and p38-MAPK, none of which are calcineurin responsive. Therefore, altering sodium balance is of therapeutic relevance in these cohorts on standard immunosuppressive regimens.

An animal model of crescentic glomerulonephritis was then used to investigate whether altering salt intake impacts the development of inflammatory kidney disease, as has been shown in models of extra-renal autoimmune conditions, such as multiple sclerosis and inflammatory bowel disease (**Table 1.1**). There was no difference in clinical outcomes with changes in salt intake in experiments undertaken. In the initial animal model, there was severe disease even in the standard diet (control) group, and the

development of disease was over a period of only 1 week. This is compared to the models of extra-renal autoimmune disease shown to be salt responsive, which are of longer duration, e.g. experimental autoimmune encephalomyelitis over 3 weeks. A subsequent experiment was therefore undertaken in which a milder and more prolonged disease was induced (to allow for the potential of clinical exacerbation with intervention), and with a longer period of salt loading prior to induction of disease. Despite this change, there was still no increase in disease severity in the high salt group; indeed, some parameters (e.g. serum creatinine) actually improved in high salt fed animals, this may be related to increased fluid intake (reflected by increased urine volume) in the high salt fed animals. The reasons for a lack of a salt effect in these animal models are unclear. There was variability within each group in terms of disease severity and a larger number of animals would have ideally been included in the investigation. Whilst IL-17 responses are important components of NTN pathogenesis, multiple other immune cells contribute and the relative effect of increased on each of these cells and their interaction is unknown. Moreover, the body compartment where the inflammatory effect of salt on immunological disease occurs is an important unknown. If this were to be at the site of the disease (i.e. in the kidney itself) it is unknown whether changes in salt intake translate to changes in renal sodium concentration, and this is something that should be assessed in future work. The degree of salt loading may need to be greater, either by increased duration or with a higher dietary salt content. Moreover, the inflammatory effect of angiotensin II, downregulated by salt loading, on some cell subtypes (e.g. Th17 cells) may have a more prominent role in inflammatory diseases affecting the kidney as opposed to inflammatory diseases at other sites.

I lastly conducted pilot studies in healthy controls and KTRs to assess the feasibility and impact on immune responsiveness of a short-term low salt diet. In both cohorts the low salt intervention was feasible with all subjects successfully completing intervention, with no side effects. There was evidence of adherence to the intervention with significant reductions in salt intake scores; however, there was no significant reduction in skin sodium concentrations in the 5 KTRs that underwent paired ^{23}Na-MRI. Moreover, post

intervention feedback from KTRs suggested that the use of lifestyle measures such as altering salt intake were of greater interest to patients in terms of prolonging graft survival than the use of more medications. This supports the need to further investigate the potential use of salt minimising diets as immunomodulatory management strategies.

In both cohorts, however, there was no detectable effect on immune responses, predominantly assessed by measuring circulating peripheral T cell subsets. As with the animal study, it may have been the intervention was of too short duration, or not undertaken in significant numbers of subjects to detect immunological changes. Variability and insensitivity of the assay may have also contributed. Increasing readouts of immune responsiveness (e.g. 7-day IL-17 responses in optimal polarising conditions) would have ideally been undertaken. Moreover, whilst studies in humans have demonstrated that increasing salt intake promotes inflammatory cell polarisation, the reverse is not necessarily true. The relationship of sodium intake to immune responsiveness may be U- or J-shaped as opposed to linear, and the optimal sodium intake in terms of minimising harmful inflammatory responses may vary across individuals. The degree of salt restriction may have actually been too great in these studies, and the counter balancing effect of increased angiotensin II on immune responses with severe salt restriction was unstudied but potentially contributory. Further work will be focused on increasing the number of subjects undergoing intervention, undertaking intervention in AIKD patients as well as KTRs, widening the assessment of immune responsiveness after intervention, and utilising a diuretic drug over a more prolonged period as an alternative mechanism for reducing sodium balance.

CONCLUSIONS

In vitro IL-17 responses in AIKD patients and KTRs are salt responsive despite the presence *in vivo* immunosuppression. A high salt diet did not worsen the nephrotoxic nephritis model of crescentic glomerulonephritis. Short-term low salt diets are feasible and safe therapeutic strategies in

healthy controls and KTRs, but did not affect circulating Th1, Th2, or Th17 cells.

6 CHAPTER 6: DISCUSSION

6.1 Summary of results and interpretation

This research project, investigating how salt (sodium chloride; NaCl) affects immunity in patients with kidney disease, consisted of 3 main areas. Initial work focused on the effect and mechanism of sodium chloride on *in vitro* IL-17 responses in healthy controls. I then investigated immunity in patients with salt depletion due to inherited SLTs. Finally, the impact of salt and the potential therapeutic relevance of using strategies to alter sodium balance in inflammatory kidney diseases were determined.

In chapter 3, I demonstrated that NaCl promotes IL-17 responses in multiple cells, specifically CD4+ (Th17) and CD8+ (Tc17) T cells. This supports previous work demonstrating NaCl promotes Th17 polarisation[52,53], but highlights that the salt effect extends beyond CD4+ subsets to Tc17 cells, which are implicated in autoimmune disease[143]. The inflammatory effect of was shown to be mediated predominantly by sodium, as opposed to osmolality, and increased extracellular sodium altered the pattern of calcium flux during T cell activation. This signalling of sodium by altered calcium flux supports data on the sodium effect in mouse dendritic cells[49], albeit in my studies of human T cells sodium flattened as opposed to augmented the calcium flux curve. Sodium channels and transporters were shown to be present on multiple immune cells, and epithelial sodium channel (ENaC, amiloride) and sodium-potassium-chloride (NKCC, furosemide) transporter inhibition abrogated salt induced IL-17 responses. This provides data to support the investigation of these commonly used diuretics as immunomodulatory therapies. Immunity in 3 patients from a single family with autosomal recessive pseudohypoaldosteronism type 1 (PHA1; inherited ENaC inactivation) was then assessed. Whilst recurrent pneumonia in PHA1 has been reported and attributed to altered airway sodium transport and mucous[138], our patients had increased upper as well as lower respiratory tract infections, alongside the presence of other infections and multiple allergies

suggesting an underlying immune defect. Patients all had increased B cells and an altered pattern of calcium flux during T cell activation that mirrored the amiloride effect. One patient had associated reduced T cell responsiveness and impaired production of multiple cytokines in response to diverse immune cell stimuli.

In chapter 4, immunity was investigated in patients with inherited SLTs (Bartter, Gitelman, and EAST syndrome). Clinical immunodeficiency was reported in a cohort of 47 patients. SLT patients had increased bacterial and fungal infections, alongside increased allergic disease compared to healthy and disease controls. Autoimmune phenomena were present in 30% of patients and the clinical phenotype mimicked the phenotype of patients with inherited defects in IL-17 immunity[81,85,87,88]. NK cells were reduced in 40% of patients, and one third had increased total IgE. T cell proliferation and activation, and antigen specific antibody responses were unaffected. SLT patients had an increased ratio of circulating Th2:Th17 cells, and impaired IL-17 responses during 7-day culture of PBMCs under optimal Th17 polarising conditions. The cause of impaired IL-17 immunity was then assessed. Phosphorylation of STAT3 and STAT1 were normal. However, the extracellular ionic environment typical in SLT (reduced sodium, potassium, and magnesium) was shown to be inhibitory to IL-17 responses. Reduced sodium stores in SLT patients were proven with ^{23}Na-MRI imaging. The pathway of sodium induced Th17 polarisation was intact in SLT patients and their IL-17 responses *in vitro* could be rescued with the addition of salt to culture conditions. This work demonstrates that salt depletion (as opposed to salt loading) has immunological and clinical consequences, which has not been demonstrated before. Moreover, previously unexplained clinical features (e.g. febrile episodes and autoimmunity) in SLT were explained.

In chapter 5, I demonstrated that patients with native AIKD and KTRs have salt responsive IL-17 responses despite the presence of *in vivo* immunosuppression. This supports attempts to reduce sodium balance to improve immune mediated outcomes in inflammatory kidney diseases. The effect of altering salt intake on the development of the nephrotoxic nephritis

model of crescentic glomerulonephritis was then assessed. Increased salt intake did not affect the development or severity of disease in 2 different variations of this model. Lastly, I investigated the feasibility of dietary salt minimisation as a potential immunomodulatory therapy in inflammatory kidney disease. In healthy controls and KTRs, short-term salt restriction was safe and feasible. However, in this relatively small cohort, no effect on immune responses was demonstrated.

6.2 Limitations and future work

In vitro work, both in terms of investigating the signalling of sodium in healthy control cells and assessing changes in patients with ion channel and transporter defects, would have been greatly enhanced by an ability to measure lymphocyte sodium flux. This was tried unsuccessfully with the use of a non-ratiometric sodium dye. Whilst using radiolabelled sodium was considered during the project, sodium movement would be best measured via patch clamping immune cells. This is a feasible but technically challenging procedure that would require a significant period of training and was beyond the scope of this project[169]. The ability to patch clamp lymphocytes would allow measurement of multiple ion fluxes during immune cell responses and be an invaluable tool in a number of potential future research projects.

The investigation of PHA1 patients was challenging due to the rare nature of the condition. The evaluation of the members of the family described in this project was incomplete. All members would have ideally undergone a broader analysis of innate and adaptive immune cell responses both through FACS immunophenotyping and stimulation assays. Recruitment of further PHA1 patients to see if any immunological findings are generalisable would likely require a national or international collaboration, and should be supplemented with further *in vitro* (e.g. ENaC known down cells) and *in vivo* (e.g. lymphocyte specific ENaC knock out animals) studies of the role of ENaC in activating adaptive immune cells.

The investigation of SLT patients concentrated on IL-17 responses as this was the focus of this project and as the clinical phenotype uncovered in SLT patients was consistent with an IL-17 defect. Whilst multiple components of immunity were assessed in SLTs, sodium has been shown to affect diverse immune cells (outlined in 1.3) and hence a broader immunological assessment should be undertaken. This may include an assessment of neutrophil function (aside from any reduction that may be associated with reduced IL-17 responses), and other CD4+ T cell subsets influenced by sodium such as Tregs and TfH cells. Moreover, the effect of aldosterone and angiotensin II was assessed on *in vitro* IL-17 responses in healthy controls, but the impact of alterations in the renin angiotensin system (which are profound in SLT patients) on immunity more generally was not.

I propose that IL-17 responses are dampened in SLT due to their unique extracellular environment. This could be supported by data from animal models of salt wasting and undertaking an unbiased approach to analyse the transcriptome of SLT patients (e.g. RNA-seq) to explore possible dysregulation of cell membrane transporters in T cells or their associated signaling pathways. We hope to investigate immunity in heterozygotes for SCL12A3, which is estimated to be prevalent in 1% of the general population[170], through immunophenotyping of subjects from the UK biobank. I also aim to investigate whether electrolyte replacement in SLT can mitigate immunological risk by adding an immunological arm to an already planned European study of salt replacement in GS. It would also be interesting to investigate immunity in patients with other causes of inherited or acquired salt wasting, such as patients with inactivating SGLT2 mutations or those on SGLT2 inhibiting drugs (who's mechanism of benefit in diabetes and cardiovascular disease is unclear), other diuretic drugs, and patients with gastrointestinal salt loss such as high output stomas.

The relevance of salt induced inflammation on immune mediated kidney diseases was investigated in the last section of the project. Whilst patients with inflammatory kidney disease had salt responsive IL-17 responses, altering salt intake in the nephrotoxic nephritis (NTN) model of crescentic

glomerulonephritis had no effect on clinical or immunological outcomes. The development of disease in this model was variable, even in the control group, and future experiments should use increased numbers of animals or consider the use of a more consistent model of disease (e.g. intraperitoneal as opposed to intravenous injection of nephrotoxic serum to induce disease is undertaken by some groups). Whilst IL-17 responses contribute to the pathogenesis of NTN, the effect of salt on other relevant immune responses (e.g. macrophage) was untested and how they may interact with IL-17 responses during salt loading in this model is unknown. Changes in RAAS components and how these may affect immunity were not determined. Moreover, whether salt loading led to alterations in renal sodium concentrations, or altered sodium concentrations at other sites was not measured. This could be done in live mice with the use of ^{23}Na-MRI or after sacrifice by measurement of sodium in dry-ashed tissue samples with flame photometry. This may provide important information on the location where sodium exerts its immunological effect, which is currently unknown.

Pilot studies were lastly undertaken in healthy controls and KTRs to assess the feasibility of low salt dietary intervention and its effect on sodium stores and immune responses. A key limitation was the small number of patients recruited to date and I plan to increase patient enrollment in future work. Moreover, I plan to broaden the assessment of immunity to include 7-day IL-17 responses. Thereafter, I have ethical approval to include patients with native AIKD and to reduce sodium balance with the use of a diuretic (furosemide) as opposed to with dietary modifications, which may have a direct effect on T cells as shown in the *in vitro* studies described above. It may be that the duration of intervention is too short to see an immunological effect albeit that salt loading over a week results in altered immune responses. Further development of the quality and reliability of our ^{23}Na-MRI images will help correlation of changes in sodium to immunity. A longer study of reducing sodium balance focusing on clinical as well as immunological outcomes in patients with inflammatory kidney diseases is the ultimate goal.

Finally, two major overarching questions remain unanswered from my and other research investigating sodium and immunity: 1. Why have our immune systems evolved to respond to changes in extracellular sodium? 2. Where in the body does sodium exert its pro-inflammatory effect? As alluded to above, it may be possible to answer the latter of these questions through improvements in ^{23}Na-MRI imaging to determine compartmental changes in sodium concentrations and correlating changes with altered immunity, and supporting this with direct measurement of sodium in mice. The immunological sodium effect is unlikely to occur within the blood due to tight regulation of sodium concentrations at this location, and I would hypothesise that its effect occurs either within the lymphatic system and/or in target organs (e.g. kidney, skin, cerebrospinal fluid) where sodium concentrations are known to increase to supra-serum levels. Why our immune systems respond to sodium is unknown. Increased sodium concentrations are created at body/environment interfaces (e.g. skin, kidney) and augmented immunity at these locations may provide an advantage. Moreover, infection is associated with localised hyper-salinity[45], which may allow for local activation of the immune system without the harmful effects of an exaggerated systemic inflammatory responses. What is becoming increasingly clear, however, it is that immunity and sodium balance are inextricably linked[171]. Our greatest threat from infection is circulatory collapse and therefore having a system whereby inflammation promotes sodium retention and vice versa may provide the combined survival advantage of maintaining circulating volume and augmenting clearance of an underlying pathogen. This would have been of particular importance when salt intake was limited. However, in an era of salt excess, the price we may now be paying for the development of this positive feedback loop is an epidemic of hypertension, cardiovascular and inflammatory disease.

6.3 Summary of planned and potential future work

i. Development of techniques to measure lymphocyte sodium (and other ion) flux

ii. Broader immunological assessment of PHA1 patients and further investigation of the role of ENaC in adaptive immune responses
iii. Investigation of immunity in heterozygotes for SLC12A3
iv. Study of the immunological effect of Na, K, and Mg replacement in SLT patients
v. Investigation of immunity in patients with other causes of inherited and acquired salt depletion (e.g. SGLT2 mutation/inhibitors)
vi. Further investigation of the effect of altering sodium balance on a more consistent animal model of inflammatory kidney disease with an assessment of broader immune responses and measurement of changes in departmental sodium stores.
vii. Improved quality and reliability of ^{23}Na-MRI imaging
viii. Complete pilot study of dietary salt restriction in KTRs and native AIKD patients with increased assessment of immune responsiveness and the use of a diuretic as well as salt restriction to reduce sodium balance

6.4 Concluding remarks

The salt content of a typical western diet far exceeds the amount with which we evolved. Salt conserving mechanisms, which once provided an evolutionary advantage in terms of maintaining intravascular volume, are now overwhelmed and salt loading with age leads to non-osmotic interstitial sodium storage, hypertension and cardiovascular disease. The work in this thesis adds to the recent evidence that demonstrates sodium also effects immunity, and that alterations in sodium balance lead to immunological disease. I demonstrate how sodium promotes inflammatory immune responses in multiple cells, that defects in sodium transport mechanisms and chronic salt wasting are associated with clinical immunodeficiency, and that altering sodium balance is a feasible therapeutic strategy in inflammatory kidney disease. In doing so, I highlight the close interaction between immunological and physiological processes. I aim to pursue this concept to further understand how physiological defects lead to immunological disease and how immunological interventions may be used to treat to physiological disease, and vice versa. This may provide new treatments and improve

outcomes in diverse conditions including kidney diseases, hypertension, cardiovascular disease, autoimmunity, and cancer.

7 REFERENCES

1. Pickering, T. G. The history and politics of salt. *J. Clin. Hypertens. Greenwich Conn* **4**, 226–228 (2002).
2. Roberts, W. C. Facts and ideas from anywhere. *Proc. Bayl. Univ. Med. Cent.* **14**, 314–322 (2001).
3. Batuman, V. Salt and hypertension: why is there still a debate? *Kidney Int. Suppl.* **3**, 316–320 (2013).
4. Powles, J. *et al.* Global, regional and national sodium intakes in 1990 and 2010: a systematic analysis of 24 h urinary sodium excretion and dietary surveys worldwide. *BMJ Open* **3**, e003733 (2013).
5. He, F. J. & MacGregor, G. A. Reducing population salt intake worldwide: from evidence to implementation. *Prog. Cardiovasc. Dis.* **52**, 363–382 (2010).
6. McCallum, L., Lip, S. & Padmanabhan, S. The hidden hand of chloride in hypertension. *Pflugers Arch.* **467**, 595–603 (2015).
7. Intersalt: an international study of electrolyte excretion and blood pressure. Results for 24 hour urinary sodium and potassium excretion. Intersalt Cooperative Research Group. *BMJ* **297**, 319–328 (1988).
8. Sacks, F. M. *et al.* Effects on blood pressure of reduced dietary sodium and the Dietary Approaches to Stop Hypertension (DASH) diet. DASH-Sodium Collaborative Research Group. *N. Engl. J. Med.* **344**, 3–10 (2001).
9. Carvalho, J. J. *et al.* Blood pressure in four remote populations in the INTERSALT Study. *Hypertens. Dallas Tex 1979* **14**, 238–246 (1989).
10. Graudal, N. A., Hubeck-Graudal, T. & Jurgens, G. Effects of low sodium diet versus high sodium diet on blood pressure, renin, aldosterone,

catecholamines, cholesterol, and triglyceride. *Cochrane Database Syst. Rev.* **4**, CD004022 (2017).

11. He, F. J., Li, J. & Macgregor, G. A. Effect of longer term modest salt reduction on blood pressure: Cochrane systematic review and meta-analysis of randomised trials. *BMJ* **346**, f1325 (2013).
12. Cook, N. R. *et al.* Long term effects of dietary sodium reduction on cardiovascular disease outcomes: observational follow-up of the trials of hypertension prevention (TOHP). *BMJ* **334**, 885–888 (2007).
13. Whelton, P. K. *et al.* Sodium, blood pressure, and cardiovascular disease: further evidence supporting the American Heart Association sodium reduction recommendations. *Circulation* **126**, 2880–2889 (2012).
14. Smyth, A. *et al.* Sodium intake and renal outcomes: a systematic review. *Am. J. Hypertens.* **27**, 1277–1284 (2014).
15. Organization, W. H. *Guideline: sodium intake for adults and children*. (World Health Organization, 2012).
16. Stevens, P. E., Levin, A. & Kidney Disease: Improving Global Outcomes Chronic Kidney Disease Guideline Development Work Group Members. Evaluation and management of chronic kidney disease: synopsis of the kidney disease: improving global outcomes 2012 clinical practice guideline. *Ann. Intern. Med.* **158**, 825–830 (2013).
17. O'Donnell, M. J. *et al.* Urinary sodium and potassium excretion and risk of cardiovascular events. *JAMA* **306**, 2229–2238 (2011).
18. Mente, A. *et al.* Urinary sodium excretion, blood pressure, cardiovascular disease, and mortality: a community-level prospective epidemiological cohort study. *Lancet Lond. Engl.* **392**, 496–506 (2018).

19. Aburto, N. J. *et al.* Effect of lower sodium intake on health: systematic review and meta-analyses. *BMJ* **346**, f1326 (2013).

20. Kawasaki, T., Itoh, K., Uezono, K. & Sasaki, H. A simple method for estimating 24 h urinary sodium and potassium excretion from second morning voiding urine specimen in adults. *Clin. Exp. Pharmacol. Physiol.* **20**, 7–14 (1993).

21. Joossens, J. V. *et al.* Dietary salt, nitrate and stomach cancer mortality in 24 countries. European Cancer Prevention (ECP) and the INTERSALT Cooperative Research Group. *Int. J. Epidemiol.* **25**, 494–504 (1996).

22. Lanaspa, M. A. *et al.* High salt intake causes leptin resistance and obesity in mice by stimulating endogenous fructose production and metabolism. *Proc. Natl. Acad. Sci. U. S. A.* **115**, 3138–3143 (2018).

23. Sundström, B., Johansson, I. & Rantapää-Dahlqvist, S. Interaction between dietary sodium and smoking increases the risk for rheumatoid arthritis: results from a nested case-control study. *Rheumatol. Oxf. Engl.* **54**, 487–493 (2015).

24. Farez, M. F., Fiol, M. P., Gaitán, M. I., Quintana, F. J. & Correale, J. Sodium intake is associated with increased disease activity in multiple sclerosis. *J. Neurol. Neurosurg. Psychiatry* **86**, 26–31 (2015).

25. Adwaney, A., Randall, D. W., Blunden, M. J., Prowle, J. R. & Kirwan, C. J. Perioperative Plasma-Lyte use reduces the incidence of renal replacement therapy and hyperkalaemia following renal transplantation when compared with 0.9% saline: a retrospective cohort study. *Clin. Kidney J.* doi:10.1093/ckj/sfx040.

26. Osté, M. C. J. *et al.* Dietary Approach to Stop Hypertension (DASH) diet and risk of renal function decline and all-cause mortality in renal transplant recipients. *Am. J. Transplant. Off. J. Am. Soc. Transplant. Am. Soc. Transpl. Surg.* (2018) doi:10.1111/ajt.14707.

27. Jula, A. M. & Karanko, H. M. Effects on left ventricular hypertrophy of long-term nonpharmacological treatment with sodium restriction in mild-to-moderate essential hypertension. *Circulation* **89**, 1023–1031 (1994).

28. Cappuccio, F. P., Kalaitzidis, R., Duneclift, S. & Eastwood, J. B. Unravelling the links between calcium excretion, salt intake, hypertension, kidney stones and bone metabolism. *J. Nephrol.* **13**, 169–177 (2000).

29. Guyton, A. C., Coleman, T. G., Young, D. B., Lohmeier, T. E. & DeClue, J. W. Salt balance and long-term blood pressure control. *Annu. Rev. Med.* **31**, 15–27 (1980).

30. Walser, M. Phenomenological analysis of renal regulation of sodium and potassium balance. *Kidney Int.* **27**, 837–841 (1985).

31. Titze, J. Sodium balance is not just a renal affair. *Curr. Opin. Nephrol. Hypertens.* **23**, 101–105 (2014).

32. Titze, J. *et al.* Long-term sodium balance in humans in a terrestrial space station simulation study. *Am. J. Kidney Dis. Off. J. Natl. Kidney Found.* **40**, 508–516 (2002).

33. Rakova, N. *et al.* Long-term space flight simulation reveals infradian rhythmicity in human Na(+) balance. *Cell Metab.* **17**, 125–131 (2013).

34. Titze, J. *et al.* Glycosaminoglycan polymerization may enable osmotically inactive Na+ storage in the skin. *Am. J. Physiol. Heart Circ. Physiol.* **287**, H203-208 (2004).

35. Machnik, A. *et al.* Macrophages regulate salt-dependent volume and blood pressure by a vascular endothelial growth factor-C-dependent buffering mechanism. *Nat. Med.* **15**, 545–552 (2009).

36. Kopp, C. *et al.* (23)Na magnetic resonance imaging of tissue sodium. *Hypertens. Dallas Tex 1979* **59**, 167–172 (2012).

37. Kopp, C. *et al.* 23Na magnetic resonance imaging-determined tissue sodium in healthy subjects and hypertensive patients. *Hypertens. Dallas Tex 1979* **61**, 635–640 (2013).

38. Go, W. Y., Liu, X., Roti, M. A., Liu, F. & Ho, S. N. NFAT5/TonEBP mutant mice define osmotic stress as a critical feature of the lymphoid microenvironment. *Proc. Natl. Acad. Sci. U. S. A.* **101**, 10673–10678 (2004).

39. Hammon, M. *et al.* 23Na Magnetic Resonance Imaging of the Lower Leg of Acute Heart Failure Patients during Diuretic Treatment. *PloS One* **10**, e0141336 (2015).

40. Kopp, C. *et al.* Elevated tissue sodium deposition in patients with type 2 diabetes on hemodialysis detected by 23Na magnetic resonance imaging. *Kidney Int.* **93**, 1191–1197 (2018).

41. Dahlmann, A. *et al.* Magnetic resonance-determined sodium removal from tissue stores in hemodialysis patients. *Kidney Int.* **87**, 434–441 (2015).

42. Titze, J. *et al.* Spooky sodium balance. *Kidney Int.* **85**, 759–767 (2014).

43. Titze, J. *et al.* Balancing wobbles in the body sodium. *Nephrol. Dial. Transplant. Off. Publ. Eur. Dial. Transpl. Assoc. - Eur. Ren. Assoc.* **31**, 1078–1081 (2016).

44. Luft, F. C., Fineberg, N. S. & Sloan, R. S. Estimating dietary sodium intake in individuals receiving a randomly fluctuating intake. *Hypertens. Dallas Tex 1979* **4**, 805–808 (1982).

45. Jantsch, J. *et al.* Cutaneous Na+ storage strengthens the antimicrobial barrier function of the skin and boosts macrophage-driven host defense. *Cell Metab.* **21**, 493–501 (2015).

46. Binger, K. J. *et al.* High salt reduces the activation of IL-4- and IL-13-stimulated macrophages. *J. Clin. Invest.* (2015) doi:10.1172/JCI80919.

47. Zhou, X. *et al.* Variation in dietary salt intake induces coordinated dynamics of monocyte subsets and monocyte-platelet aggregates in humans: implications in end organ inflammation. *PloS One* **8**, e60332 (2013).

48. Berry, M. R. *et al.* Renal Sodium Gradient Orchestrates a Dynamic Antibacterial Defense Zone. *Cell* **170**, 860-874.e19 (2017).

49. Barbaro, N. R. *et al.* Dendritic Cell Amiloride-Sensitive Channels Mediate Sodium-Induced Inflammation and Hypertension. *Cell Rep.* **21**, 1009–1020 (2017).

50. Ferguson, J. F. *et al.* High dietary salt-induced dendritic cell activation underlies microbial dysbiosis-associated hypertension. *JCI Insight* **5**, (2019).

51. Aguiar, S. L. F. *et al.* High-Salt Diet Induces IL-17-Dependent Gut Inflammation and Exacerbates Colitis in Mice. *Front. Immunol.* **8**, 1969 (2017).

52. Kleinewietfeld, M. *et al.* Sodium chloride drives autoimmune disease by the induction of pathogenic TH17 cells. *Nature* **496**, 518–522 (2013).

53. Wu, C. *et al.* Induction of pathogenic TH17 cells by inducible salt-sensing kinase SGK1. *Nature* **496**, 513–517 (2013).

54. Yang, X. *et al.* Exacerbation of lupus nephritis by high sodium chloride related to activation of SGK1 pathway. *Int. Immunopharmacol.* **29**, 568–573 (2015).

55. Mehrotra, P., Patel, J. B., Ivancic, C. M., Collett, J. A. & Basile, D. P. Th-17 cell activation in response to high salt following acute kidney injury is associated with progressive fibrosis and attenuated by AT-1R antagonism. *Kidney Int.* **88**, 776–784 (2015).

56. Wei, Y. *et al.* High salt diet stimulates gut Th17 response and exacerbates TNBS-induced colitis in mice. *Oncotarget* **8**, 70–82 (2017).

57. Hernandez, A. L. *et al.* Sodium chloride inhibits the suppressive function of FOXP3+ regulatory T cells. *J. Clin. Invest.* **125**, 4212–4222 (2015).

58. Safa, K. *et al.* Salt Accelerates Allograft Rejection through Serum- and Glucocorticoid-Regulated Kinase-1–Dependent Inhibition of Regulatory T Cells. *J. Am. Soc. Nephrol.* ASN.2014090914 (2015) doi:10.1681/ASN.2014090914.

59. Matthias, J. *et al.* Sodium chloride is an ionic checkpoint for human TH2 cells and shapes the atopic skin microenvironment. *Sci. Transl. Med.* **11**, (2019).

60. Wu, H. *et al.* High salt promotes autoimmunity by TET2-induced DNA demethylation and driving the differentiation of Tfh cells. *Sci. Rep.* **6**, (2016).

61. Cvetkovic, L., Perisic, S., Titze, J., Jäck, H.-M. & Schuh, W. The Impact of Hyperosmolality on Activation and Differentiation of B Lymphoid Cells. *Front. Immunol.* **10**, 828 (2019).

62. Wenzel, U. O., Bode, M., Kurts, C. & Ehmke, H. Salt, inflammation, IL-17 and hypertension. *Br. J. Pharmacol.* (2018) doi:10.1111/bph.14359.

63. Nikpey, E. *et al.* High-Salt Diet Causes Osmotic Gradients and Hyperosmolality in Skin Without Affecting Interstitial Fluid and Lymph. *Hypertension* HYPERTENSIONAHA.116.08539 (2017) doi:10.1161/HYPERTENSIONAHA.116.08539.

64. Szabó, G. & Magyar, Z. Electrolyte concentrations in subcutaneous tissue fluid and lymph. *Lymphology* **15**, 174–177 (1982).

65. Sica, A. & Mantovani, A. Macrophage plasticity and polarization: in vivo veritas. *J. Clin. Invest.* **122**, 787–795 (2012).

66. Jiang, H.-R. *et al.* IL-33 attenuates EAE by suppressing IL-17 and IFN-γ production and inducing alternatively activated macrophages. *Eur. J. Immunol.* **42**, 1804–1814 (2012).

67. Parsa, R. *et al.* Adoptive transfer of immunomodulatory M2 macrophages prevents type 1 diabetes in NOD mice. *Diabetes* **61**, 2881–2892 (2012).

68. Masopust, D. & Soerens, A. G. Tissue-Resident T Cells and Other Resident Leukocytes. *Annu. Rev. Immunol.* **37**, 521–546 (2019).

69. Gaffen, S. L., Jain, R., Garg, A. V. & Cua, D. J. The IL-23-IL-17 immune axis: from mechanisms to therapeutic testing. *Nat. Rev. Immunol.* **14**, 585–600 (2014).

70. McGeachy, M. J., Cua, D. J. & Gaffen, S. L. The IL-17 Family of Cytokines in Health and Disease. *Immunity* **50**, 892–906 (2019).

71. Kleinewietfeld, M. & Hafler, D. A. The plasticity of human Treg and Th17 cells and its role in autoimmunity. *Semin. Immunol.* **25**, 305–312 (2013).

72. Verbsky, J. W. & Chatila, T. A. Immune dysregulation, polyendocrinopathy, enteropathy, X-linked (IPEX) and IPEX-related disorders: an evolving web of heritable autoimmune diseases. *Curr. Opin. Pediatr.* **25**, 708–714 (2013).

73. Hirota, K. *et al.* Fate mapping of IL-17-producing T cells in inflammatory responses. *Nat. Immunol.* **12**, 255–263 (2011).

74. Gagliani, N. *et al.* Th17 cells transdifferentiate into regulatory T cells during resolution of inflammation. *Nature* **523**, 221–225 (2015).

75. Voo, K. S. *et al.* Identification of IL-17-producing FOXP3+ regulatory T cells in humans. *Proc. Natl. Acad. Sci. U. S. A.* **106**, 4793–4798 (2009).

76. Kleinewietfeld, M. & Hafler, D. A. Regulatory T cells in autoimmune neuroinflammation. *Immunol. Rev.* **259**, 231–244 (2014).

77. Krebs, C. F. *et al.* Plasticity of Th17 Cells in Autoimmune Kidney Diseases. *J. Immunol. Baltim. Md 1950* **197**, 449–457 (2016).

78. Wu, C. *et al.* SGK1 Governs the Reciprocal Development of Th17 and Regulatory T Cells. *Cell Rep.* **22**, 653–665 (2018).

79. Wulff, P. *et al.* Impaired renal Na(+) retention in the sgk1-knockout mouse. *J. Clin. Invest.* **110**, 1263–1268 (2002).

80. Lang, F. *et al.* (Patho)physiological significance of the serum- and glucocorticoid-inducible kinase isoforms. *Physiol. Rev.* **86**, 1151–1178 (2006).

81. Okada, S., Puel, A., Casanova, J.-L. & Kobayashi, M. Chronic mucocutaneous candidiasis disease associated with inborn errors of IL-17 immunity. *Clin. Transl. Immunol.* **5**, e114 (2016).

82. Beerli, R. R. *et al.* Mining the human autoantibody repertoire: isolation of potent IL17A-neutralizing monoclonal antibodies from a patient with thymoma. *mAbs* **6**, 1608–1620 (2014).

83. Jeon, C. *et al.* Monoclonal antibodies inhibiting IL-12, -23, and -17 for the treatment of psoriasis. *Hum. Vaccines Immunother.* **13**, 2247–2259 (2017).

84. Davis, S. D., Schaller, J. & Wedgwood, R. J. Job's Syndrome. Recurrent, 'cold', staphylococcal abscesses. *Lancet Lond. Engl.* **1**, 1013–1015 (1966).

85. Chandesris, M.-O. *et al.* Autosomal dominant STAT3 deficiency and hyper-IgE syndrome: molecular, cellular, and clinical features from a French national survey. *Medicine (Baltimore)* **91**, e1-19 (2012).

86. Gernez, Y. *et al.* Autosomal Dominant Hyper-IgE Syndrome in the USIDNET Registry. *J. Allergy Clin. Immunol. Pract.* **6**, 996–1001 (2018).

87. Liu, L. *et al.* Gain-of-function human STAT1 mutations impair IL-17 immunity and underlie chronic mucocutaneous candidiasis. *J. Exp. Med.* **208**, 1635–1648 (2011).

88. van de Veerdonk, F. L. *et al.* STAT1 mutations in autosomal dominant chronic mucocutaneous candidiasis. *N. Engl. J. Med.* **365**, 54–61 (2011).

89. Toubiana, J. *et al.* Heterozygous STAT1 gain-of-function mutations underlie an unexpectedly broad clinical phenotype. *Blood* **127**, 3154–3164 (2016).

90. Gan, P.-Y. *et al.* Th17 cells promote autoimmune anti-myeloperoxidase glomerulonephritis. *J. Am. Soc. Nephrol. JASN* **21**, 925–931 (2010).

91. Nogueira, E. *et al.* Serum IL-17 and IL-23 levels and autoantigen-specific Th17 cells are elevated in patients with ANCA-associated vasculitis. *Nephrol. Dial. Transplant. Off. Publ. Eur. Dial. Transpl. Assoc. - Eur. Ren. Assoc.* **25**, 2209–2217 (2010).

92. Rother, N. & van der Vlag, J. Disturbed T Cell Signaling and Altered Th17 and Regulatory T Cell Subsets in the Pathogenesis of Systemic Lupus Erythematosus. *Front. Immunol.* **6**, 610 (2015).

93. Peng, Z. *et al.* Increased number of Th22 cells and correlation with Th17 cells in peripheral blood of patients with IgA nephropathy. *Hum. Immunol.* **74**, 1586–1591 (2013).

94. Evans, R., Zdebik, A., Ciurtin, C. & Walsh, S. B. Renal involvement in primary Sjögren's syndrome. *Rheumatol. Oxf. Engl.* (2015) doi:10.1093/rheumatology/kev223.

95. Evans, R. D. R., Laing, C. M., Ciurtin, C. & Walsh, S. B. Tubulointerstitial nephritis in primary Sjögren syndrome: clinical manifestations and response to treatment. *BMC Musculoskelet. Disord.* **17**, 2 (2016).

96. Paust, H.-J. *et al.* CXCR3+ Regulatory T Cells Control TH1 Responses in Crescentic GN. *J. Am. Soc. Nephrol. JASN* **27**, 1933–1942 (2016).

97. Sullivan, J. A., Adams, A. B. & Burlingham, W. J. The emerging role of TH17 cells in organ transplantation. *Transplantation* **97**, 483–489 (2014).

98. Krebs, C. F., Schmidt, T., Riedel, J.-H. & Panzer, U. T helper type 17 cells in immune-mediated glomerular disease. *Nat. Rev. Nephrol.* **13**, 647–659 (2017).

99. Turner, J.-E. *et al.* CCR6 recruits regulatory T cells and Th17 cells to the kidney in glomerulonephritis. *J. Am. Soc. Nephrol. JASN* **21**, 974–985 (2010).

100. Krebs, C. F. *et al.* Autoimmune Renal Disease Is Exacerbated by S1P-Receptor-1-Dependent Intestinal Th17 Cell Migration to the Kidney. *Immunity* **45**, 1078–1092 (2016).

101. Gilg, J., Methven, S., Casula, A. & Castledine, C. UK Renal Registry 19th Annual Report: Chapter 1 UK RRT Adult Incidence in 2015: National and Centre-specific Analyses. *Nephron* **137 Suppl 1**, 11–44 (2017).

102. Serur, D. *et al.* Deceased-donor kidney transplantation: improvement in long-term survival. *Nephrol. Dial. Transplant. Off. Publ. Eur. Dial. Transpl. Assoc. - Eur. Ren. Assoc.* **26**, 317–324 (2011).

103. Lodhi, S. A. & Meier-Kriesche, H.-U. Kidney allograft survival: the long and short of it. *Nephrol. Dial. Transplant.* **26**, 15–17 (2011).

104. Sprangers, B., Monahan, M. & Appel, G. B. Diagnosis and treatment of lupus nephritis flares--an update. *Nat. Rev. Nephrol.* **8**, 709–717 (2012).

105. Robson, J. *et al.* Damage in the anca-associated vasculitides: long-term data from the European vasculitis study group (EUVAS) therapeutic trials. *Ann. Rheum. Dis.* **74**, 177–184 (2015).

106. El-Zoghby, Z. M. *et al.* Identifying specific causes of kidney allograft loss. *Am. J. Transplant. Off. J. Am. Soc. Transplant. Am. Soc. Transpl. Surg.* **9**, 527–535 (2009).

107. Sharples, E., Casula, A. & Byrne, C. UK Renal Registry 19th Annual Report: Chapter 3 Demographic and Biochemistry Profile of Kidney Transplant Recipients in the UK in 2015: National and Centre-specific Analyses. *Nephron* **137 Suppl 1**, 73–102 (2017).

108. Wilck, N. *et al.* Salt-responsive gut commensal modulates TH17 axis and disease. *Nature* **551**, 585–589 (2017).

109. Jörg, S. *et al.* High salt drives Th17 responses in experimental autoimmune encephalomyelitis without impacting myeloid dendritic cells. *Exp. Neurol.* **279**, 212–222 (2016).

110. Hammer, A. *et al.* Impact of combined sodium chloride and saturated long-chain fatty acid challenge on the differentiation of T helper cells in neuroinflammation. *J. Neuroinflammation* **14**, 184 (2017).

111. Spurgeon-Pechman, K. R. *et al.* Recovery from acute renal failure predisposes hypertension and secondary renal disease in response to elevated sodium. *Am. J. Physiol. Renal Physiol.* **293**, F269-278 (2007).

112. Crowley, S. D. & Rudemiller, N. P. Immunologic Effects of the Renin-Angiotensin System. *J. Am. Soc. Nephrol. JASN* **28**, 1350–1361 (2017).

113. Yi, B. *et al.* Effects of dietary salt levels on monocytic cells and immune responses in healthy human subjects: a longitudinal study. *Transl. Res. J. Lab. Clin. Med.* **166**, 103–110 (2015).

114. Luo, T. *et al.* Th17/Treg Imbalance Induced by Dietary Salt Variation Indicates Inflammation of Target Organs in Humans. *Sci. Rep.* **6**, 26767 (2016).

115. Wen, W. *et al.* Potassium supplementation inhibits IL-17A production induced by salt loading in human T lymphocytes via p38/MAPK-SGK1 pathway. *Exp. Mol. Pathol.* **100**, 370–377 (2016).

116. Scrivo, R. *et al.* The role of dietary sodium intake on the modulation of T helper 17 cells and regulatory T cells in patients with rheumatoid arthritis and systemic lupus erythematosus. *PloS One* **12**, e0184449 (2017).

117. Kleta, R. & Bockenhauer, D. Salt-Losing Tubulopathies in Children: What's New, What's Controversial? *J. Am. Soc. Nephrol. JASN* **29**, 727–739 (2018).

118. Palmer, L. G. & Schnermann, J. Integrated control of Na transport along the nephron. *Clin. J. Am. Soc. Nephrol. CJASN* **10**, 676–687 (2015).

119. Klootwijk, E. D. *et al.* Mistargeting of peroxisomal EHHADH and inherited renal Fanconi's syndrome. *N. Engl. J. Med.* **370**, 129–138 (2014).

120. Hamilton, A. J. *et al.* The HNF4A R76W mutation causes atypical dominant Fanconi syndrome in addition to a β cell phenotype. *J. Med. Genet.* **51**, 165–169 (2014).

121. Marchesin, V. *et al.* Molecular Basis for Autosomal-Dominant Renal Fanconi Syndrome Caused by HNF4A. *Cell Rep.* **29**, 4407-4421.e5 (2019).

122. Seys, E. *et al.* Clinical and Genetic Spectrum of Bartter Syndrome Type 3. *J. Am. Soc. Nephrol. JASN* **28**, 2540–2552 (2017).

123. Balavoine, A. S. *et al.* Phenotype-genotype correlation and follow-up in adult patients with hypokalaemia of renal origin suggesting Gitelman syndrome. *Eur. J. Endocrinol.* **165**, 665–673 (2011).

124. Peti-Peterdi, J. & Harris, R. C. Macula densa sensing and signaling mechanisms of renin release. *J. Am. Soc. Nephrol. JASN* **21**, 1093–1096 (2010).

125. Blanchard, A. *et al.* Gitelman syndrome: consensus and guidance from a Kidney Disease: Improving Global Outcomes (KDIGO) Controversies Conference. *Kidney Int.* **91**, 24–33 (2017).

126. Kalinski, P. Regulation of immune responses by prostaglandin E2. *J. Immunol. Baltim. Md 1950* **188**, 21–28 (2012).

127. Nijenhuis, T. *et al.* Enhanced passive Ca2+ reabsorption and reduced Mg2+ channel abundance explains thiazide-induced hypocalciuria and hypomagnesemia. *J. Clin. Invest.* **115**, 1651–1658 (2005).

128. Berry, M. R., Robinson, C. & Karet Frankl, F. E. Unexpected clinical sequelae of Gitelman syndrome: hypertension in adulthood is common and females have higher potassium requirements. *Nephrol. Dial. Transplant. Off. Publ. Eur. Dial. Transpl. Assoc. - Eur. Ren. Assoc.* **28**, 1533–1542 (2013).

129. Bockenhauer, D. *et al.* Epilepsy, ataxia, sensorineural deafness, tubulopathy, and KCNJ10 mutations. *N. Engl. J. Med.* **360**, 1960–1970 (2009).

130. Terker, A. S. *et al.* Potassium modulates electrolyte balance and blood pressure through effects on distal cell voltage and chloride. *Cell Metab.* **21**, 39–50 (2015).

131. Hoorn, E. J., Gritter, M., Cuevas, C. A. & Fenton, R. A. Regulation of the Renal NaCl Cotransporter and Its Role in Potassium Homeostasis. *Physiol. Rev.* **100**, 321–356 (2020).

132. Bernabe-Ortiz, A. *et al.* Effect of salt substitution on community-wide blood pressure and hypertension incidence. *Nat. Med.* **26**, 374–378 (2020).

133. Bartter, F. C., Pronove, P., Gill, J. R. & Maccardle, R. C. Hyperplasia of the juxtaglomerular complex with hyperaldosteronism and hypokalemic alkalosis. A new syndrome. *Am. J. Med.* **33**, 811–828 (1962).

134. Gitelman, H. J., Graham, J. B. & Welt, L. G. A new familial disorder characterized by hypokalemia and hypomagnesemia. *Trans. Assoc. Am. Physicians* **79**, 221–235 (1966).

135. Blanchard, A. *et al.* Resistance to Insulin in Patients with Gitelman Syndrome and a Subtle Intermediate Phenotype in Heterozygous Carriers: A Cross-Sectional Study. *J. Am. Soc. Nephrol. JASN* **30**, 1534–1545 (2019).

136. Zhou, H. *et al.* Complicated Gitelman syndrome and autoimmune thyroid disease: a case report with a new homozygous mutation in the SLC12A3 gene and literature review. *BMC Endocr. Disord.* **18**, 82 (2018).

137. Mancilha-Carvalho, J. de J. & Souza e Silva, N. A. The Yanomami Indians in the INTERSALT Study. *Arq. Bras. Cardiol.* **80**, 289–300 (2003).

138. Kerem, E. *et al.* Pulmonary epithelial sodium-channel dysfunction and excess airway liquid in pseudohypoaldosteronism. *N. Engl. J. Med.* **341**, 156–162 (1999).

139. Muñoz-Durango, N. *et al.* Modulation of Immunity and Inflammation by the Mineralocorticoid Receptor and Aldosterone. *BioMed Res. Int.* **2015**, 652738 (2015).

140. Hureaux, M. *et al.* High-throughput sequencing contributes to the diagnosis of tubulopathies and familial hypercalcemia hypocalciuria in adults. *Kidney Int.* **96**, 1408–1416 (2019).

141. Woellner, C. *et al.* Mutations in STAT3 and diagnostic guidelines for hyper-IgE syndrome. *J. Allergy Clin. Immunol.* **125**, 424-432.e8 (2010).

142. Norlander, A. E. *et al.* A salt-sensing kinase in T lymphocytes, SGK1, drives hypertension and hypertensive end-organ damage. *JCI Insight* **2**, (2018).

143. Srenathan, U., Steel, K. & Taams, L. S. IL-17+ CD8+ T cells: Differentiation, phenotype and role in inflammatory disease. *Immunol. Lett.* **178**, 20–26 (2016).

144. Liang, Y., Pan, H.-F. & Ye, D.-Q. Tc17 Cells in Immunity and Systemic Autoimmunity. *Int. Rev. Immunol.* **34**, 318–331 (2015).

145. Demian, W. L. *et al.* The Ion Transporter NKCC1 Links Cell Volume to Cell Mass Regulation by Suppressing mTORC1. *Cell Rep.* **27**, 1886-1896.e6 (2019).

146. Verbalis, J. G. How does the brain sense osmolality? *J. Am. Soc. Nephrol. JASN* **18**, 3056–3059 (2007).

147. Feske, S. *et al.* A mutation in Orai1 causes immune deficiency by abrogating CRAC channel function. *Nature* **441**, 179–185 (2006).

148. Li, F.-Y. *et al.* XMEN disease: a new primary immunodeficiency affecting Mg2+ regulation of immunity against Epstein-Barr virus. *Blood* **123**, 2148–2152 (2014).

149. Milner, J. D. *et al.* Impaired T(H)17 cell differentiation in subjects with autosomal dominant hyper-IgE syndrome. *Nature* **452**, 773–776 (2008).

150. Aoi, N. *et al.* Two novel genotypes of the thiazide-sensitive Na-Cl cotransporter (SLC12A3) gene in patients with Gitelman's syndrome. *Endocrine* **31**, 149–153 (2007).

151. Zha, B., Zheng, P., Liu, J. & Huang, X. Coexistence of Graves' Disease in a 14-year-old young girl with Gitelman Syndrome. *Clin. Endocrinol. (Oxf.)* **83**, 995–997 (2015).

152. Mizokami, T. *et al.* Graves' disease and Gitelman syndrome. *Clin. Endocrinol. (Oxf.)* **84**, 149–150 (2016).

153. Deliyska, B., Lazarov, V., Minkova, V., Nikolov, D. & Tishkov, I. Association of Bartter's syndrome with vasculitis. *Nephrol. Dial. Transplant. Off. Publ. Eur. Dial. Transpl. Assoc. - Eur. Ren. Assoc.* **15**, 102–103 (2000).

154. Mishima, E. *et al.* Inherited, not acquired, Gitelman syndrome in a patient with Sjögren's syndrome: importance of genetic testing to distinguish the two forms. *CEN Case Rep.* **6**, 180–184 (2017).

155. Walsh, P. R. *et al.* Clinical and diagnostic features of Bartter and Gitelman syndromes. *Clin. Kidney J.* **11**, 302–309 (2018).

156. Vaeth, M. & Feske, S. Ion channelopathies of the immune system. *Curr. Opin. Immunol.* **52**, 39–50 (2018).

157. Bettelli, E., Korn, T., Oukka, M. & Kuchroo, V. K. Induction and effector functions of T(H)17 cells. *Nature* **453**, 1051–1057 (2008).

158. Feske, S., Wulff, H. & Skolnik, E. Y. Ion Channels in Innate and Adaptive Immunity. *Annu. Rev. Immunol.* **33**, 291–353 (2015).

159. Feske, S., Giltnane, J., Dolmetsch, R., Staudt, L. M. & Rao, A. Gene regulation mediated by calcium signals in T lymphocytes. *Nat. Immunol.* **2**, 316–324 (2001).

160. Feske, S., Prakriya, M., Rao, A. & Lewis, R. S. A severe defect in CRAC Ca2+ channel activation and altered K+ channel gating in T cells from immunodeficient patients. *J. Exp. Med.* **202**, 651–662 (2005).

161. Le Deist, F. *et al.* A primary T-cell immunodeficiency associated with defective transmembrane calcium influx. *Blood* **85**, 1053–1062 (1995).

162. McCarl, C.-A. *et al.* ORAI1 deficiency and lack of store-operated Ca2+ entry cause immunodeficiency, myopathy, and ectodermal dysplasia. *J. Allergy Clin. Immunol.* **124**, 1311-1318.e7 (2009).

163. Partiseti, M. *et al.* The calcium current activated by T cell receptor and store depletion in human lymphocytes is absent in a primary immunodeficiency. *J. Biol. Chem.* **269**, 32327–32335 (1994).

164. Li, F.-Y. *et al.* Second messenger role for Mg2+ revealed by human T-cell immunodeficiency. *Nature* **475**, 471–476 (2011).

165. Kaufmann, U. *et al.* Selective ORAI1 Inhibition Ameliorates Autoimmune Central Nervous System Inflammation by Suppressing Effector but Not Regulatory T Cell Function. *J. Immunol. Baltim. Md 1950* **196**, 573–585 (2016).

166. Kaufmann, U. *et al.* Calcium Signaling Controls Pathogenic Th17 Cell-Mediated Inflammation by Regulating Mitochondrial Function. *Cell Metab.* **29**, 1104-1118.e6 (2019).

167. Tam, M., Gómez, S., González-Gross, M. & Marcos, A. Possible roles of magnesium on the immune system. *Eur. J. Clin. Nutr.* **57**, 1193–1197 (2003).

168. MacNeill, S. J., Ford, D., Evans, K. & Medcalf, J. F. Chapter 2 UK Renal Replacement Therapy Adult Prevalence in 2016: National and Centre-specific Analyses. *Nephron* **139 Suppl 1**, 47–74 (2018).

169. Gardner, P. Patch clamp studies of lymphocyte activation. *Annu. Rev. Immunol.* **8**, 231–252 (1990).

170. Ji, W. *et al.* Rare independent mutations in renal salt handling genes contribute to blood pressure variation. *Nat. Genet.* **40**, 592–599 (2008).

171. Norlander, A. E., Madhur, M. S. & Harrison, D. G. The immunology of hypertension. *J. Exp. Med.* **215**, 21–33 (2018).

8 Appendix

8.1 Structured clinical history proforma used for assessment of clinical features of altered immunity

Patient Identifier			**Date Seen**		
Consent form signed					
Diagnosis, year of diagnosis			**Genotype result**		
Other PMHx					
DHx					
History of diagnosis					
Infective symptoms or infections in childhood (location, treatment, number)	State pre/post rx/any response to tx				
Infective symptoms or infections in adulthood (location, treatment, number)	State pre/post rx/any response to tx				
Skin abscess (total #)	None	1-2	3-4	>4	
Comments (year, location, treatment)					
Pneumonia (x-ray proven, total #)	None	1	2	3	>3
Comments (year, location, treatment)					
Other serious infection (e.g. requiring hospitalization)	None	Severe			
Comments (year, location, treatment)					
URTI inc. Sinusitis, otitis (# times in worst year)	1-2	3	4-6	>6	
Comments (year, location, treatment)					
Candidiasis	None	Oral, vaginal	Fingernail	Systemic	
Comments (year, location, treatment)					
History of other infections (not requiring hospitilisation inc. UTIs)	State number UTIs in worst year, ?prophylactic abx				

Do you have a history of autoimmune disease: multiple sclerosis; IBD; psoriasis; any form of inflammatory arthritis; sjogren's syndrome; vasculitis; SLE; AI thyroid disease; other CTD	No	Yes, specify details (year diagnosis, diagnosis basis, rx):
Do you have a history of allergic disease: asthma, eczema, hay fever, contact or drug allergy	No	Yes, specify which:
Do you have any other symptoms that you think might relate to altered immunity	Inc. rec VZV, HSV, HPV	
Other comments		

8.2 Questionnaire used in pilot studies for assessment of dietary salt intake

SCORED SALT QUESTIONNAIRE

The following questions ask you about your usual eating patterns over the last 6 months.

- Please answer as honestly as possible.
- Be sure to answer every question and tick only one box per question.

1. **Breads -** How many slices of bread do you usually eat per day?

Food type	Examples	Please select one only			
		5 or more slices per day	**3-4 slices per day**	**1-2 slices per day**	**I don't usually eat any bread**
All types of bread	White, wholemeal, grain, bakery, homemade, chapatti etc. Count 1 roll, crumpet, English muffin, small wrap, or small pocket bread as = 2 slices	30	25	15	0

2. **Spreads**

Food type	Examples	Please select one only			
		At least once daily	**2-3 times per week**	**Once per week**	**Rarely or never eaten**
Fat spreads	Butter, margarine, dairy blend, olive oil spread, plant sterol spread	6	4	2	0
Yeast extract spreads	Vegemite, Promite, Marmite	4	2	1	0
Peanut spreads	Peanut butter or paste	2	1	0.5	0

3. **Cereals, Biscuits, and Baking**

Food type	Examples	Please select one only			
		At least once daily	2-3 times per week	Once per week	Rarely or never eaten
Ready-made breakfast cereals *(exclude oats and semolina)*	Corn flakes, puffed rice or corn, Froot Loops, Weet-Bix, muesli, bran flakes, Special K etc	☐5	☐3	☐2	☐0
Sweet biscuits, cookies, and baking/bakery foods	Tea biscuits, shortbread, cream biscuits, cakes, scones, sweet buns, doughnuts, muffins (savoury or sweet) etc	☐5	☐3	☐2	☐0
Sweet pastry items	Frozen waffles, Danish, pastries, croissants, tarts with pastry shell etc	☐2	☐1	☐0.5	☐0
Savoury biscuits and crackers	BBQ Shapes, rice or water crackers, Country Cheese, Jatz, Sao, Ryvita etc	☐5	☐4	☐3	☐0

4. **Cheeses and Savoury Snacks**

Food type	Examples	Please select one only			
		At least once daily	2-3 times per week	Once per week	Rarely or never eaten
Cheeses (exclude cottage and ricotta)	Block, slices, Cheddar, parmesan, Edam, brie, camembert, feta, gorgonzola, cream cheese, bottled cheese spread etc	☐12	☐6	☐4	☐0
Plain, flavoured or salted crisps, chips, pretzels	Smith's Crisps, corn chips, Pringles, Burger Rings, Cheezels etc	☐2	☐1	☐0.5	☐0
Commercial dips, pates, fish or meat spreads	French onion dip, chicken liver pate, fish paste etc	☐2	☐1	☐0.5	☐0
Olives and pickled vegetables	Olives, pickled onions, gherkins etc	☐2	☐1	☐0.5	☐0
Salted nuts, salted or buttered popcorn, or pea-or noodle-based snacks	All nuts, peanuts, bhuja mix, wasabi peas etc	☐2	☐1	☐0.5	☐0

5. **Tinned and Packet Foods and Other Meal Components**

Food type	Examples	Please select one only			
		At least once daily	2-3 times per week	Once per week	Rarely or never eaten
Tinned or packet soups	Chicken noodle soup mix, Cup-a-Soup, tinned and condensed soups, miso soup, ready-made chilled soups etc	☐3	☐2	☐1	☐0
Tinned baked beans or spaghetti	Spaghetti in tomato sauce, baked beans with cheese sauce	☐2	☐1	☐0.5	☐0
Tinned or packet casseroles, stews or curries	Steak and kidney stew, camp pie, curry in a box etc	☐2	☐1	☐0.5	☐0
Tinned legumes	Chickpeas, lentils, three bean mix, dhal, refried beans	☐2	☐1	☐0.5	☐0
Tinned vegetables	Crushed tomatoes, peas, carrots, potatoes, mushrooms in sauce, sauerkraut, creamed corn, beetroot etc	☐4	☐2.5	☐1.5	☐0
Flavoured pasta, rice, or noodles in a packet	Packet pasta meals e.g. Continental Alfredo, 2-min noodles, flavoured fried rice or cous cous	☐4	☐2	☐1	☐0
Ready-made salads	Deli or salad bar: coleslaw, potato, pasta, Greek salad Fresh produce: Caesar and other salads in packet with dressing	☐2	☐1	☐0.5	☐0

6. **Processed Meats and Seafood**

Food type	Examples	Please select one only			
		At least once daily	2-3 times per week	Once per week	Rarely or never eaten
Processed meat *(cooked, smoked or canned)*	Ham, sausages, bacon, hock, corned beef, Spam, pickled pork, Devon, luncheon, salami, rotisserie chicken etc	☐30	☐20	☐10	☐0
Processed fish or shellfish *(cooked, smoked or canned; exclude if canned in fresh/springwater)*	Tinned: tuna, sardines, mussels, crabmeat, marinara mix, anchovies Smoked: salmon, cod, kippers	☐5	☐3	☐2	☐0

7. Flavourings Added in Cooking

Food type	Examples	Please select one only			
		At least once daily	2-3 times per week	Once per week	Rarely or never eaten
Ready-made stocks (cube, powder or liquid)	Campbell's Real Chicken Stock, Bonox, stock cubes	☐5	☐3	☐2	☐0
Meal and recipe bases (dry powder mix in packet)	Maggi beef stroganoff base, slow cooker flavour sachets, taco or fajita seasonings	☐3	☐2	☐1	☐0
Bottled sauces or marinades for cooking	Pasta sauce in a jar/bottle, barbecue marinades, curry sauce in a jar, satay/black bean/sweet and sour sauces	☐10	☐5	☐3	☐0
Salt added during cooking *(include all types e.g. onion, garlic, chicken, organic, sea salt etc)*	In: vegetable or pasta cooking water, soups, mashed potato, gravy, casseroles On: grilled, pan-fried or barbecued foods	☐25	☐15	☐8	☐0

8. Flavourings Added at the Table

Food type	Examples	Please select one only			
		At least once daily	2-3 times per week	Once per week	Rarely or never eaten
Salt added at the table *(include all types e.g. onion, garlic, chicken, organic, sea salt etc)*	On: chips, meat, eggs, vegetables, soups, salads, sandwiches	☐12	☐8	☐4	☐0
Bottled table sauces and condiments	Tomato/barbecue sauce, Worcestershire sauce, soy/fish sauce, chilli sauce, fruit chutney, mustard pickles, horseradish, tartare sauce etc	☐5	☐3	☐2	☐0
Gravies and sauces made from dry packet mix	Gravox, premade liquid gravy, cheesy white sauce from dry mix	☐4	☐2.5	☐1.5	☐0
Mayonnaise or ready-made salad dressings (regular or low fat)	French/Italian/Caesar dressing, mayonnaise etc	☐3	☐2	☐1	☐0

9. **Pre-prepared Meals and Drinks and Eating Out**

Food type	Examples	Please select one only			
		At least once daily	2-3 times per week	Once per week	Rarely or never eaten
Pre-prepared, frozen or home delivered meals	Family size pies or quiches, lasagne, cannelloni, frozen pizza, frozen dinners, Meals on Wheels etc	☐4	☐3	☐2	☐0
Takeaway and deep-fried foods	Asian takeaway, pizza, fish and chips, burgers, hot dogs, fried chicken, kebabs, potato chips or wedges, Chiko Rolls, pies, pasties or sausage rolls	☐5	☐4	☐3	☐0
Restaurant, café or club meals	Food halls, Asian restaurants, buffets, canteens, The Coffee Club etc	☐4	☐3	☐2	☐0
Sports drinks or vegetable juices with added salt	Gatorade, Powerade, Isosport, V8 vegetable juice, Berri or Golden Circle tomato juice	☐2	☐1	☐0.5	☐0

8.3 Questionnaire used to assess tolerability of low salt intervention

The low salt diet was easy to adhere to for 1 week	Strongly disagree	Disagree	Neither agree nor disagree	Agree	Strongly agree
The low salt diet stopped me doing things I wanted to do	Strongly disagree	Disagree	Neither agree nor disagree	Agree	Strongly agree
The low salt diet changed the amount of money I spent on food	Strongly disagree	Disagree	Neither agree nor disagree	Agree	Strongly agree
If agree/strongly agree	Spent more	Spent less			
I had more energy on the low salt diet than my normal diet	Strongly disagree	Disagree	Neither agree nor disagree	Agree	Strongly agree
I felt less fatigued on the low salt diet than my normal diet	Strongly disagree	Disagree	Neither agree nor disagree	Agree	Strongly agree
I felt happier on the low salt diet than my normal diet	Strongly disagree	Disagree	Neither agree nor disagree	Agree	Strongly agree
I would find it easy to continue a diet of this low salt content in the longer term	Strongly disagree	Disagree	Neither agree nor disagree	Agree	Strongly agree
Having participated in the study, I am more aware of the salt content of different foods	Strongly disagree	Disagree	Neither agree nor disagree	Agree	Strongly agree
After the study, I am likely to reduce the amount of salt in my diet	Strongly disagree	Disagree	Neither agree nor disagree	Agree	Strongly agree
I would be willing to undertake changes in lifestyle if these were beneficial for my transplant outcome	Strongly disagree	Disagree	Neither agree nor disagree	Agree	Strongly agree
I would prefer to undertake changes in lifestyle than take additional medications to improve my transplant outcome	Strongly disagree	Disagree	Neither agree nor disagree	Agree	Strongly agree
Do you have any further comments on participating in the study:					

8.4 List of organisms isolated from urine sediment cultures in Salt Losing Tubulopathy patients and healthy controls

Where reliable identification could not be achieved for a cultured isolate by MALDI-TOF MS, strains are reported as “No ID”.

A. Salt losing tubulopathy patients

Patient number	Age	Sex	Diagnosis	Number of isolates	Genus	Species	Colony Forming Units/ml
29	85	Male	Gitelman	5	*Klebsiella*	*Klebsiella oxytoca*	2.4
					Enterococcus	*Enterococcus faecalis*	33.6
					Staphylococcus	*Staphylococcus epidermidis*	8.4
					Corynebacterium	*Corynebacterium singulare*	38
					Staphylococcus	*Staphylococcus haemolyticus*	3.2
12	32	Female	Bartter (3)	4	*Corynebacterium*	*Corynebacterium aurimucosum*	2.8
					Staphylococcus	*Staphylococcus haemolyticus*	0.8
					No ID	No ID	1.2
					No ID	No ID	0.4
13	34	Male	Bartter (3)	1	No ID	No ID	332
6	18	Female	Bartter (2)	3	*Streptococcus*	*Streptococcus vestibularis*	100
					Staphylococcus	*Staphylococcus haemolyticus*	100
					Staphylococcus	*Staphylococcus epidermidis*	0.4
47	31	Female	Gitelman	4	*Escherichia*	*Escherichia coli*	0.4
					Staphylococcus	*Staphylococcus hominis*	800
					Staphylococcus	*Staphylococcus epidermidis*	600
					Lactobacillus	*Lactobacillus crispatus*	800000
33	52	Male	Gitelman	2	*Staphylococcus*	*Staphylococcus haemolyticus*	800
					Enterococcus	*Enterococcis faecium*	0.4

46	43	Female	Gitelman	4	*Staphylococcus*	*Staphylococcus haemolyticus*	440
					Staphylococcus	*Staphylococcus epidermidis*	800
					Corynebacterium	*Corynebacterium aurimucosum*	72
					Enterococcus	*Enterococcus faecalis*	5.2
31	41	Female	Gitelman	4	*Escherichia*	*Escherichia coli*	3600
					Enterococcus	*Enterococcus faecalis*	60
					Enterococcus	*Enterococcus faecalis*	11600
					Corynebacterium	*Corynebacterium coyleae*	56
20	34	Male	Bartter (3)	3	*Staphylococcus*	*Staphylococcus haemolyticus*	36
					Staphylococcus	*Staphylococcus haemolyticus*	20
					Corynebacterium	*Corynebacterium singulare*	52
10	31	Male	Bartter (3)	4	*Enterococcus*	*Enterococcus faecalis*	560
					Staphylococcus	*Staphylococcus capitis*	5.2
					Staphylococcus	*Staphylococcus warneri*	2
					Streptococcus	*Streptococcus agalactiae*	2800
2	26	Female	Bartter (1)	4	*Streptococcus*	*Streptococcus agalactiae*	5600
					Aerococcus	*Aerococcus urinae*	32000
					No ID	No ID	3600
					Corynebacterium	*Corynebacterium amycolatum*	3600
27	37	Female	Gitelman	5	*Staphylococcus*	*Staphylococcus haemolyticus*	44000
					Enterococcus	*Enterococcus faecalis*	2000
					No ID	No ID	10000000
					Staphylococcus	*Staphylococcus epidermidis*	44000
					Corynebacterium	*Corynebacterium tuberculostearicum*	4000000
14	31	Male	Bartter (3)	1	*Streptococcus*	*Streptococcus oralis*	3.2
5	19	Male	Bartter (2)	2	*Klebsiella*	*Klebsiella oxytoca*	4.4
					Staphylococcus	*Staphylococcus haemolyticus*	2.8

B. Healthy Controls

Age	Sex	Number isolates	Genus	Species	Colony Forming Units/ml
30	Female	3	*Staphylococcus*	*Staphylococcus epidermidis*	32000
			Staphylococcus	*Staphylococcus hominis*	3600
			No ID	No ID	8.8
30	Female	3	*Citrobacter*	*Citrobacter koseri*	640
			Escherichia	*Escherichia coli*	24
			Enterococcus	*Enterococcus raffinosus*	5.2
22	Female	6	*Escherichia*	*Escherichia coli*	16
			Klebsiella	*Klebsiella pneumoniae*	40
			Enterococcus	*Enterococcus faecalis*	20
			Enterococcus	*Enterococcus faecalis*	5.2
			Staphylococcus	*Staphylococcus hominis*	28
			Staphylcoccus	*Stapylococcus epidermidis*	8
36	Male	0	No growth	No growth	NA
28	Male	3	*Staphylococcus*	*Staphylococcus epidermidis*	2.4
			Streptococcus	*Streptococcus mitis*	44
			Staphylococcus	*Staphylococcus epidermidis*	2.8
24	Male	3	*Staphylococcus*	*Staphylococcus haemolyticus*	0.4
			Staphylococcus	*Staphylococcus haemolyticus*	2.4
			Streptococcus	*Streptococcus mitis*	112
53	Male	4	*Staphylococcus*	*Staphylococcus hominis*	1.2
			Staphylococcus	*Staphylococcus hominis*	60
			Staphylococcus	*Staphylococcus hominis*	56
			Facklamia	*Facklamia hominis*	4
24	Female	2	*Staphylococcus*	*Staphylococcus epidermidis*	14.8
			Lactobacillus	*Lactobacillus crispatus*	1800000
50	Female	4	*Streptococcus*	*Streptococcus agalactiae*	840000
			No ID	No ID	36
			Staphylococcus	*Staphylococcus lugdenensis*	5.6

			Staphylococcus	*Staphylococcus haemolyticus*	24
42	Female	5	*Escherichia*	*Escherichia coli*	11200
			Enterococcus	*Enterococcus faecalis*	3200
			Streptococcus	*Streptococcus agalactiae*	2400
			Enterococcus	*Enerococcus faecalis*	2400
			No ID	No ID	1200
40	Male	4	*Staphylococcus*	*Staphylococcus epidermidis*	20
			Staphylococcus	*Staphylococcus capitis*	16
			Corynebacterium	*Corynebacterium tuberculostearicum*	3.6
			No ID	No ID	3200
31	Male	2	*Streptococcus*	*Streptococcus mitis*	4800
			Staphylococcus	*Staphylococcus hominis*	0.4